

**The role of Sel1L-Hrd1 ER Associated Degradation in B cell  
development and function.**

**A Dissertation**

**Presented to the Faculty of the Graduate School**

**of Cornell University**

**In Partial Fulfillment of the Requirements for the Degree of**

**Doctor of Philosophy**

**by**

**Hana Kim**

**August 2017**

© 2017 Hana Kim

## **The Role of Sel1L-ER Associated Degradation in B cell Development and Function**

Hana Kim, Ph. D.

Cornell University 2017

The Endoplasmic Reticulum (ER) serves as the site for protein synthesis, folding, maturation and modification in the cell. In mammalian cells, approximately one-third of the newly synthesized proteins enter the ER in an unfolded state. Despite various folding machineries in the ER, protein folding is inherently error prone and often results in the generation of irreparable misfolded proteins which disrupts ER homeostasis. ER-associated degradation (ERAD) is a principle quality-control mechanism responsible for restoring ER homeostasis by targeting misfolded proteins in the ER for cytosolic proteasomal degradation. The best characterized ERAD machinery in mammals is the highly conserved Sel1L-Hrd1 complex, consisting of E3 ubiquitin ligase Hrd1 and its adaptor protein Sel1L. Although studies using tissue specific knockout mice, have provided insights into the regulatory role of ERAD in highly secretory cell types such as adipocytes and intestinal epithelium, the physiological importance of Sel1L-Hrd1 ERAD in cell differentiation and development has not been explored to date.

To this end, we chose to investigate B cell development as a model system, as it requires tightly orchestrated expression of many growth factors and cell surface-associated proteins for different stages of development. We generated B cell specific Sel1L knockout mice driven by CD19-Cre (*Sel1L<sup>CD19</sup>*). Here, we report that B cell development, which requires a sequential progression of differentiation in the bone marrow, was blocked at the large pre-B cell stage in *Sel1L<sup>CD19</sup>* mice. We show that ERAD manages an early checkpoint in B cell development by selectively targeting the pre-BCR complex for proteasomal degradation, hence terminating pre-BCR signaling. In the absence of Sel1L-Hrd1 ERAD, pre-BCR accumulates at the cell surface,

leading to persistent pre-BCR signaling and cell cycling. Strikingly, our study shows that pre-BCR complex, but not BCR complex, as an endogenous protein substrate of ERAD in B cells. To further understand the physiological importance of ERAD in B cell function, we examined the mucosal immunity of *Sel1L<sup>CD19</sup>* mice. While IgG/IgM secretion in *Sel1L<sup>CD19</sup>* mice is comparable to the wild type mice, the IgA secretion level was significantly reduced. Surprisingly, *Sel1L<sup>CD19</sup>* mice exhibited exacerbated inflammatory response to dextran sodium sulfate (DSS)-induced colitis. Interestingly, this colitogenic phenotype was transmissible only between littermates bred from *Sel1L<sup>CD19</sup>* dam. Collectively, the works described in this thesis provide novel insight into the physiological importance of ERAD in B cell development. Further studies based on this dissertation may provide important mechanistic insight into protein complex substrate selection by ERAD.

# BIOGRAPHICAL SKETCH

Hana Kim was born in Seoul, South Korea in 1984 and spent her early years in Seoul, South Korea and Vancouver, Canada. The year she moved to Los Angeles with her family, she started her studies in Microbiology at California State Polytechnic University-Pomona. After receiving her bachelor's degree, she continued her pursuit of knowledge by entering master's program in Biological Sciences at California State Polytechnic University-Pomona, where she worked as a laboratory manager, while writing her thesis, Characterization of Efficacy and Immune Response of VesiVax® Universal Liposomal M2e Vaccine (L-M2e) for Scale-Up Production. Her research experience during her undergraduate and graduate years led to her interest in pursuing her Ph.D. in Immunology and Infectious Diseases at Cornell University in the Fall of 2011. In June of 2012, she joined Dr. Ling Qi's laboratory where she enjoyed the collaborative work with the members of the Qi lab. Her research focused on the ER quality control machinery and its physiological significance in B cell development and functions.

Dedicated to my parents, WonKyu and MoonSun Kim

# ACKNOWLEDGMENTS

I would like to thank my advisor Dr. Ling Qi for taking me into his lab, for his guidance and training while giving me the freedom to pursue any scientific questions. Over the years in his lab, he has trained me to see the “big picture” while paying attention to the small details. He also taught me how to effectively give presentation and write scientifically. I would like to thank my committee members Dr. Judith Appleton and Dr. Avery August for their support and encouragement, as well as advice on this thesis.

I also would like to thank the members of the Qi lab for their support and help, especially Dr. Yewei Ji, who had the patience to train me on the details of experiments and discuss any subjects regarding scientific research from day one. Thanks to my all other Qi lab colleagues: Asmita Bhattacharya, Dr. Guojun Shi, Dr. Hyang Kim and Dr. Neha Shrestha for their scientific support and advice on my thesis. I would also like to thank some of the former members, Drs. Yin He, Zhen Xue and Liu Yang for their career advice even after their graduation from Cornell.

Thanks to all my friends at Cornell, especially Kristeen Pareja, Jennifer & Thomas Pinello, and Sachi Horibata. I cannot imagine the 6 years of my life at Cornell without them. Thanks to Arla Hourigan and Cindy Grey, who were very helpful during my relocation to the University of Michigan.

Final special thanks to my parents, my sister and my Cherry, whose infinite love, support and encouragement helped me through the toughest time. It is thanks to them that I was able to finish this chapter of my life.

# TABLE OF CONTENTS

<b>BIOGRAPHICAL SKETCH .....</b>	<b>iv</b>
<b>ACKNOWLEDGMENTS .....</b>	<b>vi</b>
<b>TABLE OF CONTENTS .....</b>	<b>vii</b>
<b>LIST OF FIGURES .....</b>	<b>ix</b>
<b>LIST OF TABLES .....</b>	<b>xi</b>
<b>CHAPTER ONE: INTRODUCTION AND LITERATURE REVIEW .....</b>	<b>1</b>
<b>1.1 ENDOPLASMIC RETICULUM .....</b>	<b>2</b>
1.1.1. PROTEIN FOLDING AND POST-TRANSLATIONAL MODIFICATIONS .....	2
<b>1.2 UNFOLDED PROTEIN RESPONSE .....</b>	<b>6</b>
1.2.1. IRE1 PATHWAY .....	9
IRE1-XBP1(HAC1) pathway .....	11
Regulated Ire1-dependent decay (RIDD).....	13
Matter of life or death (inflammatory response vs apoptosis) .....	14
1.2.2. PERK PATHWAY .....	15
1.2.3. ATF6 PATHWAY .....	17
1.2.4. UPR in immunity .....	19
<b>1.3 ENDOPLASMIC RETICULUM ASSOCIATED DEGRADATION (ERAD) .....</b>	<b>23</b>
1.3.1. Recognition of misfolded proteins.....	26
1.3.2. Retrotranslocation/dislocation from the ER .....	27
1.3.3. Ubiquitination and Degradation in the cytosol.....	28
1.3.4. ERAD and Immunity.....	29
<b>1.4 B CELL DEVELOPMENT AND FUNCTION .....</b>	<b>31</b>
1.4.1. OVERVIEW .....	31
1.4.2. B CELL DEVELOPMENT IN THE BONE MARROW .....	32
1.4.3. Pre-BCR.....	36
<b>CHAPTER TWO: REVIEW- Endoplasmic reticulum quality control in cancer: Friend or Foe<sup>a</sup> .....</b>	<b>39</b>
<b>2.1 ABSTRACT .....</b>	<b>40</b>
<b>2.2 INTRODUCTION.....</b>	<b>40</b>
<b>2.3 The IRE1<math>\alpha</math> signaling pathway.....</b>	<b>41</b>
<b>2.4 THE ROLE OF IRE1A-XBP1S SIGNALING PATHWAY IN CANCER.....</b>	<b>46</b>
<b>2.5 ERAD .....</b>	<b>55</b>
<b>2.6 THE ROLE OF SEL1L-HRD1 ERAD IN CANCER.....</b>	<b>57</b>
<b>2.7 THERAPEUTICS .....</b>	<b>59</b>
<b>2.8 CONCLUSIONS .....</b>	<b>62</b>
<b>2.9 PERSPECTIVES.....</b>	<b>63</b>
<b>CHAPTER THREE: The Sel1L-Hrd1 Endoplasmic Reticulum-Associated Degradation complex manages a key checkpoint in B cell development<sup>b</sup> .....</b>	<b>67</b>
<b>3.1. ABSTRACT .....</b>	<b>68</b>
<b>3.2. INTRODUCTION.....</b>	<b>68</b>
<b>3.3. EXPERIMENTAL PROCEDURES.....</b>	<b>70</b>
<b>3.4. RESULTS.....</b>	<b>81</b>
3.4.1. Reduced peripheral B cells in B cell-specific Sel1L-deficient mice. ....	81

3.4.2. Developmental defect at the transition from the large to the small pre-B cell stage in <i>Sell1L<sup>CD19</sup></i> mice. ....	87
3.4.3. The developmental defect of <i>Sell1L<sup>CD19</sup></i> mice is independent of Chop. ....	91
3.4.4. Selective accumulation of the pre-BCR in large pre-B cells. ....	94
3.4.5. The pre-BCR complex is an endogenous Sell1L-Hrd1 ERAD substrate. ....	98
3.4.6. Enhanced ER exit of the pre-BCR in Sell1L-deficient pre-B cells. ....	102
3.4.7. Persistent pre-BCR signaling and pre-B cell cycling in <i>Sell1L<sup>CD19</sup></i> mice. ....	107
3.4.8. Sell1L-Hrd1 ERAD degrades the pre-BCR, not the BCR, complex. ....	107
3.4.9. Pre-BCR ERAD requires BiP but is independent of the unique region of $\lambda 5$ . ....	115
<b>3.5. DISCUSSION</b> .....	<b>116</b>
<b>3.6. ACKNOWLEDGEMENT</b> .....	<b>119</b>
<b>CHAPTER FOUR: B CELL SPECIFIC SEL1L ABLATION PROMOTES PROPAGATION OF COLITOGENIC MICROBIOTA</b> .....	<b>120</b>
<b>4.1 INTRODUCTION</b> .....	<b>121</b>
<b>4.2 MATERIALS AND METHODS</b> .....	<b>122</b>
<b>4.3 RESULTS</b> .....	<b>126</b>
4.3.1. Defect in Gut Associated Lymphoid Tissue (GALT) development and reduced IgA production in in <i>Sell1L<sup>CD19</sup></i> mice. ....	126
4.3.2. <i>Sell1L<sup>CD19</sup></i> mice are more susceptible to DSS induced colitis and the phenotype is transmissible .....	129
4.3.3. Colitogenic microbiota not transmissible to non-littermate wildtype mice.....	133
4.3.4. Colitogenic phenotype is vertically transmissible, only from <i>Sell1L<sup>CD19</sup></i> female mice.....	136
<b>4.4 DISCUSSION</b> .....	<b>140</b>
<b>CHAPTER FIVE: SUMMARY AND FUTURE DIRECTIONS</b> .....	<b>143</b>
<b>REFERENCE</b> .....	<b>147</b>
<b>Curriculum Vitae</b> .....	<b>191</b>

# LIST OF FIGURES

## CHAPTER ONE: INTRODUCTION AND LITERATURE REVIEW

- Figure 1. 1 The unfolded protein response (UPR) in mammals..... 8  
Figure 1. 2 Four major steps of mammalian ER-Associated Degradation (ERAD). ..... 25

## CHAPTER TWO: REVIEW- Endoplasmic reticulum quality control in cancer: Friend or Foe

- Figure 2. 1 Schematic diagrams depicting the roles of IRE1 $\alpha$  in UPR and SEL1L-HRD1 in ERAD. .... 43  
Figure 2. 2 The role of IRE1 $\alpha$ -mediated signaling pathways in cancer pathogenesis. .... 50  
Figure 2. 3 Methods for quantitation of IRE1 $\alpha$  activation and stress levels in the ER. (A and C)..... 65

## CHAPTER THREE: The Sel1L-Hrd1 Endoplasmic Reticulum-Associated Degradation complex manages a key checkpoint in B cell development

- Figure 3. 1 Reduced peripheral B lymphocyte cellularity in *Sel1L*<sup>CD19</sup> mice..... 83  
Figure 3. 2 Generation of *Sel1L*<sup>CD19</sup> mice and the reduction of mature B cells. .... 85  
Figure 3. 3 B cell developmental defects in the absence of Sel1L. .... 88  
Figure 3. 4 Developmental blockade at the transition from the large to small pre-B cells in *Sel1L*<sup>CD19</sup> mice..... 90  
Figure 3. 5 B cell developmental defect in *Sel1L*<sup>CD19</sup> mice is independent of Chop. .... 92  
Figure 3. 6 Accumulation of the pre-BCR complex in Sel1L-deficient large pre-B cells. .... 95  
Figure 3. 7 Accumulation of pre-BCR components in Sel1L-deficient large pre-B cells, .... 97  
Figure 3. 8 The pre-BCR complex is an endogenous Sel1L-Hrd1 ERAD substrate..... 100  
Figure 3. 9 Accumulation and stabilization of pre-BCR components in Sel1L-deficient large pre-B cells. .... 101  
Figure 3. 10 ERAD is indispensable for the termination of pre-BCR signaling in developing B cells..... 103  
Figure 3. 11 Consequence of ERAD deficiency on pre-BCR conformation and complex formation. .... 105  
Figure 3. 12 Sel1L-Hrd1 ERAD degrades the pre-BCR, but not the BCR complex. .... 109  
Figure 3. 13 .Sel1L-Hrd1 ERAD does not control the turnover of BCR, and ERAD-mediated pre-BCR degradation is independent of the unique region of  $\lambda 5$  ..... 111

**Figure 3. 14 Sel1L-Hrd1 ERAD-mediated pre-BCR degradation is BiP-dependent but  $\lambda 5$  unique region-independent. .... 113**

**CHAPTER FOUR: B cell specific Sel1L ablation promotes propagation of colitogenic microbiota**

**Figure 4. 1 Defect in Gut Associated Lymphoid Tissue (GALT) development and reduced IgA production in in *Sel1L<sup>CD19</sup>* mice..... 127**

**Figure 4. 2 *Sel1L<sup>CD19</sup>* and *Sel1L<sup>ff</sup>* mice are highly susceptible to DSS induced colitis. .... 130**

**Figure 4. 3 Elevated immune cell activation in DSS treated *Sel1L<sup>CD19</sup>* and *Sel1L<sup>ff</sup>* mice.. 131**

**Figure 4. 4 Colitogenic microbiota are not transmissible to non-littermate wildtype mice. .... 134**

**Figure 4. 5 Colitogenic phenotype is vertically transmissible, only from *Sel1L<sup>CD19</sup>* female mice..... 137**

**Figure 4. 6 Early exposure to reduced passive secretory IgA promotes susceptibility to colitis..... 139**

# LIST OF TABLES

<b>Table 1 The role of IRE1<math>\alpha</math> in various types of cancer. ....</b>	<b>48</b>
<b>Table 2 Therapeutic interventions in cancer targeting IRE1<math>\alpha</math> and ERAD. ....</b>	<b>61</b>

# **CHAPTER ONE: INTRODUCTION AND LITERATURE REVIEW**

## **1.1 ENDOPLASMIC RETICULUM**

Endoplasmic reticulum (ER) is the largest eukaryotic organelle and is a major site for: (a) protein synthesis and transport, protein folding; (b) lipid metabolism; (c) calcium ( $\text{Ca}^{2+}$ ) storage and release into the cytoplasm (Ma et al., 2001; Matlack et al., 1998; McMaster, 2001; Meldolesi et al., 1998). This multifunctional organelle is defined as an interconnected network with a continuous membrane, which forms abundant membrane contact sites to interact with other cellular organelles such as nucleus, Golgi, mitochondria and endosomes.

The largest domain of the ER flattens around the cell nucleus to form the nuclear envelope. The peripheral ER, which branches out from the outer nuclear envelope and spread throughout the cytoplasm, consists of two structural domains: smooth tubules and rough sheets. There are distinctive morphological differences in these two domains: the outer surfaces of the rough sheets are covered with ribosomal particles (known as rough ER or rER) for the synthesis of nascent peptides into its lumen, whereas smooth ER tubules (known as smooth ER or sER) associate significantly less with ribosome particles (Shibata et al., 2006). While rER and sER are found in all eukaryotic cells (Staehelin, 1997), the ratio of rER and sER depends on the type of cells and their functions. For example, cells that secrete large amounts of protein, such as plasma cells or pancreatic  $\beta$ -cells, are rich in rER, while cells that are highly involved in lipid synthesis or calcium signaling have abundant sER. In addition to their morphological differences, rER and sER perform distinct biological functions.

### **1.1.1. PROTEIN FOLDING AND POST-TRANSLATIONAL MODIFICATIONS**

One of the major function of the rER is to serve as a site for protein synthesis for secreted, luminal and membrane proteins (Jan et al., 2014; Reid et al., 2015). After translation, proteins can be translocated into the ER either by free ribosomes in the cytosol (post-translationally), or

during translation by ER membrane bound ribosomes (co-translationally) (Wickner et al., 2005). Co-translational translocation initiates as a signal recognition particle (SRP) recognizes and binds to the signal peptide on the emerging polypeptide. The binding of SRP stalls translation until the ribosome docks onto the translocon complex, Sec61 (SecY in yeast) complex (Robson et al., 2006). Sec61, a heterotrimeric protein channel, facilitates the translocation of polypeptides across the hydrophobic ER membrane. The active movement of the elongating polypeptide drives the translocation of growing polypeptide into the ER lumen (Park et al., 2012). On the other hand, post-translational translocation does not require SRP. The hydrophobic signal sequence in the nascent polypeptide chain is recognized by receptor proteins of the Sec62/63 complex, which is associated with Sec61 in the ER membrane (Ng et al., 1996). In the luminal side of the ER membrane, the chaperone binding immunoglobulin protein (BiP) binds the polypeptide and pulls it into the ER lumen.

The polypeptide chains fold into their correct three-dimensional conformation and polypeptides are assembled into multi-subunit proteins as soon as it enters the ER lumen (Ellgaard et al., 2003). During folding, proteins undergo transient conformational changes until they achieve the most stable and functional state, known as native state of protein. In order for nascent polypeptides to reach the final native state of protein, an array of ER resident molecular chaperones and enzymes assist folding and modification (Anfinsen et al., 1975). Folding of the polypeptide occurs while it is modified by processes such as N-linked glycosylation or disulfide bond formation.

Nascent polypeptides are glycosylated (N-linked glycosylation) while they are translocated into the ER. An oligosaccharide with 14 sugars is transferred to the side chain of an asparagine residue in the consensus sequence Asn-x-Ser/Thr by a membrane bound

oligosaccharyl transferase (Hubbard et al., 1981; Kornfeld et al., 1985). Some proteins require N-linked glycosylation for proper folding in the ER. After addition of the core oligosaccharide, two glucoses are sequentially removed by glucosidase I and glucosidase II. The calnexin/calreticulin machinery, which specifically recognizes the monoglucosylated glycan tag, interacts with sugar residues in folding intermediates and retains them in the ER (Ellgaard et al., 2003; Hebert et al., 1995). When a third glucose is removed from the glycan, the protein dissociates from calnexin/calreticulin and can leave the ER. If the protein is still unfolded, calnexin/calreticulin promotes their entry/ re-entry into the folding cycles as UDP glucose –glycoprotein glucosyl transferase (UGT) adds another glucose residue to the unfolded protein and goes through another cycle of interaction with calnexin/calreticulin. An unfolded protein undergoes continuous cycles of de- and re-glucosylation, and maintains an affinity for calnexin and calreticulin until it achieves its fully folded state.

As nascent chain emerges from the translocon, it associates with BiP (also known as Grp78), one of the most abundant ER chaperones (Hendershot, L. M., 2004). Interaction with chaperones consumes ATP and the folding of many secretory proteins is inhibited by depletion of ATP (Dorner et al., 1990); hence, the ATP cycle of BiP is tightly linked to its substrate binding (Behnke et al., 2015). BiP consists of two domains; a C-terminal substrate-binding-domain, which allows interaction with hydrophobic regions on nascent chains, and a N-terminal nucleotide-binding-domain with ATPase function (Behnke et al., 2015; Gething, 1999; Otero et al., 2010). In its ATP bound form, the substrate-binding-domain is in its open conformation, allowing binding and release of substrate. However, upon ATP hydrolysis, the lid of the substrate-binding domain closes, thus binding tightly to its substrate (Gething, 1999; Otero et al., 2010). Therefore, BiP has the ability to switch between substrate-bound and substrate free form,

which prevents misfolding and aggregation of the polypeptide and keeps it on the folding path. In addition to translocating the newly synthesized polypeptides into ER lumen and facilitating the folding and assembly of proteins, BiP also plays a critical role in many cellular processes: 1) targeting misfolded proteins for ER-associated degradation (ERAD), 2) regulating calcium homeostasis, and 3) serving as a master regulator of unfolded protein response upon ER stress (Hendershot, L. M., 2004; Lee, A. S., 2005; Li, J. et al., 2006).

In addition, disulfide formation between the side chains of cysteine residues (S-S) further assists protein folding. In the ER, formation, reduction, and isomerization of disulfides are catalyzed by protein disulfide-isomerase (PDI) family. Most PDIs have several thioredoxin-like domains, and catalytic domains with the amino acid motif CXXC (C, Cys; X, any amino acid) which contains two redox-active (Benham, 2012; Kulp et al., 2006). Most redox-active PDIs have oxidase activity and disulfide isomerase activity. When oxidized PDI introduces disulfides to unfolded/reduced substrates, the PDI has open formation (Wang, C. et al., 2013). As the disulfide of the active site transfers to the substrate via a thiol/disulfide reaction, PDI switches to a closed reduced conformation and subsequently releases of oxidized substrate. If an introduced disulfide is non-native, the substrate can bind to a molecule of reduced PDI for isomerization (Wang, C. et al., 2013). This process stabilizes the structure of secreted or membrane surface proteins. For example, the disulfide bond between subunits of immunoglobulins, in its membrane form or secreted form, stabilizes the multimer complex (Elkabetz et al., 2008; Vinci et al., 2004).

Correctly folded proteins are transported to the Golgi and proceed in the secretory pathway, *en route* to the plasma membrane or the extracellular space. However, despite various folding machineries, protein folding is innately prone to error, due to its slow and inefficient process. As a result, a subpopulation of newly synthesized polypeptides fails to reach their native

conformation and become permanently entrapped in the ER (Guerriero et al., 2012), subsequently inducing ER stress. ER stress has been observed during physiological conditions, such as nutrient deprivation and the differentiation of B lymphocytes into plasma cells, as well as in pathological conditions such as diabetes, neurodegeneration, and cancer. In the case of prolonged or overwhelming ER stress, the cell dies by apoptosis. In order to alleviate ER stress, the terminally misfolded or unfolded proteins are dislocated into the cytoplasm and degraded by the ubiquitin/proteasome system, a process known as ERAD. In addition, cells can develop an adaptive mechanism to ER stress, known as unfolded protein response (UPR).

## **1.2 UNFOLDED PROTEIN RESPONSE**

In eukaryotic cells, approximately one third of the newly synthesized membrane and secreted proteins enter the ER in an unfolded state for further modification and folding with the help of a myriad of chaperones and enzymes. Once the proteins reach their native conformation, they are transported to the Golgi complex *en route* to their final destinations. However, protein folding is a highly error-prone process, even with the assistance of many factors. In some cases, proteins which contain disease-associated mutations, such as cystic fibrosis transmembrane conductance regulator (CFTR), are structurally incapable of reaching a native conformation and become trapped in the ER (Guerriero et al., 2012). The accumulation of misfolded proteins in the ER disrupts ER homeostasis and leads to ER stress, which has been strongly associated with human disease pathogenesis (Lin, J. H. et al., 2008). In response to ER stress, eukaryotic cells have developed three pathways of protein quality control to maintain ER homeostasis and cope with the stress for survival: unfolded protein response (UPR), ER-associated degradation (ERAD), and autophagy.

Unlike in yeast cells, where UPR is initiated by single signaling cascade, Ire1p (a type I transmembrane ER protein) (Ron et al., 2007), UPR has evolved in mammalian cells to be governed by three major signaling cascades, Inositol-requiring enzyme 1 $\alpha$  (IRE1 $\alpha$ ), PKR-like ER Kinase (PERK), and activating transcription factor 6 (ATF6) (Figure 1.1). The activated UPR promotes: 1) increased ER folding capacity, 2) enhanced ERAD, and 3) attenuation of global translation to restore ER homeostasis. However, failure to reverse ER stress can induce cellular apoptosis (Walter et al., 2011).

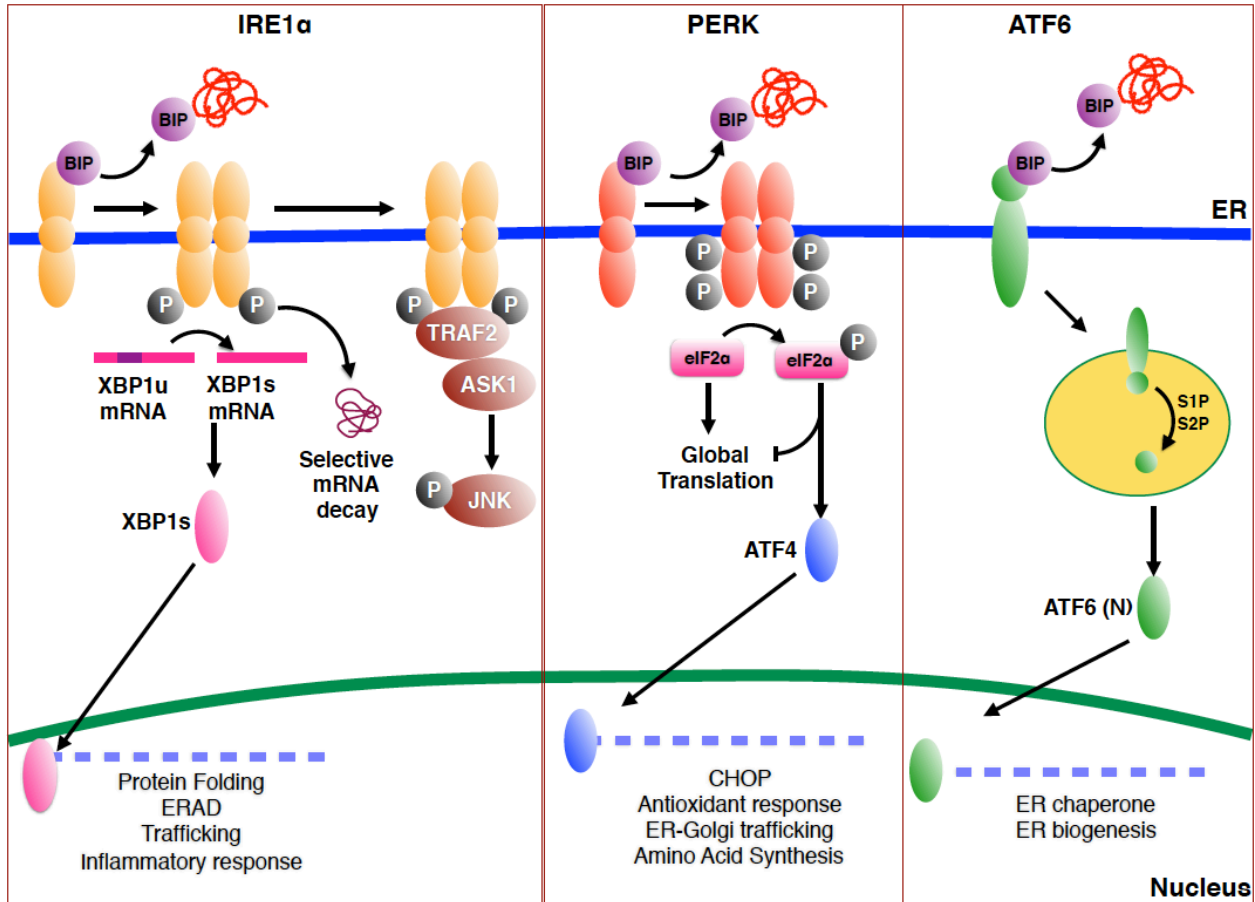


**Figure 1. 1 The unfolded protein response (UPR) in mammals.**

Accumulation of misfolded or unfolded proteins in the ER activates three UPR pathways: IRE1 $\alpha$ , PERK and ATF6. (a) Activated IRE1 $\alpha$  alternatively splices *Xbp1* mRNA to generate Xbp1s which translocates into the nucleus and regulates different genes. Binding of TRAF2 to active IRE1 cytosolic domain activates the JNK-pathway. Furthermore, activated IRE1 $\alpha$  can selectively degrade particular mRNAs by a process called regulated IRE1-dependent decay (RIDD). (b) Active PERK phosphorylates eIF2 $\alpha$  which leads to a global reduction in protein translation and translation of *Atf4* mRNA. (c) Activated ATF6 translocates to the Golgi where it is proteolytically cleaved into an active fragment, which results in the transcription of *Xbp1* mRNA and other genes related to ER chaperones and ER folding.

### 1.2.1. IRE1 PATHWAY

Inositol-requiring enzyme 1 (IRE1) is the most evolutionarily conserved UPR branch among three groups, as it is the only branch identified in lower eukaryotes such as yeast, plants, worms, flies and vertebrates (Cox et al., 1993; Koizumi et al., 2001; Mori, 2009; Shen et al., 2001; Wang, X. Z. et al., 1998). Ire1 is a type I ER-resident transmembrane protein with: 1) an N-terminal luminal dimerization domain, 2) a 20 amino acid transmembrane domain, and 3) a C-terminal cytosolic domain with Ser/Thr kinase and endoribonuclease activity (Liu, C. Y. et al., 2002). It was first identified as an indispensable gene for yeast, *Saccharomyces cerevisiae*, growth on inositol-deficient medium (Nikawa et al., 1992), and later was also found to contain site-specific endonuclease activity to splice bZIP transcription factor, *HAC1* mRNA (Nikawa et al., 1992; Sidrauski et al., 1997). In the budding yeast, *HAC1* is the only known substrate of IRE1 (Nikawa et al., 1992) and the functional homolog *HAC1* in mammals, worms, and flies is the transcription factor X-box binding protein 1 (XBP1) (Calfon et al., 2002; Ryoo et al., 2007; Souid et al., 2007; Yoshida et al., 2001).

In mammalian cells, there are two isoforms of IRE1, IRE1 $\alpha$  and IRE1 $\beta$ , both of which display kinase and RNase domain that is highly conserved to yeast Ire1p (Tirasophon et al., 1998; Wang, X. Z. et al., 1998). IRE1 $\alpha$  is ubiquitously expressed in most tissues with relatively high expression in pancreas and placenta, while IRE1 $\beta$  is selectively expressed in gastrointestinal epithelial cells and lung (Bertolotti et al., 2001; Martino et al., 2013). Hence, global deletion of *IRE1 $\alpha$*  can result in early embryonic lethality (Iwawaki et al., 2009; Zhang, K. et al., 2005), while *IRE1 $\beta$*  deletion disrupts the regulation of airway mucin production (Iwawaki et al., 2009) and increased ER stress and exacerbated colitis induced by dextran sodium sulfate (DSS) (Bertolotti et al., 2001; Kaser et al., 2008).

The mechanism by which IRE1 is activated is still ambiguous. It was first proposed that under homeostatic conditions, BiP binds to the luminal domain of IRE1, which renders IRE1 monomeric and inactive (Bertolotti et al., 2000; Kimata et al., 2003). During stress conditions, BiP dissociates from IRE1, to assist in protein folding. This subsequently results in dimerization, oligomerization, and trans-autophosphorylation of IRE1 which leads to a conformational change that activates the RNase domain. Upon activation, the IRE1 $\alpha$  kinase and RNase domain cleave *Xbp1* mRNA, mediate mRNA decay, or regulate inflammatory/apoptotic pathways. However, studies demonstrated that a mutant IRE1p, lacking the BiP binding region, can still form oligomers and splice *HAC1* mRNA (Kimata et al., 2003; Pincus et al., 2010). Moreover, crystal structure analysis of the IRE1p reveals that the ER luminal domain of IRE1p displays a major histocompatibility complex (MHC)-like groove and mutations in amino acids of the groove or in the dimerization surface abrogate the ability of IRE1p to engage the UPR (Credle et al., 2005). Hence it is more likely that the physical interaction of BiP is a fine-tuning mechanism to ensure IRE1p activation (Pincus et al., 2010).

In contrast to yeast IRE1p, the crystal structure of human IRE1 $\alpha$  revealed that the MHC-like groove might be too narrow to accommodate an unfolded protein peptide (Zhou, J. et al., 2006). Interestingly, mammalian IRE1 $\alpha$  with luminal domain mutants exhibit low affinity for BiP. Moreover, the luminal fragments of mammalian IRE1 $\alpha$  does not interact with unfolded proteins in an in vitro assay (Oikawa et al., 2009). These studies suggest that the regulation of mammalian IRE1 $\alpha$  may actually rely more on the dissociation of BiP and maybe independent of misfolded protein binding. It is likely that the IRE1 sensing mechanisms is not conserved between yeast and mammalian, due to the differences in protein structure within the sensor

domain (Zhou, J. et al., 2006). Unlike IRE1 $\alpha$ , a recent study revealed that mammalian IRE1 $\beta$  is not able to associate with BiP, while it still binds to unfolded proteins (Oikawa et al., 2012).

### ***IRE1-XBP1(HAC1) pathway***

XBP1 is a member of the cAMP response element-binding/activating transcription factor (CREB/ATF) basic region-leucine zipper (bZIP) family (Clauss et al., 1996). It was initially identified during screening for proteins that were bound to X-box, a sequence which regulates transcription of the major human histocompatibility complex (MHC) (Liou et al., 1990). In yeast, activated Ire1p cleaves the 5' and 3' exon-intron splice junction in *HAC1u*, to remove the 252-nucleotide intron (Sidrauski et al., 1997). Then two exon fragments are ligated by yeast tRNA ligase RLG1/TRL1 (Cox et al., 1996; Sidrauski et al., 1996), which yields in a mature HAC1i mRNA. The resulting *HAC1i* mRNA can be translated into a functional transcription factor that translocates to the nucleus and binds to the UPR element (UPRE) (consensus motif: CAGCGTG) and upregulates the entire yeast transcriptome (Mori et al., 1996; Sidrauski et al., 1996).

In metazoans, activated IRE1 excises 26 nucleotides (23 nucleotides in *C. elegans*) intron from the *XBP1u* mRNA. This causes a frame shift to avoid the premature stop codon and leads to the expression of more stable and active form – *Xbp1s* (Calfon et al., 2002; Lee, K. et al., 2002; Yoshida et al., 2001), which translocate into the nucleus and subsequently leads to translation of a 370 amino acid protein, as opposed to the 266 amino acid chain that is translated from *Xbp1u*. While the translation of the *HAC1u* is blocked by a mechanism that is poorly understood (Hetz et al., 2009), it has been demonstrated that *XBP1u* in mammalian can be translated into XBP1u, a protein with a rapid rate of degradation (Chen, X. et al., 2014). Two known substrates of XBP1u are XBP1s (Yoshida et al., 2006) and the active form of ATF6 (Yoshida et al., 2009). By

targeting these two proteins for degradation, XBP1u functions as a negative regulator of the UPR (Chen, X. et al., 2014).

The XBP1s activates an array of genes associated with protein folding, ERAD, lipid synthesis, protein translocation to the ER, and protein secretion (Acosta-Alvear et al., 2007; Lee, A. H., Iwakoshi, & Glimcher, 2003). For example, under ER stress condition, XBP1s induces the transcription of genes encoding ER chaperones, such as BiP, and proteins involved in ERAD, such as Derlin-2 and ER degradation enhancing  $\alpha$ -mannosidase-like protein (EDEEM), to restore ER homeostasis and promote cell survival (Lee, A. H., Iwakoshi, & Glimcher, 2003; Oda et al., 2006; Walter et al., 2011; Yoshida et al., 1998). Furthermore, given its role in upregulating genes involved in protein secretion, XBP1 or IRE1-XBP1 pathway has also been implicated in development and function of many secretory cell types. Studies with either a tissue specific, or whole body knockout of IRE1 or XBP1 have shown that this pathway is necessary for cardiac myogenesis, hepatogenesis, plasma cell differentiation, thyroglobulin production (Christis et al., 2010), as well as proliferation of pancreatic  $\beta$  cells (Lee, A. H. et al., 2005; Masaki et al., 1999; Reimold et al., 2000; Reimold et al., 2001; Xu, T. et al., 2014). Metabolic genes are also upregulated by XBP1s, glycogenesis and lipid metabolism. Taken together, these studies suggest that XBP1 plays a critical role in adapting to restore ER homeostasis and promoting cell survival.

Conversely, XBP1 is also shown to affect pro-apoptotic pathway. One of genes upregulated by XBP1s is  $p58^{IPK}$ , an inhibitor of PERK. It has been demonstrated that high levels of  $p58^{IPK}$  can downregulate the activity of the PERK/eIF2 $\alpha$ /ATF4 pathway (van Huizen et al., 2003), and as upregulation of  $p58^{IPK}$  by XBP1s occurs many hours after PERK activation, it is thought that  $p58^{IPK}$  signaling, under prolonged ER stress, represents the shift from the adaptation

strategy to the cell death phase (Szegezdi et al., 2006). Hence, XBP1s may play dual role in regulating cell survival and death.

### ***Regulated Ire1-dependent decay (RIDD)***

IRE1 mediated splicing of *XBPI* mRNA is a very unique pathway, as even a computational stimulation in mammals, searching for mRNAs with structural and regulatory similarity to XBP1, did not identify other mRNAs (Nekrutenko et al., 2006). However, Weisman group has identified a novel function IRE1 RNase, with broad range of mRNA substrates, using *Drosophila melanogaster* S2 cells (Hollien et al., 2006). It was shown that in response to ER stress induced by dithiothreitol (DTT), a subset of mRNA gets degraded by IRE1 $\alpha$  endonuclease activity, depending on their ER localization and amino acid sequence. Degradation of ER-bound mRNAs may serve to limit protein influx and unfolded protein load into the ER lumen after UPR induction. This process is called Regulated IRE1-Dependent Decays (RIDD). Although, a sequence consensus CUGCAG has been proposed as a common substrate and cleavage motif for both *XBPI* mRNA splicing and RIDD (Oikawa et al., 2010), recent study suggested that IRE1 RNase has different mechanism for cleaving RIDD substrates and *XBPI* mRNA intron. It was shown that IRE1 engaged in RIDD within an IRE1 monomer/dimer whereas catalytically active IRE1 unit engaged in *HAC1/XBPI* mRNA splicing is generated within the IRE1 oligomer (Tam et al., 2014).

RIDD also occurs in mammalian cells (Han et al., 2009; Hollien et al., 2009). Interestingly, while RIDD down-regulates many RNAs by 5-10 fold in *Drosophila* cells, in mammals the magnitude of expression changes was two-fold or even less for many targets (Hollien et al., 2009; Hollien et al., 2006)]. More significantly, the pool of mRNAs degraded by RIDD activity was in a cell-type specific manner (Han et al., 2009; Hollien et al., 2009; Hollien

et al., 2006; So et al., 2012). In addition, it was shown that IRE1 $\alpha$  can cleave premature microRNAs (miRNAs-17, -34a, -96, and -125b), thus regulating translation of pro-apoptotic protein Caspase-2 (Upton et al., 2012).

### ***Matter of life or death (inflammatory response vs apoptosis)***

While IRE1 $\alpha$  promotes cell survival through alleviating ER stress, it can also promote stress-induced apoptosis. Under ER stress, activated IRE1 $\alpha$  also recruits and activates the adaptor protein tumor necrosis factor (TNF) receptor-associated factor 2 (TRAF2) to the ER membrane. This initiates the downstream activation of apoptosis signal-regulating kinase1 (ASK1), which further activates JUN N-terminal kinase (JNK) and p38 MAPK (Nishitoh et al., 2002; Urano et al., 2000). Activated JNK protein leads to phosphorylation of activation protein-1 (AP-1), which in turn transcribes its own inflammatory gene program such as TNF, interleukin (IL-)-8, and granulocyte macrophage colony-stimulating factor (GM-CSF) (Angel et al., 2001; Davis, 2000). Activation of JNK also activates pro-apoptotic Bcl2-interacting mediator of cell death (BIM) protein (Lei et al., 2003) and inhibits the survival protein Bcl-2 (Yamamoto et al., 1999; Yoneda et al., 2001). Once phosphorylated by JNK, BIM translocates to the mitochondrial membrane and promotes mitochondrial apoptosis (Chen, D. et al., 2004). In addition, inhibition of Bcl2 by activated JNK leads to oligomerization of pro-apoptotic proteins Bax and Bak, which are inserted into the mitochondrial membrane and induce mitochondrial apoptosis (Lei et al., 2003).

Moreover, the IRE1-TRAF2 complex recruits I $\kappa$ B kinase (IKK) protein complex, and subsequent phosphorylation of I $\kappa$ B leads to its degradation, upon which releases nuclear factor- $\kappa$ B(NF- $\kappa$ B) for nuclear translocation (Ghosh, S. et al., 2002). Genes targeted by NF- $\kappa$ B include those encoding crucial pro-inflammatory cytokines, such as TNF $\alpha$  and IL-6 (Li, Y. et al., 2005;

Pahl, 1999; Rius et al., 2008; Zhang, K. et al., 2008), and enzymes involved in immunomodulation, such as cyclooxygenase-2 (Hotamisligil et al., 2008; Pahl, 1999).

There are two signaling pathways that control caspase-dependent apoptosis: the intrinsic (or mitochondrial) death pathway and the extrinsic cell (or death receptor) death pathway. Alternatively, in response to ER stress, the IRE1-TRAF2 complex can also interact with pro-caspase-12 (Morishima et al., 2004) and initiate caspase cascade which results in cell apoptosis.

In mice, the pro-caspase-12 is localized on the cytoplasmic side of the ER, and mice and mouse embryonic fibroblasts (MEFs) deficient in caspase-12 were shown to be resistant to ER stress-induced apoptosis, even though their cells still undergo apoptosis in response to other death stimuli such as TNF (Nakagawa et al., 2000). In humans, caspase-4, homologous to mouse caspase-12, is cleaved specifically by ER stress, but not by other apoptotic signals. Knocking down the expression of caspase-4 was shown to decrease ER stress-induced apoptosis (Hitomi et al., 2004; Morishima et al., 2002). However, more recent study showed that caspase-12 does not instigate ER-stress induced apoptosis, but regulates inflammation response (Saleh et al., 2006).

### **1.2.2. PERK PATHWAY**

PERK is a metazoan type I transmembrane protein (Walter et al., 2011). It is composed of an ER stress sensor in the ER lumen, with a kinase domain on its cytosolic fraction. While IRE1 $\alpha$  and PERK share a weak sequence homology in their luminal domains, it has been demonstrated that BiP binds to the luminal domain of both of these proteins (Bertolotti et al., 2000). Hence, under inactive state, PERK retains its monomeric form in a similar manner as IRE1 $\alpha$ . Upon sensing ER stress, BiP dissociates from the N-terminus of PERK and binds to misfolded proteins, while PERK undergoes dimerization/oligomerization and transphosphorylation (Sha et al., 2011). Activated PERK phosphorylates Serine 51 on the  $\alpha$ -

subunit of eukaryotic translation initiation factor-2 (eIF2 $\alpha$ ), attenuating global protein translation to reduce the flux of protein entering the ER and alleviating ER stress (Harding, Zhang, et al., 2000; Harding et al., 1999; Yan et al., 2002). Although the translation of most mRNAs is inhibited in ER-stressed cells, the translation of some mRNAs, such as activating transcription factor 4 (ATF4), is preferentially upregulated under PERK-eIF2 $\alpha$  pathway. Expression of ATF4 subsequently promotes genes involved in amino acid metabolism, anti-oxidant response, and autophagy to cells to manage pleiotropic consequences of protein misfolding in the ER (Harding, Novoa, et al., 2000; Harding et al., 2003; Okada et al., 2002; Scheuner et al., 2001).

A paradox of PERK-peIF2 $\alpha$ -ATF4 pathway is that, while it promotes adaptive pathway to restore ER homeostasis and cell survival, it simultaneously activates pro-apoptotic pathways by inducing transcription factor C/EBP homologous protein (CHOP/GADD153) (Palam et al., 2011). CHOP is a pro-apoptotic bZip transcription factor, which promotes both the transcription of BIM (Puthalakath et al., 2007) and the death receptor family member DR5 (Yamaguchi et al., 2004), while downregulating pro-survival protein BCL-2 expression (McCullough et al., 2001).

PERK signaling is also shown to phosphorylate transcription factor: nuclear factor erythroid 2-related factor 2 (Nrf2) and NF- $\kappa$ B. In unstressed cells, Nrf2 is found in the cytoplasm as a complex with Keap1, the cytoskeletal anchor. Upon ER stress, PERK phosphorylates Nrf2, independent of eIF2 $\alpha$  phosphorylation, and dissociates from Keap1 for nuclear translocation and promotes increased cell survival after chronic ER stress (Cullinan et al., 2003).

Given the dichotomy in outcomes of PERK-eIF2 $\alpha$  pathway, cells have adapted various pathways to regulate PERK activity. First, the cytosolic kinase domain of PERK can be inhibited by the action of the DNAJ family member p58<sup>IPK</sup> (van Huizen et al., 2003; Yan et al., 2002). Inhibition of PERK kinase activity relieves eIF2 $\alpha$  phosphorylation, hence removing the

translational block. In addition to inducing cell death through apoptosis, CHOP also induces growth arrest and DNA damage-inducible 34 (GADD34) as a negative feedback. As ER stress is resolved, through activation of UPR, eIF2 $\alpha$  is dephosphorylated by the GADD34-protein phosphatase1 (PP1) complex and restore mRNA translation (Connor et al., 2001). In addition to inducing GADD34, CHOP expression downregulates during the early time point of ER stress, for example by microRNA (mIR-211) as a pro-survival mechanism (Chitnis et al., 2012).

Furthermore, the UPR stress sensor of mammalian cells have evolved to integrate the intensity of the stimulus and reflect this in the signals they transduce. For example, under a very low-level of UPR activation by stress agents, thapsigargin (TG) or tunicamycin (TM), will activate PERK, ATF6, and splicing of *XBPI* mRNA, while evading terminal UPR by not upregulating CHOP (Rutkowski et al., 2006). Hence, this mechanism also allows cells to avert death as they adapt.

### 1.2.3. ATF6 PATHWAY

ATF6, a third branch of UPR, is a type II transmembrane ER stress sensor. While PERK is uniquely responsible for global inhibition of translation initiation on the cytoplasmic side (Harding et al., 1999), ATF6, along with IRE1 $\alpha$ , is concerned exclusively with activating genes which enhances the ER folding capacity (Kaufman, 2002).

Although there are two *ATF6* genes in the mammalian genome (*ATF6 $\alpha$*  and *ATF6 $\beta$* ), only *ATF6 $\alpha$*  is required to activate UPR gene expression (Wu, J. et al., 2007). Like its counterparts, IRE1 $\alpha$  and PERK, ATF6 remains inactive in ER by binding of BiP on the luminal domain of ATF6 under normal condition. As BiP dissociates from ATF6, upon ER stress, ATF6 is packaged into transport vesicle, COP II complex, and transported to Golgi apparatus (Schindler et al., 2009).

Unlike IRE1 $\alpha$  and PERK, ATF6 activation does not require phosphorylation of a kinase domain. Rather, once in Golgi Apparatus, ATF6 undergoes regulated intramembrane proteolysis (RIP), a process known to regulate sterole response element binding protein (SREBP) (Ye, J. et al., 2000). ATF6 is cleaved by two proteases: first, site-1 protease (S1P) removes the luminal domain and site-2 protease(S2O) subsequently removes the transmembrane anchor (Haze et al., 1999; Ye, J. et al., 2000). This process yields the mature transcription factor ATF6(N) (50 kDa) as a basic Leu zipper (bZIP) transcription factor. The liberated ATF6(N) translocates to the nucleus to activate the transcription of UPR target genes.

Once in the nucleus, ATF6(N) binds to ER stress-response element (ERSE) which consists of a tripartite structure CCAATN9CCACG (Li, M. et al., 2000). This interaction between ATF6(N) and ERSE increases chaperone activity, as well as degradation of unfolded proteins to restore ER homeostasis (Wu, J. et al., 2007; Yamamoto et al., 2007). For example, ATF6 upregulates BiP, protein disulfide isomerase (PDI), and ER degradation-enhancing alpha-mannosidase-like protein 1 (EDEMI), XBP1 and CHOP (Ron et al., 2007).

More recently, accumulating studies have added several ATF6 homologs as new members of UPR initiators: such as CREB-hepatocyte (CREBH), old astrocyte specifically-induced substance (OASIS; also known as CREB3-like-1), and LUMAN/CREB3. CREBH is a hepatocyte-specific bZIP transcription factor which is required for acute phase response, induced either by pro-inflammatory cytokines or ER stress (Zhang, K. et al., 2006). OASIS is induced at the transcriptional level during ER stress, specifically in astrocytes but not in other cell types, and consequently induced BiP and suppressed ER-stress-induced cell death (Kondo et al., 2005). LUMAN/CREB3, unlike CREBH and OASIS, is found in professional antigen presenting cells such as monocytes, and dendritic cells. Cumulative data has shown that LUMAN can induce

ERAD genes to prevent ER-stressed-induced cell death (Asada et al., 2011). Given the differences in activating stimuli, tissue distribution, and response element binding, this branch of UPR pathway may also be involved in regulating cellular physiology.

#### **1.2.4. UPR in immunity**

UPR pathways have been implicated in development and differentiation process in both adaptive and innate immunity. Among all immune cell types, the role of UPR in development and differentiation is the most explicitly studied B cells/plasma cells than any other cells. Due to large secretory demand as part of their function, plasma cells, among many other secretory cells, depend on a well-developed ER, as well as UPR which can quickly facilitate synthesis and trafficking of large volume of immunoglobulin load in ER. Plasma cell differentiation is regulated by the transcription factors interferon regulator factor 4 (*IRF4*), B lymphocyte-induced maturation protein 1 (BLIMP1; encoded by *Prdm1* gene), and its downstream target XBP1. Long-lived plasma cells, which produce large quantities of antibody, express high levels of BLIMP1, IRF4 and XBP1. Short-lived plasmablasts also express high levels of XBP1 but intermediate level of BLIMP1.

Upon stimulation by antigen, BLIMP1 initiates cascades of genes for plasma cell differentiation. First, BLIMP1 represses *MYC1* expression, allowing cells to exit cycling. Second, BLIMP1 also represses genes required for the identity of mature and germinal center B-cells, including BCL-6 and PAX5 (Lin, K. I. et al., 2002; Shaffer et al., 2002). While PAX5 is required for commitment to B cell lineage, it also represses the expression of XBP1, IgH, IgL and the immunoglobulin joining (J) chain (Reimold et al., 1996; Rinkenberger et al., 1996; Shaffer et al., 1997; Singh et al., 1993). Therefore, repression of PAX5 by BLIMP1, in turn, will de-repress expression of the IgH, the IgL, the J chain and XBP1. The induction of *XBPI*, by BLIMP1,

subsequently induces the gene expressions that are involved in ER expansion, degradation of misfolded proteins, trafficking between the endoplasmic reticulum and the Golgi, and targeting of secretory vesicles to the plasma membrane, which are all necessary for high levels of antibody production and secretion. Furthermore, increased *XBPI* expression is also shown to increase cell size, lysosome content, mitochondrial mass and function, ribosome number, and the size of the ER during plasma cell differentiation (Shaffer et al., 2004)

Early studies proposed that XBP1 induction during plasma differentiation is due to increased immunoglobulin synthesis and accumulated unfolded proteins in the ER, (Iwakoshi, Lee, & Glimcher, 2003; Iwakoshi, Lee, Vallabhajosyula, et al., 2003) and the generation of plasma cells is highly impaired in the absence of XBP1. However, subsequent studies have shown that ER expansion precedes the onset of immunoglobulin synthesis (van Anken et al., 2003)]. Additionally, studies using B cell-specific-*XBPI* knockout mice demonstrated that XBP1 is not required for the formation of plasma cells (Hu et al., 2009; Todd et al., 2009). Rather, XBP1 was associated with regulating the development stage after the expression of Syndecan-1 (CD138) and trafficking of plasma cells to the bone marrow (Hu et al., 2009; Todd et al., 2009). More recently, the decrease in immunoglobulin production in XBP1-deficient B cells were explained by hyperactivation of IRE1 $\alpha$ , leading to increased RIDD, and subsequently degrading I $\mu$ -heavy main mRNAs (Benhamron et al., 2014).

Interestingly, the role of two other arms of UPR, ATF6 and PERK, remains unclear. Using *in vitro* system, overexpression of a dominant-negative ATF6, a mutant in differentiating splenic B cells, diminishes IgM secretion and compromises the quality control of IgM synthesis. However, the exact timing and duration of ATF6 $\alpha$  activation during plasma cell differentiation differs from that of IRE1-XBP1 pathway (Gunn et al., 2004). On the contrary, another study

showed ATF6 $\alpha$  is not required for antibody secretion by antigen-activated marginal zone B cells and B1 cells, using ATF6 $\alpha$ -deficient (Aragon et al., 2012). PERK, although partially activated in LPS-stimulated B cells (Gass et al., 2008; Ma et al., 2010), it is not required for antibody secretion (Gass et al., 2008). These data suggest that ATF6 and PERK are not activated due to lack of ER stress. Hence, plasma cells use a “physiological” UPR and not “stress-induced” UPR, by increasing *XBPI* transcription level and splicing upon plasma cell differentiation, while maintaining basal IRE1 $\alpha$  activity.

In addition to plasma cells, IRE1 $\alpha$  activation is seen in the progenitor cells, as early as in pro-B cells (Brunsing et al., 2008; Zhang, K. et al., 2005). While IRE1 $\alpha$  knockout is embryonically lethal, fetal liver cells isolated from *IRE1*<sup>-/-</sup> mice contain CD43<sup>+</sup>B220<sup>+</sup> pro-B cells. However, the number of CD43<sup>-</sup>B220<sup>+</sup> pre-B cells and B220<sup>+</sup>IgM<sup>+</sup> immature B cells are reduced, suggesting a critical role of IRE1 $\alpha$  at pro-B cell stage for further differentiation into the next step (Zhang, K. et al., 2005). IRE1 $\alpha$  activation in pro-B cells might result from the increased secretory demand caused by synthesis of I $\mu$ g heavy chain, since the expression of VDJ recombination factors recombinase activating gene 1 (*rag1*), *rag2*, and terminal deoxynucleotidyl transferase (*TdT*) are downregulated, impairing VDJ rearrangements (Zhang, K. et al., 2005). Of note, *RAG2*<sup>-/-</sup> mice which are reconstituted with eIF2 $\alpha$  mutant fetal liver, exhibit mature splenic B-cell population with normal levels of serum immunoglobulin (Zhang, K. et al., 2005). While, this suggests that PERK-eIF2 $\alpha$  can be dispensable for B cell development and antibody secretion, whether ATF6 is involved in B cell development remains inconclusive. Taken together, further studies are necessary to provide insight into understanding how different UPR signaling branches coordinate their activities in B cell development and functions.

Among three ER stress sensors, studies have demonstrated that IRE1 $\alpha$ -XBP1 arm of the UPR is involved in dendritic cell (DC) function, as well as development. Deletion of *XBPI* in progenitor cells abrogates maturation and decreases DC survival due to increased apoptosis, which was rescued by overexpression of XBP1s (Iwakoshi et al., 2007). Conversely, in another study, XBP1 deletion in CD11c<sup>+</sup> DCs does not affect development; *XBPI* deletion, however leads to IRE1 $\alpha$  hyper-activation, followed by RIDD of components of the MHC I, thus preventing antigen class presentation (Osorio et al., 2014).

UPR also regulates macrophage functions. In macrophage, toll-like receptor 2/4 (TLR2/4) specifically activates IRE1 $\alpha$ -XBP1, which induces expression of pro-inflammatory cytokines such as IL-6, IL-1 $\beta$ , TNF and IFN- $\beta$  (Martinon et al., 2010; Smith et al., 2008; Zeng et al., 2010). In addition, under saturated fatty acid induced ER stress, ATF4 activation induces *Il6* expression in macrophage (Iwasaki et al., 2014). On the contrary, TLR-TRIF signaling in macrophage inhibits translation of *Atf4* mRNA, consequently inhibiting its downstream target CHOP, while leaving PERK-eIF2 $\alpha$  intact (Woo et al., 2009). More interestingly, ER stress-induced activation of IRE1 $\alpha$  can induce *Il-1 $\beta$*  transcription through glycogen synthase kinase 3B (GSK3B), which can simultaneously inhibit *XBPI* and its downstream target *Tnf* (Kim, S. et al., 2015).

Despite the effort to understand the role of UPR in other immune cells, such as T cells and granulocytes, there are only few studies which implicate the role of UPR in these cell development and function. While, IRE1 $\alpha$ -XBP1 pathway is one of the UPR pathways involved in eosinophil development (Bettigole et al., 2015), as well as the terminal differentiation of effector CD8<sup>+</sup> T cells (Kamimura et al., 2008), further studies are still required to understand if other arms of UPR are also involved in these immune cell types' development and functions. The critical role of UPR in immunity is also observed in *C. elegans*. During *C. elegans* development,

Xbp-1 deletion leads to larval lethality in exposure to *Pseudomonas aeruginosa* (Richardson et al., 2010).

In addition, UPR has also been implicated in the function of Paneth cells and goblet cells. Although these two types of cells are not derived specifically from common progenitor cells which produces different kinds of immune cells, these cells still play a significant role in intestinal innate immunity by producing anti-microbial peptides and mucus, respectively (Clevers et al., 2013; Kaser et al., 2008). Mice with intestinal epithelial cell (IEC)-specific *XBPI* deletion results in decreased antimicrobial function, which leads to increased susceptibility to *Listeria monocytogenes*. In addition, hyper-activation of IRE1 $\alpha$ , under *Xbp1* deletion, induces JNK activation, which results in spontaneous enteritis in these mice (Kaser et al., 2008). Recent study also shows that mice, with *Xbp1* deletion specifically in Paneth cells, developed small intestinal enteritis (Adolph et al., 2013). Moreover, IRE1 $\beta$ , which is only expressed in gastrointestinal epithelium and airway, is also required to protect mice against pathogen through regulation of mucin production (Bertolotti et al., 2001; Martino et al., 2013), further validating the importance of UPR in highly secretory epithelial cells.

### **1.3 ENDOPLASMIC RETICULUM ASSOCIATED DEGRADATION (ERAD)**

Proper folding of proteins is monitored and ensured by the quality control machinery. Accumulation of misfolded proteins, which disrupts ER homeostasis, has been associated with altered immune response, metabolic regulation, insulin resistance, tumor growth, and neuron degenerative diseases (Hetz, 2012; Sha et al., 2011). Proteins that are either terminally unfolded or misfolded are degraded via a highly-conserved quality-control machinery known as ER-associated degradation (ERAD), thereby maintaining ER homeostasis. ERAD machinery, a

highly-conserved system through yeast to mammals, proceeds through a tightly coupled steps involving: 1) substrate recognition, 2) substrate retrotranslocation/dislocation across the ER membrane, 3) ubiquitination and 4) degradation by the cytoplasmic 26S proteasome (Figure 1.2).

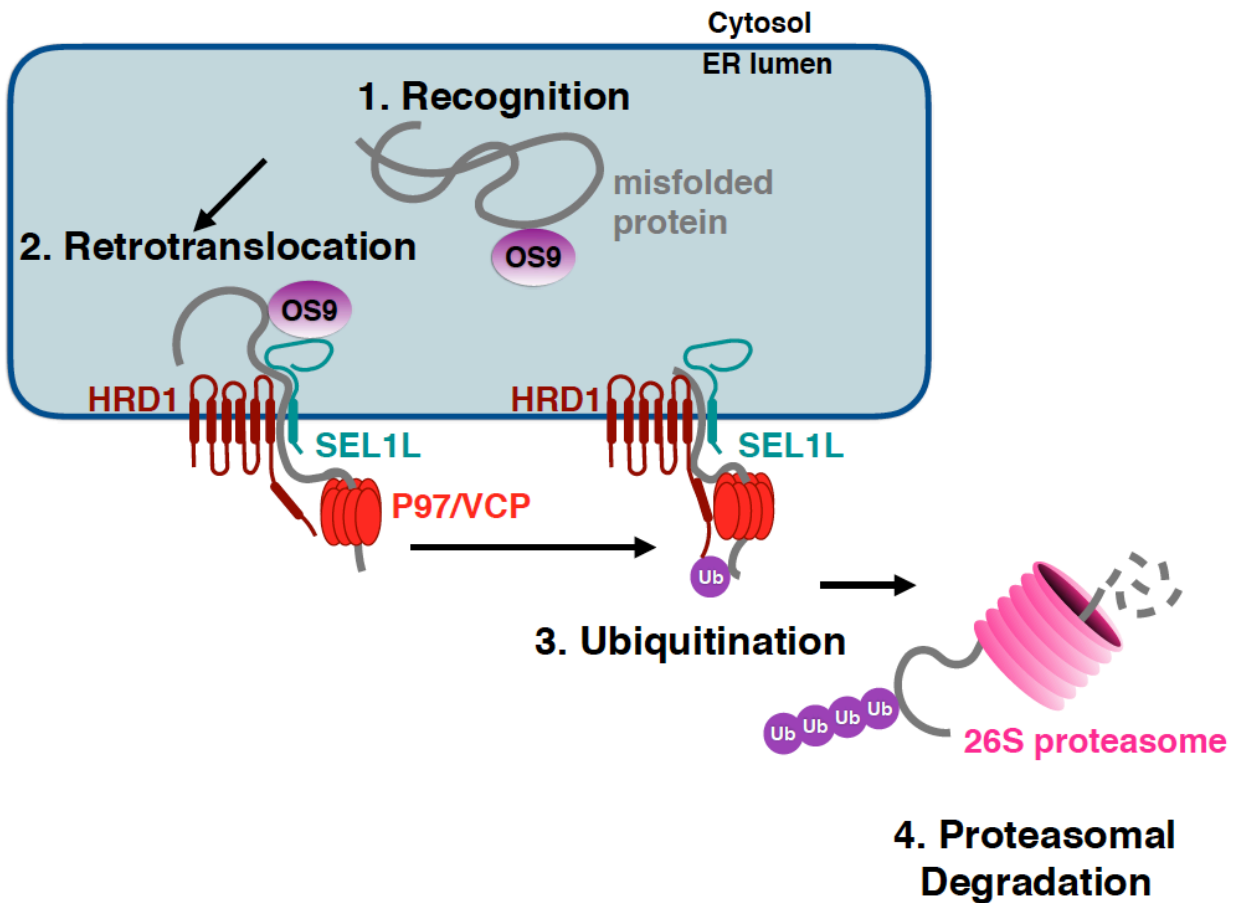


**Figure 1. 2 Four major steps of mammalian ER-Associated Degradation (ERAD).**

(a) Misfolded proteins are recognized by chaperones such as OS9 or BiP. (b) ERAD substrates are targeted to for retrotranslocation by the HRD1-SEL1L ERAD complex. (c) In the cytosol, the retrotranslocated proteins are ubiquitinated by the E3 ligase complex. (d) The ubiquitinated protein substrates are finally degraded by 26S proteasomes.

### 1.3.1. Recognition of misfolded proteins

ERAD substrate are recognized by chaperones or chaperone-like lectins, through their specific glycosylation signatures, which are generated by mannosidases that trim mannose residues from misfolded glycans. Subsequently, these misfolded glycans are further processed by the activity of EDEM1, EDEM3, and Man1c1 to remove terminal mannose residues.

Demanosylated and deglycosylated substrates, which expose alpha-16 mannose, are irreversibly targeted for degradation (Aebi et al., 2010; Hosokawa et al., 2010; Lederkremer, 2009; Olivari et al., 2006; Parodi, 2000; Tremblay et al., 1999).

The substrate recognition factors, osteosarcoma amplified 9 (OS-9) and XTP3B, bind to substrates via their mannose-6-phosphate receptor homology (MRH) domains (Bernasconi et al., 2008; Christianson et al., 2008; Hosokawa et al., 2008). Both OS9 and XTP3B may recognize misfolded regions within a substrate in addition to the glycosylation signature (Hosokawa et al., 2009). These ERAD substrate receptor proteins interact with adaptor proteins, such as SEL1L, at the ER membrane and are subsequently delivered to the retrotranslocation complex (Olzmann et al., 2013).

Alternatively, OS9 and XTP3B may bind non-glycosylated substrates indirectly via an interaction with GRP94 and BiP (Bernasconi et al., 2008; Christianson et al., 2008). The disulfide isomerase (PDIs) participates in retrotranslocation of bacteria and virus antigens (Schelhaas et al., 2007; Tsai, B. et al., 2001). It has also been suggested that non-glycosylated substrates are degraded via post-translational glycosylation (Sato et al., 2012). Despite identifying different mechanisms of recognizing diverse substrates, it is still unclear as to how the cell recognizes and discriminates between terminally misfolded proteins and folding intermediates.

### 1.3.2. Retrotranslocation/dislocation from the ER

Following the substrate recognition, the targeted unfolded proteins, whether they are soluble within the ER lumen or membrane-integrated substrates, are directed to the retrotranslocation channel in order to be degraded by the ubiquitin/proteasome system (UPS) in the cytosol (Christianson et al., 2014). As many ERAD substrates are highly hydrophobic proteins, it is absolutely essential for the processes of dislocation and degradation to be tightly coupled. Extensive studies have identified different candidates which may be responsible for forming a retrotranslocation pore on the ER membrane: Sec61 (Pilon et al., 1997; Wiertz et al., 1996; Zhou, M. et al., 1999), transmembrane protein Derlin-1 (Lilley et al., 2004; Ye, Y. et al., 2004) and E3 ligase HRD1 (Baldrige et al., 2016; Carvalho, P. et al., 2010; Stein et al., 2014). While earlier studies proposed Sec61 as translocon, which mediates the retrotranslocation of the ERAD substrate, more recent studies demonstrated that blockage of Sec61 has no effect on *in vitro* reconstituted substrate retrotranslocation (Wahlman et al., 2007). Derlin1 associates with members of the retrotranslocation complex, such as the E3 ligase HRD1, SEL1L, and deletion of Derlin1, leads to accumulation of misfolded proteins (Mehnert et al., 2014; Ye, Y. et al., 2004). Alternatively, formation of lipid droplets has been suggested as a route for partially folded ERAD substrates to reach the cytosol (Koenig et al., 2014; Ploegh, 2007), as these substrates are too big in size to pass through a protein channel (Olzmann et al., 2013). Once a substrate emerges from the dislocon complex, it is recognized by the cytoplasmic homohexameric ATPase p97/VCP (ATPase Cdc48 in yeast), which provides the driving force for pulling the ERAD substrates through the retrotranslocation complex (Ye, Y. et al., 2001, 2003).

### 1.3.3. Ubiquitination and Degradation in the cytosol

Following translocation of the misfolded substrates, E3 complexes ubiquitinate the misfolded substrates and deliver them to the cytosol for degradation. The general steps of ubiquitination involve: 1) ATP-dependent activation of ubiquitin by an E1 enzyme, 2) followed by transfer of the ubiquitin to an E2-conjugating enzyme, and 3) lastly the transfer of ubiquitin to the substrate, catalyzed by an E3 ligase (Komander et al., 2012). In mammals, ubiquitination of the E3 ligase HRD1 is selectively facilitated by UBC63 (Mueller et al., 2008), an E2 ubiquitin-conjugating enzyme, and Ubc7p in yeast (Bazirgan et al., 2006).

In yeast, two ER-anchored E3s, Hrd1p and Doa10p, are responsible for most substrate ubiquitination in ERAD. Similarly, mammalian homologues of yeast E3 ligase, such as HRD1, gp78, TRC8, RMA1, and TEB4, have been shown to mediate ubiquitination of ERAD substrates. Among dozens of mammalian E3 ligases, HRD1 is a principal ER-resident E3 ligase that forms a complex with the ER-resident SEL1L. HRD1 consists of six transmembrane domains and its cytoplasmic tail has a catalytic RING finger needed for E3 ligase activity, plus a long proline-rich C terminus. SEL1L is a type 1 transmembrane protein with a large luminal domain (Sundaram et al., 1993) As a central adaptor protein of HRD1, SEL1L forms a dimer or oligomer and interacts with the N-terminal domain of HRD1 (Jeong et al., 2016). SEL1L nucleates the whole complex by interacting with multiple ERAD components, including HRD1, Derlin1/2, p97, OS-9, XTP3-B and several housekeeping chaperones (Christianson et al., 2008; Mueller et al., 2008; Mueller et al., 2006). Just like its counterpart Hrd1p in yeast, SEL1L is necessary for the stability of HRD1 (Gardner et al., 2000; Sun et al., 2014). During ERAD process, SEL1L recruits the misfolded proteins by interacting with OS9 and XTP3B. Given these functions of SEL1L, it may not be surprising that when SEL1L expression is reduced, degradation of both luminal and integral membrane substrates is impaired (Sha et al., 2014; Sun et al., 2015). Of note,

a study has shown that SEL1L is heavily glycosylated on its luminal domain, which may be necessary for association with OS9, XTP3B and mannosidase EDEM1 (Cormier et al., 2009).

In addition to its role in retrotranslocation, p97 functions to recruit other cytosolic factors during ERAD. These include deglycosylating enzyme peptide N-glycanase (PNGase), which removes the N-linked glycans from the substrates (Hirsch et al., 2003) and deubiquitination enzymes (DUBs), which were originally proposed to remove ubiquitin on the substrate prior to the insertion to the proteasome (Ernst et al., 2009). Additionally, p97 is known to be involved in fusion of ER and Golgi membrane, cell cycle progression, apoptosis regulation, and ribosome-associated degradation (Zhang, T. et al., 2014).

The subsequent degradation of the ERAD substrates is carried out by the 26S proteasome, a protein complex composed of two parts: two 19S regulatory lid particles and the 20S barrel-shaped catalytic core particles (Bar-Nun et al., 2012). The 20S core complex cleaves the ERAD substrates into a mixture of peptides of varying size, which can be further processed by cytosolic proteases to single amino acids that can be incorporated into newly generated polypeptides (Finley, 2009).

#### **1.3.4. ERAD and Immunity**

Although substantial progress has been made towards identifying the core components of the mammalian ERAD machinery and the mechanism by which the substrates are recognized for retrotranslocation and subsequent degradation, many questions remain unanswered. Furthermore, discoveries from the use of tissue-specific ERAD knockout mouse model have only begun to shed light on the physiological importance of ERAD. While ERAD has been studied as mechanism for clearance of misfolded model substrates such as mutant CFTR, emerging evidences are suggesting novel roles of ERAD in cellular regulation and functions.

Dendritic cells are one of the antigen presenting cells in the mammalian immune system. These cells are responsible for inducing immunity against pathogens, as well as regulating immune tolerance against self-antigens (Kim, S. J. et al., 2013). Once the immature dendritic cells come into contact with a presentable antigen and phagocytose it, they degrade the antigen into small pieces of peptides which becomes present on their cell surface using MHC. Both MHC class I (MHC-I) and MHC class II (MHC-II) traffics through the ER; while MHC-I presents antigen from endogenous sources to CD8<sup>+</sup> T cells, MHC-II presents peptide from exogenous sources to CD4<sup>+</sup> T cells (Adams et al., 2013; Merad et al., 2013; Rudolph et al., 2006). Earlier studies have demonstrated how HRD1 targets the misfolded MHC-I for degradation in the in vitro cultured cell lines (Burr et al., 2011; Huang et al., 2011). Recent study, using dendritic cell-specific HRD1 knockout mice, demonstrated that HRD regulates MHC-II expression by targeting BLIMP1 for proteasomal degradation. Consequently, the HRD1-null dendritic cells failed to prime CD4<sup>+</sup> T cells without affecting CD8<sup>+</sup>T cell activation (Yang, H. et al., 2014).

HRD1 is also shown to regulate immunity induced by T cells. T cell proliferation and activation is initiated by the binding of antigenic peptides present by the MHC to the T-cell receptor (TCR), followed by engagement of the T-cell co-receptor CD28 with its ligand, B7, on APCs. *HRD1* deletion in developing thymocytes resulted in: 1) elevated p27Kip1 protein, an inhibitor of cyclin-dependent kinase (CDK); 2) subsequently inhibited T cell clonal expansion; 3) reduced T-cell numbers and attenuated CD4<sup>+</sup> T cell differentiation into Th1, Th17 and Treg lineages (Xu, Y. et al., 2016). These data further emphasize the unconventional role of ERAD in cellular regulation and functions.

## 1.4 B CELL DEVELOPMENT AND FUNCTION

### 1.4.1. OVERVIEW

The primary purpose of lymphocyte development is to form a functional and diverse antigen receptor repertoire against all potential pathogens. In order to fulfill this goal, the microenvironment, in which B cell develops, provides a sequence of signaling molecules that promotes a series of developmental programs and checkpoints. In mammals, the generation of B lymphocytes occurs primarily in the fetal liver prior to birth, and in the bone marrow during the postnatal life. Bone marrow becomes the major site of B lymphopoiesis, where B cell development occurs in a stepwise process. During B cell lymphopoiesis, progenitor B cells (pro-B) undergo IgH chain gene rearrangement and differentiation, into a large cycling precursor B cell (pre-B), which synthesizes cytoplasmic Ig $\mu$  heavy chain and assemble into pre-B cell receptor (pre-BCR) to express on the cell's surface. The cycling large pre-B cells will, then differentiate into resting small pre-B cells to begin IgL chain gene rearrangement. Subsequently, IgL chain will assemble with  $\mu$ H chains and form IgM, which is expressed on the cell surface as the B cell receptor (BCR). The immature B cells will then undergo extensive selection to eliminate cells with auto-reactivity and subsequently enter the periphery via blood stream. To further enter a mature, functional compartment, immature B cells progress through multiple transitional stages of development in the periphery lymphoid tissues, such as spleen. Mature B cells can be categorized into three subsets: 1) B1 B cells found in the peritoneal and pleural cavity, such as lung and gut epithelia; 2) marginal zone (MZ) B cells found in the splenic marginal sinus, and; 3) follicular mature (FM) B cells, which circulate in most lymphoid tissues. Although B1 B cells and MZ B cells are less abundant in number, these distinct group of B cells generate a burst of short lived plasma cells with fast kinetics (Cerutti et al., 2013; Martin, F. et al., 2001). On the other hand, since FM B cells require interaction with follicular T cells to form

germinal center, it takes up to seven days to become firmly established (Jacob et al., 1991).

Although FM B cell response is not as quick as MZ B cells, it provides highly specific response to protein antigens with higher affinity.

#### **1.4.2. B CELL DEVELOPMENT IN THE BONE MARROW**

B cell development is preceded by the first wave of “primitive hematopoiesis” in the mouse fetus at day E7.5 in the extra-embryonic environment of the yolk sac (Cumano et al., 2001; Foundation for Accountability, 2001; Godin et al., 2002). During this time of the development, fetal-type hemoglobin-expressing erythrocytes, megakaryocytes, platelets, and special types of myeloid cells, such as microglial cells, are generated (Irion et al., 2010; Schulz et al., 2012). Subsequently, during the second and third waves of hematopoiesis at E10.5, first lymphoid cells, among other cell types derived from hematopoietic progenitor cells originating from the aorta-gonad-mesonephros (AGM) region, are generated (Cumano et al., 2001). These sets of lymphoid cells migrate through embryonic blood to the developing fetal liver, omentum, thymus, and bone marrow (Cumano et al., 2007; Ohmura et al., 2001). On day E12.5, second round of hematopoiesis wave, in fetal liver and bone marrow, generates the first-B lymphoid cells and myeloid cell (Tsuneto et al., 2013); and from day E17.5 and onward, bone marrow becomes the major site of the third wave of hematopoiesis, where B cells are continuously generated from pluripotent hematopoietic stem cells (HSCs) throughout life (Hodgson et al., 1990).

While B lymphopoiesis in the fetal liver is transient due to the lack of niches that provide long-term residence, bone marrow provides niches to HSCs, along with long-lived memory T lymphocytes and plasma cells for extended period of time (Tokoyoda et al., 2010). In bone marrows, as HSCs differentiate into multipotent progenitor cells (MPPs), they lose their capacity

to self-renew and become more committed towards one lineage (Bryder et al., 2010). MPPs develop into lymphoid primed multipotent progenitors (LMPP), which has a capacity to produce granulocytes, macrophages and the classically defined lymphoid lineage, but not erythrocytes or megakaryocytes (Adolfsson et al., 2005). These LMPPs express FMS-related tyrosine kinase 3 (FLT3 or CD135) on the cell surface, which upon interaction with FLT5 ligand expressed on bone marrow stromal cells, will give rise to common lymphoid progenitors (CLPs) (Dolence et al., 2014). At this stage, cells are committed to the lymphoid lineage, defined as natural killer, B and T cells. CLPs also express high levels of FLT3, which can induce the expression of IL-7R (Borge et al., 1999). The IL-7R regulates B cell lineage commitment by regulating the expression of transcription factor early B cell factor (EBF) (Dias et al., 2005; Kikuchi et al., 2005). It has been shown that genetic deficiency in the IL-7 pathway in adult mice blocks B-cell development from the CLP stage to the pro-B cell stage (Miller et al., 2002; Peschon et al., 1994; von Freeden-Jeffry et al., 1995), underscoring the indispensable role of IL-7 in B lymphocyte development. However, CLPs do not seem to require IL-7 for survival (Miller et al., 2002). Of note, B cell development in fetal liver does not require IL-7 (Carvalho, T. L. et al., 2001).

CLPs develop into B220<sup>+</sup>CD19<sup>-</sup> pre-pro B cells, where the expression of transcription factor paired box gene 5 (*PAX5*) is initiated. *PAX5*, which is responsible for maintaining B cell lineage commitment, is expressed at about 40 % in B220<sup>+</sup>CD19<sup>-</sup> pre-pro B cells (Rumfelt et al., 2006) and up to 100 % in pro-B cells to mature B cells (Martin, C. H. et al., 2003), but transcriptionally silenced during plasma cell differentiation (Fuxa et al., 2007; Kallies et al., 2007). Since not all cells are committed to the B cell lineage in the pre-pro B cell stage, D to J rearrangements at the IgH locus can also be found even in T cells (Born et al., 1988).

In fully committed CD19<sup>+</sup> pro-B cells, the rearrangement of the immunoglobulin (Ig) gene segments, variable (V), diversity (D) and joining (J), of the IgH locus is initiated, where D<sub>H</sub> to J<sub>H</sub> rearrangements precedes V<sub>H</sub> to D<sub>H</sub>J<sub>H</sub> rearrangements. This site-specific recombination process is regulated by several factors such as IL-7, PAX5, the recombination-activating genes RAG-1 and RAG-2, and TdT (Corfe et al., 2012; Oettinger et al., 1990). When the V<sub>H</sub>D<sub>H</sub>J<sub>H</sub> rearrangements are successful, a  $\mu$ H chain is synthesized and binds to the ER chaperone called BiP and retained in the endoplasmic reticulum (Hendershot, L. M., 1990). The nascent  $\mu$ H chain pairs with surrogate light chains (SLCs), composed of VpreB and  $\lambda$ 5 polypeptides, to form pre-BCR. A pre-BCR associates with the Ig $\alpha$ / $\beta$  heterodimers, which allows the pre-BCR to be deposited on the surface of large pre-B cells. However, studies have shown that a  $\mu$ H chains can be expressed on cell surface, without forming a pre-BCR with SLC, and initiate signals (Galler et al., 2004; Schuh et al., 2003).

The expression of pre-BCR on the surface of the large pre-B cell has multiple purposes. First, signaling by the pre-BCR, in combination with the IL-7R, leads to proliferation burst via phosphoinositide-3 kinase (PI3K) and extracellular signal-regulated kinase (ERK) signaling pathways. Of note, depending on the relative fitness of the pre-BCR, the cycling large pre-B cells enter between two to five rounds of cell divisions and also grow in size (Rolink, A. G. et al., 2000). While it remains unclear whether a ligand is required at all for pre-BCR stimulation, studies have shown that the signaling is initiated either by the pre-BCR crosslinking (Anbazhagan et al., 2013) or by the bone marrow stromal cell galectin-1-(GAL1) (Gauthier et al., 2002). Second, as soon as the pre-BCR signaling is initiated, the recombination of second IgH allele is stopped by down regulating RAG expression (Philippe et al., 2008; Rolink, A. et al., 1995). This allelic exclusion prevents expression of two IgH chains by one B lineage cell

(Martensson, I. L. et al., 2010), and as a consequence, at least 98.5% B lineage cells express only one IgH chain. Moreover, the pre-BCR is believed to signal its own downregulation by silencing transcription of the genes that encode the *VpreB* and  $\lambda 5$  (Karnowski et al., 2008; Parker et al., 2005), thus limiting additional pre-BCR formation. As pre-BCR signaling decreases, large pre-B cells exit the proliferation phase, and become a resting, small pre-B cells.

The pre-BCR termination is followed by upregulation of *RAG 1* and *RAG 2* genes, which initiate  $V_L$ - $J_L$  rearrangement (Wang, Y. H. et al., 2002). However, if the rearrangement of the light chain gene fails, then it attempts to rearrange the light chain genes on the other chromosome. There are two light chain loci, *Ig $\kappa$*  and *Ig $\lambda$*  in both mice and human. During the rearrangement of IgL chain, the IgH chain loci remain closed to maintain allelic exclusion at this locus. The final product of IgL rearrangement assembles with the  $\mu$ H chain and forms BCR on the immature B cells. The complete BCR consists of two heavy chains, 2 light chains, and the subunits of Ig $\alpha$  and Ig $\beta$  (also known as CD79A and CD79B, respectively) (Kurosaki et al., 2010). These immature B cells remain in a resting state and migrate from the bone marrow via blood to the spleen.

In the periphery tissues, the immature B cell requires further maturation in order to become a functionally competent cell; otherwise, upon interaction with antigens, immature B cells respond with cell death, instead of activation and proliferation. While IgM is first expressed by pre-B cells in pre-B cells, IgD expression emerges at the transitional and mature B cells. After functional V-(D)-J recombination of IgH and IgL chain genes, mature naïve IgM<sup>+</sup>IgD<sup>+</sup> B cells co-express IgM and IgD through alternative mRNA splicing. Depending on the stimuli, B cells can be further signaled to produce other isotypes (IgA, IgG and IgE) through alternative transcript splicing and class switch recombination. The primary role of mature B cells in the

humoral component of adaptive immunity is to generate antibody and this unique function of B cells is the basis for the vast majority of successful vaccination strategies. Antibody is produced by two subpopulations of terminally differentiated B cells known as plasmablasts and plasma cells. The cycling, short-lived plasmablasts are differentiated from B1 B cells or MZ B cells through recognition of microbial molecular patterns by TLRs, whereas quiescent, long-lived plasma cells are differentiated from follicular B cells in the germinal center.

### **1.4.3. Pre-BCR**

Pre-BCRs and BCRs are two surface receptors expressed transiently on pre-B cell, and on immature B cells and following B cell subgroups, respectively. These two receptors contain transmembrane form of the Ig $\mu$  heavy chain that is non-covalently associated with a heterodimer Ig $\alpha$  and Ig $\beta$ , and the surrogate light chain (SLC), or the immunoglobulin light chain (IgL).

The SLC of the pre-BCR is composed of  $\lambda 5$  and VpreB, which are homologous to J $\lambda$ -C $\lambda$  and V $\lambda$  of the BCR, respectively (Kudo et al., 1987; Sakaguchi et al., 1986). These two proteins are non-covalently associated with each other and through  $\lambda 5$ , the SLCs form an immunoglobulin-like heterodimer with Ig $\mu$  chain to form pre-BCR, which is expressed transiently on the surface of pre-B cells (Karasuyama et al., 1990; Tsubata et al., 1990). Both the  $\lambda 5$  and the VpreB proteins have immunoglobulin domain and non-immunoglobulin domain, also known as a unique region. In VpreB, the immunoglobulin domain appears to have a V domain-like structure, but lacks the last  $\beta$ -strand ( $\beta 7$ ) of a typical V domain. Unlike  $\lambda 5$ , the unique region on the carboxyl terminal end of VpreB shows no sequence homologies to any other proteins (Melchers et al., 1999). In  $\lambda 5$  the immunoglobulin domain of the has a constant domain-like structure, with strong homologies to  $\lambda L$  chains. Unlike VpreB,  $\lambda 5$  protein has  $\beta 7$ -like strand near C $\lambda 5$ , which has strong homology to J regions of  $\lambda L$  chains. It has been proposed that  $\beta 7$ -like strand of  $\lambda 5$  is non-

covalently associated with the  $\beta$ -strands of VpreB (Melchers, 2005). Interestingly, it was demonstrated that deletion of the  $\beta$ 7 strand in  $\lambda$ 5 protein abrogates the formation of surrogate light chain (Minegishi, Hendershot, et al., 1999), suggesting that the extra  $\beta$ 7 strand is necessary to complement the incomplete VpreB domain to fold and assemble SLCs (Bornemann et al., 1997; Guelpa-Fonlupt et al., 1994; Minegishi, Hendershot, et al., 1999).  $\lambda$ 5 also has unique region, towards the amino terminal region, which shows only marginal sequence homologies to Ig domain structure (Melchers et al., 1993). Interestingly, deletion of both unique regions in VpreB and  $\lambda$ 5 did not abrogate SLC assembly (Minegishi, Hendershot, et al., 1999). However, subsequent studies demonstrated that the unique region of  $\lambda$ 5 retains the preBCR complex in the ER and limiting expression of the surface (Fang et al., 2001; Guloglu et al., 2005; Ohnishi et al., 2003), whereas the function of VpreB unique region still remains elusive.

VpreB can associate with I $\mu$  heavy chain (Seidl et al., 2001), while  $\lambda$ 5 alone cannot (Minegishi, Hendershot, et al., 1999; Seidl et al., 2001). Only when  $\lambda$ 5 is covalently associated with VpreB, does  $\lambda$ 5 form a disulfide bridge with the first constant region (CH1) of an I $\mu$  chain to form the pre-BCR (Melchers, 1999). Only the fully assembled SLC binds to  $\mu$ H chains without any structural defect (Kline et al., 1998; ten Boekel et al., 1997).

The expression of pre-BCR on the surface marks the first checkpoint in B cell development. Using pre-BCR mutant mice, the critical role of pre-BCR as a first checkpoint have been elucidated. Mice have two *VpreB* genes, *VpreB1* and *VpreB2*, and one  *$\lambda$ 5/14.1* gene encoding the SLC components on chromosome 16 (Melchers, 2005). Interestingly, *VpreB1* is expressed in all cells that express  $\lambda$ 5, whereas *VpreB2* is detected in ~30 % of these same cells; also, both gene products are functional and can form an SL chain with  $\lambda$ 5 (Dul et al., 1996)]. In model systems that are lacking either the entire SLC or its components, i.e.  $\lambda$ 5 mutant or *VpreB1*

$Vpreb2^{-/-}$ , exhibit a decrease of precursor B cell expansion, blocking further B cell development in bone marrow (Kitamura, Kudo, et al., 1992; Mundt et al., 2001; Shimizu et al., 2002). Of note, mice with *VpreB1* deletion exhibited partial block of the development at the transition from pro-B to large pre-B, demonstrating that VpreB2 alone is capable of supporting B cell development and give rise to mature B cells in the periphery (Martensson, A. et al., 1999). Furthermore, in the  $\mu$ MT mouse model and in the mouse model with a targeted deletion of  $\lambda 5$ , the efficiency with which cells progress into proliferation pre-B cell compartment is drastically reduced (Kitamura, Kudo, et al., 1992; Kitamura et al., 1991).

While ability to deposit a pre-BCR complex on the cell surface is important for development, accumulating data also suggests regulation pre-BCR signaling cascade is also a crucial factor regulating B cell development. Mice deficient of SLP-65 (also known as BLNK or BASH), an adaptor protein activated by p-Syk, show a partial block at B cell development at the pre-B cell stage. Furthermore, due to a defect of receptor down-regulation, pre-B cells from these mice express large amount of pre-BCR on their surface (Flemming et al., 2003; Jumaa et al., 2003; Jumaa et al., 1999), while temporary extended expression of  $\lambda 5$  leads to delay in the progression of maturing B lineages (Martin, D. A. et al., 2007). Taken together, these data underscore the importance of SLC expression and regulation during early B lineage differentiation.

## **CHAPTER TWO: REVIEW- Endoplasmic reticulum quality control in cancer: Friend or Foe<sup>a</sup>**

Published as: Kim, H.\* , Bhattacharya, A.\* , Qi, L. (2015). Endoplasmic reticulum quality control in cancer: Friend or Foe. *Seminars in cancer biology* 33, 25-33

(\* These authors contributed equally)

<sup>a</sup> Reprinted from *Seminars in cancer biology*,33, Kim, H.\* , Bhattacharya, A.\* , Qi, L. (2015). Endoplasmic reticulum quality control in cancer: Friend or Foe, 25-33,©2015, with permission from Elsevier, <https://doi.org/10.1016/j.semcan.2015.02.003>

## **2.1 ABSTRACT**

Quality control systems in the endoplasmic reticulum (ER) mediated by unfolded protein response (UPR) and endoplasmic reticulum associated degradation (ERAD) ensure cellular function and organismal survival. Recent studies have suggested that ER quality-control systems in cancer cells may serve as a double-edged sword that aids progression as well as prevention of tumor growth in a context-dependent manner. Here we review recent advances in our understanding of the complex relationship between ER proteostasis and cancer pathology, with a focus on the two most conserved ER quality control mechanisms – the IRE1 $\alpha$ -XBP1 pathway of the UPR and SEL1L-HRD1 complex of the ERAD.

## **2.2 INTRODUCTION**

In eukaryotic cells, approximately one third of the total proteome is folded to maturity in the endoplasmic reticulum (ER) prior to transportation to various subcellular or extracellular compartments. A myriad of chaperones, folding enzymes and nascent proteins crowd the molecular environment of the ER lumen all the while maintaining a delicate homeostasis in its protein folding machinery. Various perturbations to this equilibrium, including both physiological and pathological stimuli, can lead to an accumulation of misfolded proteins inside the ER, subjecting the cell to a condition called “ER stress” and activating a series of adaptive mechanisms to alleviate the stress and restore ER homeostasis. These mechanisms consist of two major ER quality control machineries, including unfolded protein response (UPR) and ER-associated degradation (ERAD) (Hetz et al., 2013; Ron et al., 2007; Tsai, Y. C. et al., 2010).

Originally discovered as a response to nutrient depletion, autophagy is a cellular process involved in the lysosomal degradation of cellular components and in the maintenance of energy homeostasis through recycling of amino acids and nutrients (Ryter et al., 2014). Several studies

suggest that autophagy is activated as an adaptive mechanism in cells experiencing ER stress and may play a role in the maintenance of ER homeostasis in cancer (Kroemer et al., 2010; Ogata et al., 2006). However, as the role of autophagy goes beyond the ER (Levine et al., 2008), whether the effect of autophagy in cancer is related to its function in the ER remains to be established. Hence, as the role of autophagy in cancer has recently been extensively reviewed (Gewirtz, 2014; Nagelkerke et al., 2015; Perez-Mancera et al., 2014), it will not be the focus here.

Owing to a high proliferation rate, cancer cells often experience impaired ATP generation, hypoxia, hypoglycemia and specific mutations which may perturb ER homeostasis and trigger the activation of UPR (Tsai, Y. C. et al., 2010). Persistent ER stress often activates pathways that lead to cell death, effectively eliminating cells with a potential to go rogue. On the other hand, tumor cells may hijack the ER quality control machineries to provide survival signals required for neoplasm growth and eventually avoid cell death (Croft et al., 2014). Researchers have considered targeting various components of UPR and ERAD as potent therapeutic means to specifically modulate the survival of cancer cells (Clarke et al., 2014). In this review, we will discuss the involvement of two most highly conserved branches of the ER quality control systems – the IRE1 $\alpha$  signaling pathway of the UPR and the SEL1L-HRD1 complex of the ERAD – in cancer pathogenesis.

### **2.3 The IRE1 $\alpha$ signaling pathway**

IRE1 is a type-1 ER-resident membrane protein with bifunctional cytosolic kinase and endoribonuclease (RNase) domains (Cox et al., 1993; Mori et al., 1993). In mammals, IRE1 exists in two isoforms, IRE1 $\alpha$  (Tirasophon et al., 1998) and IRE1 $\beta$  (Wang, X. Z. et al., 1998). IRE1 $\alpha$  is ubiquitously expressed and global knockout of the gene results in early embryonic lethality (Iwawaki et al., 2009; Zhang, K. et al., 2005). In contrast, IRE1 $\beta$  expression is limited to

the gastrointestinal epithelial cells (Bertolotti et al., 2001) and has no RNase activity towards the classical IRE1 $\alpha$  substrate X-box binding protein 1 (*Xbp1*) mRNA (Tsuru et al., 2013). While IRE1 $\beta$  knockout mice are viable, they are hypersensitive to experimental colitis (Bertolotti et al., 2001), which may be in part due to reduced mucin biosynthesis (Tsuru et al., 2013).

Upon ER stress, IRE1 $\alpha$  undergoes dimerization and/or oligomerization and trans-autophosphorylation, which triggers conformational change and activation of its RNase domain. Activated IRE1 $\alpha$  splices 26 nucleotides from *Xbp1* mRNA, leading to translational frameshift and the generation of an active transcription factor XBP1s. Subsequently, XBP1s enters the nucleus, where it transactivates various target genes, including those involved in protein folding, ERAD, protein trafficking, and lipid biosynthesis (Figure 2.1) (Sha et al., 2011). Additionally, IRE1 $\alpha$  has been shown to degrade a subset of mRNAs via a process called Regulated IRE1-Dependent Decay (RIDD) (Figure 2.1) (Hollien et al., 2009; Hollien et al., 2006; Sakaki et al., 2012; So et al., 2012). Moreover, IRE1 $\alpha$  cleaves some premature microRNAs as a means of regulating apoptosis (Upton et al., 2012) as well as its own mRNA level (Dai et al., 2013; Maurel & Chevet, 2013). The physiological significance of these extra-*Xbp1* activities of IRE1 $\alpha$  in vivo remains poorly characterized.

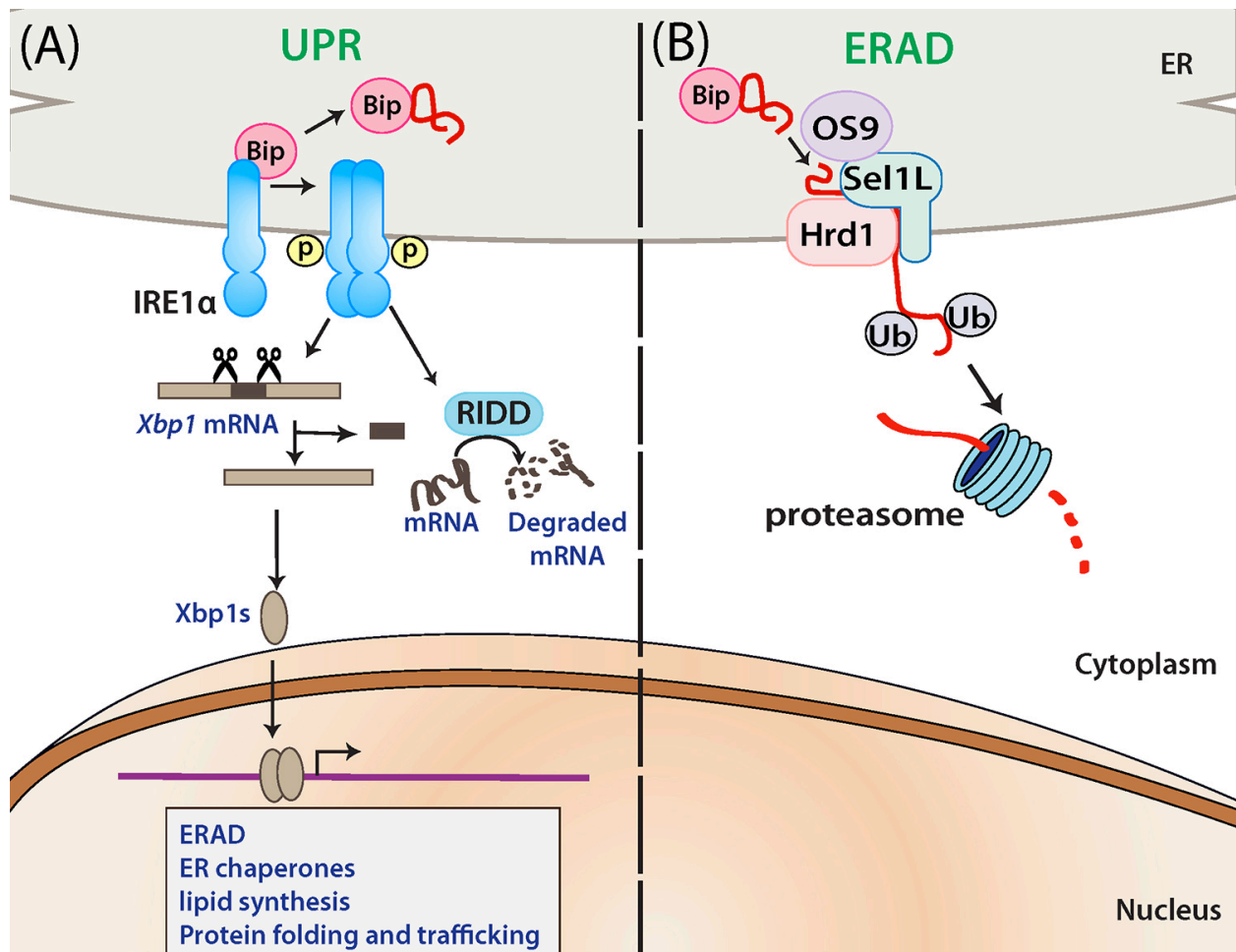


**Figure 2. 1 Schematic diagrams depicting the roles of IRE1 $\alpha$  in UPR and SEL1L-HRD1 in ERAD.**

Upon sensing ER stress, IRE1 $\alpha$  undergoes dimerization or oligomerization, and trans-autophosphorylation, activating its cytosolic endonuclease activity. Subsequently, IRE1 $\alpha$  alternatively splices *Xbp1* mRNA to generate Xbp1s which translocates into the nucleus and regulates different genes. Furthermore, activated IRE1 $\alpha$  can selectively degrade particular mRNAs by a process called regulated IRE1-dependent decay (RIDD). Unlike IRE1 $\alpha$ -XBP1 pathway, physiological significance of other IRE1 $\alpha$  pathways are not well established. (B) Misfolded proteins in the ER lumen are recognized, ubiquitinated and retrotranslocated by the

HRD1-SEL1L ERAD complex to the cytosol for proteasomal degradation. BiP and OS9 may be involved in the recognition of misfolded substrates.

Similar to IRE1 $\alpha$ -deficient mice, global deletion of XBP1 leads to embryonically lethal in mice (Iwawaki et al., 2009; Reimold et al., 2000; Zhang, K. et al., 2005). Using cell type-specific knockout mouse models, studies have demonstrated a critical role of IRE1 $\alpha$ -XBP1 pathway in secretory cells, most notably B cell-derived plasma cells and pancreatic  $\beta$  cells. Mice with B cell-specific *Xbp1* deficiency show a profound defect in plasma cell production, along with decreased levels of antigen-specific immunoglobulin (Reimold et al., 2001; Shaffer et al., 2004; Todd et al., 2009). Intriguingly, IRE1 $\alpha$  deficiency in B cells affects not only plasma cell differentiation, but also early stage of B cell development (Zhang, K. et al., 2005). While VDJ rearrangement occurs normally in XBP1<sup>-/-</sup> B cells (Reimold et al., 2001), this event is severely defective in the pro-B cell stage of IRE1 $\alpha$ <sup>-/-</sup> B cells (Zhang, K. et al., 2005). The authors propose that the cytoplasmic domain of IRE1 $\alpha$  may directly regulate transcriptional activation of genes involved in VDJ recombination such as *Rag1* (recombination-activating gene 1), *Rag2* (recombination-activating gene 2), and *TdT* (terminal deoxynucleotidyl transferase).

*In vitro*, IRE1 $\alpha$  can be activated by glucose in a concentration-dependent manner (Lipson et al., 2006) and hyperactivation of IRE1 $\alpha$  by high glucose may lead to insulin mRNA degradation in pancreatic  $\beta$  cells (Lipson et al., 2008). Intriguingly,  $\beta$  cell-specific deletion of *Xbp1* in mice results in islet atrophy and hyperglycemia associated with impaired  $\beta$  cell proliferation, insulin maturation and secretion at basal level (Lee, A. H. et al., 2011). Moreover, deficiency of XBP1 caused constitutive hyper-activation of IRE1 $\alpha$ , leading to attenuation of *insulin* mRNA via RIDD.

On the other hand, while IRE1 $\alpha$  deficiency in  $\beta$  cells causes disruption in glucose homeostasis and impairs  $\beta$  cell proliferation under metabolic stress, it did not affect pancreatic structure or islet area (Xu, T. et al., 2014). These differential phenotypes observed in  $\beta$  cell

specific IRE1 $\alpha$ - and XBP1- null mice suggest that each component of this pathway may have its own unique function in cellular physiology. Alternatively, it points to a possible role of the unspliced form of XBP1u, whose physiological role awaits further investigation. Taken together these studies highlight the indispensable role of the IRE1 $\alpha$  -XBP1 pathway in ER expansion and survival of highly secretory cell types.

## **2.4 THE ROLE OF IRE1A-XBP1S SIGNALING PATHWAY IN CANCER**

**Table 1** and **Figure 2.2** depict various possible molecular mechanisms underlying the role of IRE1 $\alpha$  in cancer. The role of IRE1 $\alpha$  in cancer is best illustrated and characterized in multiple myeloma (MM). MM is a malignant proliferation of plasma cells in the bone marrow and share phenotypical characteristics with long-lived plasma cells. Due to abundant synthesis of secretory proteins in the ER, MM cells are hypersensitive to the activation of UPR that aggravates as the disease advances (Nakamura et al., 2006). Thus, these cells require a large capacity of folding and disposal in the ER and are particularly sensitive to compounds targeting proteostasis. IRE1 $\alpha$  activation can contribute to cancer progression in several pathways mediated by its substrate XBP1s, which is highly expressed in MM (Bagratuni et al., 2010). Blocking of IRE1 $\alpha$  RNase activity by IRE1 inhibitors such as STF-083010 or 4 $\mu$ 8C or similarly reducing XBP1 expression by proteasome inhibitor or toyocamycin, an XBP1 inhibitor, attenuates the growth of MM cells, via apoptosis (Cross et al., 2012; Lee, A. H., Iwakoshi, Anderson, et al., 2003; Papandreou et al., 2011; Ri et al., 2012). Conversely, forced expression of XBP1s in B cells promotes multiple characteristics of myeloma pathogenesis with lytic bone lesions, plasmacytosis and increased monoclonal antibodies (Carrasco et al., 2007). More than 1000 genes are upregulated in XBP1s-transgenic myeloma cells compared to non-transgenic B cells, including Cyclin D1, Cyclin D2, MAF and MAFB, many of which are known to be involved in

human MM pathogenesis. In clinical studies, human MM patients with high ratio of *Xbp1s* mRNA to *Xbp1u* mRNA have a significantly lower survival rate (Bagratuni et al., 2010).

Collectively, these studies suggest a potential causative role of XBP1s in diseases pathogenesis in some MM patients and implicate IRE1 $\alpha$ -XBP1 axis as a potential therapeutic target in MM.

**Table 1 The role of IRE1 $\alpha$  in various types of cancer.**

Type of cancer	System	Mechanism	Reference
Multiple myeloma	B cell specific Xbp1s transgenic mice and patient samples	Aiding in secretory maturation of plasma cells and resistance to anti-cancer drugs	(Alexanian et al., 2012; Bagratuni et al., 2010; Carrasco et al., 2007; Leung-Hagesteijn et al., 2013)
Triple negative breast cancer	Breast cancer lines and mice with mammary glands injected with tumor cells	High Xbp1s levels aid in sustaining hypoxia (co-localizing with hypoxia markers), promoting angiogenesis and invasion in collaboration with HIF1 $\alpha$ via transcriptional regulation of various genes including VEGFA, PDK1, GLUT1, DDIT4	(Chen, X. et al., 2014)
Colon cancer	Eleven patient primary tumor samples	High levels of Xbp1 expression in colorectal carcinoma and adenoma	(Fujimoto et al., 2007)
Glioma	Human U87 glioma cell line; mouse orthotopic brain model; chick chorio-allantoic membrane	Supports tumor vascularity, blood vessel cooption and invasiveness by promoting pro-angiogenic VEGFA, IL-6, IL-8, IL-1 $\beta$ , and by inhibiting anti-angiogenic thrombospondin1, decorin.	(Auf et al., 2010)
Several cancers	Cell lines	IRE1 $\alpha$ mutations identified in tumor cells are defective in signaling	(Ghosh, R. et al., 2014; Xue et al., 2011)
Liver cancer	Hepatoma HuH7 cell line	Downregulates GPC3 (mediator of tumor growth via canonical Wnt signaling) by RIDD; itself silenced in cancer cells by oncomiR miR-1291	(Maurel, Dejeans, et al., 2013)
Colon cancer	In vivo Xbp1 intestine-specific-null mouse model	Protects against colitis-associated-cancer and Apc-mediated colorectal cancer; depletion of Xbp1 predisposes intestinal epithelium to inflammatory diseases and tumorigenesis	(Niederreiter et al., 2013)
Glioma	Human U87 glioma cell line	Suppresses attachment and migration properties by downregulating RhoA and SPARC (a matrix protein that retards cell cycle, induces cell shape change and promotes invasiveness)	(Dejeans et al., 2012)

**Abbreviations** – Apc: Adenomatous polyposis coli; DDIT4: DNA-damage-inducible transcript 4; GLUT1: Glucose transporter 1; GPC3: Glypican 3; HIF1 $\alpha$ : Hypoxia inducible factor 1 alpha; IL-6, -8, -1 $\beta$ : Interleukin 6, 8, 1beta; IRE1 $\alpha$ : Inositol requiring enzyme 1 alpha; miR: microRNA; PDK1: Phosphoinositide-dependent kinase 1; RIDD: Regulated IRE1-dependent decay; RhoA:

Ras homolog gene family member A; SPARC: Secreted protein acidic and rich in cysteine;  
VEGFA: Vascular endothelial growth factor A; XBP1s: Xbox binding protein 1 spliced

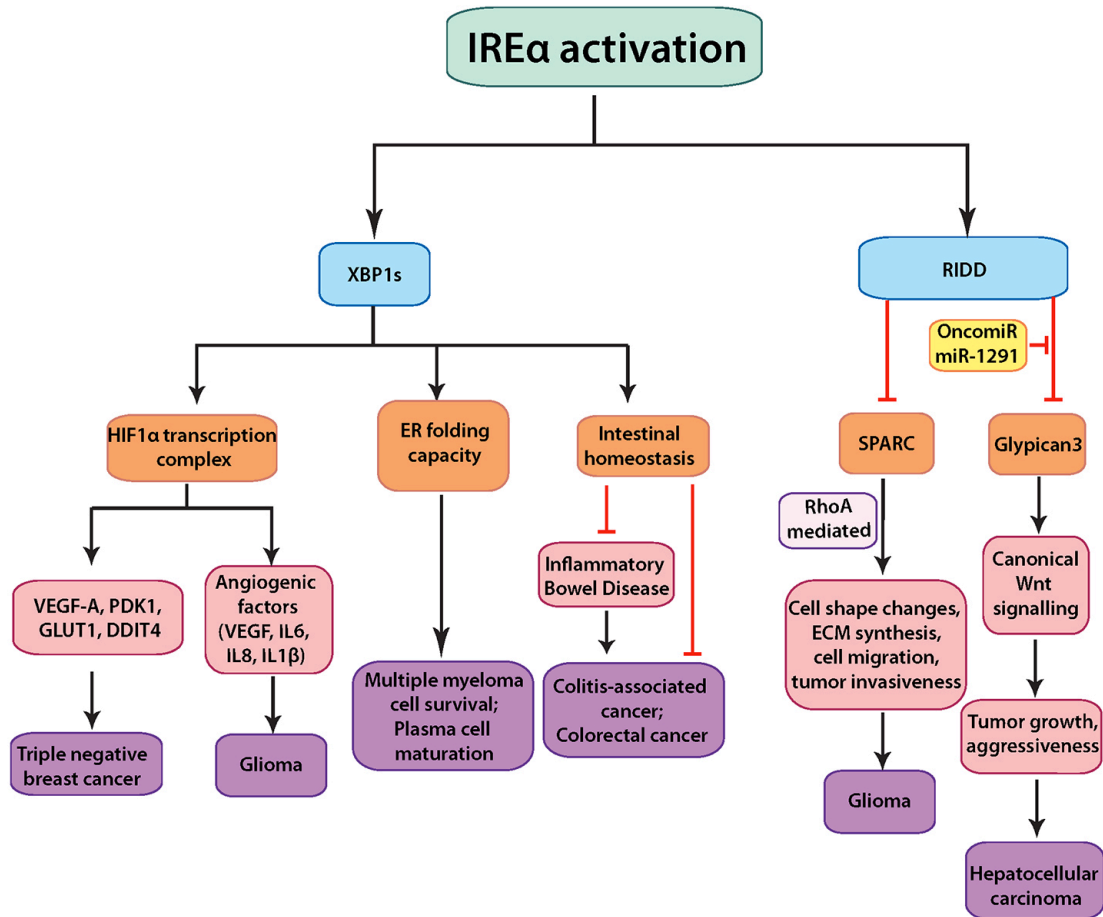


**Figure 2. 2 The role of IRE1 $\alpha$ -mediated signaling pathways in cancer pathogenesis.**

IRE1 $\alpha$  can exert XBP1s–dependent and –independent functions in cancer cells. In XBP1s–dependent pathways, IRE1 $\alpha$  activation can trigger plasma cell maturation and multiple myeloma cell survival; protection from colon cancer via maintenance of intestinal homeostasis; induction of transcription of angiogenic factors and other tumor promoting components in complex formation with HIF1 $\alpha$ , as discovered in gliomas and breast cancer. Via RIDD, IRE1 $\alpha$  downregulates SPARC mRNA thereby preventing RhoA-mediated increase in glioma invasiveness. In liver cancer, the oncogenic miR-1291 downregulates IRE1 $\alpha$ , thereby allowing

its otherwise RIDD substrate Glypican-3-to promote tumor growth and aggressiveness via canonical Wnt signal.

In addition to MM, the IRE1 $\alpha$ -XBP1 signaling pathway has been implicated in colon and breast cancers. As substantial evidence is lacking in most cases, we will discuss these studies in brief. XBP1 has been implicated in colon carcinogenesis in a 2007 clinical study, where higher levels of total *Xbp1* mRNA and protein assessed via RT-PCR and immunohistochemistry, respectively, were found in colorectal polyps, colon carcinomas and colon cancer cell lines as compared to normal and stromal tissue (Fujimoto et al., 2007). It should be pointed out that this study was limited by a small dataset of only 11 patients. In mice, loss of *Xbp1* in the intestinal epithelium leads to an increase in intestinal stem cell numbers in an IRE1 $\alpha$ -dependent manner and Stat3-dependent hyper-proliferation of intestinal epithelial cells (Niederreiter et al., 2013). Consequently, these *Xbp1* null mice are more susceptible to colitis-associated cancer as well as genetic-induced colorectal cancer associated with the mutation of adenomatous polyposis coli (*Apc-min*).

In addition to its role in ER maintenance, the -XBP1 signaling pathway may aid in the regulation of hypoxia in highly aggressive triple-negative breast cancer (TNBC) (Chen, X. et al., 2014). In breast cancer cell lines and xenograft models, loss of *Xbp1* reduces tumor growth and metastasis due to impaired angiogenesis, independently of cell proliferation or apoptosis. CHIP-seq analysis coupled with co-IP experiments reveals that XBP1s and HIF1 $\alpha$  may function within the same transcriptional complex to regulate the expression of genes involved in survival and angiogenesis such as *VEGFA* (vascular endothelial growth factor A), *PDK1* (phosphoinositide-dependent kinase 1), *GLUT1* (glucose trans-porter 1), *DDIT4* (DNA-damage-inducible transcript 4) via the recruitment of RNA polymerase II (Chen, X. et al., 2014). In line with this notion, inhibition of IRE1 $\alpha$  in gliomas reduces the expression of pro-angiogenic genes such as VEGF-A, IL-6, IL-8 and IL-1 $\beta$ , while having an opposite effect on anti-angiogenic factors and matrix

proteins such as *thrombospondin-1*, *decorin* and *osteonectin* (also known as *secreted protein acidic and rich in cysteine* or *SPARC*) (Auf et al., 2010; Drogat et al., 2007). Indeed, in tumors expressing a dominant negative IRE1 $\alpha$ , where IRE1 $\alpha$  transmembrane and luminal domains (aa 1–555) is fused upstream to full length Nck-1 (non-catalytic region of tyrosine kinase adaptor protein 1), there is a marked decrease in angiogenesis, tumor vascular density and growth (Drogat et al., 2007; Nguyen et al., 2004). Taken together, these studies point to a critical role of IRE1 $\alpha$  in mediating hypoxia and angiogenesis in tumor growth and identify the IRE1 $\alpha$ -XBP1s signaling pathway as a candidate for therapeutic intervention in targeting the angiogenic switch in tumor development.

IRE1 $\alpha$  may be involved in cancer pathogenesis via *Xbp1*-independent pathways as well (Figure 2.2). Various RIDD targets have recently been implicated in pathways promoting tumor growth and metastasis. Among them lies SPARC, a matrix-associated protein that retards cell-cycle progression, triggers changes in cell shape and induces synthesis of extracellular matrix, thereby promoting tumor cell invasiveness. (Gaddam et al., 2013; Hollien et al., 2009). IRE1 $\alpha$ , via its RNase activity, leads to a downregulation of *Sparc* mRNA levels as shown in a rat glioma model. Expression of the same aforementioned dominant negative IRE1 $\alpha$  transgene leads to an increase in tumor cell attachment and migration along with upregulation of SPARC and activation of its mediator RhoA, a cytoskeleton regulator protein (Dejeans et al., 2012; Nguyen et al., 2004).

Glypican-3 (GPC3) is an RIDD substrate as its mRNA is cleaved at the 3' UTR by IRE1 $\alpha$  in an ER stress-independent manner (Maurel, Dejeans, et al., 2013). GPC3 is a glycosylphosphatidylinositol (GPI)-anchored membrane protein that has been associated in diseases such as Wilms tumors and Simpson–Golabi–Behmel syndrome, and is highly

overexpressed in hepatoblastoma and hepatocellular carcinoma (HCC) (Jakubovic et al., 2007). GPC3 stimulates canonical Wnt signaling by forming complexes with Wnts, thereby promoting aggressiveness, tumor growth and poor prognosis (Capurro et al., 2005). In the GPC3<sup>high</sup>HCC subgroups, the oncogenic microRNA, miR-1291, is particularly up-regulated (Maurel, Dejeans, et al., 2013). Intriguingly, miR-1291 downregulates IRE1 $\alpha$  via destabilization of its mRNA by targeting a site in its 5' UTR region (Maurel, Dejeans, et al., 2013). This regulatory circuit whereby the oncomiR-1291 downregulates IRE1 $\alpha$  leading to high levels of GPC3 may promote tumor growth and invasiveness via stimulation of canonical Wnt signaling in liver cancer cells.

Finally, IRE1 $\alpha$  has also been implicated in the pathogenesis of several cancers via mechanisms yet unknown. Studies conducted using glioblastoma, serous ovarian cancer and lung adenocarcinoma models have demonstrated that mutations often accrue in IRE1 $\alpha$  genomic loci (Korennykh et al., 2009). We recently analyzed the activities of some cancer-associated IRE1 $\alpha$  mutants (P830L, S769F, L474R, and R635W) and found that a highly conserved proline residue at position 830 (Pro830) is crucial for maintaining IRE1 $\alpha$  structural integrity (Xue et al., 2011). This residue seems to act as a structural linker with adjacent tyrosine (Tyr945) and tryptophan (Trp833) residues to link the kinase and RNase domains of IRE1 $\alpha$ . The P830L mutation destabilizes IRE1 $\alpha$  and renders both kinase and RNase domains of IRE1 $\alpha$  inactive. Similarly, the Ser769Phe mutation abolishes IRE1 $\alpha$  activation and signaling, although the mechanism remains unclear (Xue et al., 2011). It is possible that cancer cells may accrue these loss-of-function IRE1 $\alpha$  mutations to attenuate the pro-apoptotic function of IRE1 $\alpha$  as recently proposed (Ghosh, R. et al., 2014). However, as whether or not IRE1 $\alpha$  signaling exerts pro- and/or anti-apoptotic effects remains controversial (Ghosh, R. et al., 2014; Lu et al., 2014), further investigations are required to delineate physiological significance of IRE1 $\alpha$  mutations in tumorigenesis.

## 2.5 ERAD

ERAD is responsible for the recognition, retrotranslocation and ubiquitination of misfolded proteins in the ER for proteasomal degradation in the cytosol (Olzmann et al., 2013). The ERAD system revolves around transmembrane ubiquitin E3 ligase proteins that connect together the substrate recognition machinery in the ER lumen and the ubiquitin-proteasome system in the cytosol. Failure to remove misfolded ER proteins may result in their accumulation and aggregation, which may account for the pathogenesis of various diseases such as cystic fibrosis,  $\alpha$ 1-antitrypsin deficiency and type-1 diabetes (Chiti et al., 2006; Guerriero et al., 2012).

There are two principle E3 ERAD complexes in yeast (Hrd1p and Doa10p), and at least half a dozen in metazoans, each of which recognizes a subset of misfolded proteins in the ER (Olzmann et al., 2013). Hrd1p forms a complex with Hrd3p in yeast (Gardner et al., 2000; Hampton et al., 1996) and with Suppressor/Enhancer of Lin-12-like (SEL1L) in mammals (Mueller et al., 2008; Mueller et al., 2006). As shown in Figure 1, SEL1L nucleates the HRD1 ERAD complex by interacting with multiple ERAD components such as HRD1, Der-lin1/2, p97, OS9, and E2 enzyme UBC6e (Christianson et al., 2011; Mueller et al., 2008; Mueller et al., 2006). A recent proteomic analysis has implicated both Sel1L-dependent and –independent HRD1-mediated degradation, which may be dictated by substrate topology or accessibility of specific E3 ligases (Christianson et al., 2011).

Physiological importance of SEL1L and HRD1 in vivo is recently emerging. Global deletion of *Sel1L* causes embryonic lethality in mice (Francisco et al., 2010; Sun et al., 2014). In the absence of *Sel1L*, the development of embryonic pancreatic epithelial cell was blocked (Li, S. et al., 2010). Using inducible and adipocyte-specific *Sel1L* -deficient mouse and cell models, we

recently demonstrated that *Sell1L* plays a critical role in the stabilization of HRD1 protein in mammals (Sha et al., 2014; Sun et al., 2014) and that the SEL1L –HRD1 complex plays a critical role in mammalian ERAD, ER homeostasis and survival in vivo (Sun et al., 2014). Acute loss of *Sell1L* in adult mice causes premature lethality and severe pathologies of secretory tissues with striking abnormalities of the ER structure integrity, suggesting a crucial role of *Sell1L* in secretory cell types in particular. On the other hand, loss of *Sell1L* in adipocytes leads to resistance to diet-induced obesity and postprandial hypertriglyceridemia due to the ER retention of lipoprotein lipase (Sha et al., 2014). In addition, variants in the *Sell1L* gene have also been identified in humans with Alzheimer's diseases (Saltini et al., 2006) and SEL1L mutations have been linked to early-onset cerebellar ataxia in canines (Kyostila et al., 2012), pointing to a possible role of SEL1L in maintaining homeostasis in neuronal/glial cells.

Global deletion of HRD1, also known as Synoviolin (encoded by the gene *Syvn1*), also causes embryonic lethality in mice (Yagishita et al., 2005). Loss of *Hrd1* in the liver upregulates the expression of *Nrf2* (nuclear factor (erythroid-derived 2)-like 2) protein and its target genes *Nqo1* (NAD(P)H quinone oxidoreductase 1) and *Gclm* (glutamate-cysteine ligase, modifier subunit). This study demonstrated that *Nrf2* is a substrate for *Hrd1*-mediated proteasomal degradation in the pathogenesis of liver cirrhosis. In this context, ER and oxidative stress response signaling pathways converge as ubiquitination of *Nrf2* by HRD1 results in downregulation of the *Nrf2*-mediated antioxidant response pathway (Wu, T. et al., 2014). In dendritic cells (DC), HRD1 seems to regulate the expression of MHC (major histocompatibility complex) class II via regulating the protein turnover of a key transcriptional repressor BLIMP1 (B lymphocyte induced maturation protein 1) (Yang, H. et al., 2014). Loss of *Hrd1* causes the accumulation of BLIMP1, which represses gene transcription of MHC class II. Dendritic cell

(DC)-specific *Hrd1* knockout mice exhibit splenomegaly with increased B cell numbers and defects in CD4<sup>+</sup> T cell priming in the autoimmune inflammatory response (Yang, H. et al., 2014). How HRD1 mediates the degradation of nuclear transcription factor and whether this function of HRD1 is SEL1L dependent remain to be demonstrated.

## **2.6 THE ROLE OF SEL1L-HRD1 ERAD IN CANCER**

While the role of ERAD in cancer remains largely unknown, SEL1L has been implicated in cancer pathogenesis. Ectopic SEL1L induction in pancreatic cancer cells leads to G1 phase cell cycle arrest via the induction of PTEN – a phosphoinositide-3-phosphatase and well-known tumor suppressor that normally inhibits cell proliferation, growth and motility. High levels of SEL1L in these cells also lead to reduction in invasiveness possibly via negative modulation of genes encoding matrix metalloproteinase inhibitors (Cattaneo et al., 2005). Furthermore, a 2012 study discovered that the SEL1L SNP (rs12435998) shares a close association with the age at diagnosis of pancreatic ductal adenocarcinoma and the patient survival time with or without pancreaticoduodenectomy by analysis of DNA obtained from Caucasian (non-smoker) patients (Liu, Q. et al., 2012).

In the context of colorectal cancer, while basal SEL1L expression level in normal mucosa of the epithelial lining is low, it is elevated in adenoma and adenocarcinoma cells (Ashktorab et al., 2012). Nonetheless, SEL1L expression pattern has so far been found to lack correlation with patient survival and the grade of colon cancer. In an investigation involving glioma stem cell lines and valproic acid (VPA), a histone deacetylase inhibitor, the same group reported that SEL1L downregulation in glioma stem cell lines leads to an impairment of neurosphere size and proliferative rate, while inducing differentiation toward a neuronal fate via Notch1 signaling (Cardano et al., 2011). VPA, a promising therapeutic agent owing to its anti-cancer and

minimally toxic properties, was found to upregulate the expression of SEL1L and other UPR genes in glioma stem cells. siRNA-mediated SEL1L knockdown in these cells negatively affects their self-renewal potential and exacerbates the cytotoxic effects of VPA. These data suggest that SEL1L may protect against VPA-mediated cytotoxicity via the maintenance of cancer stem cell properties (Cattaneo et al., 2014). In addition, correlations between low SEL1L protein levels (detected by mono-clonal antibody staining) and poor prognosis have been reported in breast carcinoma patients (Orlandi et al., 2002). In the context of esophageal cancers, while absent in normal cells, SEL1L is expressed in early neoplastic events and persists in later stages of esophageal cancer (Granelli et al., 2004).

It should be noted that, as most of these studies implicating SEL1L in cancer pathogenesis are based on association studies, interpretation of their findings should proceed with caution. Many outstanding questions remain, for example, what is the mechanism by which SEL1L is involved in tumorigenesis? How do changes in SEL1L level in tumor cells affect ER homeostasis or specific ERAD substrates? How ER homeostasis affects tumorigenesis? Nonetheless, these studies are important because they have opened avenues for more definitive future investigations using animal models. Another well-studied ERAD component is the lectin protein osteosarcoma amplified-9 (OS9) involved in the recognition and recruitment of misfolded glycoprotein or non-glycoproteins to the ERAD complex (Christianson et al., 2008; Hosokawa et al., 2009). Under hypoxic conditions, OS-9-mediated ubiquitination and subsequent degradation of HIF-1 $\alpha$ , aided by an E3 ligase and tumor suppressor von Hippel–Lindau (VHL), is instrumental in downregulating genes that promote cell survival, proliferation, invasion, angiogenesis and metastasis (Baek et al., 2005; Ivan et al., 2001). A recently identified gene CIM (Cancer Invasion or Metastasis-related) also known as ERLEC1 (Endoplasmic Reticulum Lectin-

1) has been found to sequester OS-9 away from the HIF-1 $\alpha$  complex in lung cancer cells, causing HIF-1 $\alpha$  stabilization and accumulation thereby aiding tumor growth and metastasis (Yanagisawa et al., 2010). This study proposes OS9 to be an important link between hypoxia regulation and cancer progression. Intriguingly, we have recently shown that in the absence of Sel1L, OS9 accumulates and is stabilized (Sha et al., 2014; Sun et al., 2014), suggesting that OS9 is a substrate of the Sel1L–Hrd1 ERAD complex. Thus, the Sel1L–Hrd1 ERAD complex, along with other ERAD components (such as VHL) may exert its role in tumorigenesis via the regulation of either ER homeostasis in general or specific substrates such as OS9.

## **2.7 THERAPEUTICS**

Maintaining ER proteostasis assumes high importance in cancer cells due to the increased pressure on protein folding owing to their enhanced metabolic needs, as is evident from the high basal level of expression of UPR markers in these cells. Consequently, developing interventions that aim to sensitize tumor cells to various anti-cancer agents by selectively inhibiting UPR has become a popular therapeutic strategy of late.

A recent endeavor that tested the efficacy of several IRE1 $\alpha$  inhibitors (STF-083010, 3-ethoxy-5,6-dibromosalicylaldehyde, 2-hydroxy-1-naphthaldehyde, toyocamycin, etc.) in a dosage and time-dependent manner on 14 pancreatic cancer cell lines observed growth retardation due to either cell cycle arrest or induced apoptosis as well as reduction in invasiveness demonstrated by soft agar assays and xenograft experiments (Chien et al., 2014). Irestatin is another IRE1 $\alpha$  endonuclease activity inhibitor that has been seen to impair proliferation survival under starvation conditions of malignant myeloma cells (Li, X. et al., 2011). Interestingly, while there is considerable variability in cellular responses to these IRE1 $\alpha$

inhibitors, synergistic effects have been observed when using various drug treatments in combination (Li, X. et al., 2011).

The use of oncolytic virus therapy (OVT) – viral induction of tumor cell lysis and recruitment of the immune system to the infected tissue – is quickly rising in popularity owing to its selectivity in targeting malignancies based on the inherent abnormalities of cancer cells. A major drawback of this approach lies in the great variation in the response rates of these viruses on patients. In this context, a genome-wide RNAi screen recently identified various ER stress pathway components including IRE1 $\alpha$  whose inhibition results in preconditioning of cancer cells to undergo apoptosis when challenged with rhabdoviral oncolysis. This sensitization to caspase-2-dependent cell death occurs via pro-apoptotic factors such as MCL1 (myeloid cell leukemia 1), RAIDD (RIP-Associated ICH1/CED3-Homologous Protein With Death Domain) and PIDD (p53-induced death domain) (Mahoney et al., 2011). This “one-two punch” tactic was validated using primary patient samples and can be useful in combating cancers that are otherwise individually resistant to UPR inhibition and oncolytic viruses.

Other means of sensitizing tumor cells toward proteotoxicity involve drugs that block proteasomal activity. Popular among these are the following – Bortezomib (BTZ) which leads to abrogation of NF- $\kappa$ B function and increases sensitivity to TNF $\alpha$ -related and caspase-mediated apoptosis; Nelfinavir which blocks cellular proteasomal activity by virtue of its own protease property and elicits pro-apoptotic effects marked by amassing of polyubiquitinated proteins (Schonthal, 2012); Eeyarestatin I (EerI) which is an agent that targets p97 (ATPase functioning in the transportation of ubiquitinated proteins) as a means to blocking ERAD (Wang, Q. et al., 2010). Most of these therapeutic agents and their modes of action in combating cancer have been summarized in Table 2.

**Table 2 Therapeutic interventions in cancer targeting IRE1 $\alpha$  and ERAD.**

Agent	Mechanism	Effect	Functional partners	Reference
STF-083010, 3-Ethoxy-5,6-dibromosalicylaldehyde, 2-Hydroxy-1-naphthaldehyde, toyocamycin	IRE1 $\alpha$ inhibition	Growth retardation owing to cell cycle arrest or induced apoptosis; reduction in invasiveness	Synergistic effects seen when used in combination or with gemcitabine/bortezomib	(Chien et al., 2014)
Rhabdovirus	Oncolytic virus therapy plus IRE1 $\alpha$ inhibition	IRE1 $\alpha$ inhibition preconditions cancer cells specifically and sensitizes them to apoptosis following rhabdovirus infection – called “one-two punch”	shRNA or small molecule inhibitors targeting IRE1a	(Mahoney et al., 2011)
Bortezomib	Blocks proteasome activity	Leads to abrogation of NF- $\kappa$ B function, increased sensitivity to apoptosis, thereby pushing tumor cells towards proteotoxicity	TNF $\alpha$ and caspase (mediating apoptosis)	(San Miguel et al., 2008)
Nelfinavir	Blocks proteasome activity	Exercises protease property in blocking cellular proteasome activity and inducing pro-apoptotic effects via amassing polyubiquitinated proteins	BiP/GRP78, CHOP and caspase activation induced	(Gupta et al., 2007)
Eeyarestatin I	Targeting p97 ATPase	Blocks ERAD by preventing de-ubiquitination of ERAD substrates and preferentially pushing cancer cells towards cytotoxicity		(Cross et al., 2009)
Irestatin	IRE1 $\alpha$ RNase inhibitor	Blocks UPR by abrogating XBP1s transcription, thereby impairing proliferation or inhibiting tumor cell survival in oxygen-starvation conditions		(Perry et al., 2012)

**Abbreviations** – BiP: Binding immunoglobulin protein; CHOP: C/EBP homologous protein; ERAD: Endoplasmic reticulum associated degradation; IRE1 $\alpha$ : Inositol requiring enzyme 1 alpha; GRP78: 78 kDa glucose-regulated protein; NF- $\kappa$ B: Nuclear factor kappa-light-chain-enhancer of activated B cells; shRNA: short hairpin ribonucleic acid; TNF $\alpha$ : Tumor necrosis factor alpha; UPR: Unfolded protein response; XBP1s: Xbp binding protein 1 spliced.

A 2003 study by Lee et al. (Lee, A. H., Iwakoshi, Anderson, et al., 2003) using MM cell line demonstrated XBP1 to be an important therapeutic target in cancer as proteasome inhibition in MM cells suppresses IRE1 $\alpha$  RNase activity and XBP1s generation, resulting in an increased apoptotic cell death (Lee, A. H., Iwakoshi, Anderson, et al., 2003). However, despite recent advances in therapy with proteasome inhibitors (e.g. bortezomib, carfilzomib), MM remains incurable due to the resistance to most drugs (Alexanian et al., 2012). A recent study by Leung-Hagesteijn and colleagues demonstrated that silencing of IRE1 $\alpha$  or XBP1 in MM cell lines confers resistance to proteasome inhibitors (Leung-Hagesteijn et al., 2013). The loss of XBP1 in MM results in attenuation of Ig production and a decline in ER stress and ERAD function, which reduces ER stress hypersensitivity in MM cells and accounts for the resistance to proteasomal inhibitors. Moreover, a subset of Xbp1s-negative MM cells lacks plasma cell features (Leung-Hagesteijn et al., 2013). These findings may explain the inability of proteasomal inhibitors in treating MM patients, while underscoring the importance of targeting both the committed plasma cells and the progenitors in therapeutic treatment to overcome drug resistance.

## **2.8 CONCLUSIONS**

When normal cells experience stress due to the accumulation of misfolded proteins inside the ER, a series of adaptive mechanisms are initiated, namely, UPR and ERAD. These pathways lead to global translational attenuation, the induction of specific signaling cascades and clearance of misfolded proteins in the ER aimed at restoring ER homeostasis in the cell. However, in the context of cancer cells, insults from hypoxia, nutrient deprivation, genetic mutations, and enhanced metabolic needs, can often lead to a gross accumulation of faulty proteins in the ER. Therefore, the survival of tumor cells may become especially dependent, relative to normal cells, on the adaptation to stressful conditions via UPR and ERAD. This can potentially serve as the

Achilles heel of cancer cells and allow us to view UPR and ERAD components as lucrative therapeutic targets for cancer treatment. On the other hand, it is the same UPR activation that is wielded by the tumor cells in order to mount resistance to various anti-cancer drugs, thus becoming a double edged sword in tumor cell survival. Linking ER homeostasis to cancer progression may shed further light on the cell-intrinsic processes in tumor cells and allow us to potentially target them specifically over surrounding normal cells. However, most of the studies implicating various UPR and ERAD components in cancer pathogenesis are limited by their model system of study (cell culture based experiments) and small sample sizes (sampling of patient tissue). Hence our understanding of the mechanisms by which the ER quality control systems contribute to the function and survival of cancer cells still warrants further thoughtful investigations.

## **2.9 PERSPECTIVES**

Although ER stress is thought to occur in many physiological and pathological conditions, what is lacking in most studies to date is the direct and accurate measurement of stress levels in the ER. Since cancer cells probably have an elevated protein turnover rate and are likely to accost this enhanced metabolic need by adaption via UPR and ERAD, it is quite possible that the basal levels of various components of ER chaperones are higher in tumor cells. Therefore, the induction or inhibition of these so-called “UPR markers” such as GRP78 and CHOP may not serve as a reliable indicator of ER stress. Thus, although many studies have suggested various possible roles of ER stress and IRE1 $\alpha$  signaling pathways in tumor progression, we still lack a deep and accurate understanding of exactly what the status of ER stress and the contribution of UPR pathways in cancer pathogenesis are. Hence we would like to emphasize the urgent need to directly quantitate ER stress at the level of UPR sensors such as IRE1 $\alpha$  and PERK activation.

Using the phos-tag-based approach, one can directly measure and quantitate the extent of IRE1 $\alpha$  phosphorylation (Figure. 2.3), which we have shown to correlate with the stress level in the ER. As this method is very sensitive and can detect mild ER stress under physiological and pathological conditions (He et al., 2012; Sha et al., 2009; Sha et al., 2014; Sun et al., 2014; Xue et al., 2011; Yang, L. et al., 2010) it promises to provide insights into several outstanding questions, including when and to what extent UPR and IRE1 $\alpha$  are activated during tumorigenesis, how small molecules affect IRE1 $\alpha$  signaling and ER homeostasis in tumors, and how perturbation of ER homeostasis affects the survival and death of cancer cells in humans.

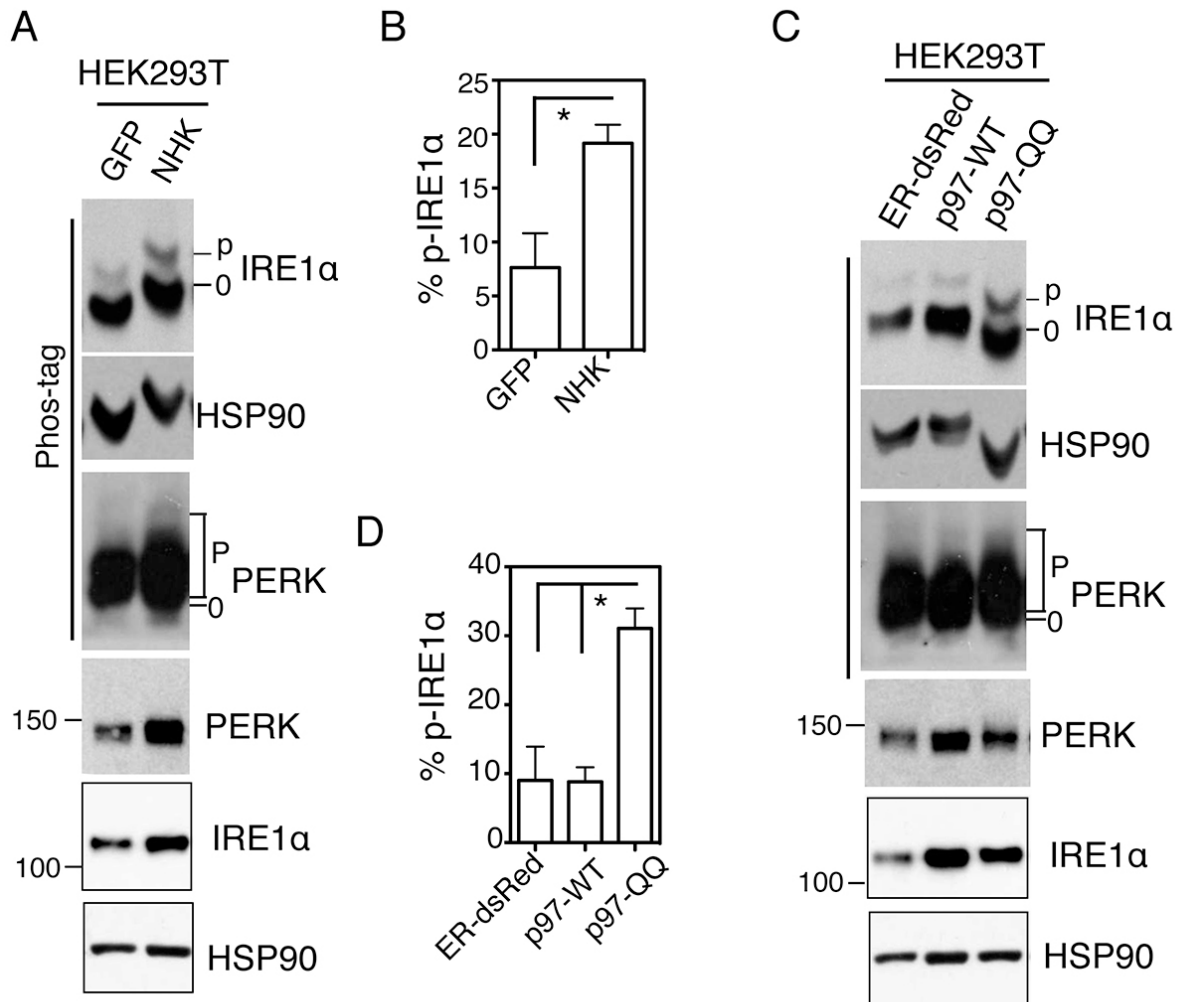


**Figure 2.3 Methods for quantitation of IRE1 $\alpha$  activation and stress levels in the ER. (A and C)**

Immunoblots of IRE1 $\alpha$  and PERK in HEK293T cells transfected with the indicated plasmids for 24 h. NHK, the unfolded form of  $\alpha$ 1-antitrypsin; p97-QQ, dominant negative form of p97-WT. ER-dsRed and GFP, negative control plasmids. HSP90, a position and loading control. (B and D)

Quantitation of percent of phosphorylated IRE1 $\alpha$  in total IRE1 $\alpha$  protein in Phos-tag gels shown in A, C. Values are mean  $\pm$  SEM \*,  $P < 0.05$  using unpaired two-tailed Student's t-test. This data is taken from (Yang, L. et al., 2010)

## **2.10 ACKNOWLEDGEMENTS**

The work in the Qi laboratory has been supported by NIH NIDDKR01DK082582, NIGMS R01GM113188, NIAAA R21AA020351, American Diabetes Association (ADA) 1-12-CD-04 and 7-08-JF-47, Juvenile Diabetes Research Foundation 47-2012-767 and 1-SRA-2014-251-Q-R, American Federation of Aging Research (RAG08061), Cornell University, HHMI International Student (59107338) and AHA Pre-doctoral Fellowship (12PRE9400033).

# **CHAPTER THREE: The Sel1L-Hrd1 Endoplasmic Reticulum-Associated Degradation complex manages a key checkpoint in B cell development<sup>b</sup>**

Published as: Ji, Y.\* , Kim, H.\* , Yang, L., Sha, H., Roman, C., Long, Q., Qi, L. (2016). The Sel1L-Hrd1 endoplasmic reticulum-associated degradation complex manages a key checkpoint in B cell development. *Cell Reports* 16, 2630-2640

(\* These authors contributed equally)

<sup>b</sup> Reprinted from *Cell Reports*, 16, Ji, Y.\* , Kim, H.\* , Yang, L., Sha, H., Roman, C., Long, Q., Qi, L. The Sel1L-Hrd1 Endoplasmic Reticulum-Associated Degradation complex manages a key checkpoint in B cell development, 2630-2640, ©2016, This article is published under the terms of the Creative Commons Attribution-NonCommercial-No Derivatives License (CC BY NC ND). <https://doi.org/10.1016/j.celrep.2016.08.003>

### **3.1. ABSTRACT**

Endoplasmic reticulum (ER)-associated degradation (ERAD) is a principle mechanism that targets ER-associated proteins for proteasomal degradation. Using various knockout mouse models, we demonstrate a critical, cell-intrinsic role of the Sel1L-Hrd1 complex of ERAD in early B cell development. Mechanistically, we show that Sel1L-Hrd1 ERAD selectively recognizes and targets the pre-B cell receptor (pre-BCR), and surprisingly not the BCR, for proteasomal degradation in a BiP-dependent manner. Loss of ERAD in B cell precursors leads to the accumulation of pre-BCR complex, persistent pre-BCR signaling and a severe developmental block at the transition from the large to small pre-B cells. Thus, this study implicates the Sel1L-Hrd1 ERAD as a key regulator of B cell development and reveals the molecular machinery and mechanism underpinning the transient nature of pre-BCR signaling.

### **3.2. INTRODUCTION**

Proteins destined for secretion or membrane localization are folded in the endoplasmic reticulum (ER). Protein folding is a complex, error-prone process that often results in the generation of irreparable misfolded, often toxic, protein by-products. A stringent quality control system is coupled to the protein folding process, ensuring that only correctly folded proteins exit the ER to proceed to their destination. ER-associated degradation (ERAD) is a fundamental quality control mechanism responsible for the recognition and translocation of terminally misfolded or unfolded proteins in the ER, targeting them for cytosolic proteasomal degradation (Olzmann et al., 2013). The use of artificial and disease-related mutant proteins as ERAD substrates has shed important insights into ERAD biology (Guerriero et al., 2012); however, very little is known about the physiological importance of ERAD and the nature of its endogenous substrates.

The best-characterized ERAD machinery in mammals is the highly conserved Sel1L-Hrd1 complex consisting of the E3 ubiquitin ligase Hrd1 and its adaptor protein Sel1L (Olzmann et al., 2013). While many biochemical insights into ERAD biology have been gained from the degradation of model substrates such as immunoglobulin (Ig) light and heavy chains, the current challenges are to identify the nature of its endogenous protein substrates and to delineate the physiological relevance and significance of ERAD in individual cell types in vivo. Using global inducible Sel1L-deficient mouse models, we recently demonstrated that Sel1L is a key component of mammalian Hrd1 ERAD machinery by stabilizing the Hrd1 protein and that the Sel1L-Hrd1 complex plays a critical role in the maintenance of ER homeostasis and animal survival (Sun et al., 2014). While Sel1L-deficient mice are embryonic lethal (Francisco et al., 2010), acute Sel1L deletion in adult mice results in pancreatic atrophy and premature lethality (Sun et al., 2014). In adipocytes, Sel1L deficiency causes intracellular retention of lipoprotein lipase, leading to hypertriglyceridemia (Sha et al., 2014). In the small intestine, epithelial Sel1L-Hrd1 ERAD is indispensable for the secretory function of Paneth cells and protects mice from pathogen-induced ileitis (Sun et al., 2016), whereas in the colon, it modulates the progression of experimental colitis in part via the degradation of IRE1 $\alpha$ , the sensor of unfolded protein response (UPR) (Sun et al., 2015). However, the physiological importance of Sel1L-Hrd1 ERAD in cell differentiation and development has not been explored to date.

To this end, we chose to investigate B cell development as a model system because of its complicated yet well-defined and developmentally restricted expression of many growth factors and cell surface-associated receptors required for different stages of development. We reasoned that ERAD may help reshape the membrane receptor proteome in the B cell development. To reach the antibody-producing mature stage, B cell precursors undergo a stepwise differentiation

process in the bone marrow (BM) from pro-B cells, cycling large pre-B cells, resting small pre-B cells, and finally to immature B cells. This process requires a productive and sequential rearrangement of the genes encoding Ig heavy (IgH) and light (IgL) chains that form B cell receptor (BCR). Prior to IgL chain rearrangement, developing B cells express a set of B lineage-specific genes called  $\lambda 5$  (CD179b) and VpreB (CD179a), which form an IgL-chain-like structure known as the surrogate light chain (SLC) to pair with I $\mu$  heavy chain to form the “pre-BCR” complex (Clark et al., 2014; Herzog et al., 2009; Lee, Y. K. et al., 1999; Pillai et al., 1987).

### 3.3. EXPERIMENTAL PROCEDURES

#### Mice

*Sell1L<sup>ff</sup>* mice on the C57B6/L background have been recently described (Sun et al., 2014) and crossed with CD19 promoter-driven Cre (*CD19-Cre*) mice from Jackson laboratory (B6.129P2(C)-Cd19tm1(cre)Cgn/J) to generate *Sell1L<sup>ff</sup>; CD19-Cre<sup>+</sup> (Sell1L<sup>CD19</sup>)* and control *Sell1L<sup>ff</sup>; CD19-Cre<sup>-</sup> (Sell1L<sup>ff</sup>)* littermates at 1:1 ratio. *Sell1L<sup>ff/+</sup>; CD19-Cre<sup>+</sup> (Sell1L<sup>CD19/+</sup>)* were generated to determine the effect of *Sell1L* heterozygosity and CD19-Cre effect on B cell development. Adult 6-8-week-old mice were used in most studies. In addition, *Sell1L<sup>CD19</sup>* mice were crossed with *Chop<sup>-/-</sup>* mice (B6.129S(Cg)-Ddit3 tm2.1Dron/J, JAX 005530) to generate *Sell1L<sup>fllox/fllox</sup>; CD19Cre<sup>+</sup>; Chop<sup>-/-</sup>* double knockout (*Sell1L<sup>CD19</sup>; Chop<sup>-/-</sup>*) mice. Inducible *Sell1L*-deficient (*Sell1L<sup>ERCre</sup>*) mice expressing estrogen-receptor-Cre (*ER<sup>Cre</sup>*) fusion protein were previously reported (Sun et al., 2014). *Sell1L<sup>ff</sup>; ER<sup>Cre-</sup>* and *Sell1L<sup>ff</sup>; ER<sup>Cre+</sup> (Sell1L<sup>ERCre</sup>)* littermates were used in the study. In all the studies, the CD19-Cre allele were maintained as heterozygous. Mice were housed under specific pathogen-free conditions. Cohoused age- and gender-matched littermates were used in all in vivo experiments. All animals were sacrificed by cervical

dislocation and tissues were immediately harvested. Frozen tissues were stored at  $-80^{\circ}\text{C}$ . All animal procedures have been approved by the Cornell IACUC (#2007-0051).

### **Flow Cytometry, Intracellular Staining, BrdU Labeling and Antibodies**

Flow cytometric analysis of peripheral immune cells was performed as we previously described (Ji et al., 2014; Ji et al., 2012). To isolate BM, tibia and femurs were isolated from mice and BM was flushed using cold PBS supplemented with 5 % FBS and 1 % penicillin/streptomycin. The RBCs in the BM suspension was lysed and resuspended in cold PBS with 5 % FBS and 1 % penicillin/streptomycin. Cell suspension were stained with either 1:100 or 1:200 fluorochrome- or biotin conjugated antibodies against CD4 (GK1.5), CD8 (YTS169), Gr-1 (RB6-8C5), CD11b (M1/70), CD45 (30-F11), CD19 (6D5), CD138 (281-2), CD2 (RM2-5), IgM (RMM-1), IgD (11-26c.2a), CD5 (53-7.3),  $\lambda$ 5 (C-16), CD43 (1B11), VpreB (R3), Pre-BCR (SL156), streptavidin-PerCP and isotype control antibodies (BioLegend or BD Biosciences). Annexin V, propidium iodide and 7-AAD were purchased from BioLegend and used per manufacturer's protocol. Secondary antibodies such as anti-IgG FITC and anti-Ig $\mu$  PE were from Jackson Immunoresearch. For intracellular staining, cells were fixed and permeabilized by BD Cytotfix/Cytoperm Fixation/Permeabilization Kit per manufacturer's protocol. For BrdU labeling, mice were injected intraperitoneally with BrdU (Sigma, 0.6 mg/10 g of body weight) at 2 hours prior to sacrifice. BM cells were collected, labeled with cell surface antibodies, and then fixed in cold 70 % ethanol at  $-20^{\circ}\text{C}$  overnight. The samples were washed and digested with Dnase I (Roche, 50 U/ml in 4.2 Mm MgCl<sub>2</sub> and 150 mM NaCl) at room temperature for 30 min. The rest of the procedures were performed as the regular flow cytometric analysis using BrdU-FITC (PRB-1, BD Biosciences). Samples were analyzed using BD LSR cell analyzer at the Flow

Cytometry Core Facility at Cornell University. Data were analyzed using the CellQuest software (BD Biosciences) and Flowjo (Flowjo.com).

### **Western Blot and Antibodies**

Preparation of whole cell lysates, endoH treatment and Western blots were performed as previously described (Sha et al., 2014; Sun et al., 2015). Antibodies used in this study were: IgG-peroxidase (goat, 1:5,000) from Sigma; HSP90 (rabbit, 1:6,000), BiP (goat, 1:1,000) and  $\alpha$ -Tubulin (mouse, 1:2000) from Santa Cruz; Sel1L (rabbit, 1:2,000) and OS9 (rabbit, 1:10,000) from Abcam; phospho-Syk and Syk (rabbit, 1:1000) from Cell Signaling; and Calnexin (rabbit, 1:8,000) from Assay Design. Hrd1-specific antibody (rabbit, 1:200) was from Dr. Richard Wojcikiewicz at SUNY Upstate Medical University (Pearce et al., 2007). Antibodies for Bag6 (rabbit, 1:10,000) and H2A (rabbit, 1:10,000) were a kind gift from Dr. Yihong Ye (NIDDK). Band density was quantitated using the Image Lab software on the ChemiDOC XRS+ system (Bio-Rad). Protein levels were normalized to HSP90 and are presented as mean  $\pm$  SEM unless otherwise specified.

### **Fluorescence-activated cell sorting (FACS)**

Tibia and femurs from 6-week-old Sel1LCD19 and *Sel1L<sup>ff</sup>* mice were flushed with cold PBS (5 % FBS, 1 % penicillin/streptomycin) using a 10 ml syringe and 27 G1/2 needle (BD) to obtain single cell suspension. Red blood cells were lysed using RBC lysis buffer (Biolegend) and washed with cold PBS and filtered through 70  $\mu$ m cell strainer. Cells were incubated with 1:100 dilution of PE anti-mouse CD43, FITC anti-mouse IgM, APC-Cy7 anti-mouse B220 and APC anti-mouse CD2 in cold PBS with 5 % FBS for 40 min at 4 °C. Cells were washed and resuspended in cold PBS and sorted using BD FACS Aria at Flow Cytometry Core Facility at Cornell University. Pro-, large pre-, small pre-, immature and mature B were gated as

B220<sup>low</sup>/IgM<sup>-</sup>/CD43<sup>high</sup>/CD2<sup>-</sup>, B220<sup>low</sup>/IgM<sup>-</sup>/CD43<sup>low</sup>/CD2<sup>-</sup>, B220<sup>low</sup>/IgM<sup>-</sup>/CD2<sup>+</sup>, B220<sup>low</sup>/IgM<sup>+</sup> and B220<sup>high</sup>/IgM<sup>+</sup> cells, respectively.

### **Isolation of peritoneal lymphocytes**

Using scissors and forceps, the outer skin of the peritoneum of an anesthetized mouse was gently pulled back to expose the inner skin lining the peritoneal cavity. Using 27 G needle, 5 ml of ice cold PBS (5 % FBS) was injected into the peritoneal cavity followed by gentle massaging to dislodge any attached cells. The fluid in the peritoneum was collected using a 25 G needle attached to a 5 ml syringe. The collected cell suspension was centrifuged at 1500 rpm for 5 min.

### **Magnetic-activated cell sorting (MACS) and Plasma cell differentiation**

Splenocytes were prepared as described above. Isolated splenocytes were stained with biotin-conjugated anti-mouse CD19 antibody (1:100, BioLegend) for 40 min at 4 °C. Cells were washed and incubated with Streptavidin particle plus (1:6, BD Biosciences) for 30 min at 4 °C. CD19<sup>+</sup> B cells were purified using Cell Separation Magnet (BD Biosciences) per manufacturer's protocol. Purified B cells were diluted in RPMI-1640 medium supplemented with 10 % heat-inactivated FBS, 50 µM β- mercaptoethanol (Invitrogen), 1 % penicillin/streptomycin (Cellgro), and 2 mM L-glutamine (Cellgro). To induce plasma cell differentiation, purified B cells were stimulated with 20 µg/ml LPS and 20 ng/ml murine IL-4 (PeproTech) for 72 hours. Cell lines Pre-B cell line 70Z/3 (ATCC) was cultured in complete RPMI supplemented with 10 % heat-inactivated FBS (Life Technologies), 50 µM β-mercaptoethanol (Invitrogen), 100 U/ml penicillin and 100 µg/ml streptomycin (Cellgro), 2 mM L-glutamine (Cellgro), 1 mM sodium pyruvate and 10 mM HEPES.

## **Generation of Sel1L knockdown cells**

Sel1L RNAi knockdown targeting sequences #7

(gatccccGGTTACTGTGGCTAGAAAttcaagagaTTCTAGCCACAGTGTAACCtttttc, tcgagaaaaGGTTACTGTGGCTAGAAAtctcttgaaTTCTAGCCACAGTGTAACCggg) was cloned into pSuper/retro vector (H1 promoter) as previously described (Sha et al., 2009). Control RNAi were against the firefly luciferase.

## **Design of Hrd1 single guide RNA (sgRNA) expression Vectors**

We used the lentiviral CRISPR-Cas9 vector from the Zhang lab, plentiCRISPRv2, which expresses the sgRNA, Cas9 protein, and puromycin resistance gene from one vector. The HRD1 sgRNA was designed using the Zhang lab software available at <http://crispr.mit.edu>. According to Zhang lab protocols ([http://www.genome-engineering.org/crispr/?page\\_id=23](http://www.genome-engineering.org/crispr/?page_id=23)), DNA oligonucleotides for the sgRNA and reverse complement sequence plus adapters needed for ligation were synthesized and cloned into the plentiCRISPRv2 vector (HRD1: forward, 5'-CACCGATCCATGCGGCATGTCGGGC-3', reverse, 5'-AAACGCCCGACATGCCGCATGGATC-3'). Empty p-lentiCRISPRv2 plasmid was used as control vector.

## **Generation of CRISPR-based knockout cell lines**

To generate lentiviral supernatant, HEK293T cells were co-transfected with 2.3 µg of sgRNA plasmid or empty plentiCRISPRv2 plasmid, 1.5 µg of pRRE(gag-pol), 0.8 µg of pVSV-G and 0.57 µg of pREV in the presence of the Lipofectamine 2000 (Life Technologies), per manufacturer's instruction. After 12 h of incubation, the medium was changed to fresh virus collecting medium (DMEM supplemented with 10 % heat-inactivated FBS and 1 % penicillin/streptomycin). 24 hours later, the viral supernatant was harvested by centrifugation and

ready to be used or stored in -80 °C. To generate knockout cells, 70Z/3 cells were infected with HRD1 CRISPR-Cas9 or empty CRISPR-Cas9 lentiviruses. 24 hours post infection, cells were selected with 2 µg/ml puromycin (Invitrogen) for 1 week. The knockout efficiency was assessed by Western blot analysis.

### **Retroviral transduction**

The cDNAs encoding mouse WT or JC λ5 (Fang et al., 2001) were subcloned into the murine retroviral vector MiG where GFP was linked to the cDNA of interest via an internal ribosome entry site. JC λ5, the truncated form of λ5, was generated by deletion of its non-Ig region and replaced with the leader sequence of conventional light chain λ1 (Guloglu et al., 2006). Retroviruses were made by co-transfection of HEK293 cells with MiG plasmids plus pψECO-encoding ecotropic helper functions. Viral supernatants and polybrene (5 µg/ml) were added to cells and incubated for 2 h, followed by centrifugation at 2500 rpm at 37 °C for 1 h. 2 weeks after infection, cells were sorted using BD FACS Aria for stably-transfected GFP+ cells for further analysis.

### **Crosslink of pre-BCR**

Pre-BCR signaling was activated as previously reported (Guo et al., 2000). 70Z/3 cells were directly stimulated with 10 µg/ml of anti-µ antibody (Jackson ImmunoResearch) at 37 °C for the indicated times. Stimulation was stopped by the addition of ice-cold PBS. Cells were pelleted by centrifugation and stored in -80 °C for Western blot analysis.

### **In vitro IL-7 stimulation**

This experiment was performed as previously described (Flemming et al., 2003). For quantitation of the absolute number, MACS sorted BM CD19<sup>+</sup> B cells were cultured in RPMI-1640 medium supplemented with 10 % heat-inactivated FBS, 50 µM β-mercaptoethanol

(Invitrogen), 1 % penicillin/streptomycin (Cellgro), and 2 mM L-glutamine (Cellgro). Purified recombinant IL-7 (PeproTech) was used at 0.1–10 ng/ml for 4 days. Viable cells were counted and normalized to the day 0 cell number. For BrdU incorporation, FACS sorted BM pro-/large pre- B cells were treated with IL-7 (1 ng/ml) for 2 days, and BrdU (10  $\mu$ M) was added for 4 hours followed by Flow Cytometric analysis as described above.

### **Immunoprecipitation (IP) using primary antibodies**

Cells were incubated with 20 mM Nethylmaleimide (NEM) in PBS for 10 min on ice, snap frozen and lysed in lysis buffer (150 mM NaCl, 1 mM EDTA, 50 mM Tris HCl, pH 7.5, protease inhibitor cocktail (Sigma), 10 mM NEM) supplemented with either 1 % Triton X-100 or 1 % Nonidet P-40 (NP-40) and incubated on ice for 15 min. Cells were centrifuged at 12,000 g at 4 °C for 10 min, supernatants were collected and protein concentration was measured using the Bradford assay. The protein lysates were incubated with Ig $\mu$ -agarose beads (Sigma) for 16 h at 4 °C with gentle rocking, followed by five washes with IP lysis buffer. Immunocomplexes were eluted by boiling for 5 min in 5X SDS sample buffer followed by SDS-PAGE and Western blot analysis.

### **Sucrose gradient sedimentation analysis**

Confluent WT and Sel1L KD 70z/3 cells in two 10 cm plates were either mock-treated or treated with 20  $\mu$ g/ml lipopolysaccharide (LPS) for 18 hours, harvested and lysed in 0.5 ml of 1 % NP40 lysis buffer as described in Immunoprecipitation. Extracts were centrifuged through 20~50 % sucrose gradients in 150 mM NaCl, 1 mM EDTA, 50 mM Tris HCl pH 7.5 and protease inhibitor, which were prepared freshly by layering higher to lower density sucrose fractions in 5 % increments in poly-allomer tubes of 11x3x60 mm (Beckman Coulter, Brea, CA, USA). Extracts were centrifuged at 58,000 rpm for 14.5 hours at 4 °C using an SW 60 Ti rotor

(Beckman Coulter). Each 4 ml gradient was divided evenly into 8 fractions (500  $\mu$ l each), and aliquots of fractions 2-8 were subjected to Western blot analyses under denaturing or non-denaturing conditions.

### **SDS-PAGE**

In non-reducing SDS-PAGE, cells were lysed in 1 % NP-40 lysis buffer without DTT. The cell lysates, diluted immunoprecipitates and sucrose gradient sedimentations were prepared in non-denaturing sample buffer with a final concentration of 20 mM pH 6.8 Tris-Cl, 0.8 % SDS, 0.04 % bromophenol blue and 4 % glycerol. Samples were heated for 10 min at 50 °C followed by Western blot analysis. For denaturing SDS-PAGE, the lysates were prepared in 5x denaturing sample buffer (50 mM Tris HCl pH 6.8, 0.2 % SDS, 10 % glycerol, 0.28 M  $\beta$ -mercaptoethanol and 0.01 % bromophenyl blue) and boiled for 5 min prior to be separated on a SDS-PAGE gel. In vitro drug treatment Cycloheximide (Millipore, Billerica, MA) was dissolved in ethanol and used at 50  $\mu$ g/ml. MG132 (Millipore, Billerica, MA) was dissolved in DMSO and used at 25  $\mu$ M. LPS was purchased from Sigma and was dissolved in water and used at 20  $\mu$ g/ml.

### **BiP depletion**

SubAB and its catalytic inactive mutant form SubA<sub>A272</sub>B were used as previously described (Paton et al., 2006). 70Z/3 cells treated with either 0.5  $\mu$ g/ml SubA<sub>A272</sub>B or SubAB WT for 45 min were lysed in lysis buffer (150 mM NaCl, 1 mM EDTA, 50 mM Tris-HCl pH 8.0, protease inhibitor and protein phosphatase inhibitor and 10 mM NEM) supplemented with 1 % NP-40. A total of ~3 mg protein lysates was pre-cleared with agarose A (Invitrogen) and then incubated with Ig $\mu$ -agarose overnight at 4 °C with gentle rocking. Ig $\mu$ -precipitated complexes were washed and eluted by boiling for 5 min in SDS sample buffer, and subjected to Western blot analyses. To measure Ig $\mu$  decay following BiP depletion, 70Z/3 cells were treated by 50

µg/ml cycloheximide together with either 0.5 µg/ml SubA<sub>A272</sub>B or SubAB WT for 0, 30, 60 and 90 min. Cells were subsequently lysed in lysis buffer supplemented with 1 % NP-40. Protein levels of Igµ at different time points were measured by Western blot.

### **Pulse labeling**

For each time point,  $4 \times 10^6$  70z/3 cells were used. Cells were cultured in cysteine and methionine-free medium (Invitrogen, 21013024) at 37 °C for 15 min and metabolically labeled with 50 µCi (35S)-cysteine and methionine (EasyTag, PerkinElmer) at 37 °C for 10 min. The pulse was stopped by the addition of 5 volumes of cold chase medium (pre-B cell culture medium supplemented with 5 mM L-methionine (Sigma, M5308) and 5 mM L-cystine (Sigma, C7352)). Then cells were quickly spin down and cultured in chase medium at 37 °C for the indicated times. Cells were spin down, snap-frozen and lysed in 0.5 % NP40 lysis buffer with NEM (20 mM). Lysates were subjected to immunoprecipitation with Igµ-agarose beads (Sigma). Immunoprecipitates were separated on a 7 % SDS-PAGE gel, which was subsequently incubated with the neutralizing buffer (30 % (v/v) methanol in PBS) for 10 min followed by the enhancer buffer (1.5 M sodium salicylate (Sigma) in 30 % (v/v) methanol) for 10 min. The gel was then dried at 80 °C for 2 hours using a gel drier (Model 583, Bio-Rad) and then subjected to autoradiography with X-film (Kodak).

### **Limited proteolysis**

WT and Sel1L KD 70z/3 cells were harvested and lysed in lysis buffer containing 50 mM HEPES (pH=7.5), 150 mM NaCl and 1 % Triton-X 100 on ice for 15 min. Aliquots of the lysates were mixed with varying concentrations of trypsin and incubated on ice for 30 min. Reaction was quenched by the addition of 5x SDS sample buffer and immediately heated at 95 °C for 10 min followed by Western blot analysis. NP-40 solubility assay WT and Sel1L KD 70z/3 cells

were incubated in the absence or presence of 20 µg/ml LPS for 18 hours, harvested, and incubated in NP-40 lysis buffer (50 mM Tris·HCl pH 8.0, 0.5 % NP-40, 150 mM NaCl, 5 mM MgCl<sub>2</sub>) supplemented with protease inhibitor (Sigma). The lysate was centrifuged at 12,000 g for 10 min and the supernatant was collected as NP-40S fraction. The pellet was then resuspended in 1x SDS sample buffer with the volume normalized to initial cell weight, heated at 95 °C for 30 min and collected as the NP-40P fraction. The NP-40S and NP-40P fractions were subsequently analyzed by Western blot.

### **Immunofluorescent staining**

For pre-B cell line staining, OP9 cells were plated on poly-L-Lysine-coated coverslips in 24-well plates and incubated for 18 hours at 37 °C. OP9 cells were washed with PBS and co-incubated with either WT or Hrd1<sup>-/-</sup> 70/z3 cells in RPMI supplemented with 10 % heat-inactivated FBS (Sigma), 50 µM β-mercaptoethanol (Invitrogen), 100 U/ml penicillin/streptomycin (Cellgro), and 2 mM L-glutamine for additional 3 hours. Cells were washed with PBS, fixed with 4 % paraformaldehyde for 20 min and permeabilized with 1 % Triton X-100 in PBS for 5 min. Cells were blocked with 5 % normal donkey serum in 0.1 % Triton X-100/PBS, then labeled with PE-anti-Igµ (1:100, Goat, Jackson ImmunoResearch) and a polyclonal rabbit anti-rodent BiP antiserum (Lee, Y. K. et al., 1999) (1:500, from Dr. Linda Hendershot at St. Jude Children's Research Hospital) for 18 hours at 4 °C. After two washes, cells were incubated with donkey anti-rabbit AF488 for 1 hour at room temperature, washed and mounted with Vectashield Mounting Medium with DAPI (Vector Laboratories, Inc.). For spleen staining, spleens were collected from *SellL<sup>ff</sup>* and *SellL<sup>CD19</sup>* mice and fixed in 10 % neutral buffered formalin overnight at 4 °C, followed by washing in 15 % sucrose overnight at 4 °C. Spleens were embedded in optical cutting temperature (O.C.T.) compound (Tissue-Tek) and

sectioned at 8  $\mu$ m thickness with a cryostat and mounted on the Superfrost slides (FISHER). The sections were washed twice with PBS and blocked in PBS with 5 % normal donkey serum and 0.5 % Tween 20 at room temperature for 20 min. The tissue sections were stained overnight with PE-anti-mouse B220 (BioLegend) at 4 °C. After two washes, the sections were washed and mounted with Prolong Gold Antifade Reagent with DAPI (Invitrogen). Fluorescent microscopic images were taken under a Zeiss LSM710 Confocal Microscope at Cornell Biotechnology Resource Center Imaging Facility.

### **RNA Extraction, Quantitative (Q), and Reverse-transcription (RT)-PCR**

RNA extraction from cells and murine tissues, and Q-PCR were carried out as previously described using Trizol (Invitrogen) (Sha et al., 2014). Q-PCR data collected on the Roche LightCycler 480 were normalized to ribosomal *132* gene in the corresponding sample.

### **Primers**

#### Genotyping:

*Sell1L* (CTGACTGAGGAAGGGTCTC; GCTAAAAACATTACAAAGGGGCA) (325 bp as wild-type allele, 286 bp as floxed allele)

*CD19-CRE* (GCGGTCTGGCAGTAAAACTATC; GTG AACAGCATTGCTGTCCTT)

*CD19-WT* (CCTCTCCCTGTCTCCTTCT; TGGTCTGAGACATTGACAATCA)

*Chop*<sup>-/-</sup> (AACGCCAGGGTTTTCCAGTCA)

*Chop*<sup>WT</sup> (GCAGGGTCAAGAGTAGTG)

#### RT-PCR/Q-PCR:

*VpreB1* (CGTCTGTCCTGCTCATGCTGC; ACGGCACAGTAATACACAGCC),

*Ig $\mu$*  (TGTGTGTACTGTGACTCACAGGGA; AGGGAGACATTGTACAGTGTGGGT),

$\lambda 5$  (GTTGGGTCTAGTGGATGGTGT; TTGGTCTGTTTGGAGGGTTGG),

*L32* (GAGCAACAAGAAAACCAAGCA; TGCACACAAGCCATCTACTCA),

*BiP* (TGTGGTACCCACCAAGAAGTC, TTCAGCTGTCACTCGGAGAAT),

*Os9* (GCTCACGCCTACTACCTCAA, GCCAGACAAGTCTCTGTGACG),

*Chop* (TATCTCATCCCCAGGAAACG, GGGCACTGACCACTCTGTTT),

*Erdj4* (CTTAGGTGTGCCAAAGTCTGC, GGCATCCGAGAGTGTTTCATA),

*Edem1* (GGGACCAAGAGGAAAAGTTTG, GAGGTGAGCAGGTCAAATCAA),

The PCR conditions are: 94 °C for 5 min, 94 °C for 1 min, 58 °C for 20 sec and 72 °C for 30 sec repeated for 25 to 30 cycles according to individual template, followed by 70 °C for 10 min.

### Statistical Analysis

Results are expressed as mean  $\pm$  SEM. Comparisons between groups were made by unpaired two-tailed Student's t test, except by one-way ANOVA with Tukey post-test in Figure 3.13. All experiments were repeated at least twice or performed with independent samples.

## 3.4. RESULTS

### 3.4.1. Reduced peripheral B cells in B cell-specific *Sel1L*-deficient mice.

Expression of *Sel1L* and *Hrd1* genes was induced around the pre-B cell stage in developing lymphocytes, preceding that of ER chaperones BiP and Edem1 (Figure 3.1.A), suggesting a possible role of *Sel1L*-*Hrd1* ERAD in early lymphopoiesis. To investigate whether *Sel1L*-*Hrd1* ERAD plays a role in B cell development, we crossed *Sel1L*<sup>flox/flox</sup> (*Sel1L*<sup>ff</sup>) mice on the C57BL/6 background (Figure 3.2A) with CD19-Cre mice to generate B cell-specific *Sel1L*-deficient mice (*Sel1L*<sup>CD19</sup>). The CD19 promoter is active specifically in B cells and throughout B cell development from the pro-B cell stage (Zhou, L. J. et al., 1991). The *Sel1L*<sup>CD19</sup> mice and their control *Sel1L*<sup>ff</sup> littermates were born in a normal Mendelian ratio (not shown) and appeared healthy with no obvious growth defects (Figure 3.1B). Immunoblot analysis confirmed the

deletion of the Sel1L protein and reduction of Hrd1 protein in the BM-derived B cells (Figure 3.1C). Spleen weights were significantly reduced in *Sel1L<sup>CD19</sup>* mice vs. controls (Figure 3.1D and Figure 3.2B). The percentage of peripheral B cells in spleen, blood, and lymph nodes was reduced by 60-75 % (Figure 3.1E) and the absolute numbers of splenic B cells were >75 % lower in *Sel1L<sup>CD19</sup>* mice compared to controls, while other cell types, including CD4<sup>+</sup>, CD8<sup>+</sup> T and myeloid cells were not affected (Figure 3.1F-G and Figure 3.2C). The reduction in B cells was not due to elevated cell death (Figure 3.2D). Similar to the conventional BM B cells (also known as B-2 cells), the percentage of peritoneal CD5<sup>+</sup> B-1 cells was decreased in *Sel1L<sup>CD19</sup>* mice vs. *Sel1L<sup>ff</sup>* controls (Figure 3.2E). Of note, there were ~20 % residual peripheral B cells in the *Sel1L<sup>CD19</sup>* mice, which is in line with the fact that CD19-Cre-mediated deletion efficacy is approximately 75-80 % in BM (Rickert et al., 1997). Hence, we concluded that Sel1L in B cells is required for B cell development.

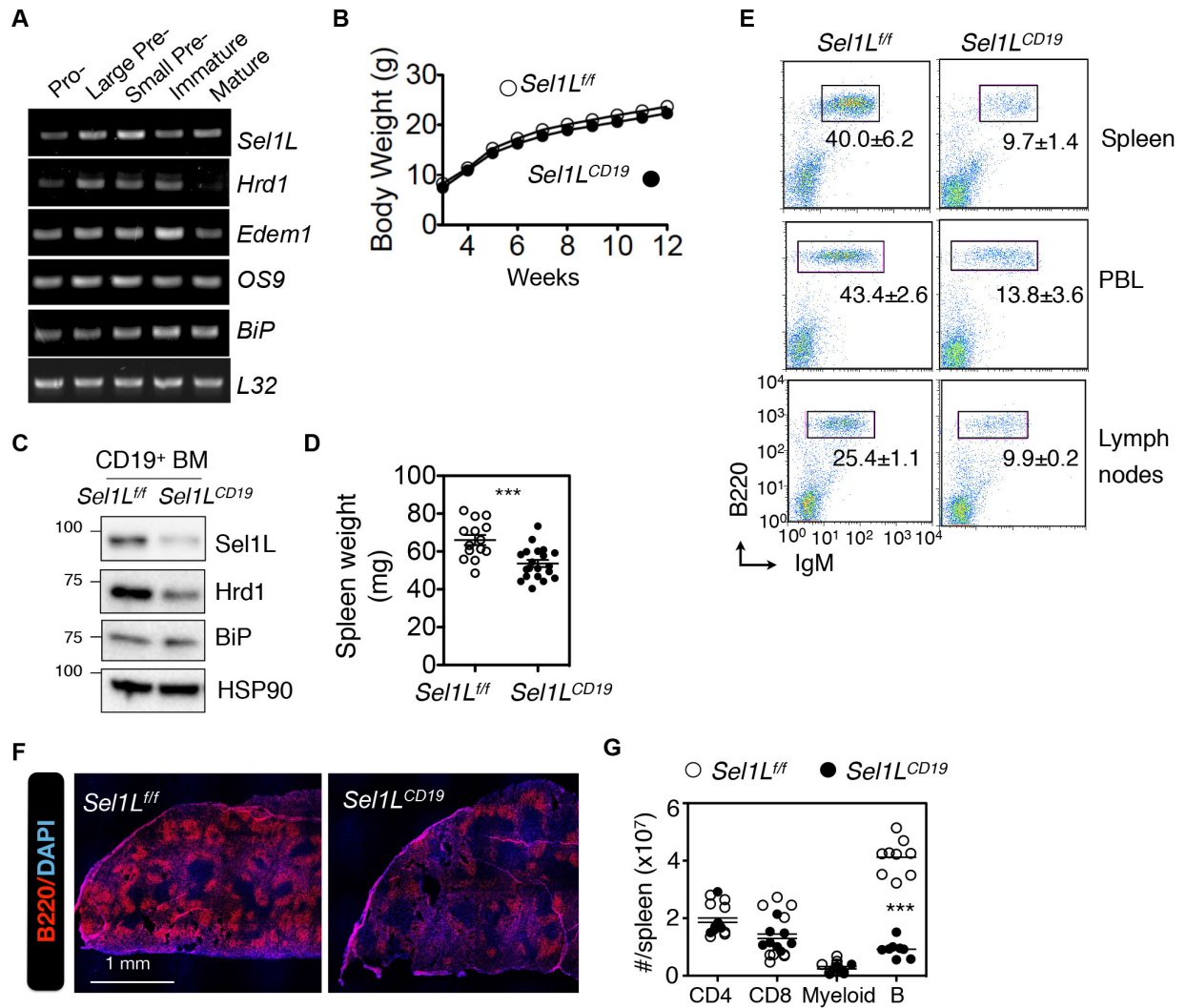


**Figure 3. 1 Reduced peripheral B lymphocyte cellularity in *Sel1L<sup>CD19</sup>* mice.**

(A) RT-PCR analysis of ERAD genes in B cell subpopulations from bone marrows (BM) of C57BL/6 mice. (B) Growth curves for male littermates. (C) Immunoblots of *Sel1L*, *Hrd1*, and *BiP* in CD19<sup>+</sup> BM cells from *Sel1L<sup>fl/fl</sup>* and *Sel1L<sup>CD19</sup>* mice. (D) Spleen mass. (E) Flow cytometric analysis of mature B cells (B220<sup>+</sup>/IgM<sup>+</sup>) in spleen, peripheral blood (PBL), and lymph nodes. (F) Representative confocal microscopic images of B cells (red) in the spleen. (G) Absolute numbers of splenic CD4<sup>+</sup>, CD8<sup>+</sup> T, myeloid, and mature B cells. Data are representative of two (A,C,F) or three (E) independent experiments. n=8 C57BL/6 mice (A), 18 mice each (B), 3 mice each (C),

15 *SellL<sup>ff</sup>* mice and 19 *SellL<sup>CD19</sup>* mice (D), 3 mice each (F), and 8-9 mice each (E,G). Values shown as mean  $\pm$  s.e.m.; N.S., not significant; \*P<0.05, \*\*\*P<0.001 by two-tailed Student's t-test

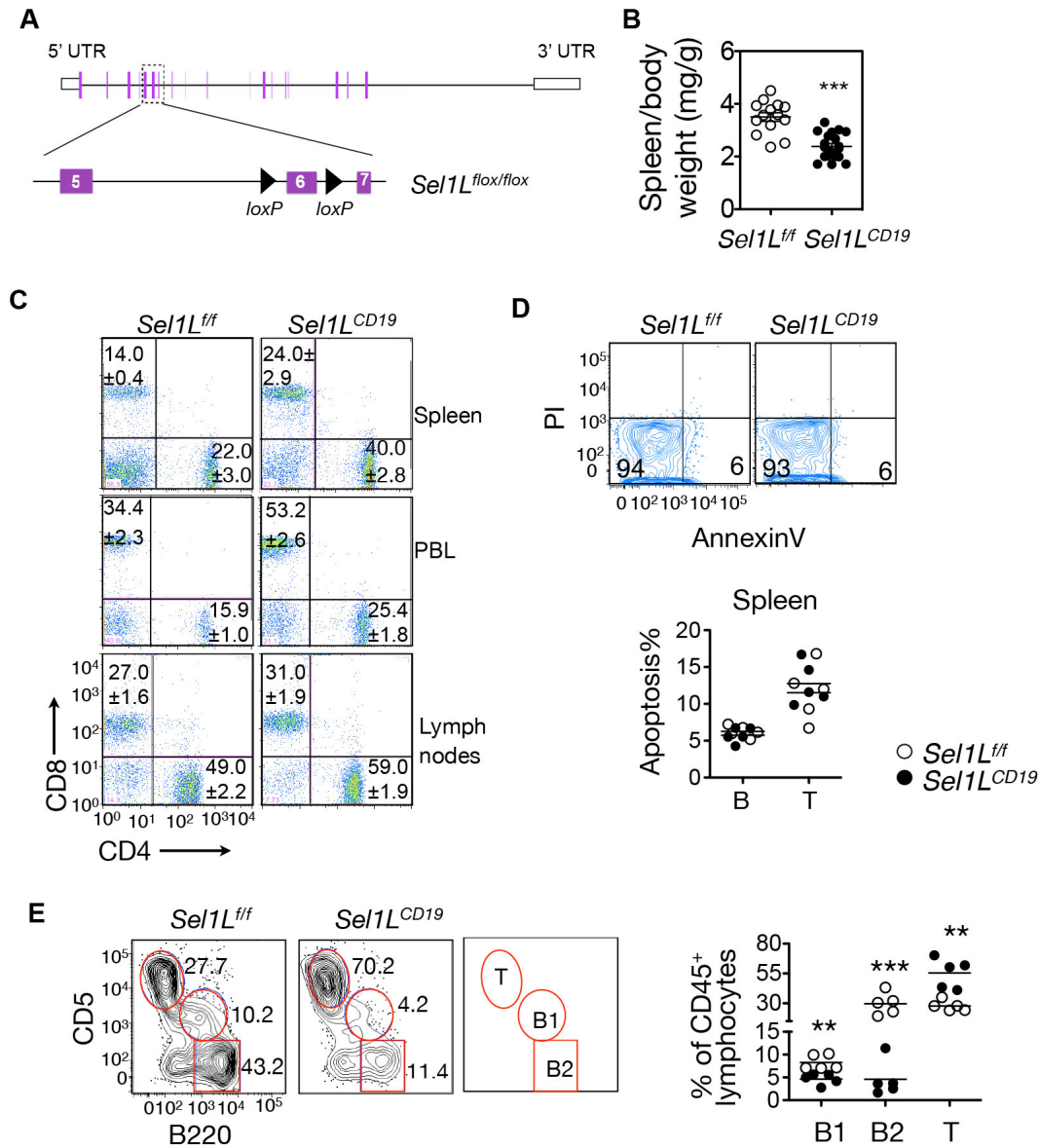


**Figure 3. 2 Generation of *Sel1L<sup>CD19</sup>* mice and the reduction of mature B cells.**

(A) Schematic diagram of *Sel1L<sup>ff</sup>* mice on the C57BL/6N background with the exon 6 flanked by two loxP sites. (B) Spleen mass normalized to body weight of *Sel1L<sup>ff</sup>* and *Sel1L<sup>CD19</sup>* littermates. (C) Flow cytometric analysis of lymphocytes from peripheral blood (PBL), spleen and lymph nodes of *Sel1L<sup>ff</sup>* and *Sel1L<sup>CD19</sup>* mice with quantitation shown in each quadrant. (D) Flow cytometric analysis of apoptotic splenocytes from *Sel1L<sup>ff</sup>* and *Sel1L<sup>CD19</sup>* mice using

Annexin-V and propidium iodide staining (PI), with quantitation shown on the right. (E) Flow cytometric analysis of lymphocytes from peritoneal cavity of *SellL<sup>ff</sup>* and *SellL<sup>CD19</sup>* mice with quantitation shown on the right. Data are representative of two independent experiments in (B-E), n= 14 *SellL<sup>ff</sup>* and 20 *SellL<sup>CD19</sup>* mice (B), 9 *SellL<sup>ff</sup>* and 8 *SellL<sup>CD19</sup>* mice (C), 5 mice each (D-E). Values shown as mean  $\pm$  s.e.m.; \*\*P< 0.01, \*\*\*P<0.001 by two-tailed Student's t-test.

### 3.4.2. Developmental defect at the transition from the large to the small pre-B cell stage in *Sell1L<sup>CD19</sup>* mice.

In adult BM, B lymphocytes develop from pluripotent hematopoietic stem cells through an ordered differentiation process, where IgH and IgL genes are sequentially rearranged and the productive rearrangement of each establishes two key checkpoints that test the functionality of each Ig component (Figure 3.3A). At the first checkpoint, the IgH (or Ig $\mu$ ) must form a signaling competent pre- BCR with the SLC; at the second checkpoint, a functional BCR must be formed between IgH and a nascent IgL after SLC expression is extinguished (Figure 3.3A). Consistent with the reduced peripheral B cellularity in *Sell1L<sup>CD19</sup>* mice, B220<sup>high</sup>/IgM<sup>+</sup> recirculating mature and B220<sup>low</sup>/IgM<sup>+</sup> immature B cells were significantly decreased in the BM of *Sell1L<sup>CD19</sup>* mice vs. *Sell1L<sup>ff</sup>* controls (Figure 3.4A-B). On the other hand, the percentage of B220<sup>low</sup> CD43<sup>hi</sup> pro-B cells was slightly elevated in *Sell1L<sup>CD19</sup>* mice while that of pre-B cells was comparable to controls (Figure 3.4A-B). These data point to a developmental defect at the pro-/pre-B cell stage in *Sell1L<sup>CD19</sup>* mice. Pro-/pre-B cells can be further classified based on the expression of SLC and the differentiation marker CD2 (Figure 3.3A). Within the pro-/pre- B cell compartment of the BM, SLC<sup>+</sup>/CD2<sup>-</sup> pre-B I and large pre-B (II) cells were twice as many, whereas SLC<sup>-</sup>/CD2<sup>+</sup> small pre-B cells were reduced by 50 % in the *Sell1L<sup>CD19</sup>* mice compared to *Sell1L<sup>ff</sup>* littermates (Figure 3.3C and Figure 3.4B). Cell death did not account for the changes in B cell populations of *Sell1L<sup>CD19</sup>* mice as apoptotic rates for various precursor populations were comparable between the cohorts (Figure 3.3C). Both *Sell1L* heterozygosity and CD19-Cre expression itself as in *Sell1L<sup>ff/+</sup>*; *CD19-Cre* (*Sell1L<sup>CD19/+</sup>*) mice had no effect on B cell development (Figure 3.3D). Thus, B cell-specific *Sell1L* deficiency results in a severe developmental defect at the transition from the large to small pre-B cells.

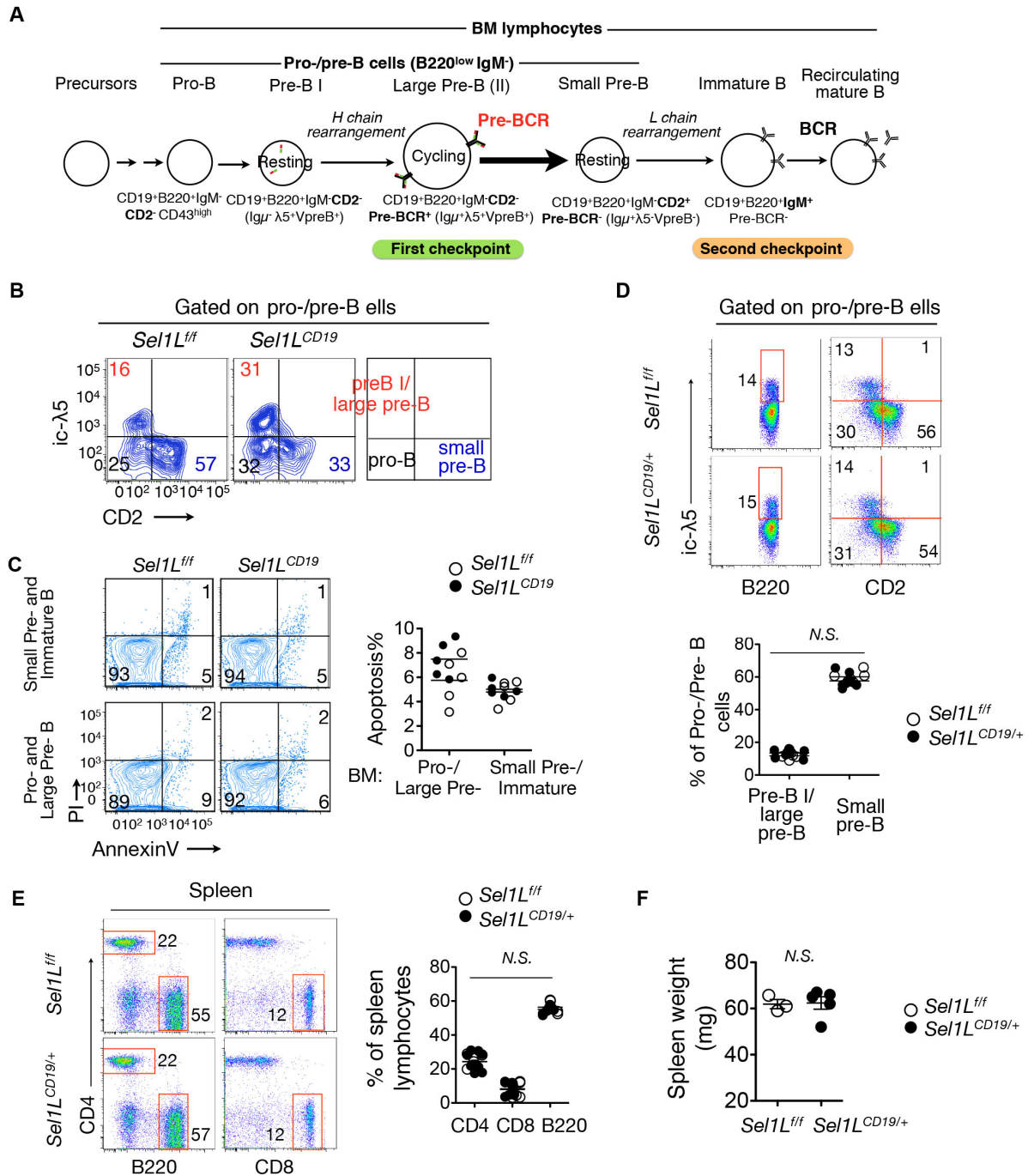


**Figure 3. 3 B cell developmental defects in the absence of Sel1L.**

(A) Schematic of B cell development in bone marrow (BM). Two checkpoints are highlighted in green and orange (B) Flow cytometric analysis of various cell populations in BM of *Sel1L<sup>ff</sup>* and

*Sell*<sup>CD19</sup> mice stained for CD2 and intracellular  $\lambda$ 5 (ic- $\lambda$ 5), gated on B220<sup>low</sup>IgM<sup>-</sup> pro-/pre-B cells, with quantitation shown in Figure 3.3C. (C) Flow cytometric analysis of apoptotic BM progenitors from *Sell*<sup>ff</sup> and *Sell*<sup>CD19</sup> mice using annexin-V and propidium iodide staining (PI) with quantitation on the right. (D-E) Flow cytometric analysis of (D) pro-/pre-B BM cells, stained for B220 and intracellular (ic)  $\lambda$ 5, and (E) of splenocytes of *Sell*<sup>ff</sup> and *Sell*<sup>CD19/+</sup> mice. (F) Spleen weights of *Sell*<sup>ff</sup> and *Sell*<sup>CD19/+</sup> mice. Data are representative of two independent experiments.

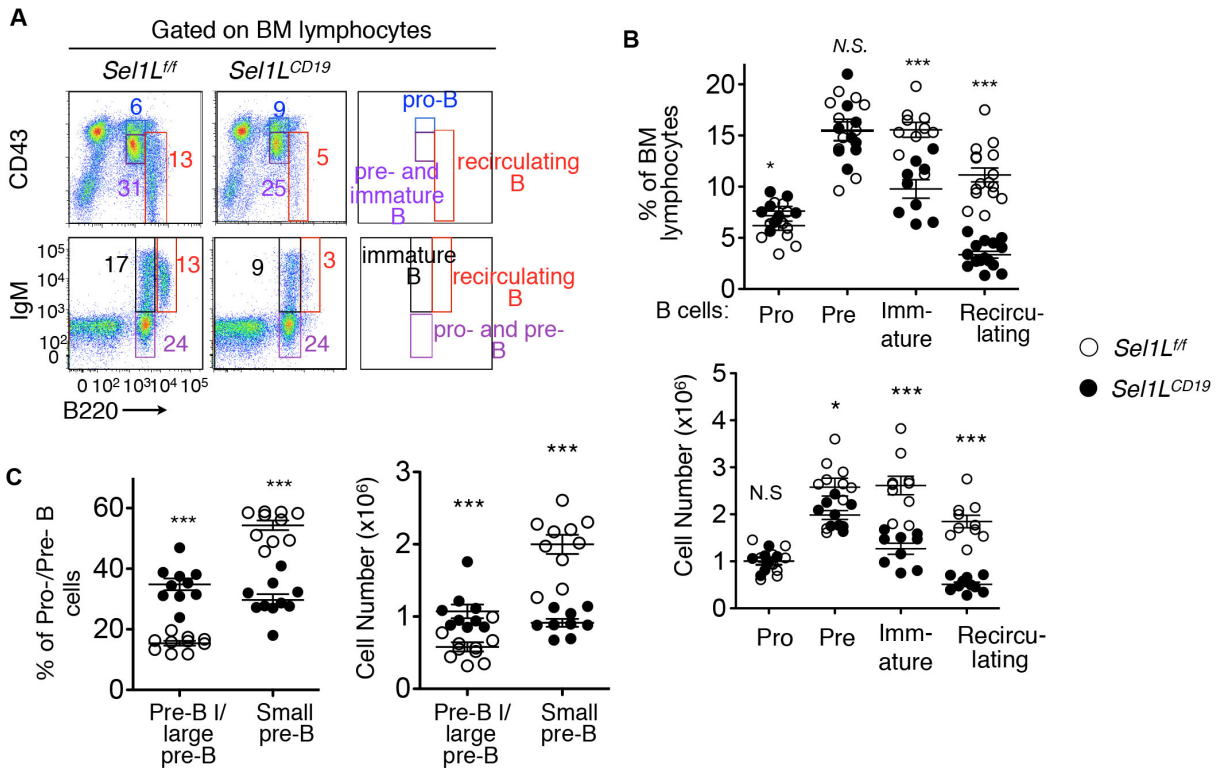


**Figure 3.4 Developmental blockade at the transition from the large to small pre-B cells in *Sel1L<sup>CD19</sup>* mice.**

(A) Flow cytometric analysis of B220-CD43 (upper) and B220-IgM (lower) in BM cells from *Sel1L<sup>ff</sup>* and *Sel1L<sup>CD19</sup>* mice, with quantitation in percentage and absolute cell number shown in (B). (C) Quantitation of flow cytometric analysis of various pro-/pre-B cell populations in BM of *Sel1L<sup>ff</sup>* and *Sel1L<sup>CD19</sup>* mice. Data are representative of three independent experiments with n= 9-10 mice each. Values shown as mean ± s.e.m.; \*P<0.05, \*\*\*P<0.001 by two-tailed Student's t-test.

### **3.4.3. The developmental defect of *Sell1L*<sup>CD19</sup> mice is independent of Chop.**

We hypothesized that impairment of an ER quality control system like ERAD could activate a stress response, and that might account for the developmental block observed. Indeed, a subset of ER stress-responsive genes such as BiP and Chop were moderately elevated in the large pre-B cells of *Sell1L*<sup>CD19</sup> mice (Figure 3.5A). To determine more directly the contribution of ER stress in B cell development of *Sell1L*<sup>CD19</sup> mice, we examined the role of Chop in *Sell1L*<sup>CD19</sup> mice by generating *Sell1L*<sup>CD19</sup>; *Chop*<sup>-/-</sup> mice. However, *Chop* deficiency had no impact on the B cell developmental defects associated with the loss of Sell1L, in terms of low spleen weight (Figure 3.5B), paucity of the B cell compartment within the peripheral lymphocyte pool (Figure 3.5C), and the developmental block at the large pre-B cell stage in the BM (Figure 3.5D-G). Thus, B cell-specific Sell1L deficiency results in a developmental block in a Chop-independent manner.

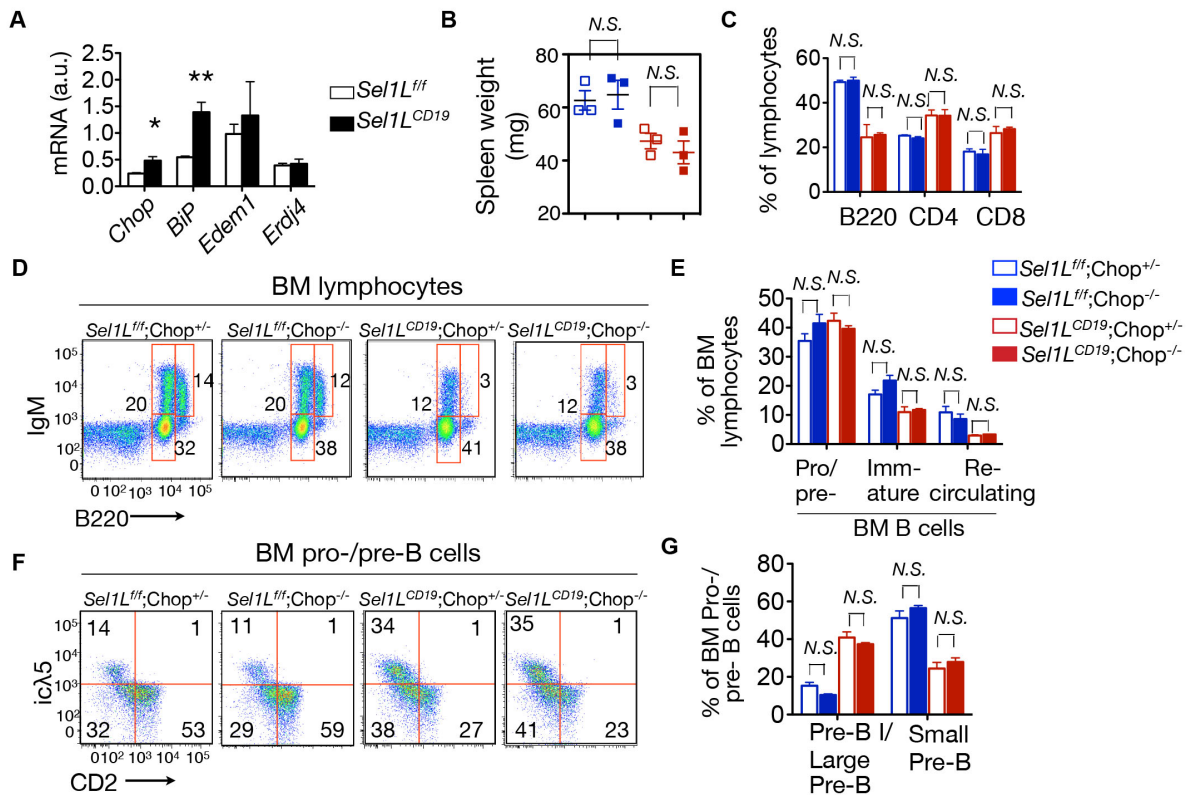


**Figure 3. B cell developmental defect in *Sel1L<sup>CD19</sup>* mice is independent of Chop.**

(A) Q-PCR analyses of BiP, Chop, Erdj4 and Edem1 mRNA levels in sorted large pre-B cells from *Sel1L<sup>ff</sup>* and *Sel1L<sup>CD19</sup>* mice. (B) Spleen weight of WT (*Sel1L<sup>ff</sup>; Chop<sup>+/-</sup>*), *Chop<sup>-/-</sup>* (*Sel1L<sup>ff</sup>; Chop<sup>-/-</sup>*), *Sel1L<sup>CD19</sup>* (*Sel1L<sup>CD19</sup>; Chop<sup>+/-</sup>*) and double knockout (*Sel1L<sup>CD19</sup>; Chop<sup>-/-</sup>*) mice. (C) Frequency of various lymphocytes in spleens from the cohorts in (B). (D) Flow cytometric analysis of pro-/pre- B cells (B220<sup>+</sup>IgM<sup>-</sup>), immature B cells (B220<sup>+</sup>IgM<sup>+</sup>) and recirculating B cells (B220<sup>hi</sup>IgM<sup>+</sup>) in BM with quantitation shown in (E). (F) Flow cytometric analysis of pre-B I/large pre-B cells (ic-λ5<sup>+</sup>/CD2<sup>-</sup>) and small pre-B cell (ic-λ5<sup>-</sup>/CD2<sup>-</sup>) populations in the BM with quantitation shown in (G). Data are representative of 2 independent experiments (n= 8 *Sel1L<sup>ff</sup>*

and 4 *SellL*<sup>CD19</sup> mice (A), 3 mice each (B) and 5 mice each (C-G)). Values shown as mean  $\pm$  s.e.m.; N.S., not significant; \*P<0.05, \*\*P<0.01, by two-tailed Student's t-test.

#### 3.4.4. Selective accumulation of the pre-BCR in large pre-B cells.

To explore the possible mechanism, we measured the protein levels of various key factors involved in B cell development at the pre-B cell stage, including c-Kit, IL-7R $\alpha$ , CD19, and the pre-BCR complex (Clark et al., 2014; Herzog et al., 2009). All of these factors are transmembrane proteins synthesized in the ER (Figure 3.6A). While total levels (intracellular and surface) of c-Kit and IL-7R $\alpha$  protein were comparable, protein levels of three main components of the pre-BCR complex were dramatically increased in the pro-/pre-B cells of *Sel1L<sup>CD19</sup>* mice (Figure 3.6B). The percentage of SLC<sup>+</sup> cells was significantly increased in *Sel1L<sup>CD19</sup>* BM (Figure 3.6C and Figure 3.7A). Accumulation of the two SLC components VpreB and  $\lambda$ 5 occurred within the same cells (Figure 3.6D). Moreover, as expression of SLC precedes that of the I $\mu$  heavy chain (Kudo et al., 1992; Lassoued et al., 1996), there is a  $\lambda$ 5-single positive pre-B I cell stage in addition to a  $\lambda$ 5<sup>+</sup>/I $\mu$ <sup>+</sup> large pre-B cells (Figure 3.3A). Strikingly, we observed a 3-fold increase in the percent of  $\lambda$ 5<sup>+</sup>/I $\mu$ <sup>+</sup> large pre-B cells in *Sel1L<sup>CD19</sup>* mice compared to that of *Sel1L<sup>ff</sup>* mice, while the percent of  $\lambda$ 5<sup>+</sup> I $\mu$ <sup>-</sup> pre-B I cells was not affected by ERAD deficiency (Figure 3.6E). In line with this finding, measurement of  $\lambda$ 5 and I $\mu$  at different developmental stages revealed their accumulation only in large pre-B cells when both were co-expressed (Figure 3.6F). These data demonstrate that Sel1L-Hrd1 ERAD recognizes and degrades the pre-BCR complex, rather than its individual components. Indeed, using a pre-BCR complex-specific antibody, we found that the proportion of pre-BCR complex-positive cells was doubled in the *Sel1L<sup>CD19</sup>* BM (Figure 3.7B). Quantitative and RT-PCR analyses revealed comparable transcript levels of VpreB,  $\lambda$ 5, and I $\mu$  genes (Figure 3.7C-D), suggesting that pre-BCR protein accumulation is a result of post-transcriptional regulation. Hence, our data identify the pre-BCR complex, rather than its individual components, as the possible Sel1L-Hrd1 ERAD substrate in developing B cells.

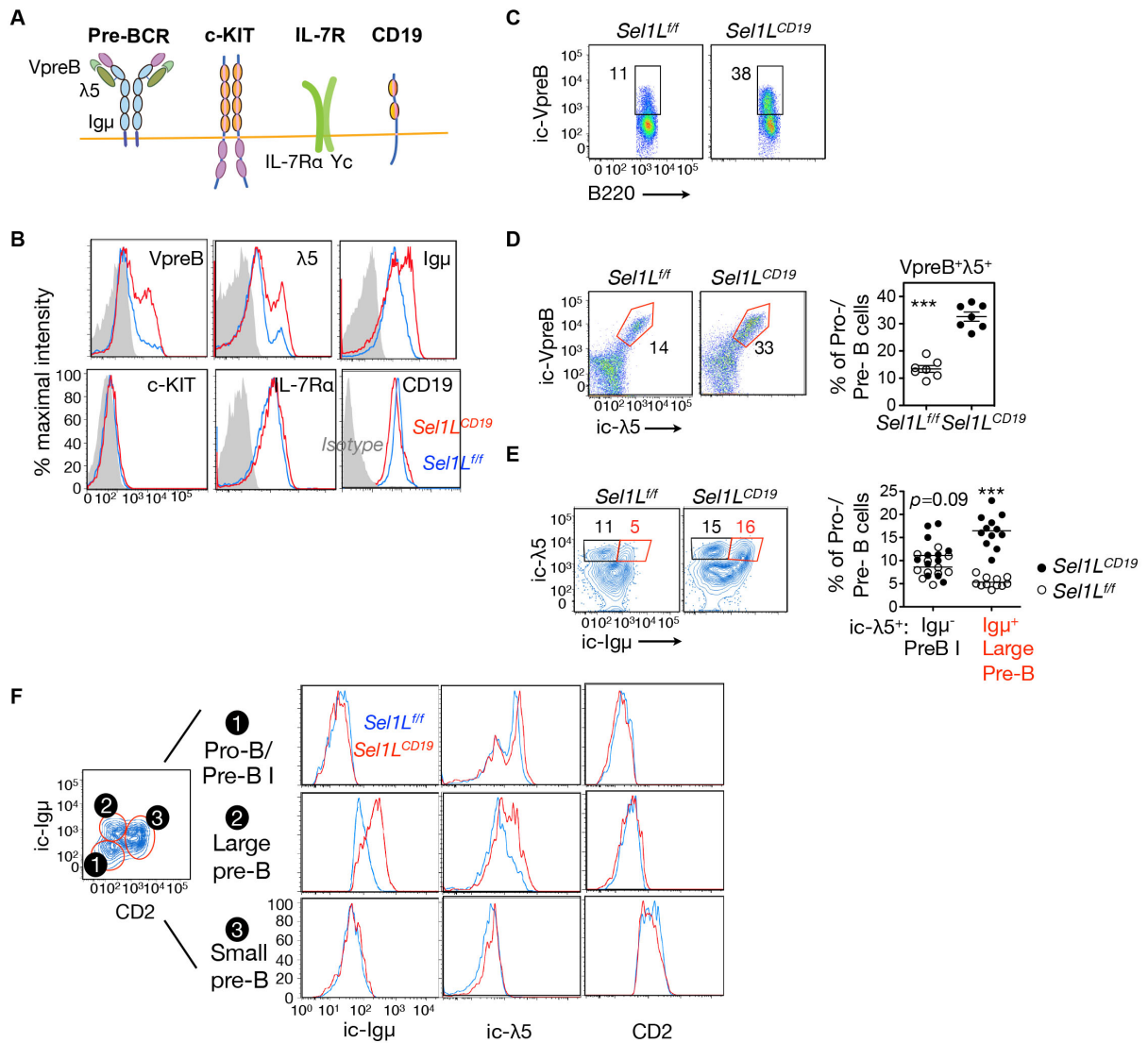


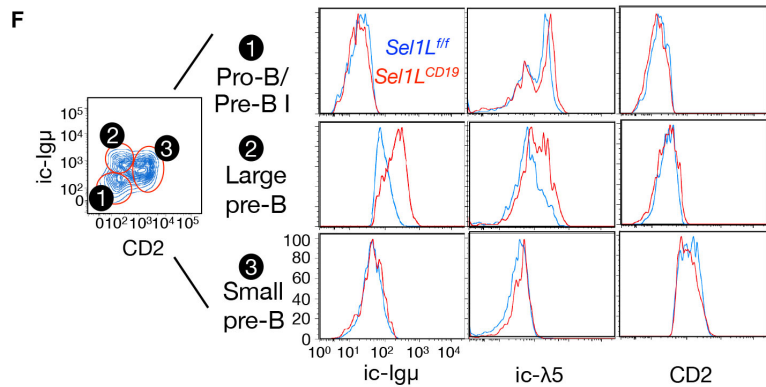
**Figure 3. 6 Accumulation of the pre-BCR complex in Sel1L-deficient large pre-B cells.**

(A) Schematic diagram of various membrane receptors involved in early B cell development. (B)

Flow cytometric histogram analysis of BM cells from *Sel1L<sup>fl/fl</sup>* and *Sel1L<sup>CD19</sup>* mice, stained for total (surface and intracellular) levels of indicated proteins, gated on B220<sup>low</sup>IgM<sup>-</sup> pro-/pre-B cells. Gray-shaded area indicates isotype control. (C) Flow cytometric analysis of BM cells from *Sel1L<sup>fl/fl</sup>* and *Sel1L<sup>CD19</sup>* mice stained for B220 and intracellular (ic) VpreB, gated on pro-/pre-B cells.

(D) Flow cytometric analysis of BM for ic-λ5 and ic-VpreB in pro-/pre-B cells with

(E) Flow cytometric analysis of BM for ic-λ5 and ic-Igμ in pro-/pre-B cells with



quantitation shown on the right. (E) Flow cytometric analysis of BM for ic- $\lambda 5$  and ic-Ig $\mu$  in pro-/pre-B cells with quantitation shown on the right. (F) Flow cytometric histogram analysis of CD2, ic-Ig $\mu$ , and ic- $\lambda 5$  in various early B cell populations in BM. Gating strategy for each population (1-3) is shown on the left. Data are representative of four (B) or two (C-F) independent experiments. n=18 mice each (B), 7 mice each (C), 7 mice each (D), 11-12 mice each (E), and 9 mice each (F). Values shown as mean  $\pm$  s.e.m.; \*\*\*P<0.001 by two-tailed Student's t-test.

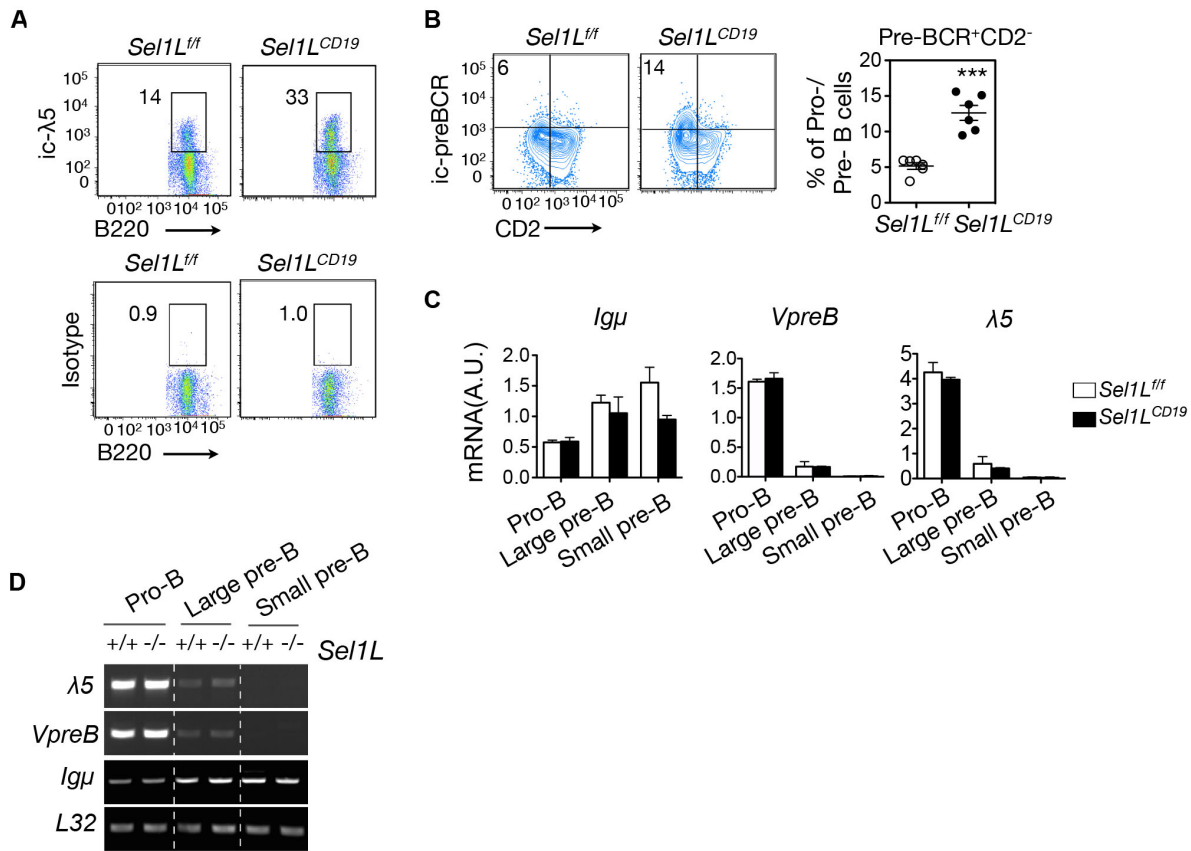


**Figure 3. 7 Accumulation of pre-BCR components in *Sel1L*-deficient large pre-B cells,** (A) Flow cytometric analysis of BM pro/pre-B cells from *Sel1L<sup>ff</sup>* and *Sel1L<sup>CD19</sup>* mice. The numbers next to the outlined area indicate the percentage of double positive cells. Representative data shown (n=7 mice each). (B) Flow cytometric analysis of CD2 and ic-preBCR in pro-/pre-B cells of *Sel1L<sup>ff</sup>* and *Sel1L<sup>CD19</sup>* mice. Quantitation is shown on the right. (C) Q-PCR analyses of pre-BCR components in various B cell progenitors isolated from BM of *Sel1L<sup>ff</sup>* and *Sel1L<sup>CD19</sup>* mice. (D) RT-PCR analysis of pre-BCR components in various B cell progenitors isolated from *Sel1L<sup>ff</sup>* and *Sel1L<sup>CD19</sup>* mice. *L32* is a loading control. Data are representative of two independent experiments. (B) 6 mice each, and (C-D) pooled cells from n=8 mice each. Values shown as mean ± s.e.m.

### 3.4.5. The pre-BCR complex is an endogenous Sel1L-Hrd1 ERAD substrate.

We next directly tested whether the pre-BCR is an ERAD substrate in pre-B cells. Protein levels of I $\mu$ ,  $\lambda$ 5, and VpreB were significantly stabilized in the BM of *Sel1L<sup>CD19</sup>* mice compared to *Sel1L<sup>ff</sup>* mice (Figure 3.8A and Figure 3.9A). By contrast, IL-7R $\alpha$  protein stability was not affected (Figure 3.8A and Figure 3.9B). To further corroborate these findings in vitro, we generated a Sel1L and Hrd1-deficient pre-BCR expressing pre-B cells, 70z/3 (Paige et al., 1978), using the RNAi and CRISPR/cas9 systems, respectively (Figure 3.8B-C). Loss of either Sel1L or Hrd1 in the 70z/3 cells increased steady-state protein levels of all three components of the pre-BCR complex (Figure 3.8B-C), and led to I $\mu$  protein stabilization, with its half-life increasing from approximately 60 min to more than 120 min (Figure 3.8D). Inhibition of proteasomal activity using MG132 or bortezomib significantly increased I $\mu$  protein stability in 70z/3 cells (Figure 3.8E and data not shown), implicating the proteasome in pre-BCR degradation. Furthermore, ubiquitination of I $\mu$  protein was reduced dramatically in *Sel1L<sup>-/-</sup>* and *Hrd1<sup>-/-</sup>* 70z/3 cells (Figure 3.8F and not shown), pointing to the indispensable role of Sel1L-Hrd1 ERAD in pre-BCR ubiquitination and degradation. Thus, we concluded that Sel1L-Hrd1 ERAD recognizes and targets the pre-BCR complex for ubiquitination and proteasomal degradation and that Sel1L-Hrd1 ERAD deficiency leads to intracellular accumulation of the pre-BCR.

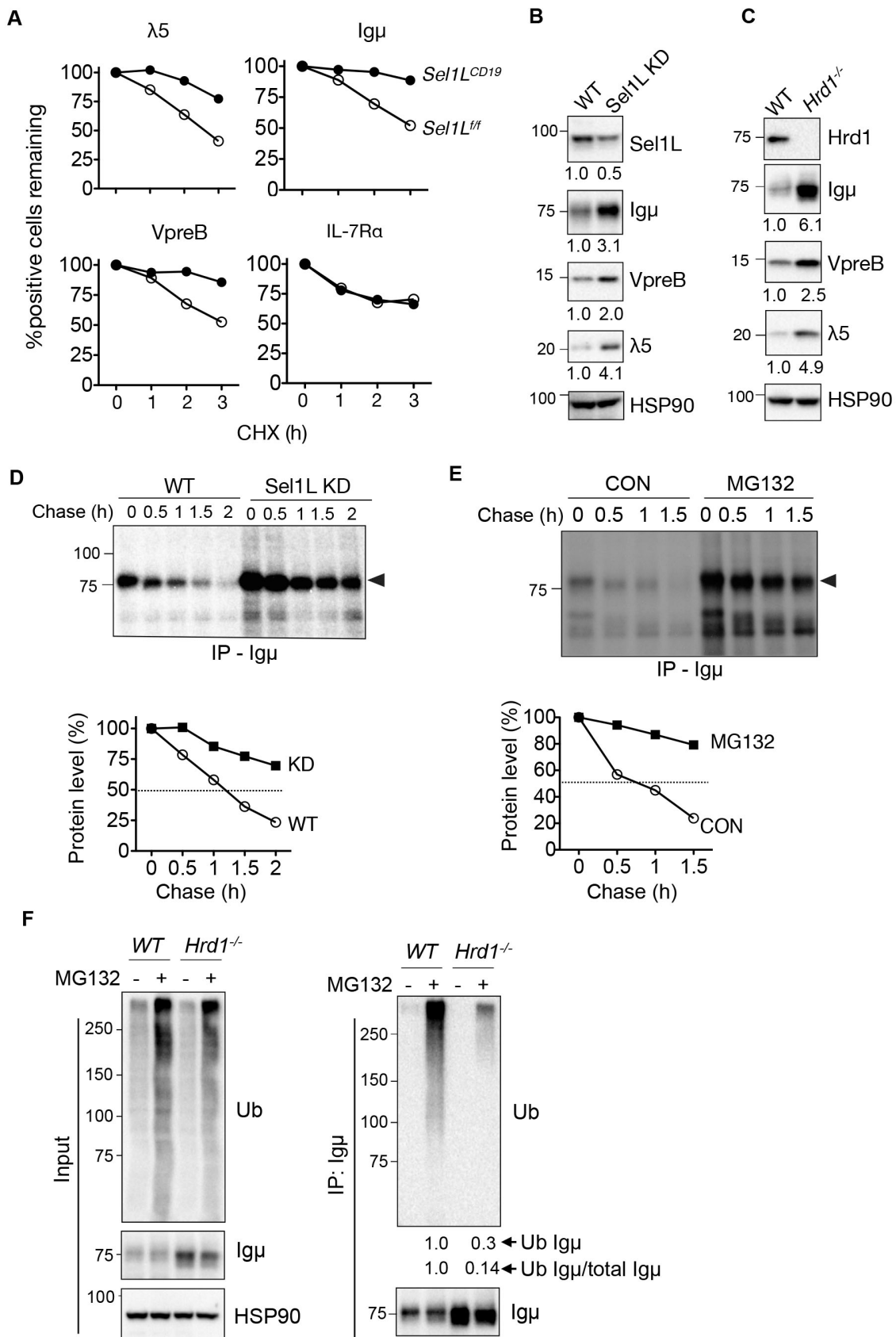


**Figure 3. 8 The pre-BCR complex is an endogenous Sel1L-Hrd1 ERAD substrate.**

(A) Protein turnover for intracellular  $\lambda 5$ , VpreB and I $\mu$  expression in fresh BM of *Sel1L<sup>ff</sup>* and *Sel1L<sup>CD19</sup>* mice treated with 50  $\mu$ g/ml cycloheximide (CHX) for the indicated times. IL-7R, a control membrane protein. (B-C) Immunoblot analysis of WT, Sel1L KD (KD) (B) and *Hrd1<sup>-/-</sup>* (C) 70Z/3 pre-B cells with quantitation (normalized to HSP90) shown below each gel. (D) Pulse-chase analysis showing I $\mu$  decay in WT and KD pre-B cells with quantitation shown on the right. (E) Pulse-chase analysis showing I $\mu$  decay in WT pre-B cells treated with or without 25  $\mu$ M MG132 for 0.5 h with quantitation shown on the right. (F) Immunoblot analysis of I $\mu$  immunoprecipitates in WT and *Hrd1<sup>-/-</sup>* pre-B cells treated with or without 25  $\mu$ M MG132 for 3 h. Quantitation of I $\mu$  ubiquitination (with or without normalization to total I $\mu$ ) shown below the blot. Data are representative of two (A,D,E), three (B-C), and four (F) independent experiments. n=3 mice each (A).

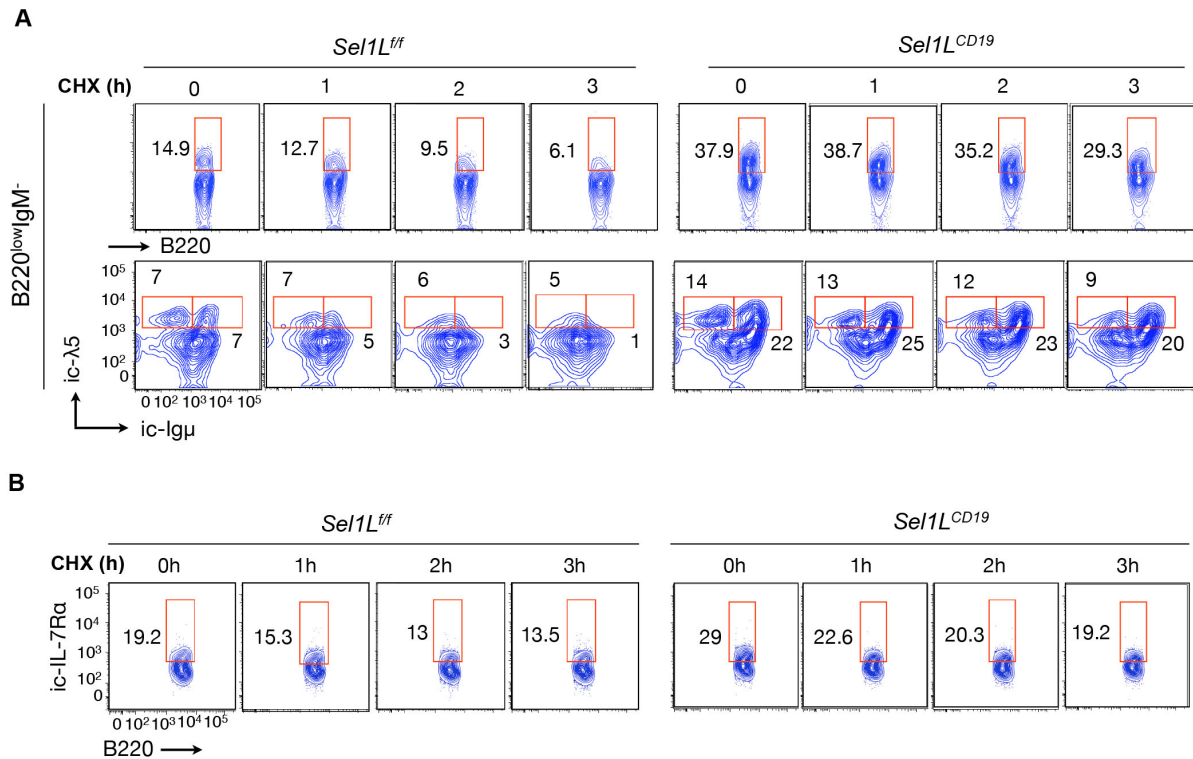


**Figure 3. 9 Accumulation and stabilization of pre-BCR components in *Sel1L*-deficient large pre-B cells.**

(A) Flow cytometric analysis for intracellular  $\lambda 5$  and Ig $\mu$  expression in fresh BM of *Sel1L<sup>ff</sup>* and *Sel1L<sup>CD19</sup>* mice treated with 50  $\mu$ g/ml cycloheximide (CHX) for the indicated times with quantitation of the percent of positive cells shown in Figure 3.8A. (B) Flow cytometric analysis of intracellular IL-7R $\alpha$  level in BM cells of *Sel1L<sup>ff</sup>* and *Sel1L<sup>CD19</sup>* mice post 50  $\mu$ g/mL cyclohexamide (CHX) treatment, gated on pro-/pre-B cells. Representative data from 2 independent experiments shown.

#### **3.4.6. Enhanced ER exit of the pre-BCR in Sel1L-deficient pre-B cells.**

We next determined the effect of Sel1L-Hrd1 ERAD deficiency on pre-BCR complex formation and intracellular trafficking. The accumulated pre-BCRs remained largely soluble (Figure 3.10A), colocalized with ER chaperone BiP (Figure 3.10B) and exhibited similar sensitivity to trypsin digestion in ERAD-deficient 70z/3 cells (Figure 3.11A). These data suggest that, in the case of pre-BCR, Sel1L-Hrd1 ERAD deficiency does not trigger a dramatic conformational change and hence protein aggregation. Moreover, accumulation of Ig $\mu$  and SLCs in ERAD-deficient 70z/3 pre-B cells increased the abundance of the high molecular weight pre-BCR complexes, as revealed by non-reducing SDS-PAGE (left two lanes, Figure 3.11B) and sucrose density gradient fractionation analyses (Figure 3.10C). Moreover, while the majority of Ig $\mu$  protein in WT pre-B cells was retained in the ER and exhibited high-mannose endoglycosidase (Endo) H-sensitivity as previously reported (Brouns et al., 1996), Sel1L deficiency resulted in a nearly 3-fold increase in endoH-resistant and peptide-N-glycosidase F (PNGase F)-sensitive Ig $\mu$  protein, indicative of increased ER exit of the pre-BCR complex in the absence of Sel1L-Hrd1 ERAD (Figure 3.10D). Consistently, more surface pre-BCR complexes were detected in ERAD-deficient pre-B cells (Figure 3.10E) and pre-B cells treated with the proteasome inhibitor MG132 (Figure 3.10F). Thus, impaired pre-BCR degradation by Sel1L-Hrd1 ERAD leads to elevated surface pre-BCR in pre-B cells.

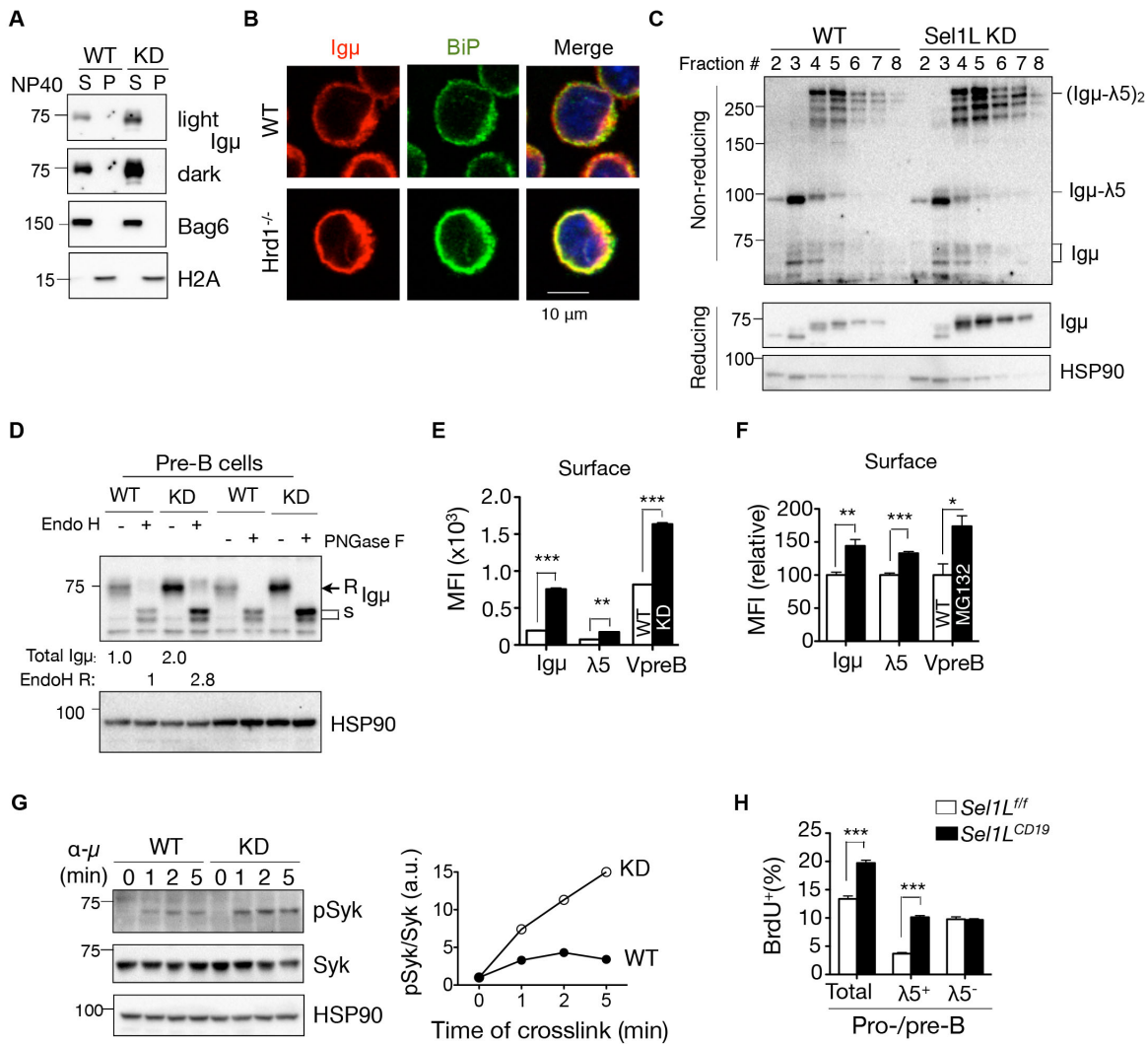


**Figure 3. 10 ERAD is indispensable for the termination of pre-BCR signaling in developing B cells.**

(A) Immunoblot analysis of Igμ in the NP-40 soluble (S) and insoluble (P) fractions of the WT and Sel1L KD pre-B cells. The distribution of Bag6 and H2A marks the S and P fractions, respectively. (B) Confocal microscopic images of Igμ (red) and BiP (green) staining in WT and *Hrd1*<sup>-/-</sup> 70z/3 cells counterstained with DAPI. (C) Sucrose gradient followed by immunoblot analysis of Igμ in WT and KD pre-B cells under non-reducing and reducing conditions. (D) Immunoblot analysis of Igμ in WT and KD pre-B cell lysates treated with EndoH or PNGase F.

(r, s= EndoH resistant, sensitive). Quantitation of total Ig $\mu$  and EndoH (r) Ig $\mu$  shown below the blot. (E-F) Quantitation of mean fluorescent intensity (MFI) of surface pre-BCR components in (E) WT and KD pre-B cells and (F) WT pre-B cells treated with or without 25  $\mu$ M MG132 for 2 h. (G) Western blot analysis of phospho-(pSyk) and total Syk (Syk) of WT and KD cells crosslinked with  $\alpha$ -Ig $\mu$  (10  $\mu$ g/ml) for the indicated times with quantitation shown on the right. (H) Quantitation of flow cytometric analysis of BrdU incorporation in pro-/pre-B cells and  $\lambda$ 5<sup>+</sup> or  $\lambda$ 5<sup>-</sup> pro-/pre-B cells of *SellL<sup>ff</sup>* and *SellL<sup>CD19</sup>* mice with original flow data shown in Figure 3.11D. Data are representative of 2-3 independent experiments. n=6 mice each for (H). Values shown as mean  $\pm$  s.e.m.; \*P< 0.05, \*\*P<0.01, \*\*\*P<0.001 by two-tailed Student's t-test.

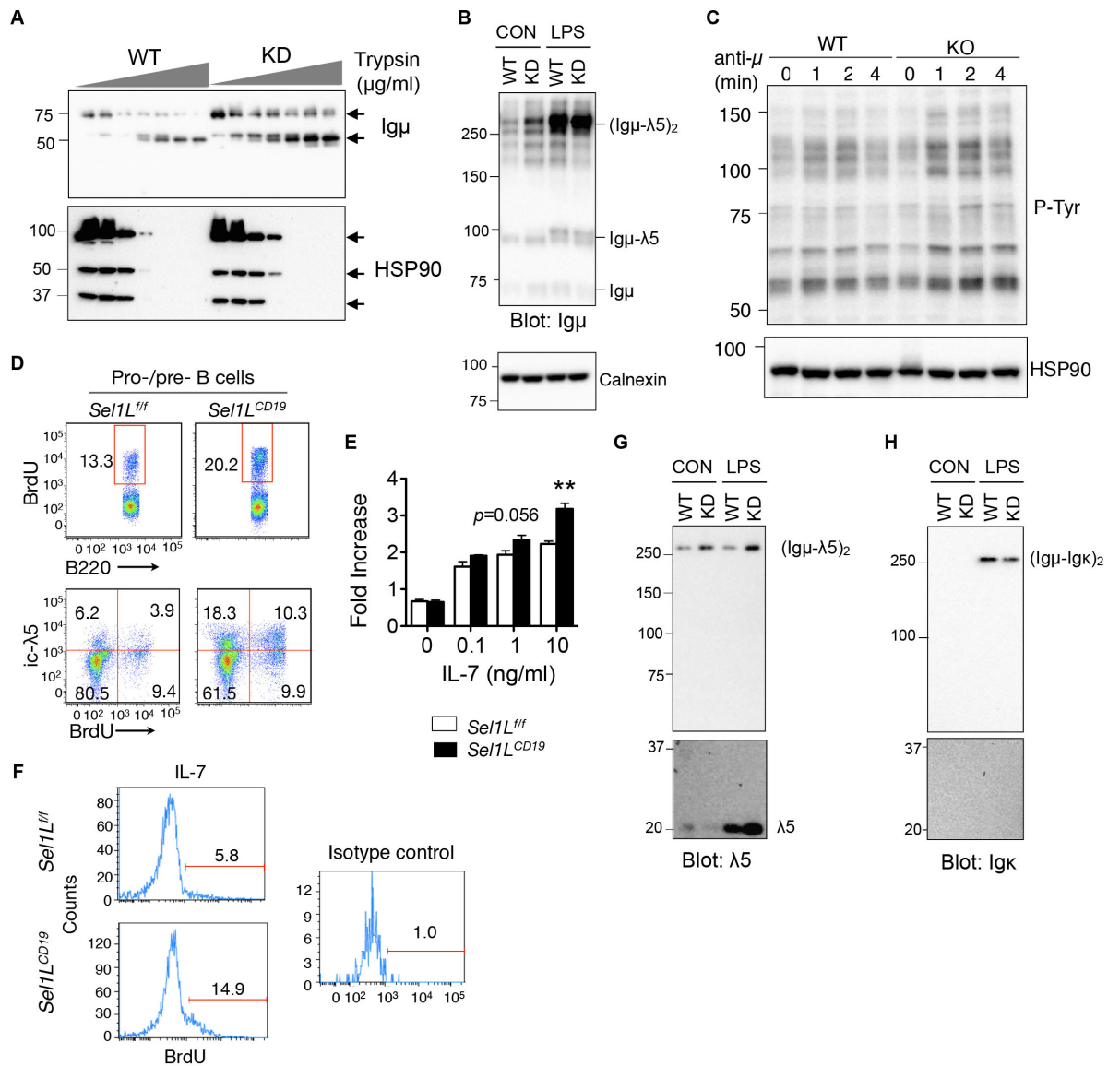


**Figure 3. 11 Consequence of ERAD deficiency on pre-BCR conformation and complex formation**

(A) Limited proteolysis digestion of WT and Sel1L KD cell lysates with varying concentrations of trypsin treatment, followed by Western blot analysis. (B, G, H) Western blot analysis of pre-BCR complex formation in mock- or LPS- (20  $\mu\text{g}/\text{mL}$ , 18h) treated WT and KD cells under non-reducing conditions. Same cell lysates were blotted for Ig $\mu$  (B),  $\lambda 5$  (G) and Ig $\kappa$  (H).

Representative data from 3 independent experiments shown. (C) Immunoblot analysis of overall

tyrosine phosphorylation in *WT* and *Hrd1*<sup>-/-</sup> pre-B cells cross-linked with  $\alpha$ -Ig $\mu$  (15  $\mu$ g/ml) at indicated times. (D) Flow cytometric analysis of BrdU incorporation in pro/pre-B cells (upper) and  $\lambda$ 5<sup>+</sup> or  $\lambda$ 5<sup>-</sup> pro-/pre-B cells (lower) of *SellL*<sup>ff</sup> and *SellL*<sup>CD19</sup> mice (n= 6 mice each), with quantitation shown in Figure 3.10H. Calnexin and HSP90, loading controls. (E-F) Effect of the IL-7 on proliferation of pro/pre-B cells in culture: (E) MACS sorted BM CD19<sup>+</sup> cells were cultured with various concentrations of IL-7 for 4 days. Absolute number of viable cells was counted and shown as cell number relative to starting point (fold increase). (F) FACS sorted BM large pre-B cells (B220<sup>low</sup>IgM<sup>-</sup>CD43<sup>low</sup>CD2<sup>-</sup>) were treated with IL-7 (1 ng/ml) for 2 days and BrdU incorporation in each population were analyzed.

### **3.4.7. Persistent pre-BCR signaling and pre-B cell cycling in *Sell1L<sup>CD19</sup>* mice.**

We next tested whether elevated surface pre-BCR results in augmented pre-BCR signaling, consequently inducing a burst of proliferation of large pre-B cells. Phosphorylation of the pre-BCR key downstream effector, spleen tyrosine kinase (Syk) (Herzog et al., 2009), was significantly increased in ERAD-deficient pre-B cells (Figure 3.10G), as was overall tyrosine phosphorylation (Figure 3.11C). Furthermore, the total number of BrdU-positive cycling pro-/pre-B cells in BM was increased by more than 50 % in *Sell1L<sup>CD19</sup>* mice compared to *Sell1L<sup>fl/fl</sup>* mice (Figure 3.10H and Figure 3.11D). Among them, only  $\lambda 5^+$  large pre-B cells were highly proliferative in *Sell1L<sup>CD19</sup>* mice, increasing more than 2.5 fold;  $\lambda 5^-$  pro-B cell proliferation did not increase in *Sell1L<sup>CD19</sup>* mice. Thus, *Sell1L* deficiency in B cells leads to elevated and sustained pre-BCR signaling and persistent proliferation of large pre-B cells. In aggregate, these findings demonstrate that the *Sell1L-Hrd1* ERAD is required to attenuate pre-BCR signaling by promoting its protein turnover.

### **3.4.8. *Sell1L-Hrd1* ERAD degrades the pre-BCR, not the BCR, complex.**

In the pre-BCR, SLC and  $Ig\mu$  assemble into a quaternary structure reminiscent of the BCR with VpreB and  $\lambda 5$  equivalent to the variable and constant regions (VL and CL), respectively, of IgL (Figure 3.12A). We compared how *Sell1L-Hrd1* ERAD targets pre-BCR for degradation by comparing the effect of ERAD on the pre-BCR vs. the BCR both in vitro and in vivo. Upon overnight LPS stimulation, 70z/3 pre-B cells differentiated into mature B cells expressing BCR with conventional  $\kappa$  chain replacing the SLC (Figure 3.11E-F), as previously reported (Paige et al., 1978). This unique feature allowed us to determine how ERAD affects the trafficking and stability of the pre-BCR vs. BCR complexes containing the same  $Ig\mu$  heavy chain in the same cell. Unlike  $Ig\mu$  in the pre-BCR, neither the steady-state protein level or stability of

Ig $\mu$  in the BCR complex, nor its endoH sensitivity (i.e. ER exit), were affected by Sel1L-Hrd1 ERAD deficiency in mature B cells (Figure 3.12B-D). This was not due to the lack of expression of ERAD components in mature B cells, as Sel1L and Hrd1 expression levels were comparable between pre- and mature B cells (Figure 3.12E).

To further test this in vivo, we analyzed mature splenic B cells from Sel1L-inducible knockout (*Sel1L<sup>ERCre</sup>*) mice expressing estrogen receptor-Cre recombinase fusion protein (ERCre) under the control of the actin promoter (Sun et al., 2014) (Figure 3.12F). Consistent with our in vitro observations, both intracellular Ig $\mu$  and surface BCR (IgM) levels were comparable between *Sel1L<sup>ff</sup>* and *Sel1L<sup>ERCre</sup>* mature B cells (Figure 3.12G). Moreover, plasma cell differentiation, cell size and total IgG levels in LPS/IL-4-treated mature primary B cells (*Sel1L<sup>ff</sup>* and *Sel1L<sup>ERCre</sup>*) were not affected by Sel1L deficiency (Figure 3.13A-C). Indeed, Ig $\mu$  interacted with several components of the ERAD machinery, including Sel1L and OS9, to a greater extent in pre-B cells compared to mature B cells (Figure 3.12H). Therefore, we concluded that the pre-BCR, but not the BCR, complex is an endogenous Sel1L-Hrd1 ERAD substrate.

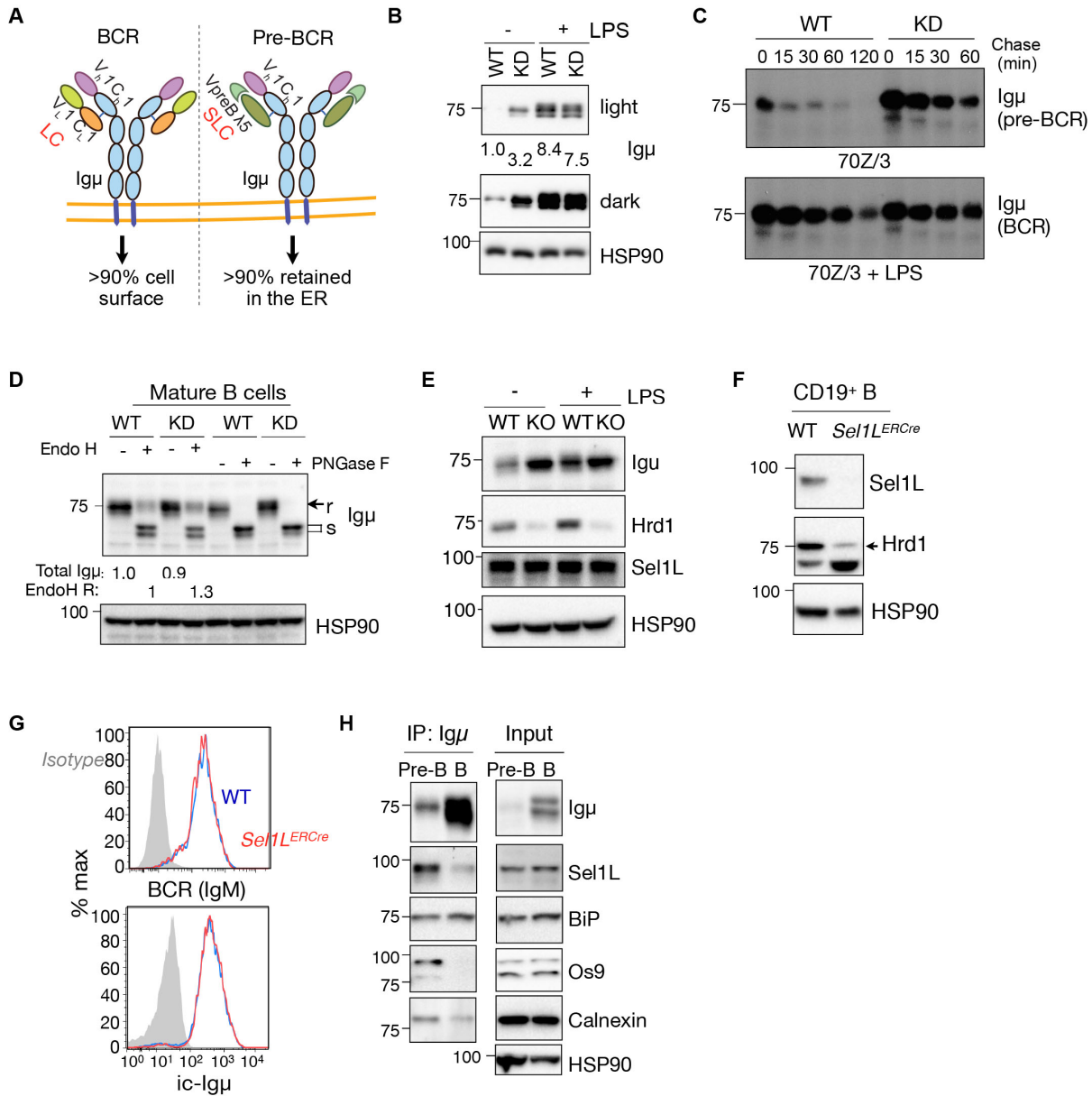


**Figure 3. 12 Sel1L-Hrd1 ERAD degrades the pre-BCR, but not the BCR complex.**

(A) Diagram depicting the difference between BCR and pre-BCR complexes. (B) Immunoblot analysis of Ig $\mu$  in WT and Sel1L KD cells (KD) treated with or without 20  $\mu$ g/mL of lipopolysaccharide (LPS) for 18 h, with quantitation shown below. (C) Pulse-chase analysis showing Ig $\mu$  decay in WT and KD 70Z/3 cells treated with or without 20  $\mu$ g/mL of LPS for 18 h. (D) Immunoblot analysis of Ig $\mu$  in WT and KD B cell lysates treated with EndoH or PNGase F.

(r/s= EndoH resistant/sensitive). Quantitation of total I $\mu$  and EndoH resistant (R) I $\mu$  shown below the blot. (E) Immunoblot analysis of ERAD proteins in *WT* and *Hrd1*<sup>-/-</sup> 70z/3 pre-B cells treated with or without 20  $\mu$ g/mL LPS for 18 h. (F) Western blot analysis of CD19<sup>+</sup> splenic B cells isolated from WT and *Sell1*-inducible knockout (*Sell1*<sup>ERCre</sup>) mice. (G) Histogram analysis of surface IgM and intracellular (ic) I $\mu$  in splenic B cells of WT and *Sell1*ERCre mice (N=3 mice each). (H) Immunoblot analysis of immunoprecipitates of I $\mu$ -agarose in pre-B 70z/3 and mature B cells. Representative of two independent experiments shown.

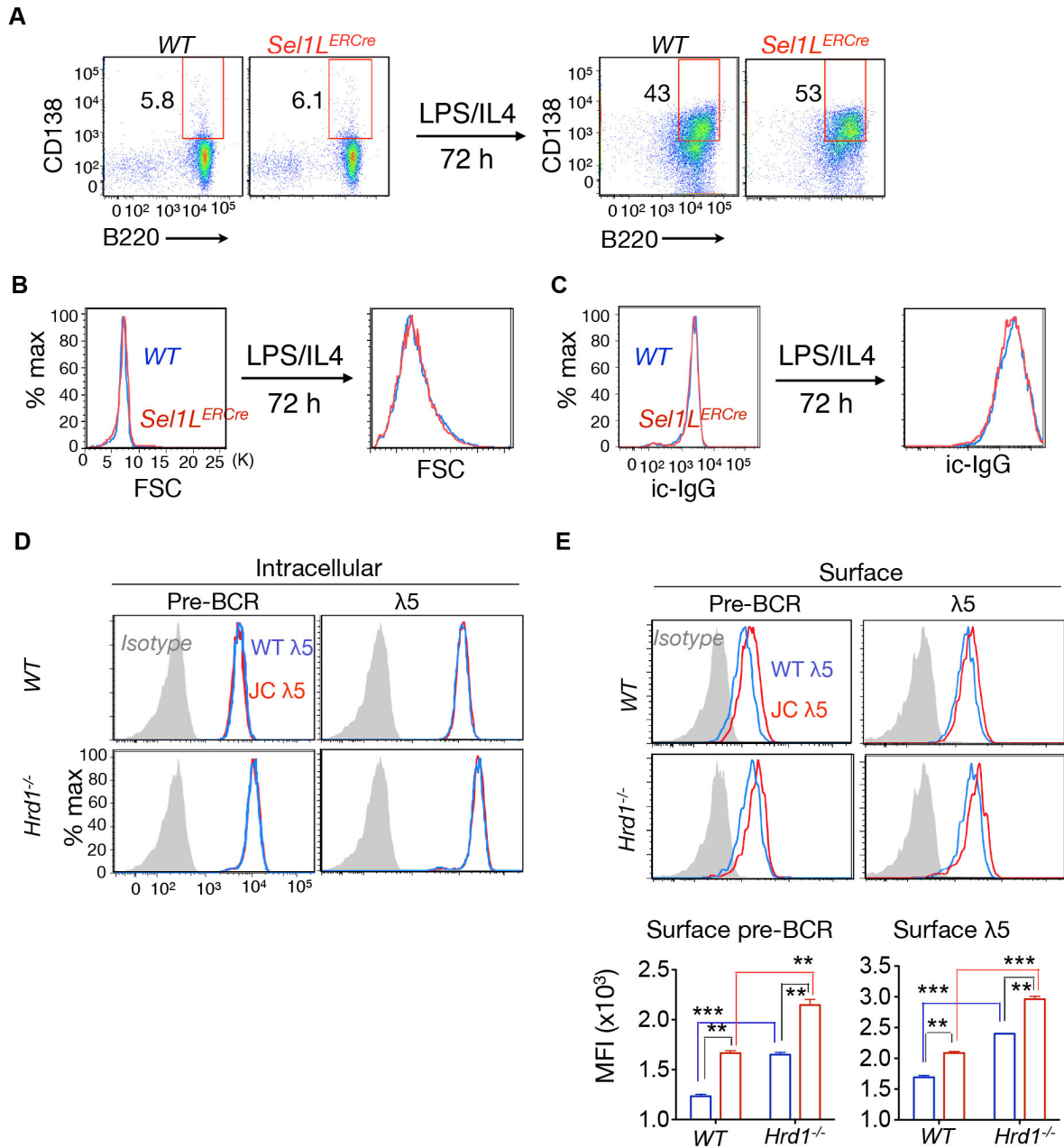


**Figure 3. 13 Sel1L-Hrd1 ERAD does not control the turnover of BCR, and ERAD-mediated pre-BCR degradation is independent of the unique region of  $\lambda 5$ .**

(A) Flow cytometric analysis of splenic B cells of WT and Sel1L-inducible knockout (*Sel1L<sup>ERCre</sup>*) mice before and after LPS/IL-4 stimulation. (B-C) Histogram analysis of cell size (B) and

intracellular (ic) IgG (C) in splenic B cells of WT and *Set1L<sup>ERCre</sup>* mice before and after LPS/IL-4 stimulation. (D-E) Flow cytometric analysis of intracellular (D) and surface (E)  $\lambda 5$  and pre-BCR in *WT* and *Hrd1<sup>-/-</sup> 70z/3* pre-B cells expressing WT or JC  $\lambda 5$ , with quantitation shown in Figure 3.14E and below respectively. Data are representative of two to three independent experiments (A-E), with n=6 mice each in (A-C). Values shown as mean  $\pm$  s.e.m.; \*\*P<0.01, \*\*\*P<0.001 by one-way ANOVA with Tukey post-test.

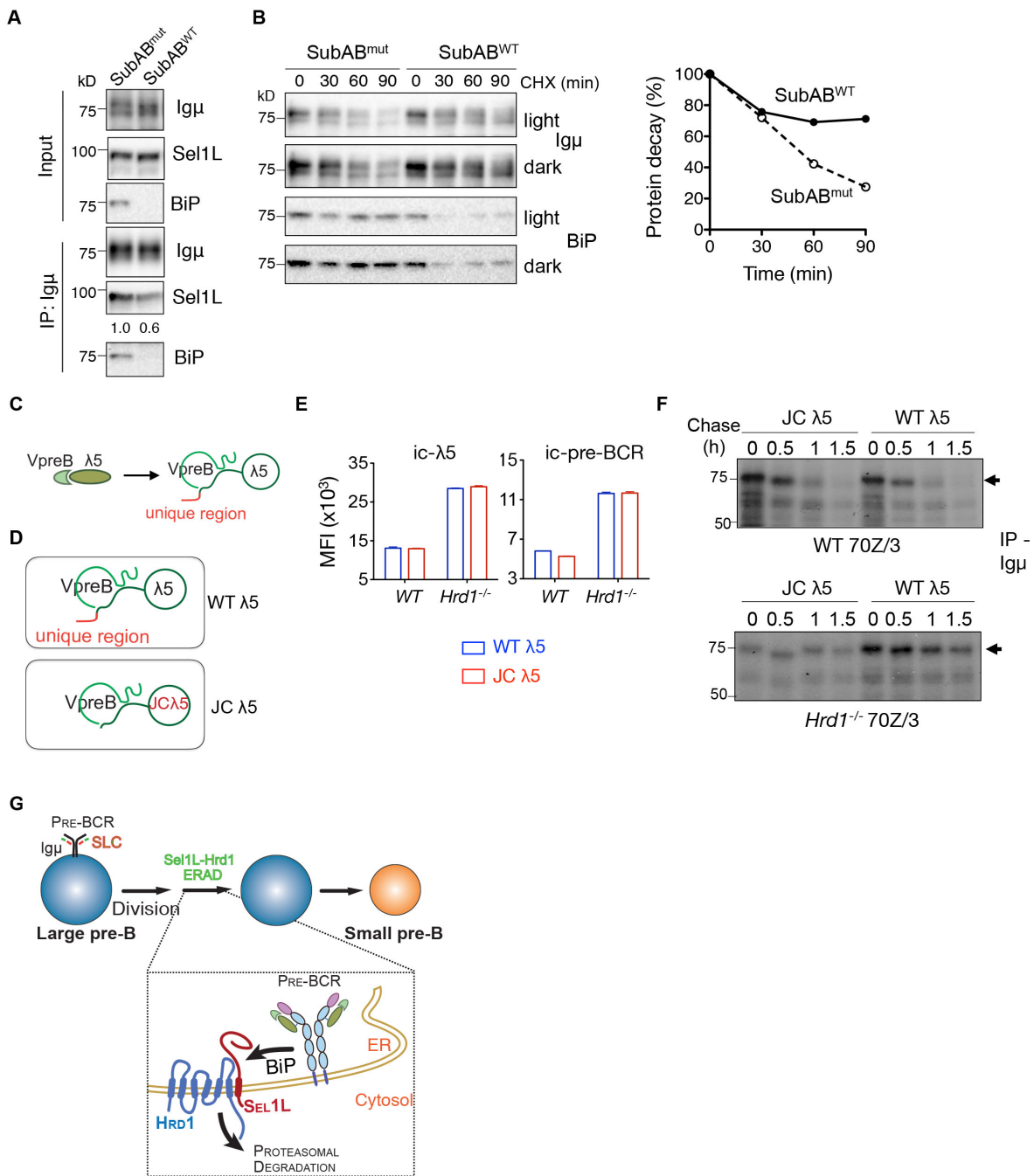


**Figure 3. 14 Sel1L-Hrd1 ERAD-mediated pre-BCR degradation is BiP-dependent but  $\lambda 5$  unique region-independent.**

(A) Immunoblot analysis of Ig $\mu$  immunoprecipitates in 70Z/3 cells treated with 0.5  $\mu$ g/ml

SubAB<sup>mut</sup> (SubA<sub>A272B</sub>) or SubAB<sup>WT</sup> for 45 min. (B) Translation shut-off assay of Ig $\mu$  in 70Z/3

cells treated by 50  $\mu\text{g/ml}$  cycloheximide (CHX) together with 0.5  $\mu\text{g/ml}$  SubAB<sup>mut</sup> or SubAB<sup>WT</sup> for the indicated times with quantitation shown on the right. (C) Schematic diagram depicting surrogate light chains (SLC). (D) Schematic diagram depicting SLC containing WT and mutant  $\lambda 5$  (JC  $\lambda 5$ ) lacking the unique region. (E) Quantitation of mean fluorescent intensity (MFI) of intracellular levels of  $\lambda 5$  (ic- $\lambda 5$ ) and pre-BCR in *WT* and *Hrd1*<sup>-/-</sup> 70z/3 pre-B cells expressing WT or JC  $\lambda 5$ . Values shown as mean  $\pm$  s.e.m. (F) Pulse-chase analysis showing I $\mu$  decay in *WT* and *Hrd1*<sup>-/-</sup> pre-B cells expressing WT or JC  $\lambda 5$ . Representative of two independent experiments shown. (G) The model: The Sel1L-Hrd1 ERAD manages the checkpoint in B cell development by targeting the pre-BCR for cytosolic proteasomal degradation (via BiP), which attenuates pre-BCR signaling and allows further B cell differentiation.

### 3.4.9. Pre-BCR ERAD requires BiP but is independent of the unique region of $\lambda 5$ .

As BiP is involved in the folding and intracellular trafficking of the pre-BCR complex (Minegishi, Hendershot, et al., 1999), we first tested whether BiP is required for pre-BCR ERAD. Depletion of BiP with the subtilase cytotoxin SubAB (Paton et al., 2006) significantly reduced the interaction between Ig $\mu$  and Sel1L (Figure 3.14A) and stabilized Ig $\mu$  protein (Figure 3.14B). Moreover, given that the pre-BCR and BCR complexes share the common Ig $\mu$  heavy chain, we speculated that a key determinant in pre-BCR recognition by ERAD may lie in the binding of SLC to Ig $\mu$ . We noted previous reports demonstrating that the unique region of  $\lambda 5$  (Figure 3.14C), which is a non-Ig portion and does not pair with either VpreB or Ig $\mu$  (Clark et al., 2014; Herzog et al., 2009), is known to retain pre-BCR complex in the ER (Fang et al., 2001; Minegishi, Hendershot, et al., 1999; Ohnishi et al., 2003). To determine the role of the unique region of  $\lambda 5$  in pre-BCR degradation, we expressed wildtype (WT  $\lambda 5$ ) and mutant  $\lambda 5$  lacking the unique region (JC  $\lambda 5$ , with only J and C parts of  $\lambda 5$ ) (Ohnishi et al., 2003) in *WT* and *Hrd1*<sup>-/-</sup> pre-B cells (Figure 3.14D).

Surprisingly, JC  $\lambda 5$  expression had no effect on total steady state intracellular levels of the pre-BCR complex in both *WT* and *Hrd1*<sup>-/-</sup> pre-B cells compared to those expressing WT  $\lambda 5$  (Figure 3.14E and Figure 3.13D). Moreover, total pre-BCR complex levels were higher in *Hrd1*<sup>-/-</sup> pre-B cells than those of WT cells expressing JC  $\lambda 5$  (Figure 3.14E), suggesting that the JC  $\lambda 5$ -containing pre-BCR complex remains to be an ERAD substrate. Consistently, JC  $\lambda 5$  expression failed to affect Ig $\mu$  protein half-life (Figure 3.14F). On the other hand, JC  $\lambda 5$  increased surface pre-BCR in WT pre-B cells as previously reported (Fang et al., 2001; Minegishi, Hendershot, et al., 1999; Ohnishi et al., 2003) (Figure 3.13E). Hence, we concluded that BiP, but not the unique region of  $\lambda 5$ , is required for the recognition of the pre-BCR complex as an ERAD substrate in pre-B cells.

### 3.5. DISCUSSION

This study shows that Sel1L-Hrd1 ERAD manages a key checkpoint in B cell development by selectively targeting the pre-BCR complex for proteasomal degradation. Indeed, Sel1L-Hrd1 ERAD complex is indispensable for the termination of pre-BCR signaling. B-cell-specific deficiency of the Sel1L-Hrd1 ERAD system blocks developmental progression at the large to small pre-B cell transition. Surprisingly, we show that the pre-BCR, not BCR, complex is an endogenous Sel1L-Hrd1 ERAD substrate in B cells and that Sel1L-Hrd1 ERAD has no obvious effect on plasma cell differentiation. Lastly, we show that ERAD-mediated pre-BCR degradation requires BiP, but independently of the unique region of  $\lambda 5$  known to be important for the ER retention of the pre-BCR complex.

Pre-BCR signaling marks a critical checkpoint in B cell development. The pre-BCR signal induces a burst of proliferation of large pre-B cells to ensure expansion of B cell precursors with a functional  $Ig\mu$  chain, a process known as “pre-BCR-dependent positive selection” (Hess et al., 2001; van Loo et al., 2007); and importantly, it downregulates its own expression via silencing the SLC genes, while upregulating recombination activating gene (Rag) expression and  $IgL$  rearrangement. Deficiency in VpreB (Mundt et al., 2001),  $\lambda 5$  (Kitamura, Kudo, et al., 1992), the transmembrane region of  $Ig\mu$  (Kitamura & Rajewsky, 1992),  $Ig\alpha$  (Kitamura & Rajewsky, 1992) and  $Ig\beta$  (Gong et al., 1996) all prevents entry into the proliferating large pre-B cell stage and leads to a marked enrichment of pro-B cells in the BM, resulting in a profound decrease in mature peripheral B cells (Herzog et al., 2009). As Sel1L deficiency leads to a B cell developmental block at a later stage, the molecular mechanism underlying the defect in the *Sel1L*<sup>CD19</sup> mice is unlikely due to a loss-of-function of the pre-BCR. Instead, our data (Wang, Y. H. et al., 2002)pre-BCR signaling. Persistent pre-BCR signaling, when the expression

of  $\lambda 5$  is extended (Martin, D. A. et al., 2007) or downstream negative effectors such as SLP-65 are inactivated (Jumaa et al., 1999), leads to elevated surface pre-BCR and continued cycling of large pre-B cells, preventing further differentiation. Similarly, *Sell1L*-deficiency in B cells results in intracellular accumulation and elevated surface pre BCR and signaling. Consequently, *Sell1L<sup>CD19</sup>* mice exhibit continued proliferation of large pre-B cells and decreased cellularity of small pre-B cells and mature B cells.

Expression and signaling from the pre-BCR complex are transient at the transition from the pro-B to the pre-B cell stage. Downregulation of pre-BCR signaling is a prerequisite for cell cycle exit and further differentiation to the resting small pre-B cell stage, such that IgL gene segment rearrangement can commence (Flemming et al., 2003; Kitamura, Kudo, et al., 1992; Melchers, 2005; Minegishi et al., 1998; Mundt et al., 2001; Parker et al., 2005; Shimizu et al., 2002). Self-limiting mechanisms include transcriptional silencing of SLC and dilution out of pre-BCRs due to large pre-B cell cycling. Our data show that the *Sell1L*-Hrd1 ERAD complex plays a key role in the termination of pre-BCR signaling in B cell development. Given the structural and composition similarity between the pre-BCR and the BCR complexes, our findings raise an intriguing question regarding substrate maturation in the ER and selection by ERAD. The binding of SLC to  $I\mu$ , unlike that of LC to  $I\mu$ , is likely to be much less efficient, associated more intensively with BiP and/or may expose folding intermediates of pre-BCR to the ERAD machinery. This model is consistent with earlier reports demonstrating that the pre-BCR complex is prone to misfolding and requires the activity of ER folding machinery (Hendershot, L. M., 1990; Minegishi, Coustan-Smith, et al., 1999), and that the majority of pre-BCR is retained in the ER, with less than 2 % reaching to the cell surface compared to 90 % of BCR reaching the cell surface in mature B cells (Brouns et al., 1996; Fagioli et al., 2001; Fang et al., 2001;

Hendershot, L. et al., 1987; Pillai et al., 1987). Moreover, the intrinsic ability of assembled pre-BCR complexes to exit the ER is limited by the unique region of  $\lambda 5$  (Fang et al., 2001; Minegishi, Hendershot, et al., 1999; Ohnishi et al., 2003). We show in this study that, while the unique region of  $\lambda 5$  controls the ER exit of the pre-BCR complex, it is dispensable for pre-BCR ERAD.

Our study demonstrates that the function of ERAD could not be accurately predicted solely on the basis of the abundance of secreted protein production. We speculate that this selectivity may derive from a particularly complex requirement for the folding of specific substrates in a cell type-specific manner, (in this case, the pre-BCR), rather than from the extent and the consequence of the UPR. Indeed, there was only very mild, if any, ER stress and cell death associated with *Sel1L*/ERAD deficiency in differentiating B cells. Moreover, *Sel1L*<sup>CD19</sup> mice exhibited phenotypes largely distinct from those with B cell-specific UPR deficiency (Hetz, 2012; Sha et al., 2011). For example, *Xbp1* deficiency blocks plasma cell differentiation from B cells, whereas it has no effect on B cell development (Reimold et al., 2001; Todd et al., 2009). IRE1 $\alpha$  deficiency causes a severe impairment of VDJ recombination of Ig genes and hence there is no expression of IgH and IgL chains of the BCR (Zhang, K. et al., 2005). This defect is associated with reduced expression of RAG1/2 and terminal deoxynucleotidyl transferase. On the other hand, the PERK-eIF2 $\alpha$  branch of the UPR is not required for B cell differentiation (Zhang, K. et al., 2005). Therefore, *Sel1L*-Hrd1 ERAD manages B cell development in an UPR-independent manner.

Polypeptides that do not meet the quality-control standards are retained within the ER and are recognized and retrotranslocated by the ERAD machinery for proteasomal degradation in the cytosol. Mammals possess a number of ERAD complexes, with the *Sel1L*-Hrd1 being the most conserved and characterized biochemically. A limited number of endogenous substrates of

Sel1L-Hrd1 ERAD complex have been identified in vitro, including ER luminal hedgehog, ATF6 and CD147 (Chen, X. et al., 2011; Horimoto et al., 2013; Tyler et al., 2012). More recently, nuclear proteins such as NRF2, Blimp1 and PGC1 $\beta$  have been identified as cell type-specific Hrd1 substrates in vivo (Fujita et al., 2015; Wu, T. et al., 2014; Yang, H. et al., 2014). We recently reported IRE1 $\alpha$  as an endogenous substrate for the Sel1L-Hrd1 ERAD in various cell types (Sun et al., 2015). Here we show that the pre-BCR complex is an endogenous ERAD substrate in developing B cells. Sel1L is required in this process likely as a key adaptor protein to stabilize Hrd1 protein as shown previously (Sun et al., 2014). Additionally, the physical interaction between the pre-BCR and Sel1L suggests that Sel1L may be intimately involved in pre-BCR turnover by recruiting the pre-BCR complex to the ligase Hrd1. As the pre-BCR is the first protein complex identified as an endogenous ERAD substrate to date, further investigation into its degradation mechanism may shed important mechanistic insights into substrate selection and protein degradation in vivo.

### **3.6. ACKNOWLEDGEMENT**

We thank Drs. Yihong Ye, Linda Hendershot, James C. Paton, and Richard Wojcikiewicz for reagents; Drs. Yihong Ye, Cynthis A. Leifer, and Margaret S. Bynoe for critical comments on our manuscript; and other members of the L.Q. lab for comment and technical assistance. This work was supported by NIH grant R03AI074801 -01 and the Dean of the College of Medicine, State University of New York-DMCNIH (to C.A.R.); grants R01GM113188 and R01DK105393, Juvenile Diabetes Research Foundation 1-SRA-2014-251-Q-R, and American Diabetes Association (ADA) 1-12-CD-04 (to L.Q.). L.Q. is the recipient of the Junior Faculty and Career Development Awards from the ADA.

**CHAPTER FOUR: B CELL SPECIFIC SEL1L  
ABLATION PROMOTES PROPAGATION OF  
COLITOGENIC MICROBIOTA**

## 4.1 INTRODUCTION

Inflammatory bowel disease (IBD) is characterized by uncontrolled inflammatory responses in the gastrointestinal tract, mounted against antigens displayed by commensal bacteria. Although the combinations of different factors have been reported to initiate this disease, the exact etiology and mechanistic basis remain unclear. Thus a comprehensive understanding of the mechanisms underlying the regulation of innate immunity and inflammation is of both fundamental and clinical relevance.

The epithelial surface of the gastrointestinal tract serves as a physical barrier against gut microbiota, thereby providing a first layer of defense against infection and inflammation. At the luminal surface of the intestinal epithelial cells is layers of mucosa, which forms second layer of protection. Final layer of protection is mounted by numerous immune cells which resides in the gut, either in gut associated lymphoid tissues (GALT) such as Peyer's patches and mesenteric lymph nodes, or scattered throughout the intestinal epithelium and lamina propria.

Amongst different immunoglobulin isotypes, immunoglobulin A (IgA) is the main antibody isotype which is secreted into the intestinal lumen. This secretory IgA (sIgA) serves as the first line of defense in protecting the intestinal epithelium cells from enteric toxins and microbiota : 1) by antigen (Ag) neutralization; 2) prevention of microbial attachment to the epithelium; 3) elimination of excessive Ag load, and; 4) the overall maintenance of mucosal homeostasis (Johansen et al., 1999; Lamm, 1997; Langford et al., 2002; Underdown et al., 1986; Uren et al., 2003). The importance of IgA production and the quality of IgA affinity in maintaining gut homeostasis has been demonstrated by several groups (Cao et al., 2012; Cataldo et al., 1998; Friman et al., 2002; Malik et al., 2016; Meini et al., 1996; Murthy et al., 2006; Okai et al., 2016). Our previous study has demonstrated that Sell1L-Hrd1 ERAD manages a key

checkpoint in B cell development by selectively targeting the pre-BCR complex for proteasomal degradation, but has no apparent effect on plasma cell differentiation (Ji et al., 2016). However, the role of *Sel1L* and *Sel1L-Hrd1* ERAD in the B cell function in mucosal immunity remains unknown.

Here, we tested sensitivity of wildtype (WT) and B cell specific *Sel1L* deficient mice to dextran sodium sulfate (DSS)-induced colitis. Our data show that *Sel1L<sup>CD19</sup>* mice are hypersensitive to DSS-induced experimental colitis and strikingly, the susceptibility to colitis is transmissible to co-housed WT littermates. These data point to the presence of colitogenic microbiota in the intestinal tract of *Sel1L<sup>CD19</sup>* mice. Mechanistically, we observed that *Sel1L<sup>CD19</sup>* mice have reduced mature B cells in the gut-associated lymphoid tissues (GALT), reduced levels of IgA in lamina propria and feces. While more mechanistic studies are under way, our data show that B-cell-specific *Sel1L-Hrd1* ERAD pathway is indispensable for B cell development and that ablation of this pathway leads to IgA deficiency and may create an intestinal niche that favors the outgrowth of colitogenic microbe(s).

## 4.2 MATERIALS AND METHODS

### Mice

*Sel1L<sup>ff</sup>* mice on the C57B/L background have been described (Sun et al., 2014) and crossed with CD19 promoter-driven Cre (*CD-19Cre*) mice from Jackson Laboratory (B6.129P2(C)-Cd19tm1(cre)Cgn/J, #006785) to generate *Sel1L<sup>ff</sup>; CD19-Cre<sup>+</sup>* (*Sel1L<sup>CD19</sup>*) and control *Sel1L<sup>ff</sup>; CD19-Cre<sup>-</sup>*(*Sel1L<sup>ff</sup>*) littermates at a 1:1 ratio. Mice were housed under specific pathogen-free conditions and fed on a low-fat diet consisting of 13 % fat, 6 7% carbohydrate, and 20 % protein (Harlan Teklad 2914, Madison, WI). For cohousing experiments, age- and gender-matched *Sel1L<sup>ff</sup>*, *Sel1L<sup>CD19</sup>* and C57BL/6J mice were co-housed at the age of 4 weeks, in

new cages at 1:1:1 ratio for 4 weeks. For cross-fostering experiments, newborn mice were exchanged between *SellL<sup>CD19</sup>* and C57BL/6J mothers within 24 hr of birth. Mice were weaned between postnatal days 21-28 and used at the age of 6-12 weeks in all in vivo experiments.

### **In vivo experiments**

Mice were fed ad libitum with 3 % (wt/vol) DSS (molecular weight 40-50 kDa; Affymetrix, Santa Clara, CA) dissolved in drinking water for 5 days and then fresh water thereafter. Body weights were monitored every other day until the end of experiments. Mice were sacrificed by cervical dislocation. Intestinal tissues were immediately harvested and fixed in 10% neutralized Formalin for histology or flushed with phosphate-buffered saline (PBS) for immune cell isolation from lamina propria. All animal procedures were approved by the Institutional Animal Care and Use Committee at Cornell University.

### **Isolation of lamina propria (LP) immune cells from colonic tissues**

In brief, the intestine was removed from mesenteric fat tissues and Peyer's patches were excised. The feces were flushed with PBS and the tissues were cut into pieces in ice-cold PBS. Tissues are incubated with pre-digestion solution containing EDTA and dithiothreitol (DTT) in Hank's balance salt solution (HBSS) for 20 minutes at 37 °C under slow rotation (40 g). The suspensions were vortexed and passed through a 100 µm cell strainer to remove epithelial cells, villus cells, subepithelial cells and intraepithelial lymphocytes (IELs). The remaining LPs and muscle layers were resuspended in digestion buffer containing collagenase D, DNase I, and dispase II and incubated at 37 °C under slow rotation (40 g) for 20 minutes. After incubation, the suspensions were vortexed and passed through a 40 µm cell strainer. The supernatants were centrifuged for 10 min at 500 g at 20 °C. The supernatants were discarded and the remaining pellets were resuspended in cold FACS buffer and centrifuged at 500 g for 10 minutes at 20 °C.

The pellets were resuspended in 10 ml of the 40 % fraction of the Percoll solution and carefully overlaid on top of 5 ml of the 80 % fraction of the Percoll solution. The 40/80 Percoll gradient was centrifuged for 20 minutes at 1000 g at 20 °C without brakes. The cells were resuspended in cold PBS (5 % FBS, 1 % Penicillin/Streptomycin) for flow cytometry analysis (Weigmann et al., 2007)

### **Flow Cytometry**

Flow cytometric analysis of immune cells was performed as we previously described (Ji et al., 2014; Ji et al., 2012). Lymphocytes isolated from colonic lamina propria were washed and resuspended in cold PBS (5 % FBS, 1 % Penicillin/Streptomycin). The cell suspension was stained with either 1:100 or 1:200 fluorochrome- or biotin conjugated antibodies against B220 (RA3-6B2), CD4 (GK1.5), CD8 (YTS169), Gr-1 (RB6-8C5), CD11b (M1/70), CD69 (H1.2F3), IgA (RMA-1), avidin-FITC and isotype control antibodies were purchased from BioLegend or BD Biosciences. The samples were collected by BD LSR cell analyzer at the Flow Cytometry Core Facility at Cornell University and the data were analyzed using the CellQuest software (BD Biosciences) and Flowjo (Flowjo.com)

### **Histological analysis, Immunofluorescent staining and Immunohistochemistry**

For the immunofluorescent staining, tissues were fixed in 10 % neutralized Formalin for 24 hours at 4 °C, immersed in 30 % sucrose solution for 24 hours at 4 °C and embedded Tissue-Tek OCT (optimum cutting temperature) solution and stored at -80 °C until sectioning. The frozen intestinal sections were washed with PBS and blocked with 5 % normal donkey serums/ 1 % Triton X-100 in PBS for 45 minutes at room temperature. The sections were incubated with Biotinylated-IgA (1:100, BioLegend) overnight at 4 °C. Next day, the sections were washed with PBS and incubated with Streptavidin-FITC (1:200) for 1 hour at room temperature. The sections

were washed at the end of the incubation and mounted with Prolong Gold Anti-fade Reagent with DAPI (Invitrogen). Fluorescent microscopic images were taken under a Nikon A1 confocal microscope at the Imaging Laboratory of the Brehm Center for Diabetes Research in University of Michigan.

For the immunohistochemistry (IHC) staining, tissues were fixed in 10 % neutralized Formalin and embedded in paraffin by the Cornell Histology Core Facility on a fee-for-service basis. The paraffin-embedded intestinal sections were rehydrated, boiled in 1 mM EDTA for antigen retrieval and stained with Histostain kit and DAB substrate from Invitrogen. Antibody used for IHCs is Ki-67 (1:50, Abcam). Sections stained with hematoxylin and eosin (H&E) and IHC were scanned using a brightfield ScanScope high-resolution digital image capture system (Aperio Technologies, Inc., Vista, CA) and photomicrographs were taken using Aperio ImageScope v.10.0 software.

For the assessment of the severity of experimental colitis, histological scores of the distal colon were blindly determined based on goblet cell loss, crypt abscesses, immune cell infiltration and epithelial erosion (0, none; 1, low; 2, moderate; 3, high; 4, maximal) as previously described (Wirtz et al., 2017).

### **Statistical analysis**

Results are expressed as mean  $\pm$  SEM. Comparisons between groups were made by unpaired two-tailed Student's t-test unless otherwise indicated. Survival curves were compared by the log-rank (Mantel–Cox) test.  $p < 0.05$  was considered statistically significant. All experiments were repeated at least two to three times, and representative data are shown.

## 4.3 RESULTS

### 4.3.1. Defect in Gut Associated Lymphoid Tissue (GALT) development and reduced IgA production in *SellL<sup>CD19</sup>* mice.

The initial analysis revealed an aberrant reduction in the total number of Peyer's patches on the small intestine of *SellL<sup>CD19</sup>* mice (Figure 4.1A). Moreover, the IHC analysis showed a dramatic reduction in the number of proliferating cells (Ki67+ cells) in the Peyer's patches of *SellL<sup>CD19</sup>* mice, suggesting a reduction in germinal center B cells (Figure 4.1B). Flow cytometry analysis of Peyer's patches and mesenteric lymph node (mLN) also revealed a significant decrease in B220<sup>+</sup>IgA<sup>+</sup> cells (Figure 4.1C) in *SellL<sup>CD19</sup>* mice. Consistent with the reduced IgA<sup>+</sup> plasma cells, the total secreted IgA level in fecal samples of *SellL<sup>CD19</sup>* mice was also reduced (Figure 4.1D). Of note, despite the reduction in IgA producing B cells, the circulating IgG and IgM concentrations remain comparable under steady state and after nitrophenylated-chicken gamma globulin (NP-CGG) antigen immunization (data not shown). Finally, immunofluorescent analysis of the large intestine revealed, that in comparison to the *SellL<sup>ff</sup>* mice, IgA-expressing plasma cells in the lamina propria were also substantially reduced in *SellL<sup>CD19</sup>* mice (Figure 4.1E).

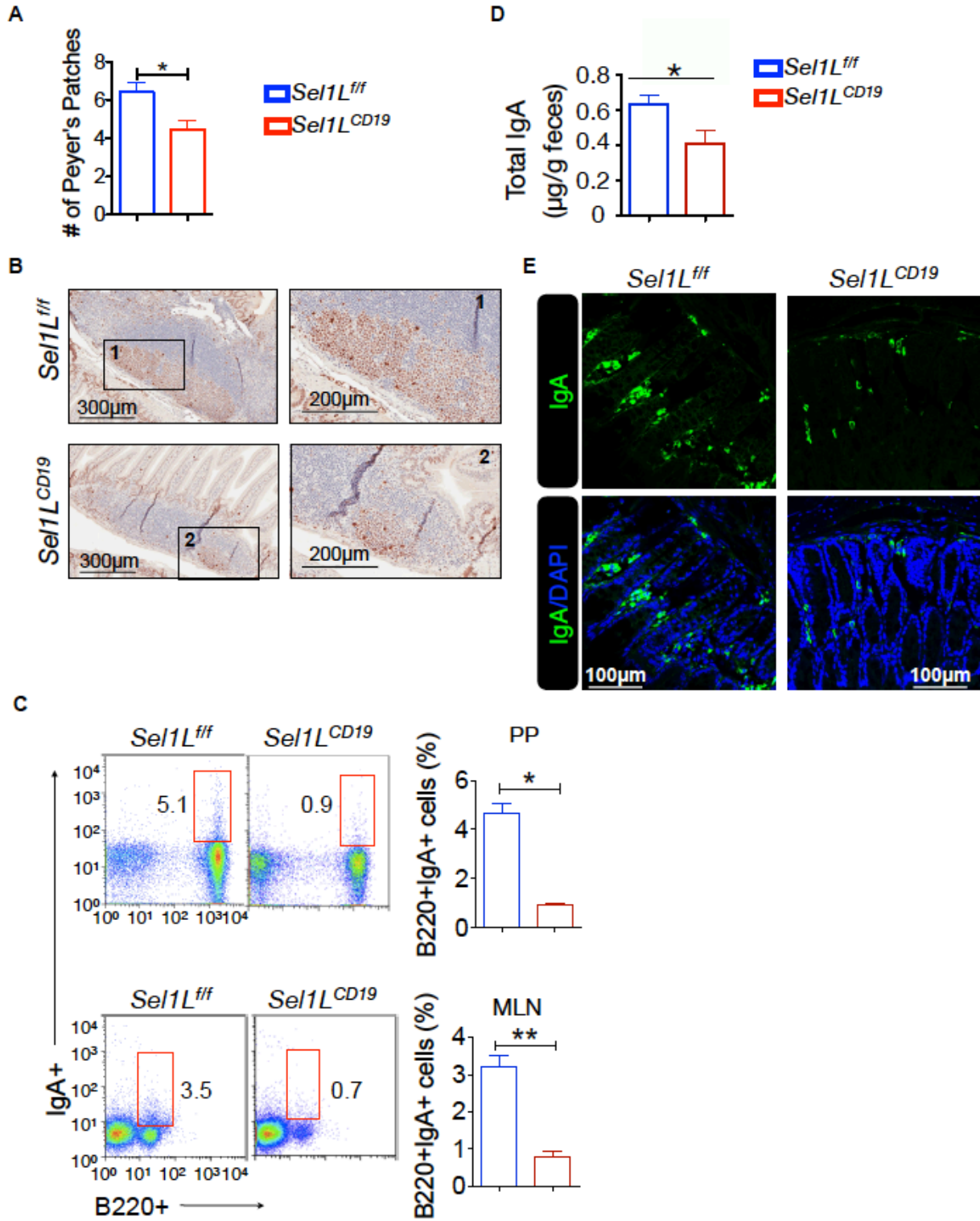


**Figure 4. 1 Defect in Gut Associated Lymphoid Tissue (GALT) development and reduced IgA production in in  $Sel1L^{CD19}$  mice.**

(A) The number of Peyer's patches (PP) from *SellL<sup>ff</sup>* mice and *SellL<sup>CD19</sup>* mice. (B) Immunohistochemistry of Ki67 of PP. Note decreased germinal center size. (C) Flow cytometric analysis of IgA<sup>+</sup> B cells from PP and mesenteric lymph nodes (MLN) of *SellL<sup>ff</sup>* mice and *SellL<sup>CD19</sup>* mice with quantitation shown on the right (D) Total IgA levels in feces of *SellL<sup>ff</sup>* mice and *SellL<sup>CD19</sup>* mice (E) Representative confocal microscopic images of IgA<sup>+</sup> B cells (green) in lamina propria of colon. Data are representative of two independent experiments in (A-E), n= 5 *SellL<sup>ff</sup>* and 5 *SellL<sup>CD19</sup>* Values shown as mean ± s.e.m.; \*\*P< 0.01, \*\*\*P<0.001 by two-tailed Student's t-test.

#### 4.3.2. *SellL*<sup>CD19</sup> mice are more susceptible to DSS induced colitis and the phenotype is transmissible

Human and mice with IgA deficiency or mice with lower number of high-affinity IgA have been shown to be more susceptible to colitis (Cao et al., 2012; Cataldo et al., 1998; Friman et al., 2002; Malik et al., 2016; Meini et al., 1996; Murthy et al., 2006; Okai et al., 2016). To address whether reduced IgA producing plasma cells in GALT leads to dysregulated inflammatory response, mice were treated with 3 % DSS in water for 5 days. As we have speculated, *SellL*<sup>CD19</sup> mice developed more severe colitis compared to single-housed JAX B6 (SH) control mice (Figure 4.2A). The knockout mice displayed colon shortening, a typical clinical features of colonic inflammation (Figure 4.2B). Histological analysis of distal colon revealed almost complete loss of crypts and goblet cells, massive immune cell infiltration, transmural edema and increased colonic mucosal erosion/ulceration in DSS-treated *SellL*<sup>CD19</sup> mice at day 10 (Figure 4.2C-D). Unexpectedly, co-housed wild type littermate *SellL*<sup>ff</sup> mice also became more susceptible to colitis when compared to JAX B6 (SH) control (Figure 4.2A-D). The flow cytometry analysis of the mLN of these 3 cohorts, under experimental colitis revealed that, while B cell population was dramatically decreased only in *SellL*<sup>CD19</sup> mice (Figure 4.3A), the neutrophil infiltration was significantly increased in both *SellL*<sup>CD19</sup> and *SellL*<sup>ff</sup> mice. (Figure 4.3B) when compared to JAX B6 (SH) mice. The activated T cell populations (CD69<sup>+</sup>CD4<sup>+</sup> and CD69<sup>+</sup>CD8<sup>+</sup> T) in *SellL*<sup>CD19</sup> and *SellL*<sup>ff</sup> mice were also higher than the JAX B6 (SH) mice, which is consistent with the histological analysis of the distal colon of these mice (Figure 4.3C-D).

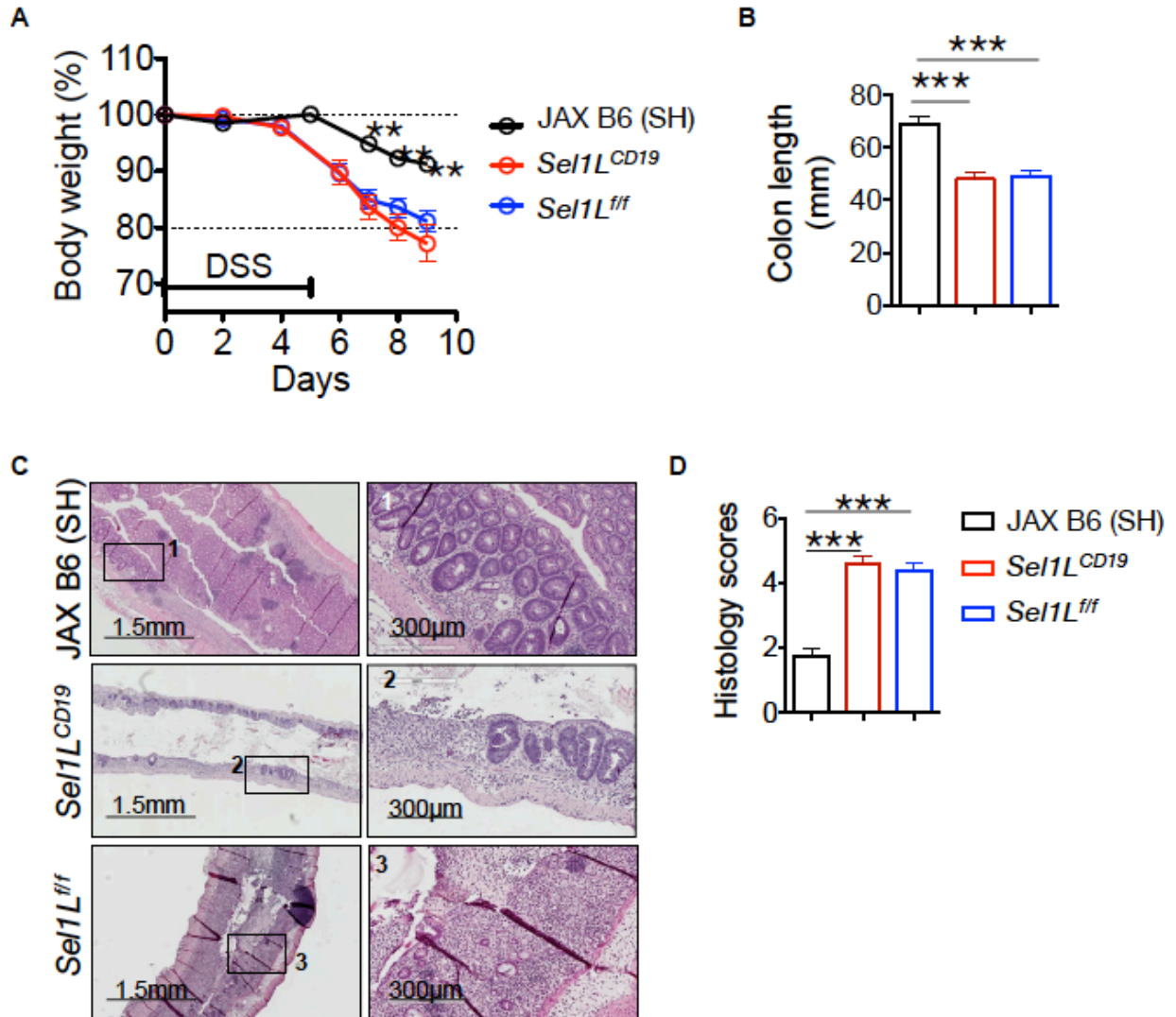


**Figure 4. 2 *Sel1L<sup>CD19</sup>* and *Sel1L<sup>fl/fl</sup>* mice are highly susceptible to DSS induced colitis.**

(A-D) 8-week-old littermates and JAX B6 single-housed (SH) mice were treated with 3 % DSS for 5 days followed by fresh water. (A) Body weight change. (B) Colon length on day 9. (C) Haematoxylin and eosin (H&E) images of colon on day 9 showing epithelial cell ulceration, severed edema and regenerative crypts. (D) Inflammatory score of colon on day 9 as a blind study. 0, none; 1, low; 2, moderate; 3, high; 4, maximal. Data are representative of two independent experiments in (A-D), n= 5 each Values shown as mean  $\pm$  s.e.m.; \*\*P< 0.01, \*\*\*P<0.001 by two-tailed Student's t-test.

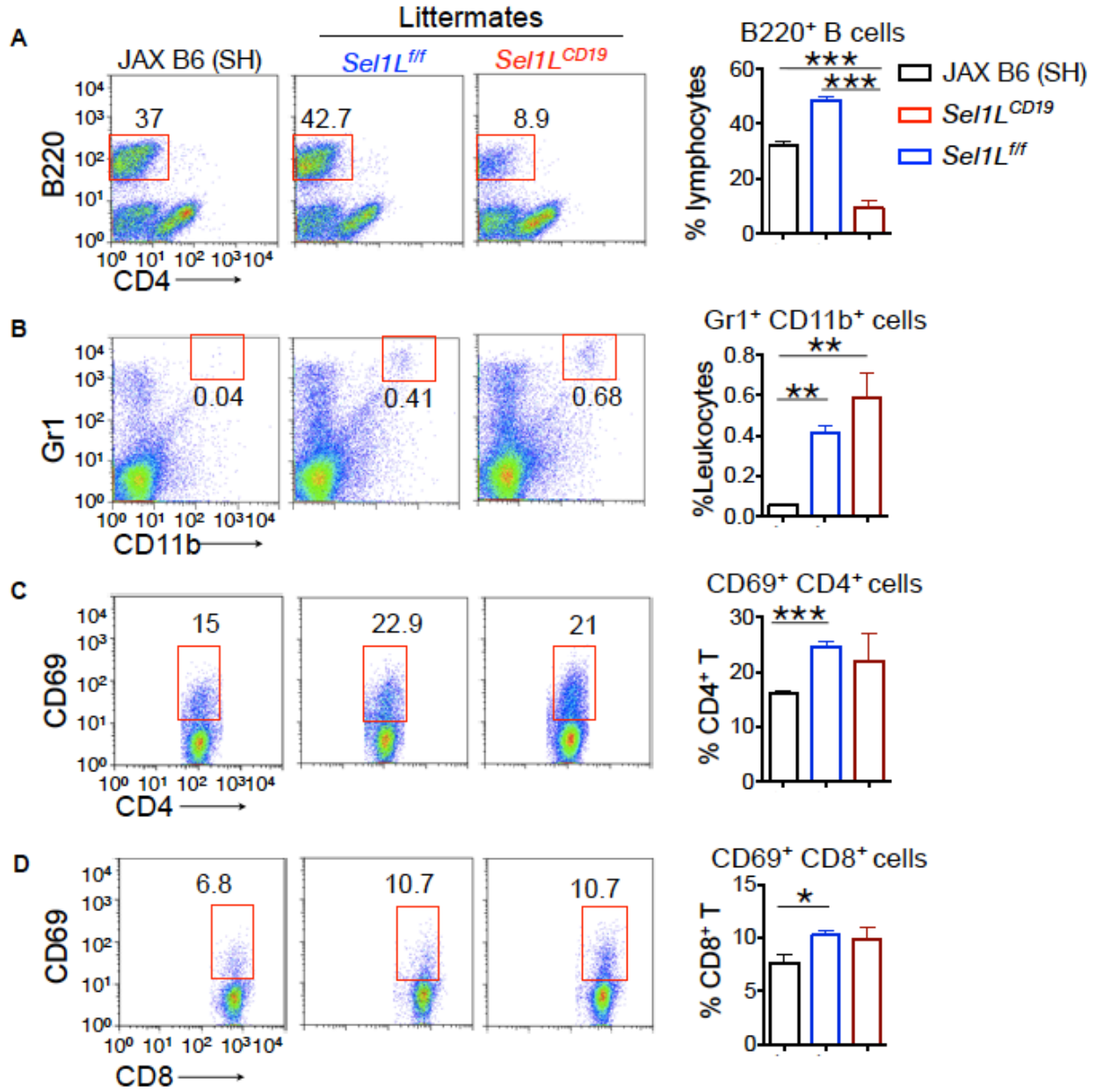


**Figure 4.3 Elevated immune cell activation in DSS treated *Sel1L<sup>CD19</sup>* and *Sel1L<sup>ff</sup>* mice.**

(A-D) Flow cytometric analysis of MLN cell isolated from *Sel1L<sup>ff</sup>* mice, *Sel1L<sup>CD19</sup>* and JAX B6 single-housed (SH) on day 9 post-DSS treatment: (A) B cells, (B) neutrophils, (C) activated CD4<sup>+</sup> T cells, and (D) activated CD8<sup>+</sup> T cells. Quantification in percentage shown on the right. Data are representative of two independent experiments in (A-D), n= 5 *Sel1L<sup>ff</sup>* and 5 *Sel1L<sup>CD19</sup>*

and 5 JAX B6(SH). Values shown as mean  $\pm$  s.e.m.; \*\*P< 0.01, \*\*\*P<0.001 by two-tailed Student's t-test.

### **4.3.3. Colitogenic microbiota not transmissible to non-littermate wildtype mice.**

To assess whether the differences in colitis severity observed between groups of littermates and JAX B6 (SH) mice were driven by differences in their intestinal microbiota, *SellL<sup>CD19</sup>* mice were co-housed with JAX B6 mice at 1:1 ratio, at 3 weeks of age, for 4 weeks before chemically inducing colitis. To our surprise, the co-housed JAX B6 mice did not develop severe colitis as we had speculated, but remained comparable to JAX B6 (SH) mice (Figure 4.4A). Consistently, the histological analysis revealed similar levels of immune cell infiltration between two cohorts of JAX B6 mice (Figure 4.4B-C) and the structure of the crypt remained intact (Figure 4.4D)

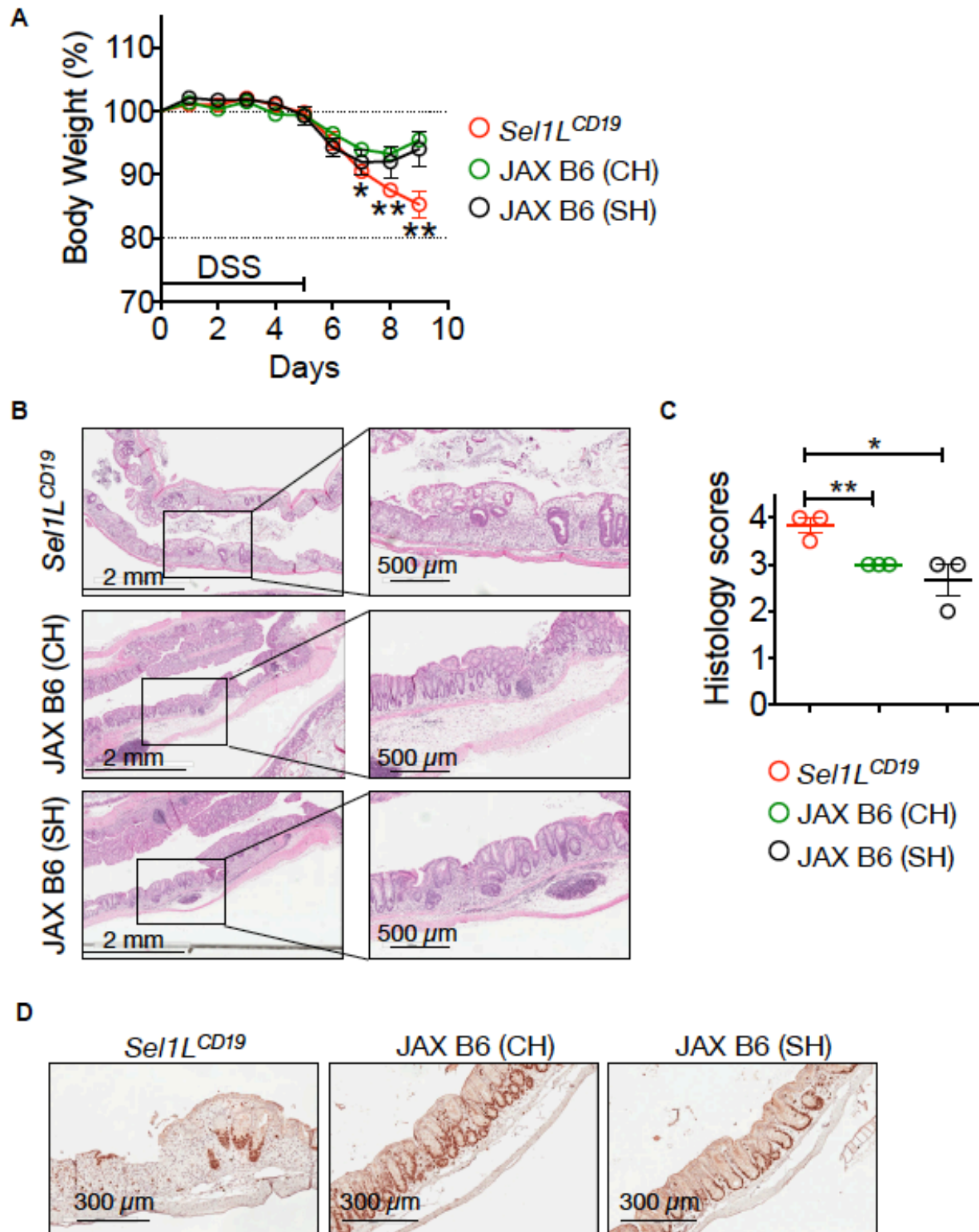


Figure 4. 4 Colitogenic microbiota are not transmissible to non-littermate wildtype mice.

(A-D) 3-week-old *SellL<sup>CD19</sup>* mice and JAX B6 mice were co-housed for 4 weeks, followed by 3% DSS treatment for 5 days. (A) Body weight change. (B) H&E images of colon on day 9 showing epithelial cell ulceration, severe edema and regenerative crypts. (C) Inflammatory score of colon on day 9 as a blind study. 0, none; 1, low; 2, moderate; 3, high; 4, maximal. (D) Immunohistochemistry of Ki67 of colon collected on day 9 post-DSS treatment. Data are representative of two independent experiments in (A-D), n= 5 *SellL<sup>ff</sup>* and 5 *SellL<sup>CD19</sup>*. Values shown as mean  $\pm$  s.e.m.; \*\*P< 0.01, \*\*\*P<0.001 by two-tailed Student's t-test

#### 4.3.4. Colitogenic phenotype is vertically transmissible, only from *SellL*<sup>CD19</sup> female mice.

Another route by which mice share intestinal microbiota is through mother to pups., as pups receive their first microbial exposure during vaginal delivery, from the vaginal and fecal microbiota of the mother. To further assess whether the intestinal microbiota, transmitted from mother to pups, contributes to differential inflammatory response, we performed cross-fostering experiments. Newborn JAX B6 mice cross-fostered (CF) at birth with *SellL*<sup>CD19</sup> mother exhibited more severe colitis compared to non-cross-fostered JAX B6 mice (Figure 4.5A-D). Interestingly, newborn *SellL*<sup>CD19</sup> mice exhibited milder body weight loss and milder colon shortening (Figure 4.5E-F) compared to non-cross-fostered *SellL*<sup>CD19</sup> mice, while histological analysis revealed similar immune cell infiltration between two cohorts (Figure 4.5G-H).

Studies have shown that newborn relies on passive secretory IgA (sIgA) in breast milk to shape the composition of microbiota, which persist into adulthood (Brandtzaeg, 2010; Janoff et al., 2012; Macpherson et al., 2012; Rogier et al., 2014). Furthermore, epidemiological studies suggest that early exposure to breast milk reduces the risk of developing inflammatory bowel disease (IBD) in children (Barclay et al., 2009). To assess whether the sIgA in breastmilk from *SellL*<sup>CD19</sup> mother is the underlying factor which induces the propagation of colitogenic microbiota in offsprings, generated *SellL*<sup>CD19</sup> offspring that would receive different amount of passive sIgA in breast milk. By breeding *SellL*<sup>ff</sup> dams, with *SellL*<sup>CD19</sup> males, we generated *SellL*<sup>CD19</sup> offsprings that received breast milk abundant of passive sIgA, compared to offsprings from *SellL*<sup>CD19</sup> dams and *SellL*<sup>ff</sup> male (Figure 4.6A). The *SellL*<sup>CD19</sup> ♂ offsprings which received breastmilk with abundant IgA, exhibited much milder colitis when compared to *SellL*<sup>CD19</sup> ♀ offsprings, which received breastmilk with less abundant IgA (Figure 4.6B). The colon shortening and immune cell infiltration in *SellL*<sup>CD19</sup> ♂ offsprings were also less severe than that of *SellL*<sup>CD19</sup> ♀ offsprings (Figure 4.6C-D)

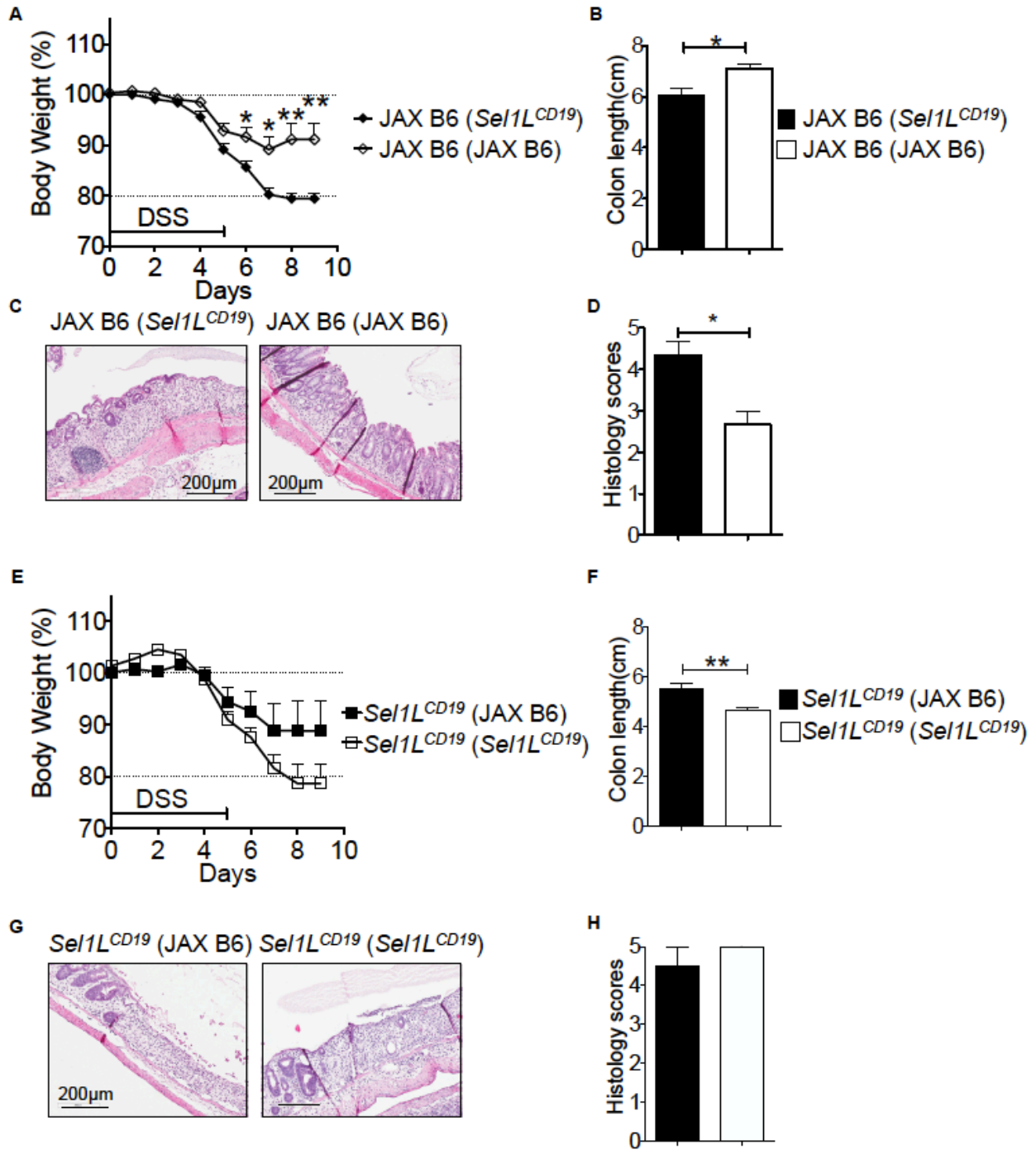


**Figure 4.5** Colitogenic phenotype is vertically transmissible, only from *Sel1L<sup>CD19</sup>* female mice.

(A-H) Newborn *Sel1L<sup>CD19</sup>* and JAX B6 mice were swapped between their respective mothers (cross-fostered), followed by induction of acute DSS colitis at 8 weeks of age.

(A, E) Body weight change and (B, F) colon length were measured in *SellL<sup>CD19</sup>* and JAX B6 mice cross-fostered with either *SellL<sup>CD19</sup>* or JAX B6 mothers. (C, G) H&E images of colon and (D, H) Inflammatory score of colon were analyzed on day 9 post 3 % DSS treatment. Data are representative of two independent experiments in (A-H), n= 5 mice each Values shown as mean  $\pm$  s.e.m.; \*\*P< 0.01, \*\*\*P<0.001 by two-tailed Student's t-test.

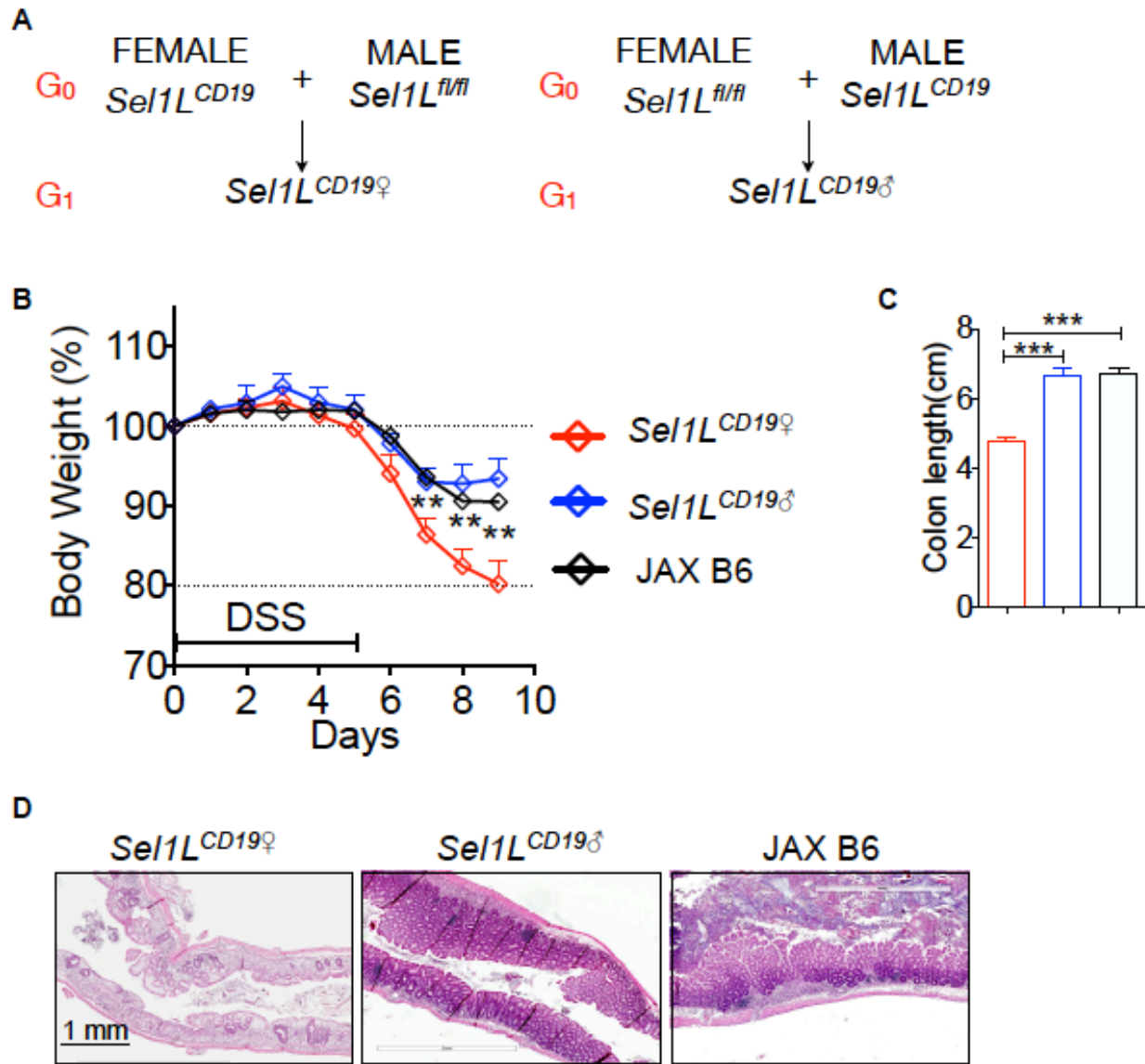


**Figure 4. 6 Early exposure to reduced passive secretory IgA promotes susceptibility to colitis.**

(A) Schematic diagram of *Sel1L*<sup>CD19♀</sup> and *Sel1L*<sup>CD19♂</sup> mice generation. (B-C) Body weight change and colon length were measured 9-days post 3 % DSS treatment. (D) H&E images of colon on 9-days post 3 % DSS treatment. Data are representative of two independent experiments in (B-D), n= 5 *Sel1L*<sup>CD19♀</sup> and 5 *Sel1L*<sup>CD19♂</sup> Values shown as mean ± s.e.m.; \*\*P< 0.01, \*\*\*P<0.001 by two-tailed Student's t-test.

## 4.4 DISCUSSION

Previously, we have demonstrated SellL-Hrd1 ERAD as a key regulator of B cell development by targeting pre-BCR for proteasomal degradation in a BiP-dependent manner (Ji et al., 2016). Here, we demonstrated that loss of SellL-Hrd1 ERAD in B cells compromises mucosal innate immune response, which promote propagation of colitogenic bacteria.

In mice intestine, approximately 50 % of IgA secreting plasma cells derive from IgM expressing cells in the peritoneal cavity, known as B1 cells (Kroese et al., 1989) . While these precursors response rapidly against potential pathogen, the end product has relatively low affinity. The remaining 50 % of IgA secreting plasma cells derived from B2 cells in Peyer's patches and the response, although slower, is of high affinity and specificity (Tissot et al., 1995). Using flow cytometry analysis, we have previously shown decreased number of circulating B220<sup>+</sup>IgM<sup>+</sup> B cells and peritoneal B1 cells in *SellL<sup>CD19</sup>* mice when compared to *SellL<sup>ff</sup>* mice. In the current study, we further observed a significant decrease in size and number of Peyer's patches and MLN, as well as decrease in B220<sup>+</sup>IgA<sup>+</sup> cells from these tissues. The number of plasma cells secreting IgA from colon lamina propria was also significantly reduced. Consequently, total secretory IgA(sIgA) measured in the fecal sample from *SellL<sup>CD19</sup>* mice was significantly lower than that of in *SellL<sup>ff</sup>* mice.

The mammalian intestine provides a niche to an estimated 100 trillion microorganisms, which majority of them maintain a symbiotic relationship with the host. While epithelial surfaces provide a physical barrier to prevent invasion by non-commensal microbes, antibody secretion by B cells, especially secretory sIgA, acts as the first line of antigen-specific immunity at the interface between the gut microbiota and the intestinal epithelium. IgA is the predominant antibody isotype in the mucosal tissue and comprises approximately 75 % of the total

immunoglobulin production in the mammalian body (Hurley et al., 2011). However, in serum, IgA antibodies make up a minor population among all isotypes, underscoring the importance of sIgA in mucosal immunity. In the present study, the effect of reduced sIgA was reflected in increased susceptibility to chemically induced colitis in *SellL<sup>CD19</sup>* mice. Interestingly, circulating IgG and IgM level in serum after immunization with NP-CGG antigen was comparable between two cohorts. These findings suggest that ERAD deficiency in B cells has drastic consequences on mucosal immunity, presumably via sIgA.

There are different ways in which the composition of the microbial communities is shaped. First, during vaginal delivery, the new born mammal receives its first microbial exposure from the vaginal and fecal microbiota of the mother as it leaves the womb (Dominguez-Bello et al., 2010; Hansen et al., 2012; Palmer et al., 2007) . Second, during postnatal life and during adulthood, the microbiota composition can change through cohabitation and coprophagy in mice (Elinav et al., 2011; Hildebrand et al., 2013). In line with these findings, *SellL<sup>ff</sup>* littermates, which have comparable level of IgA production as the irrelevant wildtype mice JAX B6, had succumbed to DSS induced colitis as its littermate *SellL<sup>CD19</sup>* mice. However, JAX B6 mice co-housed with *SellL<sup>CD19</sup>* mice for 4 weeks, right after weaning, exhibited resistance to colitis. The transfer of colitogenic microbiota to JAX B6 pups was observed only after the pups had been cross-fostered by *SellL<sup>CD19</sup>* dam. Based on this data, we speculate that the aberrant microbiota, which promote exaggerated inflammatory response in *SellL<sup>CD19</sup>* mice and *SellL<sup>ff</sup>* mice is only transmissible from dam to pups during birth (also known as vertical transmission) and is responsible for permanently shaping the life-long microbiota ecology.

As newborns are unable to produce its own sIgA (Rogier et al., 2014), the initial immune protection, which the newborn relies on, is provided through breast milk-derived sIgA antibodies;

also known as passive immunity. The initial passive immunity in suckling infants shape the composition of the gut microbiota and promote a mutualistic relationship with the host (Macpherson et al., 2012; Rogier et al., 2014). After weaning, plasma cells in the intestinal lamina propria produces IgA and provide lifelong antibody-mediated immune protection. Studies have demonstrated dysfunctional sIgA as a root of pathogenesis in IBD (Murthy et al., 2006). It has been demonstrated that cross-fostering, within 48 hours of birth, induces a permanent microbiota shift which is shaped by the nursing mother (Daft et al., 2015). Interestingly, in our cross-fostering experiment, we found that *SellL<sup>CD19</sup>* pups fostered by JAX B6 dam exhibited milder inflammatory response under DSS treatment. Furthermore, *SellL<sup>CD19</sup>* offspring from *SellL<sup>ff</sup>* dam and *SellL<sup>CD19</sup>* male breeding pairs were also protected from exacerbated inflammatory response. It has also been reported that a defect in passive sIgA of mothers can induce alteration in gut microbiota composition, subsequently leading to propagation of opportunistic and pathogenic microbes, contributing to the etiology of IBD (Rogier et al., 2014). In line with these findings, it can be speculated that early exposure of passive sIgA from *SellL<sup>CD19</sup>* dam may be the primary contributing factor in development, propagation and transfer of colitogenic microbiota in pups.

Taken together, our findings suggest that SellL-Hd1 ERAD pathway in B cells is indispensable for innate mucosal immunity and subsequently impacts gut microbiota ecology through passive sIgA. Nevertheless, the mechanism by which SellL-Hrd1 ERAD regulates IgA production and the affinity of IgA remains unknown and needs further investigation.

# **CHAPTER FIVE: SUMMARY AND FUTURE DIRECTIONS**

This thesis focused on delineating the physiological importance of ER-associated degradation (ERAD) in B cell development and its downstream impact on mucosal immunology. Humoral immunity involves a stepwise differentiation process and checkpoints during B-cell development in bone marrow, before reaching the antibody-producing mature stage. This complicated, yet refined development pathway requires the tightly orchestrated expression of many growth factors and cell surface-associated proteins. Hence, the magnitude of functional B cells reaching maturity depends on upregulation and downregulation of these proteins in a timely manner.

Along with UPR, ERAD is one of the quality control pathways responsible for maintaining ER homeostasis. Among several known mammalian ERAD complexes, Hrd E3 ligase and its adaptor protein, the Hrd1-Sel1L complex, targets the misfolded proteins in the ER for cytosolic proteasomal degradation. Various studies using tissue specific knockout animal models have revealed the physiological and pathological significance of ERAD and unveiled its tissue-specific endogenous protein substrates. In these studies, defective ERAD machinery resulted in accumulation of misfolded proteins and subsequently leading to either cell death or disease pathogenesis.

To this end, we generated B cell specific Sel1L knockout mice, under the assumption that ERAD deficiency would lead to: 1) impaired B cell development due to accumulation of misfolded proteins and; 2) defective B cell function. Indeed, we observed development block from large pre-B cell to small pre-B cell stage in B cells with ERAD deficiency (Chapter 3). While we hypothesized that impairment of an ERAD could induce ER stress response, Sel1L/ERAD deficiency in B cell resulted in a development block in a Chop-independent manner. Rather, ERAD regulates the turnover and signaling of pre-BCR. In the absence of

Sel1L/ERAD, the pre-BCR protein complex is stabilized and accumulated in large pre-B cells, leading to enhanced pre-B cell proliferation and a block of further B cell differentiation. Moreover, only pre-BCR, not BCR, complex is recognized as an endogenous substrate of Sel1L-Hrd1 ERAD. To our surprise, Sel1L/ERAD deficiency does not seem to affect either plasma cell differentiation or antibody production (IgG/IgM) of B cells in response to antigen immunization.

Further study in Appendix A revealed that ERAD deficiency in B cells compromises mucosal immune response and leads to propagation of transmissible colitogenic microbiota. While B cell development by Sel1L-Hrd1 ERAD deficiency did not interfere with IgG and IgM antibody production in response to antigen immunization, the total amount of IgA secreted into gut lumen was decreased. Under chemically induced colitis, the *Sel1L<sup>CD19</sup>* mice exhibited exaggerated inflammatory response. Interestingly, the wildtype littermate, which produces comparable levels of IgA, also exhibited exaggerated inflammatory response under DSS treatment. The current progress demonstrates that the colitogenic phenotype is only transmissible from Sel1L-Hrd1 ERAD deficient dam to pups. Moreover, Sel1L Hrd1 ERAD knockout pups bred from Sel1L-deficient male and Sel1L-sufficient female also exhibit very mild inflammatory response to DSS-induced colitis. Taken together, this study shows that Sel1L-Hrd1 ERAD is critical for IgA secretion which is responsible for maintaining gut homeostasis. Moreover, the transmissible colitogenic phenotype, between littermates, suggests that secretory IgA transferred from *Sel1L<sup>CD19</sup>* female to pups may shape the lifelong intestinal homeostasis.

Many interesting questions are raised from this dissertation. First, using non-reducing sucrose gradient fractionation analysis, we observed accumulation of high molecular weight complex in the absence of Sel1L-Hrd1 ERAD. Hence, to confirm whether this high molecular weight complex is fully assembled whole pre-BCR complex or aggregates of individual pre-BCR

compartments (Ig $\mu$ ,  $\lambda$ 5 or VpreB), further immunoprecipitation and western blot assays are required. Secondly, how ERAD distinguishes the pre-BCR complex in developing B cells versus the BCR complex in mature B cells, which share the common heavy chain Ig $\mu$ , remains to be elucidated. Consequently, it would be interesting to compare the interaction between ERAD versus the individual pre-BCR components or different combination of the pre-BCR components through in vitro mechanistic studies. Although the role of autophagy in B cell development has not been addressed in the current study, it is worth investigating whether and how autophagy affects ER homeostasis and pre-BCR expression. Hence, dissecting the crosstalk between two protein-quality control pathways, ERAD and autophagy, in B cell biology may shed further mechanistic understanding in ER homeostasis and protein quality control during cell differentiation and development. Last but not the least, more in depth studies are necessary to dissect the detailed mechanisms by which the ERAD modulates secretory IgA production and affinity in B cells, but not IgG or IgM. In addition, considering the link between passive secretory IgA (sIgA) found in breast milk and the lifelong intestinal homeostasis (Rogier et al., 2014), it is also worthwhile to investigate the microbiota composition in suckling neonates to further identify the colitogenic microbiota via bacterial 16S rRNA gene sequencing. We propose that monoassociation studies, following the identification of the colitogenic microbiota in *SellL*<sup>CD19</sup> mice will shed more insight into understanding pathogenesis of inflammatory bowel disease.

## REFERENCE

Acosta-Alvear, D., Zhou, Y., Blais, A., Tsikitis, M., Lents, N. H., Arias, C., . . . Dynlacht, B. D. (2007). XBP1 controls diverse cell type- and condition-specific transcriptional regulatory networks. *Mol Cell*, *27*(1), 53-66. doi:10.1016/j.molcel.2007.06.011

Adams, E. J., & Luoma, A. M. (2013). The adaptable major histocompatibility complex (MHC) fold: structure and function of nonclassical and MHC class I-like molecules. *Annu Rev Immunol*, *31*, 529-561. doi:10.1146/annurev-immunol-032712-095912

Adolfsson, J., Mansson, R., Buza-Vidas, N., Hultquist, A., Liuba, K., Jensen, C. T., . . . Jacobsen, S. E. (2005). Identification of Flt3+ lympho-myeloid stem cells lacking erythro-megakaryocytic potential a revised road map for adult blood lineage commitment. *Cell*, *121*(2), 295-306. doi:10.1016/j.cell.2005.02.013

Adolph, T. E., Tomczak, M. F., Niederreiter, L., Ko, H. J., Bock, J., Martinez-Naves, E., . . . Blumberg, R. S. (2013). Paneth cells as a site of origin for intestinal inflammation. *Nature*, *503*(7475), 272-276. doi:10.1038/nature12599

Aebi, M., Bernasconi, R., Clerc, S., & Molinari, M. (2010). N-glycan structures: recognition and processing in the ER. *Trends Biochem Sci*, *35*(2), 74-82. doi:10.1016/j.tibs.2009.10.001

Alexanian, R., Delasalle, K., Wang, M., Thomas, S., & Weber, D. (2012). Curability of multiple myeloma. *Bone Marrow Res*, *2012*, 916479. doi:10.1155/2012/916479

Anbazhagan, K., Rabbind Singh, A., Isabelle, P., Stella, I., Celine, A. D., Bissac, E., . . . Lassoued, K. (2013). Human pre-B cell receptor signal transduction: evidence for distinct roles of PI3kinase and MAP-kinase signalling pathways. *Immun Inflamm Dis*, *1*(1), 26-36. doi:10.1002/iid3.4

Anfinsen, C. B., & Scheraga, H. A. (1975). Experimental and theoretical aspects of protein folding. *Adv Protein Chem*, *29*, 205-300.

Angel, P., Szabowski, A., & Schorpp-Kistner, M. (2001). Function and regulation of AP-1 subunits in skin physiology and pathology. *Oncogene*, *20*(19), 2413-2423. doi:10.1038/sj.onc.1204380

Aragon, I. V., Barrington, R. A., Jackowski, S., Mori, K., & Brewer, J. W. (2012). The specialized unfolded protein response of B lymphocytes: ATF6alpha-independent development of antibody-secreting B cells. *Mol Immunol*, *51*(3-4), 347-355. doi:10.1016/j.molimm.2012.04.001

Asada, R., Kanemoto, S., Kondo, S., Saito, A., & Imaizumi, K. (2011). The signalling from endoplasmic reticulum-resident bZIP transcription factors involved in diverse cellular physiology. *J Biochem*, *149*(5), 507-518. doi:10.1093/jb/mvr041

Ashktorab, H., Green, W., Finzi, G., Sessa, F., Nouraiie, M., Lee, E. L., . . . Biunno, I. (2012). SEL1L, an UPR response protein, a potential marker of colonic cell transformation. *Dig Dis Sci*, *57*(4), 905-912. doi:10.1007/s10620-011-2026-y

Auf, G., Jabouille, A., Guerit, S., Pineau, R., Delugin, M., Bouchecareilh, M., . . . Moenner, M. (2010). Inositol-requiring enzyme 1alpha is a key regulator of angiogenesis and invasion in malignant glioma. *Proc Natl Acad Sci U S A*, *107*(35), 15553-15558. doi:10.1073/pnas.0914072107

Baek, J. H., Mahon, P. C., Oh, J., Kelly, B., Krishnamachary, B., Pearson, M., . . . Semenza, G. L. (2005). OS-9 interacts with hypoxia-inducible factor 1alpha and prolyl hydroxylases to promote oxygen-dependent degradation of HIF-1alpha. *Mol Cell*, *17*(4), 503-512. doi:10.1016/j.molcel.2005.01.011

Bagratuni, T., Wu, P., Gonzalez de Castro, D., Davenport, E. L., Dickens, N. J., Walker, B. A., . . . Davies, F. E. (2010). XBP1s levels are implicated in the biology and outcome of myeloma mediating different clinical outcomes to thalidomide-based treatments. *Blood*, *116*(2), 250-253. doi:10.1182/blood-2010-01-263236

Baldrige, R. D., & Rapoport, T. A. (2016). Autoubiquitination of the Hrd1 Ligase Triggers Protein Retrotranslocation in ERAD. *Cell*, *166*(2), 394-407. doi:10.1016/j.cell.2016.05.048

Bar-Nun, S., & Glickman, M. H. (2012). Proteasomal AAA-ATPases: structure and function. *Biochim Biophys Acta*, *1823*(1), 67-82. doi:10.1016/j.bbamcr.2011.07.009

Barclay, A. R., Russell, R. K., Wilson, M. L., Gilmour, W. H., Satsangi, J., & Wilson, D. C. (2009). Systematic review: the role of breastfeeding in the development of pediatric inflammatory bowel disease. *J Pediatr*, *155*(3), 421-426. doi:10.1016/j.jpeds.2009.03.017

Bazirgan, O. A., Garza, R. M., & Hampton, R. Y. (2006). Determinants of RING-E2 fidelity for Hrd1p, a membrane-anchored ubiquitin ligase. *J Biol Chem*, *281*(51), 38989-39001. doi:10.1074/jbc.M608174200

Behnke, J., Feige, M. J., & Hendershot, L. M. (2015). BiP and its nucleotide exchange factors Grp170 and Sill: mechanisms of action and biological functions. *J Mol Biol*, *427*(7), 1589-1608. doi:10.1016/j.jmb.2015.02.011

Benham, A. M. (2012). The protein disulfide isomerase family: key players in health and disease. *Antioxid Redox Signal*, *16*(8), 781-789. doi:10.1089/ars.2011.4439

Benhamron, S., Hadar, R., Iwawaky, T., So, J. S., Lee, A. H., & Tirosh, B. (2014). Regulated IRE1-dependent decay participates in curtailing immunoglobulin secretion from plasma cells. *Eur J Immunol*, *44*(3), 867-876. doi:10.1002/eji.201343953

Bernasconi, R., Pertel, T., Luban, J., & Molinari, M. (2008). A dual task for the Xbp1-responsive OS-9 variants in the mammalian endoplasmic reticulum: inhibiting secretion of misfolded protein conformers and enhancing their disposal. *J Biol Chem*, *283*(24), 16446-16454. doi:10.1074/jbc.M802272200

Bertolotti, A., Wang, X., Novoa, I., Jungreis, R., Schlessinger, K., Cho, J. H., . . . Ron, D. (2001). Increased sensitivity to dextran sodium sulfate colitis in IRE1beta-deficient mice. *J Clin Invest*, *107*(5), 585-593. doi:10.1172/JCI11476

Bertolotti, A., Zhang, Y., Hendershot, L. M., Harding, H. P., & Ron, D. (2000). Dynamic interaction of BiP and ER stress transducers in the unfolded-protein response. *Nat Cell Biol*, *2*(6), 326-332. doi:10.1038/35014014

Bettigole, S. E., Lis, R., Adoro, S., Lee, A. H., Spencer, L. A., Weller, P. F., & Glimcher, L. H. (2015). The transcription factor XBP1 is selectively required for eosinophil differentiation. *Nat Immunol*, *16*(8), 829-837. doi:10.1038/ni.3225

Borge, O. J., Adolfsson, J., Martensson, A., Martensson, I. L., & Jacobsen, S. E. (1999). Lymphoid-restricted development from multipotent candidate murine stem cells: distinct and complimentary functions of the c-kit and flt3-ligands. *Blood*, *94*(11), 3781-3790.

Born, W., White, J., Kappler, J., & Marrack, P. (1988). Rearrangement of IgH genes in normal thymocyte development. *J Immunol*, *140*(9), 3228-3232.

Bornemann, K. D., Brewer, J. W., Perez, E., Doerre, S., Sita, R., & Corley, R. B. (1997). Secretion of soluble pre-B cell receptors by pre-B cells. *J Immunol*, *158*(6), 2551-2557.

Brandtzaeg, P. (2010). The mucosal immune system and its integration with the mammary glands. *J Pediatr*, *156*(2 Suppl), S8-15. doi:10.1016/j.jpeds.2009.11.014

Brouns, G. S., de Vries, E., Neefjes, J. J., & Borst, J. (1996). Assembled pre-B cell receptor complexes are retained in the endoplasmic reticulum by a mechanism that is not selective for the pseudo-light chain. *J Biol Chem*, *271*(32), 19272-19278.

Brunsing, R., Omori, S. A., Weber, F., Bicknell, A., Friend, L., Rickert, R., & Niwa, M. (2008). B- and T-cell development both involve activity of the unfolded protein response pathway. *J Biol Chem*, *283*(26), 17954-17961. doi:10.1074/jbc.M801395200

Bryder, D., & Sigvardsson, M. (2010). Shaping up a lineage--lessons from B lymphopoiesis. *Curr Opin Immunol*, *22*(2), 148-153. doi:10.1016/j.coi.2010.02.001

Burr, M. L., Cano, F., Svobodova, S., Boyle, L. H., Boname, J. M., & Lehner, P. J. (2011). HRD1 and UBE2J1 target misfolded MHC class I heavy chains for endoplasmic reticulum-associated degradation. *Proc Natl Acad Sci U S A*, *108*(5), 2034-2039. doi:10.1073/pnas.1016229108

Calfon, M., Zeng, H., Urano, F., Till, J. H., Hubbard, S. R., Harding, H. P., . . . Ron, D. (2002). IRE1 couples endoplasmic reticulum load to secretory capacity by processing the XBP-1 mRNA. *Nature*, *415*(6867), 92-96. doi:10.1038/415092a

Cao, A. T., Yao, S., Gong, B., Elson, C. O., & Cong, Y. (2012). Th17 cells upregulate polymeric Ig receptor and intestinal IgA and contribute to intestinal homeostasis. *J Immunol*, *189*(9), 4666-4673. doi:10.4049/jimmunol.1200955

Capurro, M. I., Xiang, Y. Y., Lobe, C., & Filmus, J. (2005). Glypican-3 promotes the growth of hepatocellular carcinoma by stimulating canonical Wnt signaling. *Cancer Res*, *65*(14), 6245-6254. doi:10.1158/0008-5472.CAN-04-4244

Cardano, M., Diaferia, G. R., Cattaneo, M., Dessi, S. S., Long, Q., Conti, L., . . . Biunno, I. (2011). mSEL-1L (Suppressor/enhancer Lin12-like) protein levels influence murine neural stem cell self-renewal and lineage commitment. *J Biol Chem*, *286*(21), 18708-18719. doi:10.1074/jbc.M110.210740

Carrasco, D. R., Sukhdeo, K., Protopopova, M., Sinha, R., Enos, M., Carrasco, D. E., . . . DePinho, R. A. (2007). The differentiation and stress response factor XBP-1 drives multiple myeloma pathogenesis. *Cancer Cell*, *11*(4), 349-360. doi:10.1016/j.ccr.2007.02.015

Carvalho, P., Stanley, A. M., & Rapoport, T. A. (2010). Retrotranslocation of a misfolded luminal ER protein by the ubiquitin-ligase Hrd1p. *Cell*, *143*(4), 579-591. doi:10.1016/j.cell.2010.10.028

Carvalho, T. L., Mota-Santos, T., Cumano, A., Demengeot, J., & Vieira, P. (2001). Arrested B lymphopoiesis and persistence of activated B cells in adult interleukin 7(-/-) mice. *J Exp Med*, *194*(8), 1141-1150.

Cataldo, F., Marino, V., Ventura, A., Bottaro, G., & Corazza, G. R. (1998). Prevalence and clinical features of selective immunoglobulin A deficiency in coeliac disease: an Italian multicentre study. Italian Society of Paediatric Gastroenterology and Hepatology (SIGEP) and "Club del Tenue" Working Groups on Coeliac Disease. *Gut*, *42*(3), 362-365.

Cattaneo, M., Baronchelli, S., Schiffer, D., Mellai, M., Caldera, V., Saccani, G. J., . . . Biunno, I. (2014). Down-modulation of SEL1L, an unfolded protein response and endoplasmic reticulum-associated degradation protein, sensitizes glioma stem cells to the cytotoxic effect of valproic acid. *J Biol Chem*, *289*(5), 2826-2838. doi:10.1074/jbc.M113.527754

Cattaneo, M., Fontanella, E., Canton, C., Delia, D., & Biunno, I. (2005). SEL1L affects human pancreatic cancer cell cycle and invasiveness through modulation of PTEN and genes related to cell-matrix interactions. *Neoplasia*, *7*(11), 1030-1038.

Cerutti, A., Cols, M., & Puga, I. (2013). Marginal zone B cells: virtues of innate-like antibody-producing lymphocytes. *Nat Rev Immunol*, *13*(2), 118-132. doi:10.1038/nri3383

Chen, D., & Zhou, Q. (2004). Caspase cleavage of BimEL triggers a positive feedback amplification of apoptotic signaling. *Proc Natl Acad Sci U S A*, *101*(5), 1235-1240. doi:10.1073/pnas.0308050100

Chen, X., Iliopoulos, D., Zhang, Q., Tang, Q., Greenblatt, M. B., Hatziapostolou, M., . . . Glimcher, L. H. (2014). XBP1 promotes triple-negative breast cancer by controlling the HIF1alpha pathway. *Nature*, *508*(7494), 103-107. doi:10.1038/nature13119

Chen, X., Tukachinsky, H., Huang, C. H., Jao, C., Chu, Y. R., Tang, H. Y., . . . Salic, A. (2011). Processing and turnover of the Hedgehog protein in the endoplasmic reticulum. *J Cell Biol*, *192*(5), 825-838. doi:10.1083/jcb.201008090

Chien, W., Ding, L. W., Sun, Q. Y., Torres-Fernandez, L. A., Tan, S. Z., Xiao, J., . . . Koeffler, P. H. (2014). Selective inhibition of unfolded protein response induces apoptosis in pancreatic cancer cells. *Oncotarget*, *5*(13), 4881-4894. doi:10.18632/oncotarget.2051

Chiti, F., & Dobson, C. M. (2006). Protein misfolding, functional amyloid, and human disease. *Annu Rev Biochem*, *75*, 333-366. doi:10.1146/annurev.biochem.75.101304.123901

Chitnis, N. S., Pytel, D., Bobrovnikova-Marjon, E., Pant, D., Zheng, H., Maas, N. L., . . . Diehl, J. A. (2012). miR-211 is a prosurvival microRNA that regulates chop expression in a PERK-dependent manner. *Mol Cell*, *48*(3), 353-364. doi:10.1016/j.molcel.2012.08.025

Christianson, J. C., Olzmann, J. A., Shaler, T. A., Sowa, M. E., Bennett, E. J., Richter, C. M., . . . Kopito, R. R. (2011). Defining human ERAD networks through an integrative mapping strategy. *Nat Cell Biol*, *14*(1), 93-105. doi:10.1038/ncb2383

Christianson, J. C., Shaler, T. A., Tyler, R. E., & Kopito, R. R. (2008). OS-9 and GRP94 deliver mutant alpha1-antitrypsin to the Hrd1-SEL1L ubiquitin ligase complex for ERAD. *Nat Cell Biol*, *10*(3), 272-282. doi:10.1038/ncb1689

Christianson, J. C., & Ye, Y. (2014). Cleaning up in the endoplasmic reticulum: ubiquitin in charge. *Nat Struct Mol Biol*, *21*(4), 325-335. doi:10.1038/nsmb.2793

Christis, C., Fullaondo, A., Schildknecht, D., Mkrtchian, S., Heck, A. J., & Braakman, I. (2010). Regulated increase in folding capacity prevents unfolded protein stress in the ER. *J Cell Sci*, *123*(Pt 5), 787-794. doi:10.1242/jcs.041111

Clark, M. R., Mandal, M., Ochiai, K., & Singh, H. (2014). Orchestrating B cell lymphopoiesis through interplay of IL-7 receptor and pre-B cell receptor signalling. *Nat Rev Immunol*, *14*(2), 69-80. doi:10.1038/nri3570

Clarke, H. J., Chambers, J. E., Liniker, E., & Marciniak, S. J. (2014). Endoplasmic reticulum stress in malignancy. *Cancer Cell*, *25*(5), 563-573. doi:10.1016/j.ccr.2014.03.015

Clauss, I. M., Chu, M., Zhao, J. L., & Glimcher, L. H. (1996). The basic domain/leucine zipper protein hXBP-1 preferentially binds to and transactivates CRE-like sequences containing an ACGT core. *Nucleic Acids Res*, *24*(10), 1855-1864.

Clevers, H. C., & Bevins, C. L. (2013). Paneth cells: maestros of the small intestinal crypts. *Annu Rev Physiol*, *75*, 289-311. doi:10.1146/annurev-physiol-030212-183744

Connor, J. H., Weiser, D. C., Li, S., Hallenbeck, J. M., & Shenolikar, S. (2001). Growth arrest and DNA damage-inducible protein GADD34 assembles a novel signaling complex containing protein phosphatase 1 and inhibitor 1. *Mol Cell Biol*, *21*(20), 6841-6850. doi:10.1128/MCB.21.20.6841-6850.2001

Corfe, S. A., & Paige, C. J. (2012). The many roles of IL-7 in B cell development; mediator of survival, proliferation and differentiation. *Semin Immunol*, *24*(3), 198-208. doi:10.1016/j.smim.2012.02.001

Cormier, J. H., Tamura, T., Sunryd, J. C., & Hebert, D. N. (2009). EDEM1 recognition and delivery of misfolded proteins to the SEL1L-containing ERAD complex. *Mol Cell*, *34*(5), 627-633. doi:10.1016/j.molcel.2009.05.018

Cox, J. S., Shamu, C. E., & Walter, P. (1993). Transcriptional induction of genes encoding endoplasmic reticulum resident proteins requires a transmembrane protein kinase. *Cell*, *73*(6), 1197-1206.

Cox, J. S., & Walter, P. (1996). A novel mechanism for regulating activity of a transcription factor that controls the unfolded protein response. *Cell*, *87*(3), 391-404.

Credle, J. J., Finer-Moore, J. S., Papa, F. R., Stroud, R. M., & Walter, P. (2005). On the mechanism of sensing unfolded protein in the endoplasmic reticulum. *Proc Natl Acad Sci U S A*, *102*(52), 18773-18784. doi:10.1073/pnas.0509487102

Croft, A., Tay, K. H., Boyd, S. C., Guo, S. T., Jiang, C. C., Lai, F., . . . Zhang, X. D. (2014). Oncogenic activation of MEK/ERK primes melanoma cells for adaptation to endoplasmic reticulum stress. *J Invest Dermatol*, *134*(2), 488-497. doi:10.1038/jid.2013.325

Cross, B. C., Bond, P. J., Sadowski, P. G., Jha, B. K., Zak, J., Goodman, J. M., . . . Harding, H. P. (2012). The molecular basis for selective inhibition of unconventional mRNA splicing by an IRE1-binding small molecule. *Proc Natl Acad Sci U S A*, *109*(15), E869-878. doi:10.1073/pnas.1115623109

Cross, B. C., McKibbin, C., Callan, A. C., Roboti, P., Piacenti, M., Rabu, C., . . . Swanton, E. (2009). Eeyarestatin I inhibits Sec61-mediated protein translocation at the endoplasmic reticulum. *J Cell Sci*, *122*(Pt 23), 4393-4400. doi:10.1242/jcs.054494

Cullinan, S. B., Zhang, D., Hannink, M., Arvisais, E., Kaufman, R. J., & Diehl, J. A. (2003). Nrf2 is a direct PERK substrate and effector of PERK-dependent cell survival. *Mol Cell Biol*, *23*(20), 7198-7209.

Cumano, A., Ferraz, J. C., Klaine, M., Di Santo, J. P., & Godin, I. (2001). Intraembryonic, but not yolk sac hematopoietic precursors, isolated before circulation, provide long-term multilineage reconstitution. *Immunity*, *15*(3), 477-485.

Cumano, A., & Godin, I. (2007). Ontogeny of the hematopoietic system. *Annu Rev Immunol*, *25*, 745-785. doi:10.1146/annurev.immunol.25.022106.141538

Daft, J. G., Ptacek, T., Kumar, R., Morrow, C., & Lorenz, R. G. (2015). Cross-fostering immediately after birth induces a permanent microbiota shift that is shaped by the nursing mother. *Microbiome*, *3*, 17. doi:10.1186/s40168-015-0080-y

Dai, B. H., Geng, L., Wang, Y., Sui, C. J., Xie, F., Shen, R. X., . . . Yang, J. M. (2013). microRNA-199a-5p protects hepatocytes from bile acid-induced sustained endoplasmic reticulum stress. *Cell Death Dis*, *4*, e604. doi:10.1038/cddis.2013.134

Davis, R. J. (2000). Signal transduction by the JNK group of MAP kinases. *Cell*, *103*(2), 239-252.

Dejeans, N., Pluquet, O., Lhomond, S., Grise, F., Bouche-careilh, M., Juin, A., . . . Chevet, E. (2012). Autocrine control of glioma cells adhesion and migration through IRE1alpha-mediated cleavage of SPARC mRNA. *J Cell Sci*, *125*(Pt 18), 4278-4287. doi:10.1242/jcs.099291

Dias, S., Silva, H., Jr., Cumano, A., & Vieira, P. (2005). Interleukin-7 is necessary to maintain the B cell potential in common lymphoid progenitors. *J Exp Med*, *201*(6), 971-979. doi:10.1084/jem.20042393

Dolence, J. J., Gwin, K. A., Shapiro, M. B., & Medina, K. L. (2014). Flt3 signaling regulates the proliferation, survival, and maintenance of multipotent hematopoietic progenitors that generate B cell precursors. *Exp Hematol*, *42*(5), 380-393 e383. doi:10.1016/j.exphem.2014.01.001

Dominguez-Bello, M. G., Costello, E. K., Contreras, M., Magris, M., Hidalgo, G., Fierer, N., & Knight, R. (2010). Delivery mode shapes the acquisition and structure of the initial microbiota across multiple body habitats in newborns. *Proc Natl Acad Sci U S A*, *107*(26), 11971-11975. doi:10.1073/pnas.1002601107

Dorner, A. J., Wasley, L. C., & Kaufman, R. J. (1990). Protein dissociation from GRP78 and secretion are blocked by depletion of cellular ATP levels. *Proc Natl Acad Sci U S A*, *87*(19), 7429-7432.

Drogat, B., Auguste, P., Nguyen, D. T., Bouche-careilh, M., Pineau, R., Nalbantoglu, J., . . . Moenner, M. (2007). IRE1 signaling is essential for ischemia-induced vascular endothelial growth factor-A expression and contributes to angiogenesis and tumor growth in vivo. *Cancer Res*, *67*(14), 6700-6707. doi:10.1158/0008-5472.CAN-06-3235

Dul, J. L., Argon, Y., Winkler, T., ten Boekel, E., Melchers, F., & Martensson, I. L. (1996). The murine VpreB1 and VpreB2 genes both encode a protein of the surrogate light chain and are co-expressed during B cell development. *Eur J Immunol*, *26*(4), 906-913. doi:10.1002/eji.1830260428

Elinav, E., Strowig, T., Kau, A. L., Henao-Mejia, J., Thaiss, C. A., Booth, C. J., . . . Flavell, R. A. (2011). NLRP6 inflammasome regulates colonic microbial ecology and risk for colitis. *Cell*, *145*(5), 745-757. doi:10.1016/j.cell.2011.04.022

Elkabetz, Y., Ofir, A., Argon, Y., & Bar-Nun, S. (2008). Alternative pathways of disulfide bond formation yield secretion-competent, stable and functional immunoglobulins. *Mol Immunol*, *46*(1), 97-105. doi:10.1016/j.molimm.2008.07.005

Ellgaard, L., & Helenius, A. (2003). Quality control in the endoplasmic reticulum. *Nat Rev Mol Cell Biol*, *4*(3), 181-191. doi:10.1038/nrm1052

Ernst, R., Mueller, B., Ploegh, H. L., & Schlieker, C. (2009). The otubain YOD1 is a deubiquitinating enzyme that associates with p97 to facilitate protein dislocation from the ER. *Mol Cell*, *36*(1), 28-38. doi:10.1016/j.molcel.2009.09.016

Fagioli, C., & Sitia, R. (2001). Glycoprotein quality control in the endoplasmic reticulum. Mannose trimming by endoplasmic reticulum mannosidase I times the proteasomal degradation of unassembled immunoglobulin subunits. *J Biol Chem*, *276*(16), 12885-12892. doi:10.1074/jbc.M009603200

Fang, T., Smith, B. P., & Roman, C. A. (2001). Conventional and surrogate light chains differentially regulate Ig mu and Dmu heavy chain maturation and surface expression. *J Immunol*, 167(7), 3846-3857.

Finley, D. (2009). Recognition and processing of ubiquitin-protein conjugates by the proteasome. *Annu Rev Biochem*, 78, 477-513.  
doi:10.1146/annurev.biochem.78.081507.101607

Flemming, A., Brummer, T., Reth, M., & Jumaa, H. (2003). The adaptor protein SLP-65 acts as a tumor suppressor that limits pre-B cell expansion. *Nat Immunol*, 4(1), 38-43.  
doi:10.1038/ni862

Foundation for Accountability, P. O. R. U. S. A. (2001). Health care choices: sharing the quality message. *Issue Brief Cent Medicare Educ*, 2(1), 1-12.

Francisco, A. B., Singh, R., Li, S., Vani, A. K., Yang, L., Munroe, R. J., . . . Long, Q. (2010). Deficiency of suppressor enhancer Lin12 1 like (SEL1L) in mice leads to systemic endoplasmic reticulum stress and embryonic lethality. *J Biol Chem*, 285(18), 13694-13703. doi:10.1074/jbc.M109.085340

Friman, V., Nowrouzian, F., Adlerberth, I., & Wold, A. E. (2002). Increased frequency of intestinal Escherichia coli carrying genes for S fimbriae and haemolysin in IgA-deficient individuals. *Microb Pathog*, 32(1), 35-42. doi:10.1006/mpat.2001.0477

Fujimoto, T., Yoshimatsu, K., Watanabe, K., Yokomizo, H., Otani, T., Matsumoto, A., . . . Ogawa, K. (2007). Overexpression of human X-box binding protein 1 (XBP-1) in colorectal adenomas and adenocarcinomas. *Anticancer Res*, 27(1A), 127-131.

Fujita, H., Yagishita, N., Aratani, S., Saito-Fujita, T., Morota, S., Yamano, Y., . . . Nakajima, T. (2015). The E3 ligase synoviolin controls body weight and mitochondrial biogenesis through negative regulation of PGC-1beta. *EMBO J*, 34(8), 1042-1055.  
doi:10.15252/embj.201489897

Fuxa, M., & Busslinger, M. (2007). Reporter gene insertions reveal a strictly B lymphoid-specific expression pattern of Pax5 in support of its B cell identity function. *J Immunol*, 178(5), 3031-3037.

Gaddam, D., Stevens, N., & Hollien, J. (2013). Comparison of mRNA localization and regulation during endoplasmic reticulum stress in Drosophila cells. *Mol Biol Cell*, 24(1), 14-20. doi:10.1091/mbc.E12-06-0491

Galler, G. R., Mundt, C., Parker, M., Pelanda, R., Martensson, I. L., & Winkler, T. H. (2004). Surface mu heavy chain signals down-regulation of the V(D)J-recombinase machinery in the absence of surrogate light chain components. *J Exp Med*, *199*(11), 1523-1532. doi:10.1084/jem.20031523

Gardner, R. G., Swarbrick, G. M., Bays, N. W., Cronin, S. R., Wilhovsky, S., Seelig, L., . . . Hampton, R. Y. (2000). Endoplasmic reticulum degradation requires lumen to cytosol signaling. Transmembrane control of Hrd1p by Hrd3p. *J Cell Biol*, *151*(1), 69-82.

Gass, J. N., Jiang, H. Y., Wek, R. C., & Brewer, J. W. (2008). The unfolded protein response of B-lymphocytes: PERK-independent development of antibody-secreting cells. *Mol Immunol*, *45*(4), 1035-1043. doi:10.1016/j.molimm.2007.07.029

Gauthier, L., Rossi, B., Roux, F., Termine, E., & Schiff, C. (2002). Galectin-1 is a stromal cell ligand of the pre-B cell receptor (BCR) implicated in synapse formation between pre-B and stromal cells and in pre-BCR triggering. *Proc Natl Acad Sci U S A*, *99*(20), 13014-13019. doi:10.1073/pnas.202323999

Gething, M. J. (1999). Role and regulation of the ER chaperone BiP. *Semin Cell Dev Biol*, *10*(5), 465-472. doi:10.1006/scdb.1999.0318

Gewirtz, D. A. (2014). The four faces of autophagy: implications for cancer therapy. *Cancer Res*, *74*(3), 647-651. doi:10.1158/0008-5472.CAN-13-2966

Ghosh, R., Wang, L., Wang, E. S., Perera, B. G., Igarria, A., Morita, S., . . . Papa, F. R. (2014). Allosteric inhibition of the IRE1alpha RNase preserves cell viability and function during endoplasmic reticulum stress. *Cell*, *158*(3), 534-548. doi:10.1016/j.cell.2014.07.002

Ghosh, S., & Karin, M. (2002). Missing pieces in the NF-kappaB puzzle. *Cell*, *109 Suppl*, S81-96.

Godin, I., & Cumano, A. (2002). The hare and the tortoise: an embryonic haematopoietic race. *Nat Rev Immunol*, *2*(8), 593-604. doi:10.1038/nri857

Gong, S., & Nussenzweig, M. C. (1996). Regulation of an early developmental checkpoint in the B cell pathway by Ig beta. *Science*, *272*(5260), 411-414.

Granelli, P., Cattaneo, M., Ferrero, S., Bottiglieri, L., Bosari, S., Fichera, G., & Biunno, I. (2004). SEL1L and squamous cell carcinoma of the esophagus. *Clin Cancer Res*, *10*(17), 5857-5861. doi:10.1158/1078-0432.CCR-04-0075

Guelpa-Fonlupt, V., Bossy, D., Alzari, P., Fumoux, F., Fougereau, M., & Schiff, C. (1994). The human pre-B cell receptor: structural constraints for a tentative model of the pseudo-light ( $\psi$  L) chain. *Mol Immunol*, *31*(14), 1099-1108.

Guerriero, C. J., & Brodsky, J. L. (2012). The delicate balance between secreted protein folding and endoplasmic reticulum-associated degradation in human physiology. *Physiol Rev*, *92*(2), 537-576. doi:10.1152/physrev.00027.2011

Guloglu, F. B., Bajor, E., Smith, B. P., & Roman, C. A. (2005). The unique region of surrogate light chain component  $\lambda 5$  is a heavy chain-specific regulator of precursor B cell receptor signaling. *J Immunol*, *175*(1), 358-366.

Guloglu, F. B., & Roman, C. A. (2006). Precursor B cell receptor signaling activity can be uncoupled from surface expression. *J Immunol*, *176*(11), 6862-6872.

Gunn, K. E., Gifford, N. M., Mori, K., & Brewer, J. W. (2004). A role for the unfolded protein response in optimizing antibody secretion. *Mol Immunol*, *41*(9), 919-927. doi:10.1016/j.molimm.2004.04.023

Guo, B., Kato, R. M., Garcia-Lloret, M., Wahl, M. I., & Rawlings, D. J. (2000). Engagement of the human pre-B cell receptor generates a lipid raft-dependent calcium signaling complex. *Immunity*, *13*(2), 243-253.

Gupta, A. K., Li, B., Cerniglia, G. J., Ahmed, M. S., Hahn, S. M., & Maity, A. (2007). The HIV protease inhibitor nelfinavir downregulates Akt phosphorylation by inhibiting proteasomal activity and inducing the unfolded protein response. *Neoplasia*, *9*(4), 271-278.

Hampton, R. Y., Gardner, R. G., & Rine, J. (1996). Role of 26S proteasome and HRD genes in the degradation of 3-hydroxy-3-methylglutaryl-CoA reductase, an integral endoplasmic reticulum membrane protein. *Mol Biol Cell*, *7*(12), 2029-2044.

Han, D., Lerner, A. G., Vande Walle, L., Upton, J. P., Xu, W., Hagen, A., . . . Papa, F. R. (2009). IRE1 $\alpha$  kinase activation modes control alternate endoribonuclease outputs to determine divergent cell fates. *Cell*, *138*(3), 562-575. doi:10.1016/j.cell.2009.07.017

Hansen, C. H., Nielsen, D. S., Kverka, M., Zakostelska, Z., Klimesova, K., Hudcovic, T., . . . Hansen, A. K. (2012). Patterns of early gut colonization shape future immune responses of the host. *PLoS One*, *7*(3), e34043. doi:10.1371/journal.pone.0034043

Harding, H. P., Novoa, I., Zhang, Y., Zeng, H., Wek, R., Schapira, M., & Ron, D. (2000). Regulated translation initiation controls stress-induced gene expression in mammalian cells. *Mol Cell*, *6*(5), 1099-1108.

Harding, H. P., Zhang, Y., Bertolotti, A., Zeng, H., & Ron, D. (2000). Perk is essential for translational regulation and cell survival during the unfolded protein response. *Mol Cell*, *5*(5), 897-904.

Harding, H. P., Zhang, Y., & Ron, D. (1999). Protein translation and folding are coupled by an endoplasmic-reticulum-resident kinase. *Nature*, *397*(6716), 271-274. doi:10.1038/16729

Harding, H. P., Zhang, Y., Zeng, H., Novoa, I., Lu, P. D., Calton, M., . . . Ron, D. (2003). An integrated stress response regulates amino acid metabolism and resistance to oxidative stress. *Mol Cell*, *11*(3), 619-633.

Haze, K., Yoshida, H., Yanagi, H., Yura, T., & Mori, K. (1999). Mammalian transcription factor ATF6 is synthesized as a transmembrane protein and activated by proteolysis in response to endoplasmic reticulum stress. *Mol Biol Cell*, *10*(11), 3787-3799.

He, Y., Beatty, A., Han, X., Ji, Y., Ma, X., Adelstein, R. S., . . . Qi, L. (2012). Nonmuscle myosin IIB links cytoskeleton to IRE1alpha signaling during ER stress. *Dev Cell*, *23*(6), 1141-1152. doi:10.1016/j.devcel.2012.11.006

Hebert, D. N., Simons, J. F., Peterson, J. R., & Helenius, A. (1995). Calnexin, calreticulin, and Bip/Kar2p in protein folding. *Cold Spring Harb Symp Quant Biol*, *60*, 405-415.

Hendershot, L., Bole, D., & Kearney, J. F. (1987). The role of immunoglobulin heavy chain binding protein in immunoglobulin transport. *Immunol Today*, *8*(4), 111-114. doi:10.1016/0167-5699(87)90861-9

Hendershot, L. M. (1990). Immunoglobulin heavy chain and binding protein complexes are dissociated in vivo by light chain addition. *J Cell Biol*, *111*(3), 829-837.

Hendershot, L. M. (2004). The ER function BiP is a master regulator of ER function. *Mt Sinai J Med*, 71(5), 289-297.

Herzog, S., Reth, M., & Jumaa, H. (2009). Regulation of B-cell proliferation and differentiation by pre-B-cell receptor signalling. *Nat Rev Immunol*, 9(3), 195-205. doi:10.1038/nri2491

Hess, J., Werner, A., Wirth, T., Melchers, F., Jack, H. M., & Winkler, T. H. (2001). Induction of pre-B cell proliferation after de novo synthesis of the pre-B cell receptor. *Proc Natl Acad Sci U S A*, 98(4), 1745-1750. doi:10.1073/pnas.041492098

Hetz, C. (2012). The unfolded protein response: controlling cell fate decisions under ER stress and beyond. *Nat Rev Mol Cell Biol*, 13(2), 89-102. doi:10.1038/nrm3270

Hetz, C., Chevet, E., & Harding, H. P. (2013). Targeting the unfolded protein response in disease. *Nat Rev Drug Discov*, 12(9), 703-719. doi:10.1038/nrd3976

Hetz, C., & Glimcher, L. H. (2009). Fine-tuning of the unfolded protein response: Assembling the IRE1alpha interactome. *Mol Cell*, 35(5), 551-561. doi:10.1016/j.molcel.2009.08.021

Hildebrand, F., Nguyen, T. L., Brinkman, B., Yunta, R. G., Cauwe, B., Vandenaabeele, P., . . . Raes, J. (2013). Inflammation-associated enterotypes, host genotype, cage and inter-individual effects drive gut microbiota variation in common laboratory mice. *Genome Biol*, 14(1), R4. doi:10.1186/gb-2013-14-1-r4

Hirsch, C., Blom, D., & Ploegh, H. L. (2003). A role for N-glycanase in the cytosolic turnover of glycoproteins. *EMBO J*, 22(5), 1036-1046. doi:10.1093/emboj/cdg107

Hitomi, J., Katayama, T., Eguchi, Y., Kudo, T., Taniguchi, M., Koyama, Y., . . . Tohyama, M. (2004). Involvement of caspase-4 in endoplasmic reticulum stress-induced apoptosis and Abeta-induced cell death. *J Cell Biol*, 165(3), 347-356. doi:10.1083/jcb.200310015

Hodgson, W. C., King, R. G., & Boura, A. L. (1990). Augmented potentiation of renal vasoconstrictor responses by thromboxane A2 receptor stimulation in the alloxan-diabetic rat. *J Pharm Pharmacol*, 42(6), 423-427.

Hollien, J., Lin, J. H., Li, H., Stevens, N., Walter, P., & Weissman, J. S. (2009). Regulated Ire1-dependent decay of messenger RNAs in mammalian cells. *J Cell Biol*, *186*(3), 323-331. doi:10.1083/jcb.200903014

Hollien, J., & Weissman, J. S. (2006). Decay of endoplasmic reticulum-localized mRNAs during the unfolded protein response. *Science*, *313*(5783), 104-107. doi:10.1126/science.1129631

Horimoto, S., Ninagawa, S., Okada, T., Koba, H., Sugimoto, T., Kamiya, Y., . . . Mori, K. (2013). The unfolded protein response transducer ATF6 represents a novel transmembrane-type endoplasmic reticulum-associated degradation substrate requiring both mannose trimming and SEL1L protein. *J Biol Chem*, *288*(44), 31517-31527. doi:10.1074/jbc.M113.476010

Hosokawa, N., Kamiya, Y., Kamiya, D., Kato, K., & Nagata, K. (2009). Human OS-9, a lectin required for glycoprotein endoplasmic reticulum-associated degradation, recognizes mannose-trimmed N-glycans. *J Biol Chem*, *284*(25), 17061-17068. doi:10.1074/jbc.M809725200

Hosokawa, N., Tremblay, L. O., Sleno, B., Kamiya, Y., Wada, I., Nagata, K., . . . Herscovics, A. (2010). EDEM1 accelerates the trimming of alpha1,2-linked mannose on the C branch of N-glycans. *Glycobiology*, *20*(5), 567-575. doi:10.1093/glycob/cwq001

Hosokawa, N., Wada, I., Nagasawa, K., Moriyama, T., Okawa, K., & Nagata, K. (2008). Human XTP3-B forms an endoplasmic reticulum quality control scaffold with the HRD1-SEL1L ubiquitin ligase complex and BiP. *J Biol Chem*, *283*(30), 20914-20924. doi:10.1074/jbc.M709336200

Hotamisligil, G. S., & Erbay, E. (2008). Nutrient sensing and inflammation in metabolic diseases. *Nat Rev Immunol*, *8*(12), 923-934. doi:10.1038/nri2449

Hu, C. C., Dougan, S. K., McGehee, A. M., Love, J. C., & Ploegh, H. L. (2009). XBP-1 regulates signal transduction, transcription factors and bone marrow colonization in B cells. *EMBO J*, *28*(11), 1624-1636. doi:10.1038/emboj.2009.117

Huang, L., Marvin, J. M., Tatsis, N., & Eisenlohr, L. C. (2011). Cutting Edge: Selective role of ubiquitin in MHC class I antigen presentation. *J Immunol*, *186*(4), 1904-1908. doi:10.4049/jimmunol.1003411

- Hubbard, S. C., & Ivatt, R. J. (1981). Synthesis and processing of asparagine-linked oligosaccharides. *Annu Rev Biochem*, *50*, 555-583. doi:10.1146/annurev.bi.50.070181.003011
- Hurley, W. L., & Theil, P. K. (2011). Perspectives on immunoglobulins in colostrum and milk. *Nutrients*, *3*(4), 442-474. doi:10.3390/nu3040442
- Irion, S., Clarke, R. L., Luche, H., Kim, I., Morrison, S. J., Fehling, H. J., & Keller, G. M. (2010). Temporal specification of blood progenitors from mouse embryonic stem cells and induced pluripotent stem cells. *Development*, *137*(17), 2829-2839. doi:10.1242/dev.042119
- Ivan, M., Kondo, K., Yang, H., Kim, W., Valiando, J., Ohh, M., . . . Kaelin, W. G., Jr. (2001). HIF $\alpha$  targeted for VHL-mediated destruction by proline hydroxylation: implications for O<sub>2</sub> sensing. *Science*, *292*(5516), 464-468. doi:10.1126/science.1059817
- Iwakoshi, N. N., Lee, A. H., & Glimcher, L. H. (2003). The X-box binding protein-1 transcription factor is required for plasma cell differentiation and the unfolded protein response. *Immunol Rev*, *194*, 29-38.
- Iwakoshi, N. N., Lee, A. H., Vallabhajosyula, P., Otipoby, K. L., Rajewsky, K., & Glimcher, L. H. (2003). Plasma cell differentiation and the unfolded protein response intersect at the transcription factor XBP-1. *Nat Immunol*, *4*(4), 321-329. doi:10.1038/ni907
- Iwakoshi, N. N., Pypaert, M., & Glimcher, L. H. (2007). The transcription factor XBP-1 is essential for the development and survival of dendritic cells. *J Exp Med*, *204*(10), 2267-2275. doi:10.1084/jem.20070525
- Iwasaki, Y., Suganami, T., Hachiya, R., Shirakawa, I., Kim-Saijo, M., Tanaka, M., . . . Ogawa, Y. (2014). Activating transcription factor 4 links metabolic stress to interleukin-6 expression in macrophages. *Diabetes*, *63*(1), 152-161. doi:10.2337/db13-0757
- Iwawaki, T., Akai, R., Yamanaka, S., & Kohno, K. (2009). Function of IRE1 alpha in the placenta is essential for placental development and embryonic viability. *Proc Natl Acad Sci U S A*, *106*(39), 16657-16662. doi:10.1073/pnas.0903775106
- Jacob, J., Kassir, R., & Kelsoe, G. (1991). In situ studies of the primary immune response to (4-hydroxy-3-nitrophenyl)acetyl. I. The architecture and dynamics of responding cell populations. *J Exp Med*, *173*(5), 1165-1175.

Jakubovic, B. D., & Jothy, S. (2007). Glypican-3: from the mutations of Simpson-Golabi-Behmel genetic syndrome to a tumor marker for hepatocellular carcinoma. *Exp Mol Pathol*, 82(2), 184-189. doi:10.1016/j.yexmp.2006.10.010

Jan, C. H., Williams, C. C., & Weissman, J. S. (2014). Principles of ER cotranslational translocation revealed by proximity-specific ribosome profiling. *Science*, 346(6210), 1257521. doi:10.1126/science.1257521

Janoff, E. N., Gustafson, C., & Frank, D. N. (2012). The world within: living with our microbial guests and guides. *Transl Res*, 160(4), 239-245. doi:10.1016/j.trsl.2012.05.005

Jeong, H., Sim, H. J., Song, E. K., Lee, H., Ha, S. C., Jun, Y., . . . Lee, C. (2016). Crystal structure of SEL1L: Insight into the roles of SLR motifs in ERAD pathway. *Sci Rep*, 6, 20261. doi:10.1038/srep20261

Ji, Y., Kim, H., Yang, L., Sha, H., Roman, C. A., Long, Q., & Qi, L. (2016). The SellL-Hrd1 Endoplasmic Reticulum-Associated Degradation Complex Manages a Key Checkpoint in B Cell Development. *Cell Rep*, 16(10), 2630-2640. doi:10.1016/j.celrep.2016.08.003

Ji, Y., Sun, S., Goodrich, J. K., Kim, H., Poole, A. C., Duhamel, G. E., . . . Qi, L. (2014). Diet-induced alterations in gut microflora contribute to lethal pulmonary damage in TLR2/TLR4-deficient mice. *Cell Rep*, 8(1), 137-149. doi:10.1016/j.celrep.2014.05.040

Ji, Y., Sun, S., Xia, S., Yang, L., Li, X., & Qi, L. (2012). Short term high fat diet challenge promotes alternative macrophage polarization in adipose tissue via natural killer T cells and interleukin-4. *J Biol Chem*, 287(29), 24378-24386. doi:10.1074/jbc.M112.371807

Johansen, F. E., Pekna, M., Norderhaug, I. N., Haneberg, B., Hietala, M. A., Krajci, P., . . . Brandtzaeg, P. (1999). Absence of epithelial immunoglobulin A transport, with increased mucosal leakiness, in polymeric immunoglobulin receptor/secretory component-deficient mice. *J Exp Med*, 190(7), 915-922.

Jumaa, H., Bossaller, L., Portugal, K., Storch, B., Lotz, M., Flemming, A., . . . Reth, M. (2003). Deficiency of the adaptor SLP-65 in pre-B-cell acute lymphoblastic leukaemia. *Nature*, 423(6938), 452-456. doi:10.1038/nature01608

Jumaa, H., Wollscheid, B., Mitterer, M., Wienands, J., Reth, M., & Nielsen, P. J. (1999). Abnormal development and function of B lymphocytes in mice deficient for the signaling adaptor protein SLP-65. *Immunity*, *11*(5), 547-554.

Kallies, A., Hasbold, J., Fairfax, K., Pridans, C., Emslie, D., McKenzie, B. S., . . . Nutt, S. L. (2007). Initiation of plasma-cell differentiation is independent of the transcription factor Blimp-1. *Immunity*, *26*(5), 555-566. doi:10.1016/j.immuni.2007.04.007

Kamimura, D., & Bevan, M. J. (2008). Endoplasmic reticulum stress regulator XBP-1 contributes to effector CD8<sup>+</sup> T cell differentiation during acute infection. *J Immunol*, *181*(8), 5433-5441.

Karasuyama, H., Kudo, A., & Melchers, F. (1990). The proteins encoded by the VpreB and lambda 5 pre-B cell-specific genes can associate with each other and with mu heavy chain. *J Exp Med*, *172*(3), 969-972.

Karnowski, A., Cao, C., Matthias, G., Carotta, S., Corcoran, L. M., Martensson, I. L., . . . Matthias, P. (2008). Silencing and nuclear repositioning of the lambda5 gene locus at the pre-B cell stage requires Aiolos and OBF-1. *PLoS One*, *3*(10), e3568. doi:10.1371/journal.pone.0003568

Kaser, A., Lee, A. H., Franke, A., Glickman, J. N., Zeissig, S., Tilg, H., . . . Blumberg, R. S. (2008). XBP1 links ER stress to intestinal inflammation and confers genetic risk for human inflammatory bowel disease. *Cell*, *134*(5), 743-756. doi:10.1016/j.cell.2008.07.021

Kaufman, R. J. (2002). Orchestrating the unfolded protein response in health and disease. *J Clin Invest*, *110*(10), 1389-1398. doi:10.1172/JCI16886

Kikuchi, K., Lai, A. Y., Hsu, C. L., & Kondo, M. (2005). IL-7 receptor signaling is necessary for stage transition in adult B cell development through up-regulation of EBF. *J Exp Med*, *201*(8), 1197-1203. doi:10.1084/jem.20050158

Kim, S., Joe, Y., Kim, H. J., Kim, Y. S., Jeong, S. O., Pae, H. O., . . . Chung, H. T. (2015). Endoplasmic reticulum stress-induced IRE1alpha activation mediates cross-talk of GSK-3beta and XBP-1 to regulate inflammatory cytokine production. *J Immunol*, *194*(9), 4498-4506. doi:10.4049/jimmunol.1401399

- Kim, S. J., Gregersen, P. K., & Diamond, B. (2013). Regulation of dendritic cell activation by microRNA let-7c and BLIMP1. *J Clin Invest*, *123*(2), 823-833. doi:10.1172/JCI64712
- Kimata, Y., Kimata, Y. I., Shimizu, Y., Abe, H., Farcasanu, I. C., Takeuchi, M., . . . Kohno, K. (2003). Genetic evidence for a role of BiP/Kar2 that regulates Ire1 in response to accumulation of unfolded proteins. *Mol Biol Cell*, *14*(6), 2559-2569. doi:10.1091/mbc.E02-11-0708
- Kitamura, D., Kudo, A., Schaal, S., Muller, W., Melchers, F., & Rajewsky, K. (1992). A critical role of lambda 5 protein in B cell development. *Cell*, *69*(5), 823-831.
- Kitamura, D., & Rajewsky, K. (1992). Targeted disruption of mu chain membrane exon causes loss of heavy-chain allelic exclusion. *Nature*, *356*(6365), 154-156. doi:10.1038/356154a0
- Kitamura, D., Roes, J., Kuhn, R., & Rajewsky, K. (1991). A B cell-deficient mouse by targeted disruption of the membrane exon of the immunoglobulin mu chain gene. *Nature*, *350*(6317), 423-426. doi:10.1038/350423a0
- Kline, G. H., Hartwell, L., Beck-Engeser, G. B., Keyna, U., Zaharevitz, S., Klinman, N. R., & Jack, H. M. (1998). Pre-B cell receptor-mediated selection of pre-B cells synthesizing functional mu heavy chains. *J Immunol*, *161*(4), 1608-1618.
- Koenig, P. A., & Ploegh, H. L. (2014). Protein quality control in the endoplasmic reticulum. *F1000Prime Rep*, *6*, 49. doi:10.12703/P6-49
- Koizumi, N., Martinez, I. M., Kimata, Y., Kohno, K., Sano, H., & Chrispeels, M. J. (2001). Molecular characterization of two Arabidopsis Ire1 homologs, endoplasmic reticulum-located transmembrane protein kinases. *Plant Physiol*, *127*(3), 949-962.
- Komander, D., & Rape, M. (2012). The ubiquitin code. *Annu Rev Biochem*, *81*, 203-229. doi:10.1146/annurev-biochem-060310-170328
- Kondo, S., Murakami, T., Tatsumi, K., Ogata, M., Kanemoto, S., Otori, K., . . . Imaizumi, K. (2005). OASIS, a CREB/ATF-family member, modulates UPR signalling in astrocytes. *Nat Cell Biol*, *7*(2), 186-194. doi:10.1038/ncb1213

Korennykh, A. V., Egea, P. F., Korostelev, A. A., Finer-Moore, J., Zhang, C., Shokat, K. M., . . . Walter, P. (2009). The unfolded protein response signals through high-order assembly of Ire1. *Nature*, *457*(7230), 687-693. doi:10.1038/nature07661

Kornfeld, R., & Kornfeld, S. (1985). Assembly of asparagine-linked oligosaccharides. *Annu Rev Biochem*, *54*, 631-664. doi:10.1146/annurev.bi.54.070185.003215

Kroemer, G., Marino, G., & Levine, B. (2010). Autophagy and the integrated stress response. *Mol Cell*, *40*(2), 280-293. doi:10.1016/j.molcel.2010.09.023

Kroese, F. G., Butcher, E. C., Stall, A. M., & Herzenberg, L. A. (1989). A major peritoneal reservoir of precursors for intestinal IgA plasma cells. *Immunol Invest*, *18*(1-4), 47-58.

Kudo, A., & Melchers, F. (1987). A second gene, VpreB in the lambda 5 locus of the mouse, which appears to be selectively expressed in pre-B lymphocytes. *EMBO J*, *6*(8), 2267-2272.

Kudo, A., Thalmann, P., Sakaguchi, N., Davidson, W. F., Pierce, J. H., Kearney, J. F., . . . Melchers, F. (1992). The expression of the mouse VpreB/lambda 5 locus in transformed cell lines and tumors of the B lineage differentiation pathway. *Int Immunol*, *4*(8), 831-840.

Kulp, M. S., Frickel, E. M., Ellgaard, L., & Weissman, J. S. (2006). Domain architecture of protein-disulfide isomerase facilitates its dual role as an oxidase and an isomerase in Ero1p-mediated disulfide formation. *J Biol Chem*, *281*(2), 876-884. doi:10.1074/jbc.M511764200

Kurosaki, T., Shinohara, H., & Baba, Y. (2010). B cell signaling and fate decision. *Annu Rev Immunol*, *28*, 21-55. doi:10.1146/annurev.immunol.021908.132541

Kyostila, K., Cizinauskas, S., Seppala, E. H., Suhonen, E., Jeserevics, J., Sukura, A., . . . Lohi, H. (2012). A SEL1L mutation links a canine progressive early-onset cerebellar ataxia to the endoplasmic reticulum-associated protein degradation (ERAD) machinery. *PLoS Genet*, *8*(6), e1002759. doi:10.1371/journal.pgen.1002759

Lamm, M. E. (1997). Interaction of antigens and antibodies at mucosal surfaces. *Annu Rev Microbiol*, *51*, 311-340. doi:10.1146/annurev.micro.51.1.311

Langford, T. D., Housley, M. P., Boes, M., Chen, J., Kagnoff, M. F., Gillin, F. D., & Eckmann, L. (2002). Central importance of immunoglobulin A in host defense against *Giardia* spp. *Infect Immun*, *70*(1), 11-18.

Lassoued, K., Illges, H., Benlagha, K., & Cooper, M. D. (1996). Fate of surrogate light chains in B lineage cells. *J Exp Med*, *183*(2), 421-429.

Lederkremer, G. Z. (2009). Glycoprotein folding, quality control and ER-associated degradation. *Curr Opin Struct Biol*, *19*(5), 515-523. doi:10.1016/j.sbi.2009.06.004

Lee, A. H., Chu, G. C., Iwakoshi, N. N., & Glimcher, L. H. (2005). XBP-1 is required for biogenesis of cellular secretory machinery of exocrine glands. *EMBO J*, *24*(24), 4368-4380. doi:10.1038/sj.emboj.7600903

Lee, A. H., Heidtman, K., Hotamisligil, G. S., & Glimcher, L. H. (2011). Dual and opposing roles of the unfolded protein response regulated by IRE1alpha and XBP1 in proinsulin processing and insulin secretion. *Proc Natl Acad Sci U S A*, *108*(21), 8885-8890. doi:10.1073/pnas.1105564108

Lee, A. H., Iwakoshi, N. N., Anderson, K. C., & Glimcher, L. H. (2003). Proteasome inhibitors disrupt the unfolded protein response in myeloma cells. *Proc Natl Acad Sci U S A*, *100*(17), 9946-9951. doi:10.1073/pnas.1334037100

Lee, A. H., Iwakoshi, N. N., & Glimcher, L. H. (2003). XBP-1 regulates a subset of endoplasmic reticulum resident chaperone genes in the unfolded protein response. *Mol Cell Biol*, *23*(21), 7448-7459.

Lee, A. S. (2005). The ER chaperone and signaling regulator GRP78/BiP as a monitor of endoplasmic reticulum stress. *Methods*, *35*(4), 373-381. doi:10.1016/j.ymeth.2004.10.010

Lee, K., Tirasophon, W., Shen, X., Michalak, M., Prywes, R., Okada, T., . . . Kaufman, R. J. (2002). IRE1-mediated unconventional mRNA splicing and S2P-mediated ATF6 cleavage merge to regulate XBP1 in signaling the unfolded protein response. *Genes Dev*, *16*(4), 452-466. doi:10.1101/gad.964702

Lee, Y. K., Brewer, J. W., Hellman, R., & Hendershot, L. M. (1999). BiP and immunoglobulin light chain cooperate to control the folding of heavy chain and ensure the fidelity of immunoglobulin assembly. *Mol Biol Cell*, *10*(7), 2209-2219.

Lei, K., & Davis, R. J. (2003). JNK phosphorylation of Bim-related members of the Bcl2 family induces Bax-dependent apoptosis. *Proc Natl Acad Sci U S A*, *100*(5), 2432-2437. doi:10.1073/pnas.0438011100

Leung-Hagesteijn, C., Erdmann, N., Cheung, G., Keats, J. J., Stewart, A. K., Reece, D. E., . . . Tiedemann, R. E. (2013). Xbp1s-negative tumor B cells and pre-plasmablasts mediate therapeutic proteasome inhibitor resistance in multiple myeloma. *Cancer Cell*, *24*(3), 289-304. doi:10.1016/j.ccr.2013.08.009

Levine, B., & Kroemer, G. (2008). Autophagy in the pathogenesis of disease. *Cell*, *132*(1), 27-42. doi:10.1016/j.cell.2007.12.018

Li, J., & Lee, A. S. (2006). Stress induction of GRP78/BiP and its role in cancer. *Curr Mol Med*, *6*(1), 45-54.

Li, M., Baumeister, P., Roy, B., Phan, T., Foti, D., Luo, S., & Lee, A. S. (2000). ATF6 as a transcription activator of the endoplasmic reticulum stress element: thapsigargin stress-induced changes and synergistic interactions with NF-Y and YY1. *Mol Cell Biol*, *20*(14), 5096-5106.

Li, S., Francisco, A. B., Munroe, R. J., Schimenti, J. C., & Long, Q. (2010). SEL1L deficiency impairs growth and differentiation of pancreatic epithelial cells. *BMC Dev Biol*, *10*, 19. doi:10.1186/1471-213X-10-19

Li, X., Zhang, K., & Li, Z. (2011). Unfolded protein response in cancer: the physician's perspective. *J Hematol Oncol*, *4*, 8. doi:10.1186/1756-8722-4-8

Li, Y., Schwabe, R. F., DeVries-Seimon, T., Yao, P. M., Gerbod-Giannone, M. C., Tall, A. R., . . . Tabas, I. (2005). Free cholesterol-loaded macrophages are an abundant source of tumor necrosis factor-alpha and interleukin-6: model of NF-kappaB- and map kinase-dependent inflammation in advanced atherosclerosis. *J Biol Chem*, *280*(23), 21763-21772. doi:10.1074/jbc.M501759200

Lilley, B. N., & Ploegh, H. L. (2004). A membrane protein required for dislocation of misfolded proteins from the ER. *Nature*, *429*(6994), 834-840. doi:10.1038/nature02592

Lin, J. H., Walter, P., & Yen, T. S. (2008). Endoplasmic reticulum stress in disease pathogenesis. *Annu Rev Pathol*, *3*, 399-425. doi:10.1146/annurev.pathmechdis.3.121806.151434

Lin, K. I., Angelin-Duclos, C., Kuo, T. C., & Calame, K. (2002). Blimp-1-dependent repression of Pax-5 is required for differentiation of B cells to immunoglobulin M-secreting plasma cells. *Mol Cell Biol*, 22(13), 4771-4780.

Liou, H. C., Boothby, M. R., Finn, P. W., Davidon, R., Nabavi, N., Zeleznik-Le, N. J., . . . Glimcher, L. H. (1990). A new member of the leucine zipper class of proteins that binds to the HLA DR alpha promoter. *Science*, 247(4950), 1581-1584.

Lipson, K. L., Fonseca, S. G., Ishigaki, S., Nguyen, L. X., Foss, E., Bortell, R., . . . Urano, F. (2006). Regulation of insulin biosynthesis in pancreatic beta cells by an endoplasmic reticulum-resident protein kinase IRE1. *Cell Metab*, 4(3), 245-254. doi:10.1016/j.cmet.2006.07.007

Lipson, K. L., Ghosh, R., & Urano, F. (2008). The role of IRE1alpha in the degradation of insulin mRNA in pancreatic beta-cells. *PLoS One*, 3(2), e1648. doi:10.1371/journal.pone.0001648

Liu, C. Y., Wong, H. N., Schauerte, J. A., & Kaufman, R. J. (2002). The protein kinase/endoribonuclease IRE1alpha that signals the unfolded protein response has a luminal N-terminal ligand-independent dimerization domain. *J Biol Chem*, 277(21), 18346-18356. doi:10.1074/jbc.M112454200

Liu, Q., Chen, J., Mai, B., Amos, C., Killary, A. M., Sen, S., . . . Frazier, M. L. (2012). A single-nucleotide polymorphism in tumor suppressor gene SEL1L as a predictive and prognostic marker for pancreatic ductal adenocarcinoma in Caucasians. *Mol Carcinog*, 51(5), 433-438. doi:10.1002/mc.20808

Lu, M., Lawrence, D. A., Marsters, S., Acosta-Alvear, D., Kimmig, P., Mendez, A. S., . . . Ashkenazi, A. (2014). Opposing unfolded-protein-response signals converge on death receptor 5 to control apoptosis. *Science*, 345(6192), 98-101. doi:10.1126/science.1254312

Ma, Y., & Hendershot, L. M. (2001). The unfolding tale of the unfolded protein response. *Cell*, 107(7), 827-830.

Ma, Y., Shimizu, Y., Mann, M. J., Jin, Y., & Hendershot, L. M. (2010). Plasma cell differentiation initiates a limited ER stress response by specifically suppressing the PERK-dependent branch of the unfolded protein response. *Cell Stress Chaperones*, 15(3), 281-293. doi:10.1007/s12192-009-0142-9

Macpherson, A. J., Geuking, M. B., Slack, E., Hapfelmeier, S., & McCoy, K. D. (2012). The habitat, double life, citizenship, and forgetfulness of IgA. *Immunol Rev*, *245*(1), 132-146. doi:10.1111/j.1600-065X.2011.01072.x

Mahoney, D. J., Lefebvre, C., Allan, K., Brun, J., Sanaei, C. A., Baird, S., . . . Stojdl, D. F. (2011). Virus-tumor interactome screen reveals ER stress response can reprogram resistant cancers for oncolytic virus-triggered caspase-2 cell death. *Cancer Cell*, *20*(4), 443-456. doi:10.1016/j.ccr.2011.09.005

Malik, A., Sharma, D., Zhu, Q., Karki, R., Guy, C. S., Vogel, P., & Kanneganti, T. D. (2016). IL-33 regulates the IgA-microbiota axis to restrain IL-1alpha-dependent colitis and tumorigenesis. *J Clin Invest*, *126*(12), 4469-4481. doi:10.1172/JCI88625

Martensson, A., Argon, Y., Melchers, F., Dul, J. L., & Martensson, I. L. (1999). Partial block in B lymphocyte development at the transition into the pre-B cell receptor stage in Vpre-B1-deficient mice. *Int Immunol*, *11*(3), 453-460.

Martensson, I. L., Almqvist, N., Grimsholm, O., & Bernardi, A. I. (2010). The pre-B cell receptor checkpoint. *FEBS Lett*, *584*(12), 2572-2579. doi:10.1016/j.febslet.2010.04.057

Martin, C. H., Aifantis, I., Scimone, M. L., von Andrian, U. H., Reizis, B., von Boehmer, H., & Gounari, F. (2003). Efficient thymic immigration of B220+ lymphoid-restricted bone marrow cells with T precursor potential. *Nat Immunol*, *4*(9), 866-873. doi:10.1038/ni965

Martin, D. A., Lu, L., Cascalho, M., & Wu, G. E. (2007). Maintenance of surrogate light chain expression induces developmental delay in early B cell compartment. *J Immunol*, *179*(8), 4996-5005.

Martin, F., Oliver, A. M., & Kearney, J. F. (2001). Marginal zone and B1 B cells unite in the early response against T-independent blood-borne particulate antigens. *Immunity*, *14*(5), 617-629.

Martino, M. B., Jones, L., Brighton, B., Ehre, C., Abdulah, L., Davis, C. W., . . . Ribeiro, C. M. (2013). The ER stress transducer IRE1beta is required for airway epithelial mucin production. *Mucosal Immunol*, *6*(3), 639-654. doi:10.1038/mi.2012.105

Martinson, F., Chen, X., Lee, A. H., & Glimcher, L. H. (2010). TLR activation of the transcription factor XBP1 regulates innate immune responses in macrophages. *Nat Immunol*, *11*(5), 411-418. doi:10.1038/ni.1857

Masaki, T., Yoshida, M., & Noguchi, S. (1999). Targeted disruption of CRE-binding factor TREB5 gene leads to cellular necrosis in cardiac myocytes at the embryonic stage. *Biochem Biophys Res Commun*, 261(2), 350-356. doi:10.1006/bbrc.1999.0972

Matlack, K. E., Mothes, W., & Rapoport, T. A. (1998). Protein translocation: tunnel vision. *Cell*, 92(3), 381-390.

Maurel, M., & Chevet, E. (2013). Endoplasmic reticulum stress signaling: the microRNA connection. *Am J Physiol Cell Physiol*, 304(12), C1117-1126. doi:10.1152/ajpcell.00061.2013

Maurel, M., Dejeans, N., Taouji, S., Chevet, E., & Grosset, C. F. (2013). MicroRNA-1291-mediated silencing of IRE1alpha enhances Glypican-3 expression. *RNA*, 19(6), 778-788. doi:10.1261/rna.036483.112

McCullough, K. D., Martindale, J. L., Klotz, L. O., Aw, T. Y., & Holbrook, N. J. (2001). Gadd153 sensitizes cells to endoplasmic reticulum stress by down-regulating Bcl2 and perturbing the cellular redox state. *Mol Cell Biol*, 21(4), 1249-1259. doi:10.1128/MCB.21.4.1249-1259.2001

McMaster, C. R. (2001). Lipid metabolism and vesicle trafficking: more than just greasing the transport machinery. *Biochem Cell Biol*, 79(6), 681-692.

Mehnert, M., Sommer, T., & Jarosch, E. (2014). Der1 promotes movement of misfolded proteins through the endoplasmic reticulum membrane. *Nat Cell Biol*, 16(1), 77-86. doi:10.1038/ncb2882

Meini, A., Pillan, N. M., Villanacci, V., Monafò, V., Ugazio, A. G., & Plebani, A. (1996). Prevalence and diagnosis of celiac disease in IgA-deficient children. *Ann Allergy Asthma Immunol*, 77(4), 333-336. doi:10.1016/S1081-1206(10)63329-7

Melchers, F. (1999). Fit for life in the immune system? Surrogate L chain tests H chains that test L chains. *Proc Natl Acad Sci U S A*, 96(6), 2571-2573.

Melchers, F. (2005). The pre-B-cell receptor: selector of fitting immunoglobulin heavy chains for the B-cell repertoire. *Nat Rev Immunol*, 5(7), 578-584. doi:10.1038/nri1649

Melchers, F., Karasuyama, H., Haasner, D., Bauer, S., Kudo, A., Sakaguchi, N., . . . Rolink, A. (1993). The surrogate light chain in B-cell development. *Immunol Today*, *14*(2), 60-68. doi:10.1016/0167-5699(93)90060-X

Melchers, F., ten Boekel, E., Yamagami, T., Andersson, J., & Rolink, A. (1999). The roles of preB and B cell receptors in the stepwise allelic exclusion of mouse IgH and L chain gene loci. *Semin Immunol*, *11*(5), 307-317. doi:10.1006/smim.1999.0187

Meldolesi, J., & Pozzan, T. (1998). The endoplasmic reticulum Ca<sup>2+</sup> store: a view from the lumen. *Trends Biochem Sci*, *23*(1), 10-14.

Merad, M., Sathe, P., Helft, J., Miller, J., & Mortha, A. (2013). The dendritic cell lineage: ontogeny and function of dendritic cells and their subsets in the steady state and the inflamed setting. *Annu Rev Immunol*, *31*, 563-604. doi:10.1146/annurev-immunol-020711-074950

Miller, J. P., Izon, D., DeMuth, W., Gerstein, R., Bhandoola, A., & Allman, D. (2002). The earliest step in B lineage differentiation from common lymphoid progenitors is critically dependent upon interleukin 7. *J Exp Med*, *196*(5), 705-711.

Minegishi, Y., Coustan-Smith, E., Rapalus, L., Ersoy, F., Campana, D., & Conley, M. E. (1999). Mutations in Igalpha (CD79a) result in a complete block in B-cell development. *J Clin Invest*, *104*(8), 1115-1121. doi:10.1172/JCI7696

Minegishi, Y., Coustan-Smith, E., Wang, Y. H., Cooper, M. D., Campana, D., & Conley, M. E. (1998). Mutations in the human lambda5/14.1 gene result in B cell deficiency and agammaglobulinemia. *J Exp Med*, *187*(1), 71-77.

Minegishi, Y., Hendershot, L. M., & Conley, M. E. (1999). Novel mechanisms control the folding and assembly of lambda5/14.1 and VpreB to produce an intact surrogate light chain. *Proc Natl Acad Sci U S A*, *96*(6), 3041-3046.

Mori, K. (2009). Signalling pathways in the unfolded protein response: development from yeast to mammals. *J Biochem*, *146*(6), 743-750. doi:10.1093/jb/mvp166

Mori, K., Kawahara, T., Yoshida, H., Yanagi, H., & Yura, T. (1996). Signalling from endoplasmic reticulum to nucleus: transcription factor with a basic-leucine zipper motif is required for the unfolded protein-response pathway. *Genes Cells*, *1*(9), 803-817.

Mori, K., Ma, W., Gething, M. J., & Sambrook, J. (1993). A transmembrane protein with a cdc2+/CDC28-related kinase activity is required for signaling from the ER to the nucleus. *Cell*, 74(4), 743-756.

Morishima, N., Nakanishi, K., Takenouchi, H., Shibata, T., & Yasuhiko, Y. (2002). An endoplasmic reticulum stress-specific caspase cascade in apoptosis. Cytochrome c-independent activation of caspase-9 by caspase-12. *J Biol Chem*, 277(37), 34287-34294. doi:10.1074/jbc.M204973200

Morishima, N., Nakanishi, K., Tsuchiya, K., Shibata, T., & Seiwa, E. (2004). Translocation of Bim to the endoplasmic reticulum (ER) mediates ER stress signaling for activation of caspase-12 during ER stress-induced apoptosis. *J Biol Chem*, 279(48), 50375-50381. doi:10.1074/jbc.M408493200

Mueller, B., Klemm, E. J., Spooner, E., Claessen, J. H., & Ploegh, H. L. (2008). SEL1L nucleates a protein complex required for dislocation of misfolded glycoproteins. *Proc Natl Acad Sci U S A*, 105(34), 12325-12330. doi:10.1073/pnas.0805371105

Mueller, B., Lilley, B. N., & Ploegh, H. L. (2006). SEL1L, the homologue of yeast Hrd3p, is involved in protein dislocation from the mammalian ER. *J Cell Biol*, 175(2), 261-270. doi:10.1083/jcb.200605196

Mundt, C., Licence, S., Shimizu, T., Melchers, F., & Martensson, I. L. (2001). Loss of precursor B cell expansion but not allelic exclusion in VpreB1/VpreB2 double-deficient mice. *J Exp Med*, 193(4), 435-445.

Murthy, A. K., Dubose, C. N., Banas, J. A., Coalson, J. J., & Arulanandam, B. P. (2006). Contribution of polymeric immunoglobulin receptor to regulation of intestinal inflammation in dextran sulfate sodium-induced colitis. *J Gastroenterol Hepatol*, 21(9), 1372-1380. doi:10.1111/j.1440-1746.2006.04312.x

Nagelkerke, A., Sweep, F. C., Geurts-Moespot, A., Bussink, J., & Span, P. N. (2015). Therapeutic targeting of autophagy in cancer. Part I: molecular pathways controlling autophagy. *Semin Cancer Biol*, 31, 89-98. doi:10.1016/j.semcancer.2014.05.004

Nakagawa, T., Zhu, H., Morishima, N., Li, E., Xu, J., Yankner, B. A., & Yuan, J. (2000). Caspase-12 mediates endoplasmic-reticulum-specific apoptosis and cytotoxicity by amyloid-beta. *Nature*, 403(6765), 98-103. doi:10.1038/47513

Nakamura, M., Gotoh, T., Okuno, Y., Tatetsu, H., Sonoki, T., Uneda, S., . . . Hata, H. (2006). Activation of the endoplasmic reticulum stress pathway is associated with survival of myeloma cells. *Leuk Lymphoma*, *47*(3), 531-539. doi:10.1080/10428190500312196

Nekrutenko, A., & He, J. (2006). Functionality of unspliced XBP1 is required to explain evolution of overlapping reading frames. *Trends Genet*, *22*(12), 645-648. doi:10.1016/j.tig.2006.09.012

Ng, D. T., Brown, J. D., & Walter, P. (1996). Signal sequences specify the targeting route to the endoplasmic reticulum membrane. *J Cell Biol*, *134*(2), 269-278.

Nguyen, D. T., Kebache, S., Fazel, A., Wong, H. N., Jenna, S., Emadali, A., . . . Chevet, E. (2004). Nck-dependent activation of extracellular signal-regulated kinase-1 and regulation of cell survival during endoplasmic reticulum stress. *Mol Biol Cell*, *15*(9), 4248-4260. doi:10.1091/mbc.E03-11-0851

Niederreiter, L., Fritz, T. M., Adolph, T. E., Krismer, A. M., Offner, F. A., Tschurtschenthaler, M., . . . Kaser, A. (2013). ER stress transcription factor Xbp1 suppresses intestinal tumorigenesis and directs intestinal stem cells. *J Exp Med*, *210*(10), 2041-2056. doi:10.1084/jem.20122341

Nikawa, J., & Yamashita, S. (1992). IRE1 encodes a putative protein kinase containing a membrane-spanning domain and is required for inositol phototrophy in *Saccharomyces cerevisiae*. *Mol Microbiol*, *6*(11), 1441-1446.

Nishitoh, H., Matsuzawa, A., Tobiume, K., Saegusa, K., Takeda, K., Inoue, K., . . . Ichijo, H. (2002). ASK1 is essential for endoplasmic reticulum stress-induced neuronal cell death triggered by expanded polyglutamine repeats. *Genes Dev*, *16*(11), 1345-1355. doi:10.1101/gad.992302

Oda, Y., Okada, T., Yoshida, H., Kaufman, R. J., Nagata, K., & Mori, K. (2006). Derlin-2 and Derlin-3 are regulated by the mammalian unfolded protein response and are required for ER-associated degradation. *J Cell Biol*, *172*(3), 383-393. doi:10.1083/jcb.200507057

Oettinger, M. A., Schatz, D. G., Gorka, C., & Baltimore, D. (1990). RAG-1 and RAG-2, adjacent genes that synergistically activate V(D)J recombination. *Science*, *248*(4962), 1517-1523.

Ogata, M., Hino, S., Saito, A., Morikawa, K., Kondo, S., Kanemoto, S., . . . Imaizumi, K. (2006). Autophagy is activated for cell survival after endoplasmic reticulum stress. *Mol Cell Biol*, 26(24), 9220-9231. doi:10.1128/MCB.01453-06

Ohmura, K., Kawamoto, H., Lu, M., Ikawa, T., Ozaki, S., Nakao, K., & Katsura, Y. (2001). Immature multipotent hemopoietic progenitors lacking long-term bone marrow-reconstituting activity in the aorta-gonad-mesonephros region of murine day 10 fetuses. *J Immunol*, 166(5), 3290-3296.

Ohnishi, K., & Melchers, F. (2003). The nonimmunoglobulin portion of lambda5 mediates cell-autonomous pre-B cell receptor signaling. *Nat Immunol*, 4(9), 849-856. doi:10.1038/ni959

Oikawa, D., Kimata, Y., Kohno, K., & Iwawaki, T. (2009). Activation of mammalian IRE1alpha upon ER stress depends on dissociation of BiP rather than on direct interaction with unfolded proteins. *Exp Cell Res*, 315(15), 2496-2504. doi:10.1016/j.yexcr.2009.06.009

Oikawa, D., Kitamura, A., Kinjo, M., & Iwawaki, T. (2012). Direct association of unfolded proteins with mammalian ER stress sensor, IRE1beta. *PLoS One*, 7(12), e51290. doi:10.1371/journal.pone.0051290

Oikawa, D., Tokuda, M., Hosoda, A., & Iwawaki, T. (2010). Identification of a consensus element recognized and cleaved by IRE1 alpha. *Nucleic Acids Res*, 38(18), 6265-6273. doi:10.1093/nar/gkq452

Okada, T., Yoshida, H., Akazawa, R., Negishi, M., & Mori, K. (2002). Distinct roles of activating transcription factor 6 (ATF6) and double-stranded RNA-activated protein kinase-like endoplasmic reticulum kinase (PERK) in transcription during the mammalian unfolded protein response. *Biochem J*, 366(Pt 2), 585-594. doi:10.1042/BJ20020391

Okai, S., Usui, F., Yokota, S., Hori, I. Y., Hasegawa, M., Nakamura, T., . . . Shinkura, R. (2016). High-affinity monoclonal IgA regulates gut microbiota and prevents colitis in mice. *Nat Microbiol*, 1(9), 16103. doi:10.1038/nmicrobiol.2016.103

Olivari, S., Cali, T., Salo, K. E., Paganetti, P., Ruddock, L. W., & Molinari, M. (2006). EDEM1 regulates ER-associated degradation by accelerating de-mannosylation of folding-defective polypeptides and by inhibiting their covalent aggregation. *Biochem Biophys Res Commun*, 349(4), 1278-1284. doi:10.1016/j.bbrc.2006.08.186

- Olzmann, J. A., Kopito, R. R., & Christianson, J. C. (2013). The mammalian endoplasmic reticulum-associated degradation system. *Cold Spring Harb Perspect Biol*, 5(9). doi:10.1101/cshperspect.a013185
- Orlandi, R., Cattaneo, M., Troglio, F., Casalini, P., Ronchini, C., Menard, S., & Biunno, I. (2002). SEL1L expression decreases breast tumor cell aggressiveness in vivo and in vitro. *Cancer Res*, 62(2), 567-574.
- Osorio, F., Tavernier, S. J., Hoffmann, E., Saeys, Y., Martens, L., Veters, J., . . . Lambrecht, B. N. (2014). The unfolded-protein-response sensor IRE-1alpha regulates the function of CD8alpha+ dendritic cells. *Nat Immunol*, 15(3), 248-257. doi:10.1038/ni.2808
- Otero, J. H., Lizak, B., & Hendershot, L. M. (2010). Life and death of a BiP substrate. *Semin Cell Dev Biol*, 21(5), 472-478. doi:10.1016/j.semcdb.2009.12.008
- Pahl, H. L. (1999). Activators and target genes of Rel/NF-kappaB transcription factors. *Oncogene*, 18(49), 6853-6866. doi:10.1038/sj.onc.1203239
- Paige, C. J., Kincade, P. W., & Ralph, P. (1978). Murine B cell leukemia line with inducible surface immunoglobulin expression. *J Immunol*, 121(2), 641-647.
- Palam, L. R., Baird, T. D., & Wek, R. C. (2011). Phosphorylation of eIF2 facilitates ribosomal bypass of an inhibitory upstream ORF to enhance CHOP translation. *J Biol Chem*, 286(13), 10939-10949. doi:10.1074/jbc.M110.216093
- Palmer, C., Bik, E. M., DiGiulio, D. B., Relman, D. A., & Brown, P. O. (2007). Development of the human infant intestinal microbiota. *PLoS Biol*, 5(7), e177. doi:10.1371/journal.pbio.0050177
- Papandreou, I., Denko, N. C., Olson, M., Van Melckebeke, H., Lust, S., Tam, A., . . . Koong, A. C. (2011). Identification of an Ire1alpha endonuclease specific inhibitor with cytotoxic activity against human multiple myeloma. *Blood*, 117(4), 1311-1314. doi:10.1182/blood-2010-08-303099
- Park, E., & Rapoport, T. A. (2012). Mechanisms of Sec61/SecY-mediated protein translocation across membranes. *Annu Rev Biophys*, 41, 21-40. doi:10.1146/annurev-biophys-050511-102312

Parker, M. J., Licence, S., Erlandsson, L., Galler, G. R., Chakalova, L., Osborne, C. S., . . . Martensson, I. L. (2005). The pre-B-cell receptor induces silencing of VpreB and lambda5 transcription. *EMBO J*, *24*(22), 3895-3905. doi:10.1038/sj.emboj.7600850

Parodi, A. J. (2000). Protein glucosylation and its role in protein folding. *Annu Rev Biochem*, *69*, 69-93. doi:10.1146/annurev.biochem.69.1.69

Paton, A. W., Beddoe, T., Thorpe, C. M., Whisstock, J. C., Wilce, M. C., Rossjohn, J., . . . Paton, J. C. (2006). AB5 subtilase cytotoxin inactivates the endoplasmic reticulum chaperone BiP. *Nature*, *443*(7111), 548-552. doi:10.1038/nature05124

Pearce, M. M., Wang, Y., Kelley, G. G., & Wojcikiewicz, R. J. (2007). SPFH2 mediates the endoplasmic reticulum-associated degradation of inositol 1,4,5-trisphosphate receptors and other substrates in mammalian cells. *J Biol Chem*, *282*(28), 20104-20115. doi:10.1074/jbc.M701862200

Perez-Mancera, P. A., Young, A. R., & Narita, M. (2014). Inside and out: the activities of senescence in cancer. *Nat Rev Cancer*, *14*(8), 547-558. doi:10.1038/nrc3773

Perry, J. W., Ahmed, M., Chang, K. O., Donato, N. J., Showalter, H. D., & Wobus, C. E. (2012). Antiviral activity of a small molecule deubiquitinase inhibitor occurs via induction of the unfolded protein response. *PLoS Pathog*, *8*(7), e1002783. doi:10.1371/journal.ppat.1002783

Peschon, J. J., Morrissey, P. J., Grabstein, K. H., Ramsdell, F. J., Maraskovsky, E., Gliniak, B. C., . . . Davison, B. L. (1994). Early lymphocyte expansion is severely impaired in interleukin 7 receptor-deficient mice. *J Exp Med*, *180*(5), 1955-1960.

Philippe, A., Weber, S., Esquivel, E. L., Houbron, C., Hamard, G., Ratelade, J., . . . Antignac, C. (2008). A missense mutation in podocin leads to early and severe renal disease in mice. *Kidney Int*, *73*(9), 1038-1047. doi:10.1038/ki.2008.27

Pillai, S., & Baltimore, D. (1987). Formation of disulphide-linked mu 2 omega 2 tetramers in pre-B cells by the 18K omega-immunoglobulin light chain. *Nature*, *329*(6135), 172-174. doi:10.1038/329172a0

Pilon, M., Schekman, R., & Romisch, K. (1997). Sec61p mediates export of a misfolded secretory protein from the endoplasmic reticulum to the cytosol for degradation. *EMBO J*, *16*(15), 4540-4548. doi:10.1093/emboj/16.15.4540

Pincus, D., Chevalier, M. W., Aragon, T., van Anken, E., Vidal, S. E., El-Samad, H., & Walter, P. (2010). BiP binding to the ER-stress sensor Ire1 tunes the homeostatic behavior of the unfolded protein response. *PLoS Biol*, *8*(7), e1000415. doi:10.1371/journal.pbio.1000415

Ploegh, H. L. (2007). A lipid-based model for the creation of an escape hatch from the endoplasmic reticulum. *Nature*, *448*(7152), 435-438. doi:10.1038/nature06004

Puthalakath, H., O'Reilly, L. A., Gunn, P., Lee, L., Kelly, P. N., Huntington, N. D., . . . Strasser, A. (2007). ER stress triggers apoptosis by activating BH3-only protein Bim. *Cell*, *129*(7), 1337-1349. doi:10.1016/j.cell.2007.04.027

Reid, D. W., & Nicchitta, C. V. (2015). Diversity and selectivity in mRNA translation on the endoplasmic reticulum. *Nat Rev Mol Cell Biol*, *16*(4), 221-231. doi:10.1038/nrm3958

Reimold, A. M., Etkin, A., Clauss, I., Perkins, A., Friend, D. S., Zhang, J., . . . Glimcher, L. H. (2000). An essential role in liver development for transcription factor XBP-1. *Genes Dev*, *14*(2), 152-157.

Reimold, A. M., Iwakoshi, N. N., Manis, J., Vallabhajosyula, P., Szomolanyi-Tsuda, E., Gravalles, E. M., . . . Glimcher, L. H. (2001). Plasma cell differentiation requires the transcription factor XBP-1. *Nature*, *412*(6844), 300-307. doi:10.1038/35085509

Reimold, A. M., Ponath, P. D., Li, Y. S., Hardy, R. R., David, C. S., Strominger, J. L., & Glimcher, L. H. (1996). Transcription factor B cell lineage-specific activator protein regulates the gene for human X-box binding protein 1. *J Exp Med*, *183*(2), 393-401.

Ri, M., Tashiro, E., Oikawa, D., Shinjo, S., Tokuda, M., Yokouchi, Y., . . . Iida, S. (2012). Identification of Toyocamycin, an agent cytotoxic for multiple myeloma cells, as a potent inhibitor of ER stress-induced XBP1 mRNA splicing. *Blood Cancer J*, *2*(7), e79. doi:10.1038/bcj.2012.26

Richardson, C. E., Kooistra, T., & Kim, D. H. (2010). An essential role for XBP-1 in host protection against immune activation in *C. elegans*. *Nature*, *463*(7284), 1092-1095. doi:10.1038/nature08762

Rickert, R. C., Roes, J., & Rajewsky, K. (1997). B lymphocyte-specific, Cre-mediated mutagenesis in mice. *Nucleic Acids Res*, *25*(6), 1317-1318.

Rinkenberger, J. L., Wallin, J. J., Johnson, K. W., & Koshland, M. E. (1996). An interleukin-2 signal relieves BSAP (Pax5)-mediated repression of the immunoglobulin J chain gene. *Immunity*, 5(4), 377-386.

Rius, J., Guma, M., Schachtrup, C., Akassoglou, K., Zinkernagel, A. S., Nizet, V., . . . Karin, M. (2008). NF-kappaB links innate immunity to the hypoxic response through transcriptional regulation of HIF-1alpha. *Nature*, 453(7196), 807-811. doi:10.1038/nature06905

Robson, A., & Collinson, I. (2006). The structure of the Sec complex and the problem of protein translocation. *EMBO Rep*, 7(11), 1099-1103. doi:10.1038/sj.embor.7400832

Rogier, E. W., Frantz, A. L., Bruno, M. E., Wedlund, L., Cohen, D. A., Stromberg, A. J., & Kaetzel, C. S. (2014). Secretory antibodies in breast milk promote long-term intestinal homeostasis by regulating the gut microbiota and host gene expression. *Proc Natl Acad Sci U S A*, 111(8), 3074-3079. doi:10.1073/pnas.1315792111

Rolink, A., Ghia, P., Grawunder, U., Haasner, D., Karasuyama, H., Kalberer, C., . . . Melchers, F. (1995). In-vitro analyses of mechanisms of B-cell development. *Semin Immunol*, 7(3), 155-167.

Rolink, A. G., Winkler, T., Melchers, F., & Andersson, J. (2000). Precursor B cell receptor-dependent B cell proliferation and differentiation does not require the bone marrow or fetal liver environment. *J Exp Med*, 191(1), 23-32.

Ron, D., & Walter, P. (2007). Signal integration in the endoplasmic reticulum unfolded protein response. *Nat Rev Mol Cell Biol*, 8(7), 519-529. doi:10.1038/nrm2199

Rudolph, M. G., Stanfield, R. L., & Wilson, I. A. (2006). How TCRs bind MHCs, peptides, and coreceptors. *Annu Rev Immunol*, 24, 419-466. doi:10.1146/annurev.immunol.23.021704.115658

Rumfelt, L. L., Zhou, Y., Rowley, B. M., Shinton, S. A., & Hardy, R. R. (2006). Lineage specification and plasticity in CD19- early B cell precursors. *J Exp Med*, 203(3), 675-687. doi:10.1084/jem.20052444

Rutkowski, D. T., Arnold, S. M., Miller, C. N., Wu, J., Li, J., Gunnison, K. M., . . . Kaufman, R. J. (2006). Adaptation to ER stress is mediated by differential stabilities of pro-survival and pro-apoptotic mRNAs and proteins. *PLoS Biol*, 4(11), e374. doi:10.1371/journal.pbio.0040374

Ryoo, H. D., Domingos, P. M., Kang, M. J., & Steller, H. (2007). Unfolded protein response in a *Drosophila* model for retinal degeneration. *EMBO J*, *26*(1), 242-252. doi:10.1038/sj.emboj.7601477

Ryter, S. W., Mizumura, K., & Choi, A. M. (2014). The impact of autophagy on cell death modalities. *Int J Cell Biol*, *2014*, 502676. doi:10.1155/2014/502676

Sakaguchi, N., & Melchers, F. (1986). Lambda 5, a new light-chain-related locus selectively expressed in pre-B lymphocytes. *Nature*, *324*(6097), 579-582. doi:10.1038/324579a0

Sakaki, K., Yoshina, S., Shen, X., Han, J., DeSantis, M. R., Xiong, M., . . . Kaufman, R. J. (2012). RNA surveillance is required for endoplasmic reticulum homeostasis. *Proc Natl Acad Sci U S A*, *109*(21), 8079-8084. doi:10.1073/pnas.1110589109

Saleh, M., Mathison, J. C., Wolinski, M. K., Bensinger, S. J., Fitzgerald, P., Droin, N., . . . Nicholson, D. W. (2006). Enhanced bacterial clearance and sepsis resistance in caspase-12-deficient mice. *Nature*, *440*(7087), 1064-1068. doi:10.1038/nature04656

Saltini, G., Dominici, R., Lovati, C., Cattaneo, M., Michelini, S., Malferrari, G., . . . Biunno, I. (2006). A novel polymorphism in SEL1L confers susceptibility to Alzheimer's disease. *Neurosci Lett*, *398*(1-2), 53-58. doi:10.1016/j.neulet.2005.12.038

San Miguel, J. F., Schlag, R., Khuageva, N. K., Dimopoulos, M. A., Shpilberg, O., Kropff, M., . . . Investigators, V. T. (2008). Bortezomib plus melphalan and prednisone for initial treatment of multiple myeloma. *N Engl J Med*, *359*(9), 906-917. doi:10.1056/NEJMoa0801479

Sato, T., Sako, Y., Sho, M., Momohara, M., Suico, M. A., Shuto, T., . . . Kai, H. (2012). STT3B-dependent posttranslational N-glycosylation as a surveillance system for secretory protein. *Mol Cell*, *47*(1), 99-110. doi:10.1016/j.molcel.2012.04.015

Schelhaas, M., Malmstrom, J., Pelkmans, L., Haugstetter, J., Ellgaard, L., Grunewald, K., & Helenius, A. (2007). Simian Virus 40 depends on ER protein folding and quality control factors for entry into host cells. *Cell*, *131*(3), 516-529. doi:10.1016/j.cell.2007.09.038

Scheuner, D., Song, B., McEwen, E., Liu, C., Laybutt, R., Gillespie, P., . . . Kaufman, R. J. (2001). Translational control is required for the unfolded protein response and in vivo glucose homeostasis. *Mol Cell*, *7*(6), 1165-1176.

Schindler, A. J., & Schekman, R. (2009). In vitro reconstitution of ER-stress induced ATF6 transport in COPII vesicles. *Proc Natl Acad Sci U S A*, *106*(42), 17775-17780. doi:10.1073/pnas.0910342106

Schonthal, A. H. (2012). Endoplasmic reticulum stress: its role in disease and novel prospects for therapy. *Scientifica (Cairo)*, *2012*, 857516. doi:10.6064/2012/857516

Schuh, W., Meister, S., Roth, E., & Jack, H. M. (2003). Cutting edge: signaling and cell surface expression of a mu H chain in the absence of lambda 5: a paradigm revisited. *J Immunol*, *171*(7), 3343-3347.

Schulz, C., Gomez Perdiguero, E., Chorro, L., Szabo-Rogers, H., Cagnard, N., Kierdorf, K., . . . Geissmann, F. (2012). A lineage of myeloid cells independent of Myb and hematopoietic stem cells. *Science*, *336*(6077), 86-90. doi:10.1126/science.1219179

Seidl, T., Rolink, A., & Melchers, F. (2001). The VpreB protein of the surrogate light-chain can pair with some mu heavy-chains in the absence of the lambda 5 protein. *Eur J Immunol*, *31*(7), 1999-2006. doi:10.1002/1521-4141(200107)31:7<1999::AID-IMMU1999>3.0.CO;2-K

Sha, H., He, Y., Chen, H., Wang, C., Zenno, A., Shi, H., . . . Qi, L. (2009). The IRE1alpha-XBP1 pathway of the unfolded protein response is required for adipogenesis. *Cell Metab*, *9*(6), 556-564. doi:10.1016/j.cmet.2009.04.009

Sha, H., He, Y., Yang, L., & Qi, L. (2011). Stressed out about obesity: IRE1alpha-XBP1 in metabolic disorders. *Trends Endocrinol Metab*, *22*(9), 374-381. doi:10.1016/j.tem.2011.05.002

Sha, H., Sun, S., Francisco, A. B., Ehrhardt, N., Xue, Z., Liu, L., . . . Qi, L. (2014). The ER-associated degradation adaptor protein Sel1L regulates LPL secretion and lipid metabolism. *Cell Metab*, *20*(3), 458-470. doi:10.1016/j.cmet.2014.06.015

Shaffer, A. L., Lin, K. I., Kuo, T. C., Yu, X., Hurt, E. M., Rosenwald, A., . . . Staudt, L. M. (2002). Blimp-1 orchestrates plasma cell differentiation by extinguishing the mature B cell gene expression program. *Immunity*, *17*(1), 51-62.

Shaffer, A. L., Peng, A., & Schlissel, M. S. (1997). In vivo occupancy of the kappa light chain enhancers in primary pro- and pre-B cells: a model for kappa locus activation. *Immunity*, *6*(2), 131-143.

Shaffer, A. L., Shapiro-Shelef, M., Iwakoshi, N. N., Lee, A. H., Qian, S. B., Zhao, H., . . . Staudt, L. M. (2004). XBP1, downstream of Blimp-1, expands the secretory apparatus and other organelles, and increases protein synthesis in plasma cell differentiation. *Immunity*, *21*(1), 81-93. doi:10.1016/j.immuni.2004.06.010

Shearer, A. G., & Hampton, R. Y. (2005). Lipid-mediated, reversible misfolding of a sterol-sensing domain protein. *EMBO J*, *24*(1), 149-159. doi:10.1038/sj.emboj.7600498

Shen, X., Ellis, R. E., Lee, K., Liu, C. Y., Yang, K., Solomon, A., . . . Kaufman, R. J. (2001). Complementary signaling pathways regulate the unfolded protein response and are required for *C. elegans* development. *Cell*, *107*(7), 893-903.

Shibata, Y., Voeltz, G. K., & Rapoport, T. A. (2006). Rough sheets and smooth tubules. *Cell*, *126*(3), 435-439. doi:10.1016/j.cell.2006.07.019

Shimizu, T., Mundt, C., Licence, S., Melchers, F., & Martensson, I. L. (2002). VpreB1/VpreB2/lambda 5 triple-deficient mice show impaired B cell development but functional allelic exclusion of the IgH locus. *J Immunol*, *168*(12), 6286-6293.

Sidrauski, C., Cox, J. S., & Walter, P. (1996). tRNA ligase is required for regulated mRNA splicing in the unfolded protein response. *Cell*, *87*(3), 405-413.

Sidrauski, C., & Walter, P. (1997). The transmembrane kinase Ire1p is a site-specific endonuclease that initiates mRNA splicing in the unfolded protein response. *Cell*, *90*(6), 1031-1039.

Singh, M., & Birshstein, B. K. (1993). NF-HB (BSAP) is a repressor of the murine immunoglobulin heavy-chain 3' alpha enhancer at early stages of B-cell differentiation. *Mol Cell Biol*, *13*(6), 3611-3622.

Smith, J. A., Turner, M. J., DeLay, M. L., Klenk, E. I., Sowders, D. P., & Colbert, R. A. (2008). Endoplasmic reticulum stress and the unfolded protein response are linked to synergistic IFN-beta induction via X-box binding protein 1. *Eur J Immunol*, *38*(5), 1194-1203. doi:10.1002/eji.200737882

So, J. S., Hur, K. Y., Tarrío, M., Ruda, V., Frank-Kamenetsky, M., Fitzgerald, K., . . . Lee, A. H. (2012). Silencing of lipid metabolism genes through IRE1alpha-mediated mRNA decay lowers plasma lipids in mice. *Cell Metab*, *16*(4), 487-499. doi:10.1016/j.cmet.2012.09.004

Song, B. L., Sever, N., & DeBose-Boyd, R. A. (2005). Gp78, a membrane-anchored ubiquitin ligase, associates with Insig-1 and couples sterol-regulated ubiquitination to degradation of HMG CoA reductase. *Mol Cell*, *19*(6), 829-840. doi:10.1016/j.molcel.2005.08.009

Soud, S., Lepesant, J. A., & Yanicostas, C. (2007). The xbp-1 gene is essential for development in Drosophila. *Dev Genes Evol*, *217*(2), 159-167. doi:10.1007/s00427-006-0124-1

Staehelin, L. A. (1997). The plant ER: a dynamic organelle composed of a large number of discrete functional domains. *Plant J*, *11*(6), 1151-1165.

Stein, A., Ruggiano, A., Carvalho, P., & Rapoport, T. A. (2014). Key steps in ERAD of luminal ER proteins reconstituted with purified components. *Cell*, *158*(6), 1375-1388. doi:10.1016/j.cell.2014.07.050

Sun, S., Lourie, R., Cohen, S. B., Ji, Y., Goodrich, J. K., Poole, A. C., . . . Qi, L. (2016). Epithelial Sel1L is required for the maintenance of intestinal homeostasis. *Mol Biol Cell*, *27*(3), 483-490. doi:10.1091/mbc.E15-10-0724

Sun, S., Shi, G., Han, X., Francisco, A. B., Ji, Y., Mendonca, N., . . . Qi, L. (2014). Sel1L is indispensable for mammalian endoplasmic reticulum-associated degradation, endoplasmic reticulum homeostasis, and survival. *Proc Natl Acad Sci U S A*, *111*(5), E582-591. doi:10.1073/pnas.1318114111

Sun, S., Shi, G., Sha, H., Ji, Y., Han, X., Shu, X., . . . Qi, L. (2015). IRE1alpha is an endogenous substrate of endoplasmic-reticulum-associated degradation. *Nat Cell Biol*, *17*(12), 1546-1555. doi:10.1038/ncb3266

Sundaram, M., & Greenwald, I. (1993). Suppressors of a lin-12 hypomorph define genes that interact with both lin-12 and glp-1 in *Caenorhabditis elegans*. *Genetics*, *135*(3), 765-783.

Szegezdi, E., Logue, S. E., Gorman, A. M., & Samali, A. (2006). Mediators of endoplasmic reticulum stress-induced apoptosis. *EMBO Rep*, *7*(9), 880-885. doi:10.1038/sj.embor.7400779

Tam, A. B., Koong, A. C., & Niwa, M. (2014). Ire1 has distinct catalytic mechanisms for XBP1/HAC1 splicing and RIDD. *Cell Rep*, *9*(3), 850-858. doi:10.1016/j.celrep.2014.09.016

- ten Boekel, E., Melchers, F., & Rolink, A. G. (1997). Changes in the V(H) gene repertoire of developing precursor B lymphocytes in mouse bone marrow mediated by the pre-B cell receptor. *Immunity*, 7(3), 357-368.
- Tirasophon, W., Welihinda, A. A., & Kaufman, R. J. (1998). A stress response pathway from the endoplasmic reticulum to the nucleus requires a novel bifunctional protein kinase/endoribonuclease (Ire1p) in mammalian cells. *Genes Dev*, 12(12), 1812-1824.
- Tissot, S., Normand, S., Khalfallah, Y., Delafosse, B., Viale, J. P., Annat, G., . . . Riou, J. P. (1995). Effects of a continuous lipid infusion on glucose metabolism in critically ill patients. *Am J Physiol*, 269(4 Pt 1), E753-758.
- Todd, D. J., McHeyzer-Williams, L. J., Kowal, C., Lee, A. H., Volpe, B. T., Diamond, B., . . . Glimcher, L. H. (2009). XBP1 governs late events in plasma cell differentiation and is not required for antigen-specific memory B cell development. *J Exp Med*, 206(10), 2151-2159. doi:10.1084/jem.20090738
- Tokoyoda, K., Hauser, A. E., Nakayama, T., & Radbruch, A. (2010). Organization of immunological memory by bone marrow stroma. *Nat Rev Immunol*, 10(3), 193-200. doi:10.1038/nri2727
- Tremblay, L. O., & Herscovics, A. (1999). Cloning and expression of a specific human alpha 1,2-mannosidase that trims Man9GlcNAc2 to Man8GlcNAc2 isomer B during N-glycan biosynthesis. *Glycobiology*, 9(10), 1073-1078.
- Tsai, B., Rodighiero, C., Lencer, W. I., & Rapoport, T. A. (2001). Protein disulfide isomerase acts as a redox-dependent chaperone to unfold cholera toxin. *Cell*, 104(6), 937-948.
- Tsai, Y. C., & Weissman, A. M. (2010). The Unfolded Protein Response, Degradation from Endoplasmic Reticulum and Cancer. *Genes Cancer*, 1(7), 764-778. doi:10.1177/1947601910383011
- Tsubata, T., & Reth, M. (1990). The products of pre-B cell-specific genes (lambda 5 and VpreB) and the immunoglobulin mu chain form a complex that is transported onto the cell surface. *J Exp Med*, 172(3), 973-976.
- Tsuneto, M., Tokoyoda, K., Kajikhina, E., Hauser, A. E., Hara, T., Tani-Ichi, S., . . . Melchers, F. (2013). B-cell progenitors and precursors change their microenvironment in

fetal liver during early development. *Stem Cells*, 31(12), 2800-2812.  
doi:10.1002/stem.1421

Tsuru, A., Fujimoto, N., Takahashi, S., Saito, M., Nakamura, D., Iwano, M., . . . Kohno, K. (2013). Negative feedback by IRE1beta optimizes mucin production in goblet cells. *Proc Natl Acad Sci U S A*, 110(8), 2864-2869. doi:10.1073/pnas.1212484110

Tyler, R. E., Pearce, M. M., Shaler, T. A., Olzmann, J. A., Greenblatt, E. J., & Kopito, R. R. (2012). Unassembled CD147 is an endogenous endoplasmic reticulum-associated degradation substrate. *Mol Biol Cell*, 23(24), 4668-4678. doi:10.1091/mbc.E12-06-0428

Underdown, B. J., & Schiff, J. M. (1986). Immunoglobulin A: strategic defense initiative at the mucosal surface. *Annu Rev Immunol*, 4, 389-417.  
doi:10.1146/annurev.iy.04.040186.002133

Upton, J. P., Wang, L., Han, D., Wang, E. S., Huskey, N. E., Lim, L., . . . Oakes, S. A. (2012). IRE1alpha cleaves select microRNAs during ER stress to derepress translation of proapoptotic Caspase-2. *Science*, 338(6108), 818-822. doi:10.1126/science.1226191

Urano, F., Wang, X., Bertolotti, A., Zhang, Y., Chung, P., Harding, H. P., & Ron, D. (2000). Coupling of stress in the ER to activation of JNK protein kinases by transmembrane protein kinase IRE1. *Science*, 287(5453), 664-666.

Uren, T. K., Johansen, F. E., Wijburg, O. L., Koentgen, F., Brandtzaeg, P., & Strugnell, R. A. (2003). Role of the polymeric Ig receptor in mucosal B cell homeostasis. *J Immunol*, 170(5), 2531-2539.

van Anken, E., Romijn, E. P., Maggioni, C., Mezghrani, A., Sitia, R., Braakman, I., & Heck, A. J. (2003). Sequential waves of functionally related proteins are expressed when B cells prepare for antibody secretion. *Immunity*, 18(2), 243-253.

van Huizen, R., Martindale, J. L., Gorospe, M., & Holbrook, N. J. (2003). P58IPK, a novel endoplasmic reticulum stress-inducible protein and potential negative regulator of eIF2alpha signaling. *J Biol Chem*, 278(18), 15558-15564. doi:10.1074/jbc.M212074200

van Loo, P. F., Dingjan, G. M., Maas, A., & Hendriks, R. W. (2007). Surrogate-light-chain silencing is not critical for the limitation of pre-B cell expansion but is for the termination of constitutive signaling. *Immunity*, 27(3), 468-480.  
doi:10.1016/j.immuni.2007.07.018

Vinci, F., Catharino, S., Frey, S., Buchner, J., Marino, G., Pucci, P., & Ruoppolo, M. (2004). Hierarchical formation of disulfide bonds in the immunoglobulin Fc fragment is assisted by protein-disulfide isomerase. *J Biol Chem*, *279*(15), 15059-15066. doi:10.1074/jbc.M311480200

von Freeden-Jeffry, U., Vieira, P., Lucian, L. A., McNeil, T., Burdach, S. E., & Murray, R. (1995). Lymphopenia in interleukin (IL)-7 gene-deleted mice identifies IL-7 as a nonredundant cytokine. *J Exp Med*, *181*(4), 1519-1526.

Wahlman, J., DeMartino, G. N., Skach, W. R., Bulleid, N. J., Brodsky, J. L., & Johnson, A. E. (2007). Real-time fluorescence detection of ERAD substrate retrotranslocation in a mammalian in vitro system. *Cell*, *129*(5), 943-955. doi:10.1016/j.cell.2007.03.046

Walter, P., & Ron, D. (2011). The unfolded protein response: from stress pathway to homeostatic regulation. *Science*, *334*(6059), 1081-1086. doi:10.1126/science.1209038

Wang, C., Li, W., Ren, J., Fang, J., Ke, H., Gong, W., . . . Wang, C. C. (2013). Structural insights into the redox-regulated dynamic conformations of human protein disulfide isomerase. *Antioxid Redox Signal*, *19*(1), 36-45. doi:10.1089/ars.2012.4630

Wang, Q., Shinkre, B. A., Lee, J. G., Weniger, M. A., Liu, Y., Chen, W., . . . Ye, Y. (2010). The ERAD inhibitor Eeyarestatin I is a bifunctional compound with a membrane-binding domain and a p97/VCP inhibitory group. *PLoS One*, *5*(11), e15479. doi:10.1371/journal.pone.0015479

Wang, X. Z., Harding, H. P., Zhang, Y., Jolicoeur, E. M., Kuroda, M., & Ron, D. (1998). Cloning of mammalian Ire1 reveals diversity in the ER stress responses. *EMBO J*, *17*(19), 5708-5717. doi:10.1093/emboj/17.19.5708

Wang, Y. H., Stephan, R. P., Scheffold, A., Kunkel, D., Karasuyama, H., Radbruch, A., & Cooper, M. D. (2002). Differential surrogate light chain expression governs B-cell differentiation. *Blood*, *99*(7), 2459-2467.

Weigmann, B., Tubbe, I., Seidel, D., Nicolaev, A., Becker, C., & Neurath, M. F. (2007). Isolation and subsequent analysis of murine lamina propria mononuclear cells from colonic tissue. *Nat Protoc*, *2*(10), 2307-2311. doi:10.1038/nprot.2007.315

Wickner, W., & Schekman, R. (2005). Protein translocation across biological membranes. *Science*, *310*(5753), 1452-1456. doi:10.1126/science.1113752

Wiertz, E. J., Tortorella, D., Bogyo, M., Yu, J., Mothes, W., Jones, T. R., . . . Ploegh, H. L. (1996). Sec61-mediated transfer of a membrane protein from the endoplasmic reticulum to the proteasome for destruction. *Nature*, *384*(6608), 432-438. doi:10.1038/384432a0

Wirtz, S., Popp, V., Kindermann, M., Gerlach, K., Weigmann, B., Fichtner-Feigl, S., & Neurath, M. F. (2017). Chemically induced mouse models of acute and chronic intestinal inflammation. *Nat Protoc*, *12*(7), 1295-1309. doi:10.1038/nprot.2017.044

Woo, C. W., Cui, D., Arellano, J., Dorweiler, B., Harding, H., Fitzgerald, K. A., . . . Tabas, I. (2009). Adaptive suppression of the ATF4-CHOP branch of the unfolded protein response by toll-like receptor signalling. *Nat Cell Biol*, *11*(12), 1473-1480. doi:10.1038/ncb1996

Wu, J., Rutkowski, D. T., Dubois, M., Swathirajan, J., Saunders, T., Wang, J., . . . Kaufman, R. J. (2007). ATF6alpha optimizes long-term endoplasmic reticulum function to protect cells from chronic stress. *Dev Cell*, *13*(3), 351-364. doi:10.1016/j.devcel.2007.07.005

Wu, T., Zhao, F., Gao, B., Tan, C., Yagishita, N., Nakajima, T., . . . Zhang, D. D. (2014). Hrd1 suppresses Nrf2-mediated cellular protection during liver cirrhosis. *Genes Dev*, *28*(7), 708-722. doi:10.1101/gad.238246.114

Xu, T., Yang, L., Yan, C., Wang, X., Huang, P., Zhao, F., . . . Liu, Y. (2014). The IRE1alpha-XBP1 pathway regulates metabolic stress-induced compensatory proliferation of pancreatic beta-cells. *Cell Res*, *24*(9), 1137-1140. doi:10.1038/cr.2014.55

Xu, Y., Zhao, F., Qiu, Q., Chen, K., Wei, J., Kong, Q., . . . Fang, D. (2016). The ER membrane-anchored ubiquitin ligase Hrd1 is a positive regulator of T-cell immunity. *Nat Commun*, *7*, 12073. doi:10.1038/ncomms12073

Xue, Z., He, Y., Ye, K., Gu, Z., Mao, Y., & Qi, L. (2011). A conserved structural determinant located at the interdomain region of mammalian inositol-requiring enzyme 1alpha. *J Biol Chem*, *286*(35), 30859-30866. doi:10.1074/jbc.M111.273714

Yagishita, N., Ohneda, K., Amano, T., Yamasaki, S., Sugiura, A., Tsuchimochi, K., . . . Nakajima, T. (2005). Essential role of synoviolin in embryogenesis. *J Biol Chem*, *280*(9), 7909-7916. doi:10.1074/jbc.M410863200

Yamaguchi, H., & Wang, H. G. (2004). CHOP is involved in endoplasmic reticulum stress-induced apoptosis by enhancing DR5 expression in human carcinoma cells. *J Biol Chem*, *279*(44), 45495-45502. doi:10.1074/jbc.M406933200

Yamamoto, K., Ichijo, H., & Korsmeyer, S. J. (1999). BCL-2 is phosphorylated and inactivated by an ASK1/Jun N-terminal protein kinase pathway normally activated at G(2)/M. *Mol Cell Biol*, *19*(12), 8469-8478.

Yamamoto, K., Sato, T., Matsui, T., Sato, M., Okada, T., Yoshida, H., . . . Mori, K. (2007). Transcriptional induction of mammalian ER quality control proteins is mediated by single or combined action of ATF6alpha and XBP1. *Dev Cell*, *13*(3), 365-376. doi:10.1016/j.devcel.2007.07.018

Yan, W., Frank, C. L., Korth, M. J., Sopher, B. L., Novoa, I., Ron, D., & Katze, M. G. (2002). Control of PERK eIF2alpha kinase activity by the endoplasmic reticulum stress-induced molecular chaperone P58IPK. *Proc Natl Acad Sci U S A*, *99*(25), 15920-15925. doi:10.1073/pnas.252341799

Yanagisawa, K., Konishi, H., Arima, C., Tomida, S., Takeuchi, T., Shimada, Y., . . . Takahashi, T. (2010). Novel metastasis-related gene CIM functions in the regulation of multiple cellular stress-response pathways. *Cancer Res*, *70*(23), 9949-9958. doi:10.1158/0008-5472.CAN-10-1055

Yang, H., Qiu, Q., Gao, B., Kong, S., Lin, Z., & Fang, D. (2014). Hrd1-mediated BLIMP-1 ubiquitination promotes dendritic cell MHCII expression for CD4 T cell priming during inflammation. *J Exp Med*, *211*(12), 2467-2479. doi:10.1084/jem.20140283

Yang, L., Xue, Z., He, Y., Sun, S., Chen, H., & Qi, L. (2010). A Phos-tag-based approach reveals the extent of physiological endoplasmic reticulum stress. *PLoS One*, *5*(7), e11621. doi:10.1371/journal.pone.0011621

Ye, J., Rawson, R. B., Komuro, R., Chen, X., Dave, U. P., Prywes, R., . . . Goldstein, J. L. (2000). ER stress induces cleavage of membrane-bound ATF6 by the same proteases that process SREBPs. *Mol Cell*, *6*(6), 1355-1364.

Ye, Y., Meyer, H. H., & Rapoport, T. A. (2001). The AAA ATPase Cdc48/p97 and its partners transport proteins from the ER into the cytosol. *Nature*, *414*(6864), 652-656. doi:10.1038/414652a

Ye, Y., Meyer, H. H., & Rapoport, T. A. (2003). Function of the p97-Ufd1-Npl4 complex in retrotranslocation from the ER to the cytosol: dual recognition of nonubiquitinated polypeptide segments and polyubiquitin chains. *J Cell Biol*, 162(1), 71-84. doi:10.1083/jcb.200302169

Ye, Y., Shibata, Y., Yun, C., Ron, D., & Rapoport, T. A. (2004). A membrane protein complex mediates retro-translocation from the ER lumen into the cytosol. *Nature*, 429(6994), 841-847. doi:10.1038/nature02656

Yoneda, T., Imaizumi, K., Oono, K., Yui, D., Gomi, F., Katayama, T., & Tohyama, M. (2001). Activation of caspase-12, an endoplasmic reticulum (ER) resident caspase, through tumor necrosis factor receptor-associated factor 2-dependent mechanism in response to the ER stress. *J Biol Chem*, 276(17), 13935-13940. doi:10.1074/jbc.M010677200

Yoshida, H., Haze, K., Yanagi, H., Yura, T., & Mori, K. (1998). Identification of the cis-acting endoplasmic reticulum stress response element responsible for transcriptional induction of mammalian glucose-regulated proteins. Involvement of basic leucine zipper transcription factors. *J Biol Chem*, 273(50), 33741-33749.

Yoshida, H., Matsui, T., Yamamoto, A., Okada, T., & Mori, K. (2001). XBP1 mRNA is induced by ATF6 and spliced by IRE1 in response to ER stress to produce a highly active transcription factor. *Cell*, 107(7), 881-891.

Yoshida, H., Oku, M., Suzuki, M., & Mori, K. (2006). pXBP1(U) encoded in XBP1 pre-mRNA negatively regulates unfolded protein response activator pXBP1(S) in mammalian ER stress response. *J Cell Biol*, 172(4), 565-575. doi:10.1083/jcb.200508145

Yoshida, H., Uemura, A., & Mori, K. (2009). pXBP1(U), a negative regulator of the unfolded protein response activator pXBP1(S), targets ATF6 but not ATF4 in proteasome-mediated degradation. *Cell Struct Funct*, 34(1), 1-10.

Zeng, L., Liu, Y. P., Sha, H., Chen, H., Qi, L., & Smith, J. A. (2010). XBP-1 couples endoplasmic reticulum stress to augmented IFN-beta induction via a cis-acting enhancer in macrophages. *J Immunol*, 185(4), 2324-2330. doi:10.4049/jimmunol.0903052

Zhang, K., & Kaufman, R. J. (2008). From endoplasmic-reticulum stress to the inflammatory response. *Nature*, 454(7203), 455-462. doi:10.1038/nature07203

Zhang, K., Shen, X., Wu, J., Sakaki, K., Saunders, T., Rutkowski, D. T., . . . Kaufman, R. J. (2006). Endoplasmic reticulum stress activates cleavage of CREBH to induce a systemic inflammatory response. *Cell*, *124*(3), 587-599. doi:10.1016/j.cell.2005.11.040

Zhang, K., Wong, H. N., Song, B., Miller, C. N., Scheuner, D., & Kaufman, R. J. (2005). The unfolded protein response sensor IRE1alpha is required at 2 distinct steps in B cell lymphopoiesis. *J Clin Invest*, *115*(2), 268-281. doi:10.1172/JCI21848

Zhang, T., & Ye, Y. (2014). The final moments of misfolded proteins en route to the proteasome. *DNA Cell Biol*, *33*(8), 477-483. doi:10.1089/dna.2014.2452

Zhou, J., Liu, C. Y., Back, S. H., Clark, R. L., Peisach, D., Xu, Z., & Kaufman, R. J. (2006). The crystal structure of human IRE1 luminal domain reveals a conserved dimerization interface required for activation of the unfolded protein response. *Proc Natl Acad Sci U S A*, *103*(39), 14343-14348. doi:10.1073/pnas.0606480103

Zhou, L. J., Ord, D. C., Hughes, A. L., & Tedder, T. F. (1991). Structure and domain organization of the CD19 antigen of human, mouse, and guinea pig B lymphocytes. Conservation of the extensive cytoplasmic domain. *J Immunol*, *147*(4), 1424-1432.

Zhou, M., & Schekman, R. (1999). The engagement of Sec61p in the ER dislocation process. *Mol Cell*, *4*(6), 925-934.

# Curriculum Vitae

## BIOSKETCH

NAME Hana Kim	POSITION TITLE Ph.D. candidate
EMAIL hk739@cornell.edu	DISSERTATION ADVISOR Dr. Ling Qi, Professor of Molecular & Integrative Physiology

### A. EDUCATION/TRAINING

- 9/2011 – 8/2017 Ph.D., Immunology and Infectious Disease  
Cornell University, Ithaca, NY (Advisor: Dr. Ling Qi, Professor)  
GPA: 3.63
- 9/2008 - 7/2011 M.S. Biological Sciences California State Polytechnic University, Pomona, CA  
(Advisor: Dr. Jill Adler-Moore, Professor)  
GPA: 3.51
- 6/2005 - 6/2008 B.S. Microbiology California State Polytechnic University, Pomona, CA (Advisor:  
Dr. Jill Adler-Moore, Professor)  
GPA: 3.48

### B. RESEARCH POSITIONS

- 8/2016 - present Research Intern. *University of Michigan, Ann Arbor, MI* (Advisor: Dr. Ling Qi, Professor)
- 9/2011 - present PhD Candidate. *Cornell University, Ithaca, NY* (Advisor: Dr. Ling Qi, Associate Professor)
- 9/2008 - 7/2011 Graduate research student. *California State Polytechnic University, Pomona, CA* (Advisor: Dr. Jill Adler-Moore, Professor)
- 6/2008 - 8/2010 Research Assistant. *California State Polytechnic University, Pomona, CA* (Advisor: Dr. Jill Adler-Moore, Professor)
- 9/2007 - 6/2008 Undergraduate research student. *California State Polytechnic University, Pomona, CA* (Advisor: Dr. Jill Adler-Moore, Professor)

### C. OTHER WORK EXPERIENCES

- 8/2016 - present Laboratory Manager, *University of Michigan, Ann Arbor, MI*
- 1/2016 - 7/2016 Laboratory Manager, *Cornell University, Ithaca, NY*
- 9/2013 - 5/2016 Teaching Assistant, *Cornell University, Ithaca, NY*
- 9/2008 - 5/2011 Teaching Assistant, *California State Polytechnic, Pomona, CA*

### D. PUBLICATIONS

- 1) Ji Y\*, Sun S\*, Shrestha N, Darragh L, Shirakawa J, Xing Y, He Y, Carboneau B, Kim G, **Kim H**, Shu X, An D, Ma M, Oberhozler J, Soleimanpour S, Gannon M, Liu C, Naji A, Kulkarni R, Wang Y, Kersten S, Qi L. Toll-like receptors 2 and 4 act as brakes on adaptive  $\beta$ -cell mass expansion in diet-induced obesity. *Nature immunology*. *Under revision*
- 2) Ji Y\*, **Kim H**\*, Yang L, Sha H, Roman C, Long Q, Qi L. The Sel1L-Hrd1 endoplasmic reticulum-associated degradation complex manages a key checkpoint in B cell development. *Cell Report*. 2016 September. PMID 27568564 (\*Contributed equally)

- 3) Sun S\*, Shi G\*, Sha H, Ji Y, Han X, Shu X, Ma H, Inoue T, Gao B, **Kim H**, Bu P, Guber RD, Shen X, Lee AH, Iwawaki T, Paton AW, Paton JC, Fang D, Tsai B, Yates JR 3rd, Wu H, Kersten S, Long Q, Duhamel GE, Simpson KW, Qi L. IRE1 $\alpha$  is an endogenous substrate of endoplasmic reticulum associated degradation. *Nature cell biology*. 2015 December. PMID 26551274
- 4) **Kim H\***, Bhattacharya A\*, Qi L. Endoplasmic reticulum quality control in cancer: Friend or foe. *Semin Cancer Biol*. 2015 Mar 18. PMID 25794824 (\*Contributed equally)
- 5) Ji Y\*, Sun S\*, Goodrich JK, **Kim H**, Poole AC, Duhamel GE, Ley RE, Qi L. Diet-induced alterations in gut microflora contribute to lethal pulmonary damage in TLR2/TLR4-deficient mice. *Cell Rep*. 2014 Jul 10. PMID 24953658
- 6) Iwata TN, Cowley TJ, Sloma M, Ji Y, **Kim H**, Qi L, Lee SS. The transcriptional co-regulator HCF-1 is required for INS-1  $\beta$ -cell glucose-stimulated insulin secretion. *PLoS One*. 2013 Nov 8. PMID 24250814
- 7) Adler-Moore, J., M. Munoz, **H. Kim**, J. Romero, T. Tumpey, H. Zeng, C. Petro, W. Ernst, S. Kosina, G. Jimenez, and G. Fujii. 2011. Characterization of the murine Th2 response to immunization with liposomal M2e influenza vaccine. *Vaccine*. 2011 May 3. PMID 21545821

#### E. ABSTRACT PRESENTATIONS:

- *The Sel1L-Hrd1 Endoplasmic Reticulum-Associated Degradation Complex Manages a Key checkpoint in B cell development*  
**Hana Kim**, Yewei Ji, Liu Yang, Ling Qi  
 October 13<sup>th</sup>, 2016  
 3<sup>rd</sup> Annual Protein Folding Diseases Initiative Symposium, Ann Arbor, Michigan
- *The Sel1L-Hrd1 Endoplasmic Reticulum-Associated Degradation Complex Manages a Key checkpoint in B cell development*  
 Yewei Ji, **Hana Kim**, Liu Yang, Ling Qi  
 June 18<sup>th</sup>, 2015  
 FASEB Science Research Conferences – From Unfolded Proteins in the ER to Disease, Saxtons Rivers, Vermont
- *B cell Specific Sel1L Ablation Promotes Propagation of Colitogenic Microbiota*  
**Hana Kim**, Yewei Ji, Iris Sun, Liu Yang, Ling Qi  
 February 4<sup>th</sup>, 2014  
 Biological and Biomedical Sciences Recruitment 2014 Poster Session, Ithaca, NY
- *Broad Neutralization of Type A Influenza Virus Strains by Anti-M2 Ectodomain Antibodies*  
**Hana Kim**<sup>1</sup>, Juan Romero<sup>1</sup>, Chris Petro<sup>1</sup>, William Ernst<sup>2</sup>, Gary Fujii<sup>2</sup>, Hui Zeng<sup>3</sup>, Terrence Tumpey<sup>3</sup>, Jill Adler-Moore<sup>1</sup>  
 October 28th, 2010  
 10<sup>th</sup> Agricultural Research Institute Showcase Pomona, CA
- *Broad Neutralization of Type A Influenza Virus Strains by Anti-M2 Ectodomain Antibodies*  
**Hana Kim**<sup>1</sup>, Juan Romero<sup>1</sup>, Chris Petro<sup>1</sup>, William Ernst<sup>2</sup>, Gary Fujii<sup>2</sup>, Hui Zeng<sup>3</sup>, Terrence Tumpey<sup>3</sup>, Jill Adler-Moore<sup>1</sup>  
 July 17-21, 2010  
 American Society for Virology 29<sup>th</sup> Annual Meeting

## **F. Research Skills/ Competencies**

### 1) Research skills:

- Extensively trained in primary B cell isolation, activation, proliferation and differentiation.
- Highly skilled in animal handling, which includes, but not limited to intraperitoneal injection, tail vein injection, bone marrow transplantation, glucose tolerance test/ Insulin sensitivity test
- Trained in cryosectioning, immunohistochemistry (IHC) and immunofluorescence (IF) staining of mouse tissues such as spleen, pancreas, liver and intestine
- Trained in confocal microscopy and image analysis
- Highly skilled in designing and performing multicolor flow cytometry and analyze the data
- Extensively trained in immunoassays such as ELISA, ELISPOT, Multiplex
- Skilled in biochemistry techniques with experiences in protein isolation, immunoblot analysis and co-immunoprecipitation

### 2) Software:

- Knowledge on Microsoft Office, GraphPad Prism, FlowJo, Image J Analysis and Adobe Photoshop

### 3) Language proficiency:

- English and Korean (Native)

## **G. HONORS**

- 2006-08 Golden Key International Honor Society, California State Polytechnic University, Pomona, CA
- 2006-08 Dean's List, California State Polytechnic University, Pomona, CA
- 2006-07 International Student Scholarships, California State Polytechnic University, Pomona, CA
- 2005-06 President's Honors List, California State Polytechnic University, Pomona, CA
- 2004-05 President's List, Mount San Antonio College, Walnut, CA
- 2002-04 Dean's List, Mount San Antonio College, Walnut, CA